Structural modifications of the RNA-binding protein, fused in sarcoma: Implications for amyotrophic lateral sclerosis

Hannah Kirby Robinson

September 2015

A thesis submitted to Cardiff University for the degree of

Doctor of Philosophy

Neuroscience & Mental Health
Research Institute

ABSTRACT

Amyotrophic lateral sclerosis (ALS) is an aggressive neurodegenerative disease characterised by the loss of upper and lower motor neurons, resulting in progressive paralysis, muscular atrophy and eventual death, on average, within 2-5 years post-diagnosis. In ~5% of patients with familial ALS (fALS), causative mutations occur within the gene encoding the RNA-binding protein, Fused in Sarcoma (FUS). Normally, FUS is predominantly localised to the nucleus and has several known roles in transcription, splicing and mRNA transport. Yet, in ALS patients with mutant forms of FUS, the protein becomes dramatically mislocalised to the cytoplasm and abnormal proteinaceous inclusions of FUS in the cytoplasm are observed post-mortem. Several questions remain: How do large pathological inclusions of FUS form? Is pathology induced via a gain or loss of protein function? Can aggregation in the cytoplasm of this normally nuclear protein be sufficient to produce toxicity? This thesis provides detailed characterisation of a novel pathway through which FUS may aggregate following its mislocalisation to the cytoplasm. This pathway is distinct from recruitment into stress-induced stress granules and can lead to the formation of large RNA-based FUS aggregates in a concentration-dependent manner. It was demonstrated that reduced protein-RNA interaction through transcriptional inhibition resulted in the dissolution and reassembly of these FUS aggregates into higher order RNA-free structures, reminiscent of inclusions seen in ALS-FUS patients. We also show *in vivo* that an initial insult of FUS aggregation in the cytoplasm is sufficient to elicit ALS-like pathology. In addition, how loss of FUS from the nucleus could affect the nuclear architecture was investigated, highlighting an important role for FUS in the maintenance of a protective subnuclear body, the paraspeckle, the disruption of which may contribute to the pathogenesis of FUSopathies. As such, this thesis identifies several novel mechanisms involved in the development and progression of FUSopathy, which may be useful for future therapeutic strategies targeting ALS caused by FUS mutation.

ACKNOWLEDGEMENTS

This thesis project was funded by a scholarship from the Neuroscience and Mental Health Research Institute at Cardiff University together with project grants from Motor Neurone Disease Association and Wellcome Trust.

In the first instance I wish to thank Prof. Vladimir Buchman for welcoming me as a member of his group and for his expert guidance and support over the past 4 years. I also thank Dr Natalia Ninkina for always providing words of wisdom and unwavering optimism when I have needed it most. For teaching me the practical skills that were required throughout my PhD (and for being an incredibly patient mentor), I am indebted to Dr Tatyana Shelkovnikova. I am also grateful to past members of the VLB lab, for their support, namely, Dr Owen Peters, Dr Natalie Connor-Robson and Dr Alexey Ustyugov.

I extend my gratitude to members of the 4th floor office - because life is better when you are laughing. Thank you for putting up with me.

I am incredibly grateful for the support given by Dr Alexander Shaw who has been with me every step of the way.

Finally, I thank my family, and in particular, my parents Corrine and Ian, for always believing in me.

CONTENTS

LIST OF FIGURES

LIST OF TABLES

LIST OF ABBREVIATIONS

ALS	amyotrophic lateral sclerosis
ASO(s)	antisense oligonucleotide(s)
BSA	bovine serum albumin
CAZ	Cabeza
DAB	diaminobenzidine
DBHS	*Drosophila* behaviour human splicing
DDX5	DEAD box helicase 5
DENN	differentially expressed in normal and neoplastic cells
DRB	5,6-dichloro-1-beta-D-ribofuranosylbenzimidazole
EM	electron microscopy
EWS	Ewing's sarcoma protein
FA(-)(s)	RNA-free FAs formed by RNA-binding-competent ALS-associated FUS following prolonged transcriptional inhibition
FA(s)	FUS aggregate(s)
fALS	familial amyotrophic lateral sclerosis
FG(s)	FUS granule(s)
FMRP	fragile X mental retardation protein
FTD	frontotemporal dementia
FTLD	frontotemporal lobar degeneration
FUS	fused in sarcoma
G3BP1	GTPase-activating protein-binding protein 1
GFAP	glial fibrillary acidic protein
GFP	green fluorescent protein
GOF	gain of function
GWAS	genome-wide association studies
HCI(s)	hyaline conglomerate inclusion(s)
HEK-293	human embryonic kidney-293
iPSC(s)	induced pluripotent stem cell(s)
KO	knock-out
LA (LA+)	luria agar (with antibiotics)
LB (LB+)	luria broth (with antibiotics)
LMN(s)	lower motor neuron(s)
LOF	loss of function
mGluR5	metabotropic glutamate receptor 5
MN(s)	motor neuron(s)
MS	multiple sclerosis
MTA	methylthioadenosine
MTAP	methylthioadenosine phosphorylase
MTOC(s)	microtubule organising centre(s)
NLS	nuclear localisation signal
NMJ(s)	neuromuscular junction(s)
OPTN	optineurin
PBS	phosphate buffered saline

PFA	paraformaldehyde
PFN1	profilin 1
PIC(s)	pre-initiation complex(es)
PrP	prion protein
PVDF	polyvinylidene difluoride
qPCR	quantitative polymerase chain reaction
RCAI	*R. communis* agglutinin I
RNAP2	RNA polymerase II
RNAP3	RNA polymerase III
RNP	ribonucleoprotein
RRM	RNA recognition motif
SA	sodium arsenite
sALS	sporadic amyotrophic lateral sclerosis
SDS-PAGE	sodium dodecyl sulphate polyacrylamide gel electrophoresis
SG(s)	stress granule(s)
Sigma 1	sigma non-opioid receptor 1
SMA	spinal muscular atrophy
SMN	survival of motor neuron protein
snRNPs	small nuclear ribonucleic particles
SOD1	Cu/Zn superoxide dismutase 1
TAF15	TATA-box binding protein associated factor 15
TANK1	tank-binding kinase 1
TDP-43	TAR DNA binding protein-43
TFIID	transcription factor IID
TG	transgenic
TIA-1	T cell intracellular antigen 1
TIAR	TIA-1 related protein
TUBA4A	tubulin alpha 4A
UBI(s)	ubiquitin-positive inclusion(s)
UBQLN2	ubiquilin 2
UMN(s)	upper motor neuron(s)
UPS	ubiquitin-proteasome system
VCP	valosin-containing protein
WT	wild-type
YFP	yellow fluorescent protein
ZF	zinc finger

GENERAL INTRODUCTION

1.1 Amyotrophic lateral sclerosis

The third most common neurodegenerative disease worldwide, amyotrophic lateral sclerosis (ALS), also known as Lou Gehrig's disease, has a reported incidence of between 1.5–2.5 per 100,000/year (Logroscino *et al.*, 2008) and is the named cause of death on approximately 1 in 1000 death certificates in the UK (Talbot, 2009). This form of motor neuron disease, characterised by a loss of both upper (UMNs) and lower motor neurons (LMNs) is severely debilitating, resulting in increasing muscular atrophy and progressive paralysis (Figure 1.1). Although a highly heterogeneous disease, a diagnosis of ALS is always terminal and patients typically succumb to the disease between two and five years post-symptom onset (Logroscino *et al.*, 2008). Further, the single currently licensed pharmacotherapy for ALS, Riluzole, delays disease progression by only a few months (Bensimon *et al.*, 1994; Miller *et al.*, 2003). As well as the severe physical and emotional impact that a diagnosis of ALS has for a patient and their family, with a lifetime risk of developing ALS at 1:400 (Hardiman *et al.*, 2011) and prevalence of ~5.2 per 100,000 (Worms, 2001), the economic cost to society must be considered. In a study determining the cost of brain disorders in Europe, an individual with neuromuscular disease, of which ALS is a subset, was found to cost around €30,000 per year (Gustavsson *et al.*, 2011). Taken together, this highlights the essential need for better understanding and, in turn, improved therapeutics for the disease.

1.2 Clinical features and diagnosis of ALS

A diagnosis of ALS is often difficult to provide and is largely given following the elimination of similarly presenting neuromuscular diseases. Without a definitive test for ALS, there is usually a severe delay to diagnosis, often taking between 9 and 13 months following initial symptom presentation (Cellura *et al.*, 2012). For diagnosis, clinical examinations are used to determine the degree to which upper and lower motor neurons are affected. A key sign of UMN involvement, highlighting loss of normal corticospinal transmission, is muscular spasticity, or stiffness. The presence of the 'Babinski sign', an abnormal dorsiflexion of the big toe following blunt stimulation to the sole of the foot, can also be used to indicate UMN involvement, as functional corticospinal transmission is normally required to suppress this. Muscle weakness, atrophy and fasciculations are instead indicative of LMN involvement. Frequently, there is a co-occurrence of UMN and LMN signs in a single region, e.g. arms or legs, and asymmetry of these signs is probable (Kiernan *et al.*, 2011). Patients may also undergo more objective measures such as electromyography to monitor neuromuscular activity.

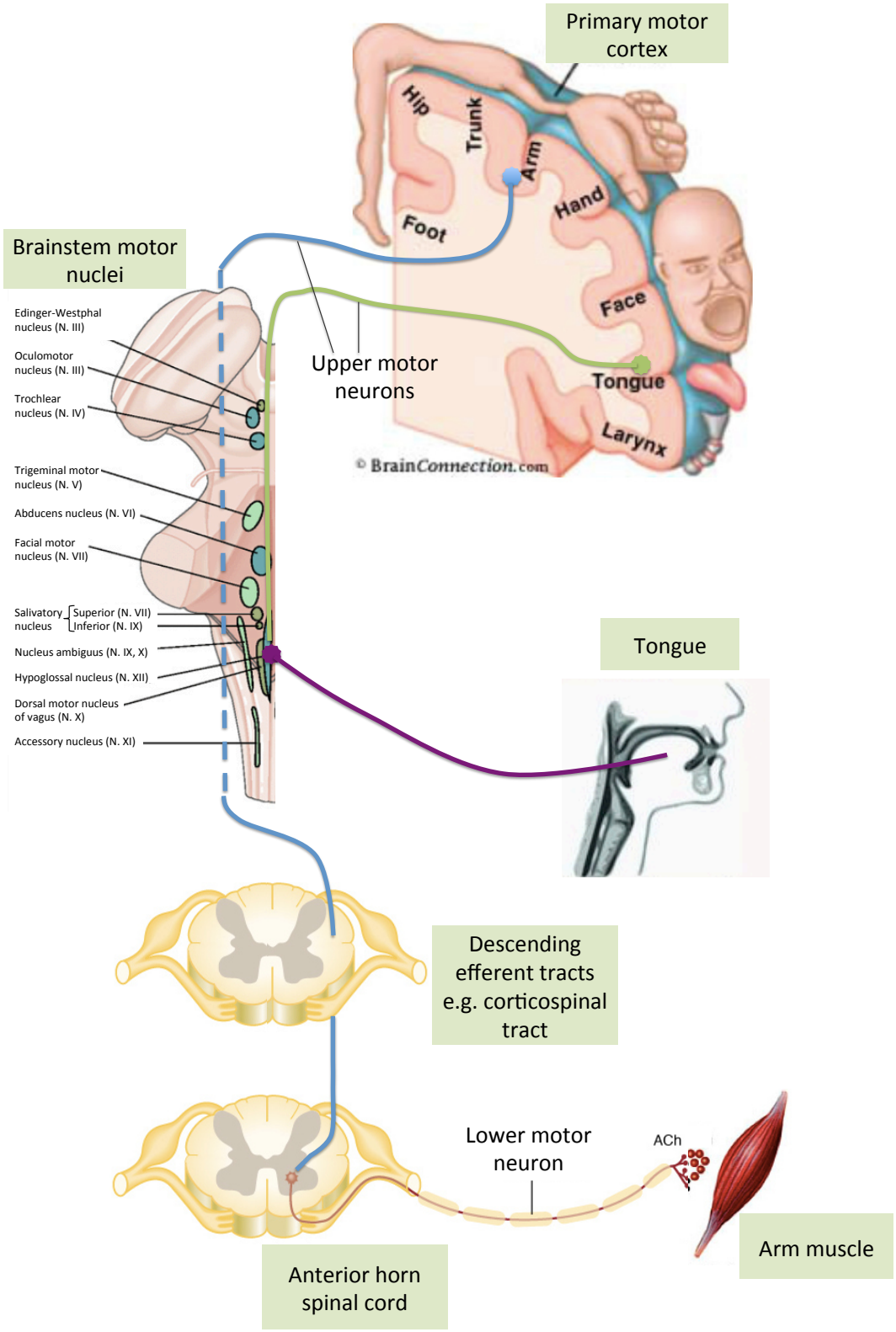

Figure 1.1. Representative schematic highlighting UMN and LMN projections that are degenerated in ALS. Primary motor cortex (PMC) is topographically mapped in columns, with different bodily movements assigned varying degrees of cortical area. UMNs, large pyramidal cells originating in layer 5 PMC project to either specific brainstem motor nuclei (green) or descend through spinal cord efferent tracts until reaching the required vertebral level and passing into the anterior horn of spinal cord (blue). Here, they synapse directly, or indirectly via interneurons, onto LMNs that innervate target muscles (red and purple). Both UMNs and LMNs are degenerated in ALS. Ach, acetyl choline. Figure created using images from Kandel (2013) and BrainConnection.com (2014).

Based upon the number of UMN and LMN signs of involvement, patients are classed as having clinically possible, clinically probable or clinically definite ALS. The currently favoured Awaji-shima criteria for diagnosis of ALS (de Carvalho *et al.*, 2008) (Figure 1.2), has evolved from the original El Escorial criteria (Brooks, 1994) to give an equal weighting to objective electromyography measures and clinical examinations, providing increased sensitivity of diagnosis compared to previous criteria (Douglass et al., 2010).

The initial presentation of ALS is not uniform, further complicating diagnoses. Classical limb onset ALS is the most typical, occurring in approximately two thirds of patients and bulbar and respiratory onset patterns occur to a lesser extent (Wijesekera and Leigh, 2009; Traynor *et al.*, 2000). In bulbar onset patients, degeneration of motor neuronal populations may initially present as dysphagia or dysarthria. Although ALS may outwardly begin within a given region, it is unforgivingly progressive and symptoms 'spread' to include other motor neuron groups, with limb onset patients also usually experiencing bulbar involvement eventually. In late stages of the disease, patients reach a 'totally locked in' state, where paralysis is widespread and loss of respiratory control is the major cause of death (Roche *et al.*, 2012). Interestingly, innervation of oculomotor regions and pelvic floor muscles is rarely affected (Mannen *et al.*, 1977).

An average age of onset of between 50 and 60 years is typically accepted for ALS (Cleveland and Rothstein, 2001). Although age itself may be identified as a risk factor within this range, because prevalence decreases after 80 years of age, ALS is more likely a disease affecting a susceptible subgroup rather than simply an aged population (Logroscino *et al.*, 2010). On an individual basis, age of onset is highly variable, with some forms of ALS diagnosed in teenage years and earlier (Turner *et al.*, 2012). Further, gender is also considered to be a risk factor, with an increased occurrence in men, although this remains unexplained (Logroscino *et al.*, 2010).

Aside from Riluzole, treatment is mainly palliative. Alongside pain relief, patients are, where required, given the option of gastrostomy to facilitate feeding and respiratory ventilation to support breathing, either non-invasively or via tracheostomy, although the quality of life must be addressed in these individuals (Blackhall, 2012).

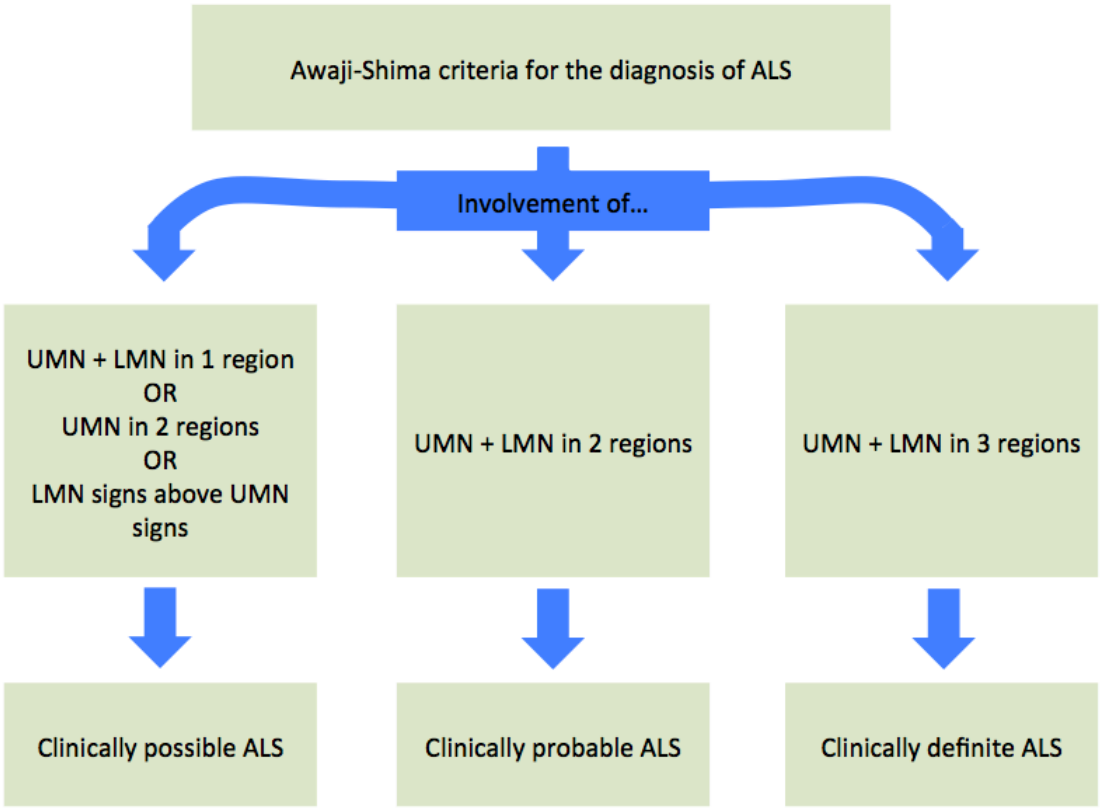

Figure 1.2. Schematic representation of the Awaji-Shima criteria for the diagnosis of ALS. Abbreviations: UMN, upper motor neuron(s); LMN, lower motor neuron(s). Adapted from (Douglass *et al.*, 2010)

In addition to motor symptoms, cognitive and/or behavioural symptoms are observed in ~50% of ALS patients and about 15% of these cases qualify for a diagnosis of frontotemporal dementia (FTD) (Ringholz *et al.*, 2005; Lillo and Hodges, 2009). FTD results from frontal and temporal lobe degeneration (FTLD), and often presents as semantic dementia, lack of behavioral inhibition and speech disturbances (Seltman and Matthews, 2012). Inversely, a large fraction of patients with FTD are given a diagnosis of definite ALS or display initial motor symptoms (Lomen-Hoerth *et al.*, 2002). Considerable clinical overlap of FTLD and ALS, combined with overlapping pathology and genetics have recently led to the understanding that ALS and FTLD are likely the opposite ends of a continuum of disease (Figure 1.3) (Goldstein and Abrahams, 2013; Robberecht and Philips, 2013).

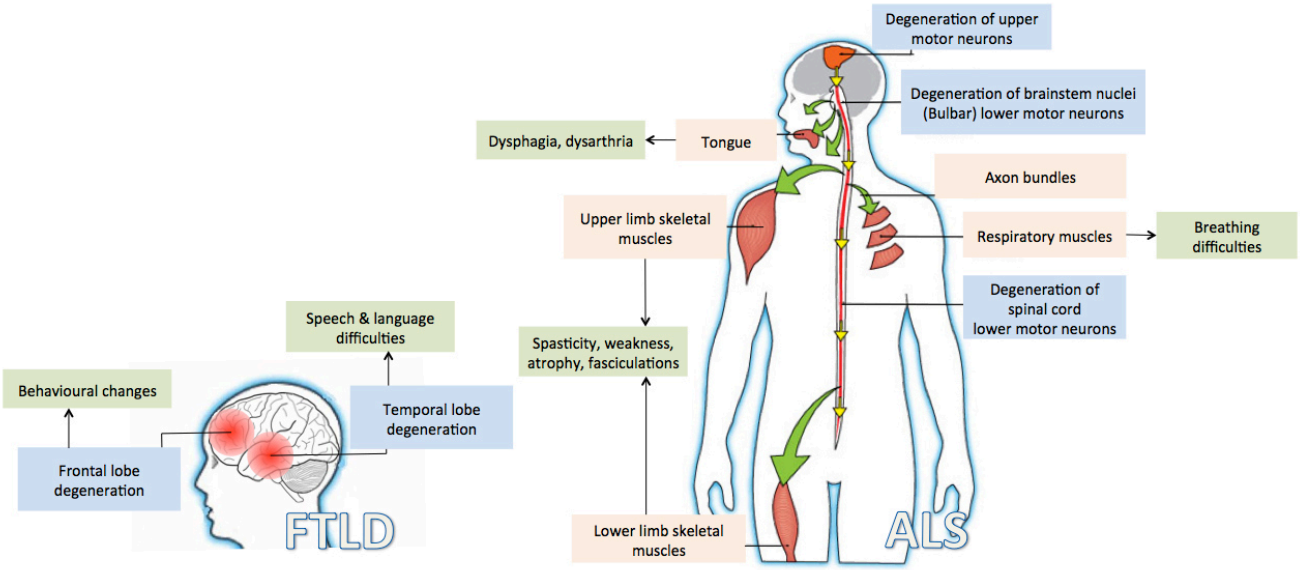

Figure 1.3. Summary of the clinical signs of ALS and FTLD. Clinical signs associated with ALS and FTLD (green) result from the degeneration of specific neuronal populations (blue). Main affected areas are shown in light orange. Image adapted from Muscular Dystrophy Association (2014).

1.3 Genetics of ALS

A small fraction (~10%) of ALS patients have familial ALS (fALS) following a clear Mendelian pattern of inheritance and accompanied by a family history of the disease. However, the majority of patients (~90%) are instead thought to have sporadic ALS (sALS) with no observable family history. FALS and sALS are, however, clinically indistinguishable. In addition, an increasing number of genetic abnormalities and increased heritability are linked to supposedly sALS, which together with an often sparse family history, blurs the boundary between these two classifications (Al-Chalabi *et al.*, 2010; Talbot, 2013). Genetic counseling and limited genetic testing is available for those with clear family history, although with a wealth of genes now known to harbor ALS-causing mutations and a degree of fALS not yet genetically explained, genetic testing may fail to provide a definitive conclusion in many instances.

1.3.1 Genes with ALS-causing mutations

Understanding of the genetic background of ALS has greatly accelerated over the past 20 years, with ~70% familial ALS now genetically accounted for and the list of ALS-associated genes rapidly growing (Table 1.1) (Renton *et al.*, 2014).

Table 1.1. Major genes known to carry ALS-causing mutations

Gene/ protein	Location	Inheritance	Estimated % accounted		Protein functions	Reference(s)
			fALS	sALS		
***SOD1*/ SOD1**	21q22	AD & AR	20	1-2	Superoxide metabolism	Rosen *et al.* (1993)
***TARDBP*/ TDP-43**	1p36	AD	4	1	RNA metabolism	Sreedharan *et al.* (2008)
***FUS*/ FUS**	16p11	AD & AR	4	1	RNA metabolism	Kwiatkowski *et al.* (2009); Vance *et al.* (2009)
***VCP*/ VCP**	9p13	AD	1	1	Proteostatic protein	Johnson *et al.* (2010)
***OPTN*/ optineurin**	10p13	AD & AR	<1	<1	Proteostatic protein	Maruyama *et al.* (2010)
***UBQLN2*/ ubiquilin 2**	Xp11	XD	<1	<1	Proteostatic protein	Deng *et al.* (2011)
SQSTM1/ p62	5q35	AD	1	<1	Proteostatic protein	Fecto *et al.* (2011)
***C9ORF72*/ C9orf72**	9p21	AD	40	7	DENN protein	Renton *et al.* (2011); DeJesus-Hernandez *et al.* (2011)
***PFN1*/ profilin 1**	17p13	AD	<1	<1	Cytoskeleton dynamics	Wu *et al.* (2012)

Abbreviations: AD, autosomal dominant; AR, autosomal recessive; XD, X-linked dominant; DENN, differentially expressed in normal and neoplasia. Adapted from (Renton *et al.*, 2014).

SOD1

The first known genetic cause of ALS was provided by Rosen *et al.* (1993) with their identification of 11 causal mutations in the gene encoding Cu/Zn superoxide dismutase 1 (SOD1) in 13 families showing dominantly inherited fALS with high penetrance. Since, over 150 dominant ALS-causing mutations, predominantly missense, have been

observed across all 5 exons of *SOD1* (Chen *et al.*, 2013) and a single recessive substitution mutation, D90A, has been identified (Andersen *et al.*, 1995). *SOD1* mutation is thought to account for ~20% of fALS and ~1-2% of sALS (Pasinelli and Brown, 2006). Altered speeds of progression have been linked to different mutations; patients homozygous for D90A show a much slower progression than those with the frequently occurring A4V mutation (Rosen *et al.*, 1994), and although highly heterogeneous, there is a tendency for ALS-SOD1 patients to present mainly with LMN signs (Ravits *et al.*, 2013). Present in the cytosol and the inner mitochondrial space, SOD1 polypeptide forms a functional homodimer that acts as a cellular defence mechanism against toxic superoxide, a by-product of oxidative phosphorylation, converting it to oxygen and hydrogen peroxide. Although discussed in more detail later, mutations in this protein have led to the implication of oxidative stress, amongst other mechanisms, in the pathophysiology of ALS (Barber and Shaw, 2010). However, the subsequent discovery of other genes with ALS-causing mutations is unveiling novel pathological mechanisms alongside those provided in the first instance by SOD1.

TARDBP

In recent years, defects in RNA metabolism and processing are being increasingly linked to ALS through the identification of mutations in genes encoding RNA-binding proteins. In 2008, ALS-causing mutations were discovered in *TARDBP*, encoding TAR DNA-binding protein-43 (TDP-43), a 43 kDa, predominantly nuclear protein involved in many cellular processes including transcription, mRNA transport and RNA processing (Sreedharan *et al.*, 2008). Mutations in *TARDBP* are thought to account for ~4% fALS and ~1% sALS (Lagier-Tourenne *et al.*, 2010). These mutations (>30) are largely missense and most commonly occur in exon 6, encoding the C-terminus of the protein, a glycine-rich region involved in protein-protein interactions (Figure 1.4). Mutations in *TARDBP* have shown a dominant pattern of inheritance and lead to a predominantly upper limb onset with slow progression (Corcia *et al.*, 2012).

FUS

The identification of ALS-causing mutations in another gene, *FUS,* encoding a second RNA binding protein, Fused in Sarcoma (FUS), further implicated altered RNA processing in ALS (Kwiatkowski *et al.*, 2009; Vance *et al.*, 2009). Although many of its normal cellular functions remain unknown, FUS protein has been shown to shuttle between the nucleus and the cytoplasm and engage in mRNA transport, RNA metabolism, transcription and splicing events (Lagier-Tourenne *et al.*, 2010; Zinszner

et al., 1997b). Approximately 50 mutations have been identified in ALS patients, the majority of which have been missense mutations occurring predominantly in exon 15, encoding the C-terminus, comprised of a nuclear localisation signal (NLS) and RNA-binding domains (Figure 1.4). Variants in the 3'UTR of *FUS* have also been detected in ALS patients and were shown to result in overexpression of the protein (Sabatelli *et al.*, 2013). Rare C-terminal truncation mutations have also been identified. The R495X truncation, resulting in the loss of 31 C-terminal amino acids, has been associated with a severe clinical phenotype (Waibel *et al.*, 2010). Additionally, a genomic variant (10747 A>G) at a splice site for intron 13 has been discovered, resulting in the skipping of exon 14 and the introduction of a premature stop codon, producing a FUS protein comprising only the first 466 amino acids (p.G466VfsX14). This patient was 20 years old with prominent bulbar signs and died following respiratory failure 22 months post symptom onset (DeJesus-Hernandez *et al.*, 2010). In another kindred, a dominantly inherited truncation of the NLS (p.G504WfsX12) was also shown to produce an aggressive form of ALS (Kent *et al.*, 2014). However, it must be noted that not all mutations to *FUS* are pathogenic. Whilst a number of small insertions and deletions (indels) have been identified in *FUS* in ALS patients, they have also been noted at a similar frequency in controls (Rutherford *et al.*, 2012).

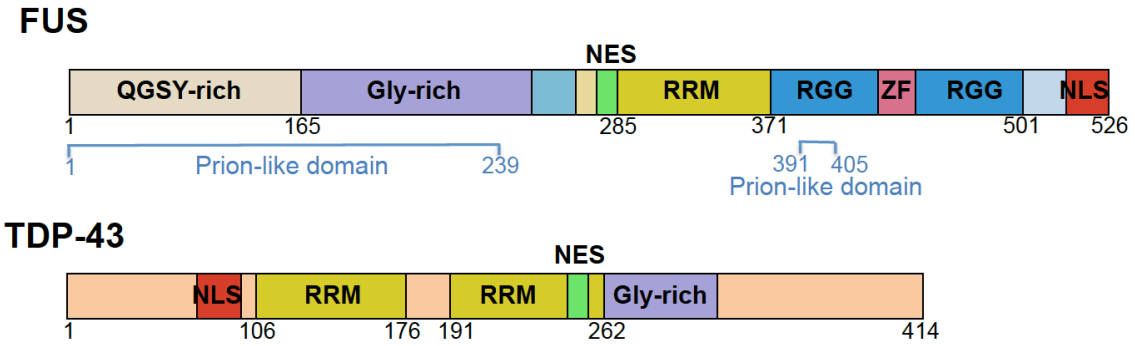

Figure 1.4. Protein domains of the RNA-binding proteins FUS and TDP-43. Proposed prion-like domains of FUS indicated in below in blue (Cushman *et al.*, 2010). Numbers indicate amino acid sequence residue at boundaries. NES, nuclear export sequence; RRM, RNA-recognition motif; ZF, zinc finger; NLS, nuclear localisation signal.

Like *TARDBP*, mutations in the *FUS* gene account for ~4% fALS and ~1% sALS. The vast majority are dominantly inherited, although one rare recessive mutation, G517Q, has been reported (Kwiatkowski *et al.*, 2009). Patients with *FUS* mutations have mainly LMN and bulbar involvement with rapid progression (Al-Chalabi and Hardiman, 2013) and whilst the age of onset for these patients is highly varied, on average, *FUS* mutations lead to an extreme and aggressive, early-onset phenotype. Notably, there have been a number of cases of juvenile-onset ALS caused by *FUS* mutation (Baumer *et al.*, 2010).

In conjunction with TDP-43 and FUS, other RNA processing proteins are increasingly being implicated genetically in ALS pathogenesis. In 2013, mutations in the prion-like domains of hnRNPa1 and hnRNPa2b1 were identified as causative of multisystem proteinopathy and ALS (Kim *et al.*, 2013) and in 2014, mutations in *MATR3*, encoding another RNA-DNA binding protein, matrin-3, were discovered (Johnson *et al.*, 2014). More recently, missense and deleterious mutations were identified in *GLE1*, encoding the global mRNA processing factor, hGle1 (Kaneb *et al.*, 2015), further substantiating the need to understand these RNA processing proteins in ALS.

C9orf72

In addition to the emerging picture of altered RNA metabolism in ALS, perhaps one of the biggest advances for the field of ALS genetics in recent years has been the identification of an intronic hexanucleotide repeat expansion in *C9orf72* that accounts for ~40% of fALS and ~7% sALS (Majounie *et al.*, 2012). Remarkably, whilst SOD1, TDP-43 and FUS mutations predominantly affect motor systems and are only rarely linked to FTLD (Borroni *et al.*, 2009; Huey *et al.*, 2012; Katz *et al.*, 2012), this hexanucleotide repeat has not only been shown to account for a significant proportion of ALS cases, but can also cause FTLD and an ALS-FTLD syndrome (DeJesus-Hernandez *et al.*, 2011; Renton *et al.*, 2011), firmly linking these disorders. This GGGGCC (G_4C_2) repeat sequence is usually present in the population as 2-19 repeats, but the pathogenic expansion range is, on average, 250-1500 repeats, although some small (20-22) repeats are also shown to be associated with a disease phenotype (Gomez-Tortosa *et al.*, 2013) and much larger repeats have been identified (van Blitterswijk *et al.*, 2013a). Interestingly, these G_4C_2 expansions have also been noted in other forms of neurodegenerative disease and surprisingly, repeat lengths of >400 occur at a frequency of 1/600 in the UK population (Beck *et al.*, 2013). With abnormally

expanded RNA being transcribed as a result of this mutation, this discovery again suggests that ALS may be a disease of disrupted RNA processing.

It is therefore of great importance to understand how these genes, with clear roles in RNA processing, may be implicated in ALS, not simply with the aim to understand the mechanisms underlying specific genetic subsets of ALS, but to identify disease pathways that could be common to ALS as a whole.

Additional genetic causes of ALS

Although occurring to a lesser extent, each accounting for no more than 1% of fALS or sALS, mutations within genes encoding proteaostatic proteins have also been associated with ALS. These proteins include valosin-containing protein (VCP) (Johnson *et al.*, 2010), optineurin (OPTN) (Maruyama *et al.*, 2010), ubiquilin 2 (UBQLN2) (Deng *et al.*, 2011) and p62 (Fecto *et al.*, 2011; Teyssou *et al.*, 2013), highlighting a potential inability of cells to appropriately process and/or clear proteins as an additional pathogenic mechanism in ALS. Moreover, a recent study has confirmed that mutations in *TBK1*, in which variants have previously associated with increased risk of ALS (Cirulli *et al.*, 2015), are causative of ALS (Freischmidt *et al.*, 2015). Largely evoking loss of function, these mutations rendered the tank-binding kinase 1 (TANK1) protein unable to bind optineurin, again providing evidence of altered protein clearance pathways in the pathophysiology of ALS.

There are also a number of other genes that have been implicated to some degree in ALS. Mutations in the gene encoding the cytoskeleton regulating protein, profilin 1 (PFN1) have been shown to cause some dominant cases of ALS (Wu *et al.*, 2012) and mutations in the genes encoding alsin (Hadano *et al.*, 2001), spatacsin (Orlacchio *et al.*, 2010), senataxin (Chen *et al.*, 2004) and sigma non-opioid receptor 1 (sigma 1) (Al-Saif *et al.*, 2011) have all been identified in juvenile forms of the disease. Mutations in the genes *ELP3* (Simpson *et al.*, 2009), *FIG4* (Chow *et al.*, 2009), *DCTN1* (Munch *et al.*, 2004), *VAPB* (Nishimura *et al.*, 2004), *NEFH* (Al-Chalabi *et al.*, 1999), *ANG* (Greenway *et al.*, 2006) and *CHCHD10* (Bannwarth *et al.*, 2014) have also been identified in some ALS cases although their contribution to the disease is not well understood. Further, by screening ALS patients with unaffected parents, Chesi *et al.* (2013) uncovered an enrichment of *de novo* mutations in genes encoding chromatin regulating proteins, including crest protein.

1.3.2 Genetic risk of ALS

Supplementary to identifying genes in which mutations are causal of ALS, individual genetic variants may be associated with the disease. Genome-wide association studies (GWAS), where the prevalence of common genetic variants is compared between ALS cases and healthy controls, have been invaluable in their identification of novel loci for further screening. Notably, the *C9ORF72* locus was identified following a large hit on chromosome 9p21 that arose from a GWAS study of 405 ALS patients and 497 controls (Laaksovirta *et al.*, 2010). More recently, a number of exome sequencing studies have identified variants associated with ALS. Indeed, Smith *et al.* (2014) showed that rare variants in the tubulin alpha 4A (*TUBA4A*) gene were significantly enriched in ALS patients compared to controls, suggesting a disease association of this cytoskeletal-regulating protein. Meanwhile, as mentioned above, variants in *TBK1* were identified in a separate exome-wide association study (Cirulli *et al.*, 2015).

As well as the slight phenotypic variations that can be observed as a result of differing genetic causes of the disease, there are distinct differences in the pathology observed post-mortem between genetic subsets, providing further clues about the mechanisms of disease aetiology and progression.

1.4 Pathology of ALS

It is now almost 150 years since physiologist Jean-Martin Charcot first described ALS (Rowland, 2001). He was the first to link the observed spasticity of patients with the pathology seen in the lateral spinal cord and his terminology used in his naming of the disease reflected this, with ‘amyotrophic’ describing the weakening and atrophy of muscles and ‘lateral sclerosis’ reflecting the hardening of the anterior and lateral corticospinal tracts associated with the disease (Goetz, 2000; Wijesekera and Leigh, 2009).

1.4.1 Motor neuron loss

Today, we know that this paralysis arises from the degeneration of upper and lower motor neurons, causing a loss of muscular innervation. The literature surrounding quantification of UMN loss is varied (Gredal *et al.*, 2000; Maekawa *et al.*, 2004). This is likely due to difficulties in classification of cell types, differences in cortical regions investigated and inter-study variation in methodology. However, the findings in brainstem nuclei have been consistent. A significant loss of motor neurons in trigeminal, facial, hypoglossal and ambiguous nuclei, all supplying skeletal muscle, is frequently seen (DePaul *et al.*, 1988). Additionally, there is evidence of differential

susceptibility of motor neurons to degeneration, with oculomotor, abducens and trochlear brainstem motor nuclei unaffected in these patients (Reiner *et al.*, 1995). In spinal cord, an average loss of ~55% of LMNs has been described in the anterior horns, ranging between 8-90% (Ravits *et al.*, 2007). Reflecting a spread of degeneration, in the same study, Ravits *et al.* (2007) identified increased losses (68%) of LMNs in the clinical region of onset compared to those in more remote regions (44%). A loss of myelination and axons in anterior spinal cord, and occurrence of fibrosis of anterior roots are also observed (Hughes, 1982). The onset of early clinical signs in ALS patients, specifically muscle weakness and atrophy, coincides with the initial loss of innervation from the muscle which has been suggested to precede neuronal death in a 'dying back' hypothesis (Fischer *et al.*, 2004). On another note, the hardening observed in the spinal cord by Charcot has since been attributed to an infiltration of the region by glia. This occurs in response to the degeneration of motor neurons and is termed astrogliosis (Rowland and Shneider, 2001).

1.4.2 Pathological inclusions

Although the loss of motor neurons within ALS appears an obvious pathology considering the clinical signs of impaired muscular innervation, another key hallmark of ALS is perhaps more unexpected. A diverse array of pathological, cellular inclusions has been observed in the surviving motor neurons in ALS patients post-mortem (Figure 1.5). Inclusion bodies, commonly foci of aggregated protein, are a typical feature of neurodegenerative diseases (Alves-Rodrigues *et al.*, 1998; Kopito, 2000), yet their role in pathogenesis is not well understood. In early studies, identification and classification of these inclusions in ALS was based on their morphology, location and appearance following histological staining, but more recent advances in immunological techniques have provided increased understanding of their protein composition.

Bunina bodies

Bunina bodies are found within surviving motor neurons of the spinal cord in few fALS and almost all sALS patients (Bunina, 1962; Piao *et al.*, 2003; Okamoto *et al.*, 2008). These small (2-5 μm diameter) eosinophillic structures are localised to the cytoplasm and dendrites and although their composition is not well characterised, it has been revealed that they consist of electron dense material (Okamoto *et al.*, 1993) and are frequently positive for cystatin C and transferrin (Okamoto *et al.*, 1993; Mizuno *et al.*, 2006).

Axonal spheroids

Axonal spheroids are distinct swellings of axons containing cytoskeletal components and organelles, and are common to the majority of diseases where neurons of the central nervous system are damaged (Coleman, 2005). In ALS they occur within both UMNs and LMNs and are often positive for neurofilament, ubiquitin, synaptophysin and peripherin (Corbo and Hays, 1992; Troost *et al.*, 1992; Schiffer *et al.*, 1995).

Hyaline conglomerate inclusions

Hyaline conglomerate inclusions (HCIs) are found predominantly within neurons of the motor cortex and, to a lesser degree, in spinal cord motor neurons in ALS patients post-mortem and comprise accumulations of cytoskeletal intermediate filament proteins, namely peripherin and hyperphosphorylated neurofilament subunits. These inclusions are largely identified within fALS caused by *SOD1* mutation (Hays *et al.*, 2006) although identification of SOD1-immunoreactivity in these HCIs is varied (Shaw *et al.*, 1997; Shibata *et al.*, 1996).

Ubiquitinated inclusions

With improved immunological techniques came the identification of cytoplasmic and intranuclear, non-amyloid, ubiquitin-positive inclusions (UBIs) in surviving motor neurons and glia (Leigh *et al.*, 1991). These inclusions are morphologically diverse and are often reported in the literature as being skein-like, round or Lewy body-like, tangled or even rod-like. These are the most widespread type of inclusion amongst ALS patients, seen in the surviving motor neurons or glia of ~100% of sALS cases (Piao *et al.*, 2003). As such, UBIs have become a major pathological hallmark of the disease and a key topic of investigation for understanding the underlying pathophysiological mechanisms.

In fALS patients with *SOD1* mutation, ubiquitinated inclusions are shown to be positive for SOD1 protein (Shibata *et al.*, 1994; Jonsson *et al.*, 2004). These inclusions are found in the cytoplasm of motor neurons and glia of the anterior spinal cord (Kato *et al.*, 1996; Bruijn *et al.*, 1997). Electron microscopy has revealed these SOD1-positive structures to be composed of granule-coated fibrils (15-25 nm diameter) and to be commonly associated with accumulations of neurofilaments (Kokubo *et al.*, 1999). SOD1 is also present in UBIs in some sporadic cases, highlighting a role for WT SOD1 in ALS (Forsberg *et al.*, 2010). However, in the majority of ALS patients without *SOD1*

mutation, UBIs are negative for SOD1 protein (Mackenzie *et al.*, 2007), potentially exposing ALS-SOD1 as mechanistically distinct from other ALS subtypes.

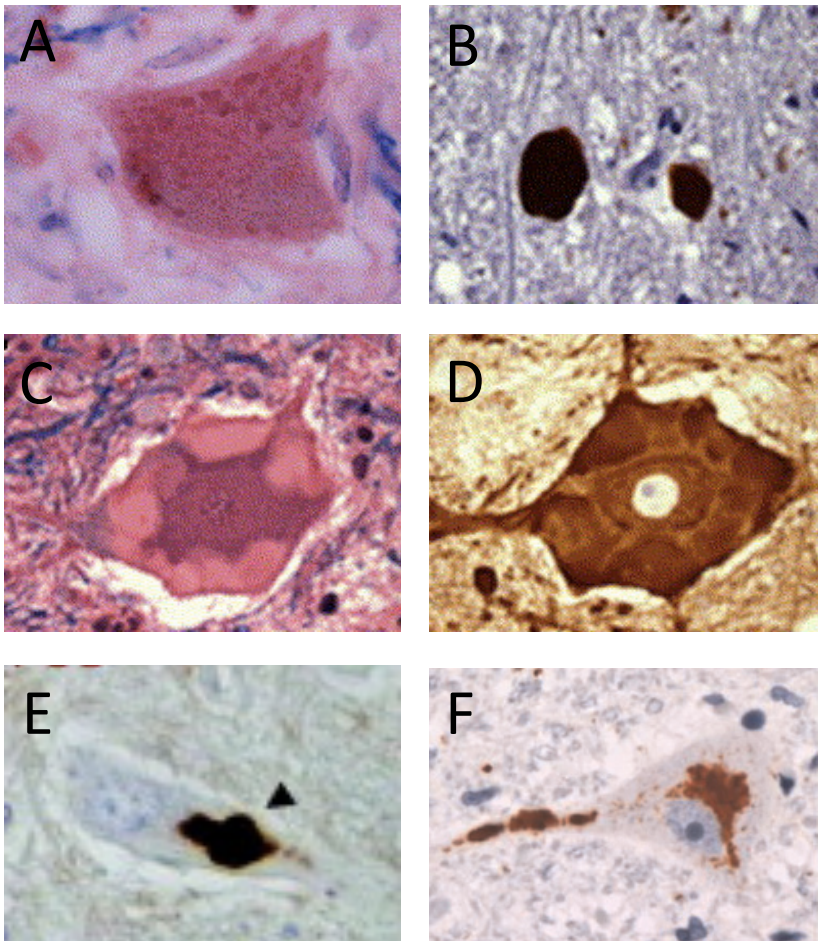

Figure 1.5. Proteinopathy in ALS. Examples from the literature of the diverse array of abnormal protein structures that are seen in the surviving motor neurons of ALS patients. (A) Bunina bodies visualised with haemotoxylin, luxol fast blue and eosin staining. (B) Axonal spheroids highlighted by peripherin immunohistochemistry. (C) Haemotoxylin, luxol fast blue and eosin staining of hyaline conglomerate inclusions (HCIs). (D) HGI as labelled by neurofilament immunohistochemistry. (A-D) from Xiao *et al.* (2006). (E) FUS-positive UBI (arrow) (Dormann and Haass, 2011). (F) SOD1-positive UBIs (Pokrishevsky *et al.*, 2012).

In 2006, prior to the discovery of its genetic link with ALS, the normally nuclear protein, TDP-43, was found to be a major component of SOD1-negative UBIs, present in ~90% ALS patients (Arai *et al.*, 2006; Neumann *et al.*, 2006; Mackenzie *et al.*, 2007). Aside from a single case study, TDP-43-positive UBIs are not seen in cases with *SOD1* mutation (Okamoto *et al.*, 2011; Mackenzie *et al.*, 2007). Mutations in *TARDBP* are, however, much less prevalent than the occurrence of TDP-43-positive UBIs in both

sALS and fALS, highlighting endogenous full-length TDP-43 in the pathophysiology of ALS (Lagier-Tourenne *et al.*, 2010; Sreedharan *et al.*, 2008). As well as their presence in surviving motor neurons, TDP-43-positive UBIs have been noted, albeit to a lesser extent, in the hippocampus and frontal and temporal lobes of ALS patients (Neumann *et al.*, 2006). Upon biochemical analysis, TDP-43 in the disease state has been shown to be hyperphosphorylated and produce 25 kDa and 35 kDa fragments, since determined to be caused by cleavage of full length TDP-43 by caspases (Zhang *et al.*, 2007; Zhang *et al.*, 2009). Together with this, TDP-43 positive UBIs in the brain and spinal cord are differentially enriched for C-terminal fragments; inclusions in the cortex display increased reactivity to C-terminal antibodies whereas those in the spinal cord show equal labelling with N- and C-terminus antibodies (Igaz *et al.*, 2008).

UBIs in ALS which are negative for TDP-43 and SOD1 instead comprise FUS, also genetically implicated in ALS (Fig. 1.5) (Kwiatkowski *et al.*, 2009; Vance *et al.*, 2009). These inclusions occur in both fALS, as a result of mutations in the *FUS* gene, and in sALS and non-SOD1 fALS that lack *FUS* mutation (Hewitt *et al.*, 2010; Deng *et al.*, 2010). FUS-positive inclusions and TDP-43-positive inclusions are, for the most part, distinct, although some rare cases of inclusions positive for both proteins have been identified (Deng *et al.*, 2010). Additionally, FUS-positive inclusions that lack ubiquitin staining are often present (Vance *et al.*, 2009). FUS-positive inclusions have not been noted in ALS-SOD1, again highlighting mechanistic differences in the pathophysiology of ALS subtypes (Deng *et al.*, 2010). Unlike ALS with TDP-43-positive inclusions, where most patients are diagnosed with late-onset sALS, most ALS patients with FUS-positive inclusions suffer with earlier onset or juvenile ALS (Huang *et al.*, 2010; Baumer *et al.*, 2010).

Interestingly, TDP-43- and FUS-positive inclusions are not limited to ALS. As well as the clinical and genetic overlap of ALS with FTLD, there is an established pathological overlap, with the presence of these inclusions in subtypes of FTLD. The inclusions seen in around half of FTLD patients comprise hyperphosphorylated tau protein (FTLD-tau), yet in remaining cases, TDP-43- (FTLD-TDP43) or FUS-positive (FTLD-FUS) UBIs are observed (Urwin *et al.*, 2010; Neumann *et al.*, 2006; Arai *et al.*, 2006). In FTLD, inclusions are found within the frontal and temporal cortices and are not restricted to motor neurons or glia as with ALS (Neumann *et al.*, 2006). The composition of these UBIs also differs between the two disease classifications, with reactivity to other TET/FET family proteins, TATA-box binding protein associated factor 15 (TAF15) and Ewing's Sarcoma (EWS), being indicative of FTLD-FUS over ALS-FUS

(Neumann *et al.*, 2011). FTLD-FUS UBIs also label with transportin, yet this is rare in ALS-FUS (Neumann *et al.*, 2006). In addition to ALS and FTLD, UBIs comprised of these RNA-binding proteins are found within other neurological disorders. TDP-43-positive UBIs have been observed in Alzheimer's disease (Amador-Ortiz *et al.*, 2007) and FUS-positive inclusions have also been noted in basophilic inclusion body disease (Munoz *et al.*, 2009), neuronal intermediate filament disease (Neumann *et al.*, 2009), Huntington's disease (Doi *et al.*, 2008) and spinocerebellar ataxia (Doi *et al.*, 2010).

Dipeptides in ALS-C9orf72

Whilst TDP-43-positive inclusions are a major pathology in patients with *C9orf72* repeat expansion (Figure 1.6), short dipeptides produced from the G_4C_2 repeat, thought to be translated through a repeat-associated non-ATG initiated mechanism (RAN translation), have also been seen in aggregated forms (Mori *et al.*, 2013).

The presence of pathological inclusions of aggregated protein, both mutant and full length 'wild type' (WT), in ALS (Figure 1.6) and other neurological disorders raises many questions about the relationship of these proteins to the pathogenesis of disease. It will be important to understand how these pathological structures may be formed and the contribution that these proteins have to the disease process with the hope of revealing novel therapeutic targets.

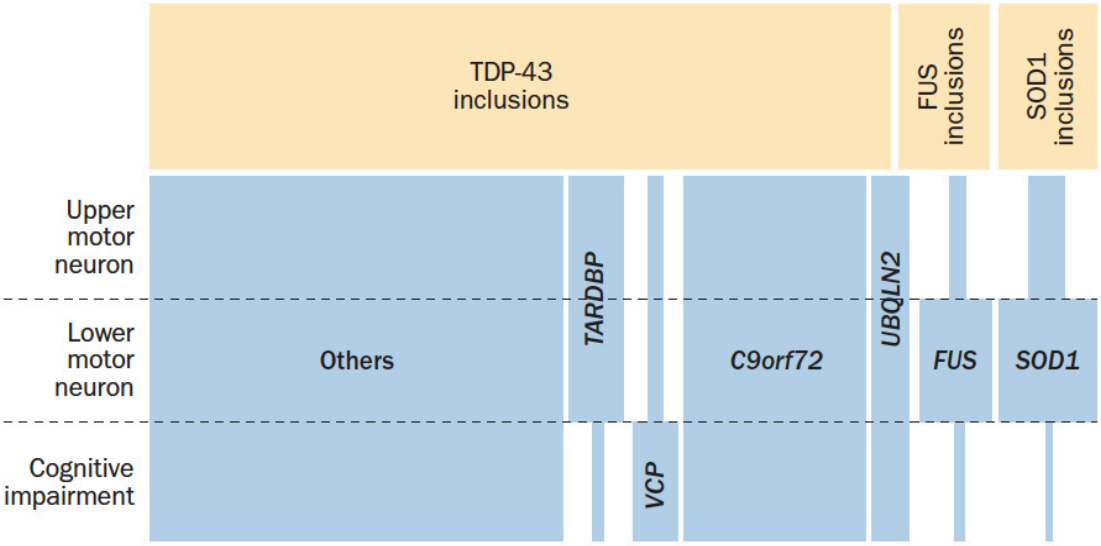

Figure 1.6. The type of pathological inclusions and phenotype seen in ALS patients varies with their genetic background. Pathological compartments (cream) are sized based on their frequency in the ALS population. Underlying genetics of each of these pathologies are shown below (blue) and are also sized based on their frequency in each phenotypic instance. Abbreviations: TDP-43/*TARDBP*, TAR DNA binding protein; FUS, Fused in sarcoma; SOD1, superoxide dismutase 1; *VCP*, valosin-containing protein; *UBQLN2*, ubiquilin 2. Image taken from Al-Chalabi and Hardiman (2013).

1.6 Mechanisms of disease

It is clear that ALS is as a highly complex and multifactorial disease. The proteins implicated in ALS display functionally diverse cellular roles and sometimes a seemingly non-integrative involvement in disease pathogenesis, highlighted by a predominant lack of co-occurrence of these proteins in pathological inclusions. The discovery of each ALS-linked protein has brought with it new understanding of potential disease mechanisms and, to date, some of these have included abnormal protein homeostasis, altered RNA metabolism, mitochondrial dysfunction, axonal transport defects, oxidative stress and immune activation, although the extent to which these mechanisms overlap remains largely unknown (Ling *et al.*, 2013; Ferraiuolo *et al.*, 2011). Whilst this thesis focused on the role of FUS protein in the pathogenesis of ALS, potential mechanisms of the disease implicated through other major genetic contributors will be briefly outlined to place this work into context for interested readers.

1.6.1 SOD1

As discussed previously, SOD1 is an abundant and ubiquitously expressed protein with a role in catalysing the conversion of toxic superoxides into water or hydrogen peroxide (McCord and Fridovich, 1969), although on a side note, more recently, an additional function for SOD1 in signaling the repression of cellular respiration has been proposed (Reddi and Culotta, 2013). Soon after its genetic link with ALS was established in 1993, gain of toxic SOD1 function quickly became the focus of research, largely driven by findings in animal models (Turner and Talbot, 2008). Notably, mice overexpressing a human ALS-associated form of SOD1 (G93A), having little to no effect on its enzymatic activity, produced an ALS-like phenotype including reduced survival, paralysis and spinal cord motor neuron loss (Gurney *et al.*, 1994). Further, mice expressing mutant mouse SOD1 at high levels also demonstrated a decline in motor function combined with motor neuron degeneration (Ripps *et al.*, 1995). Conversely, mice lacking SOD1 displayed normal phenotypes and vulnerability to motor neuron loss was only observed following axonal trauma (Reaume *et al.*, 1996). Cementing this, Bruijn *et al.* (1998) showed that mice expressing an ALS-associated mutant form of SOD1 were affected by the disease process equally, independent of whether they were on a high or low endogenous mouse SOD1 background. Although loss of SOD1 has been, for the most part, ruled out as a major pathological mechanism in ALS-SOD1, there is some support for loss of SOD1 function as a potential disease modifier (Saccon *et al.*, 2013).

The misfolding of mutant SOD1 isoforms in ALS is well established (Robberecht and Philips, 2013). Misfolded SOD1 isoforms evade normal degradation pathways and instead oligomerise and coalesce into larger aggregates, which can be seen in both ALS-SOD1 patients and several SOD1 animal models (Watanabe *et al.*, 2001). Interestingly, WT SOD1 may also misfold and become involved in the disease process (for review see Rotunno and Bosco (2013)).

However, it remains unclear as to how these aggregated SOD1 forms are involved in the progression of disease. Mutant SOD1 isoforms do not appear to lose enzymatic function (Cleveland, 1999), indeed enzyme function was shown not to correlate with age of onset or progression of ALS (Cudkowicz *et al.*, 1997), again suggesting that loss of normal function is not causative. Instead, several pathological mechanisms have been implicated through investigation of mutant SOD1. The ubiquitin proteasome system is thought to be overwhelmed by SOD1 isoforms (Robberecht and Philips, 2013) and endoplasmic reticulum stress caused by processing masses of misfolded protein may lead to the activation of cell death pathways (Nishitoh *et al.*, 2008; Lindholm *et al.*, 2006). Mutant SOD1 also aggregates within mitochondria (Jaarsma *et al.*, 2001; Pasinelli *et al.*, 2004), which can result in mitochondrial damage (Higgins *et al.*, 2003), again implicating a pathogenic role for oxidative stress within ALS (Barber and Shaw, 2010). Furthermore, there is evidence to suggest that because of mutant SOD1 in the mitochondria, motor neurons are more sensitive to glutamatergic excitotoxicity, which has itself been implicated in ALS (Van Den Bosch *et al.*, 2006). Axonal transport deficits have been identified in animal models of ALS-SOD1 and, in particular, mitochondrial transport is reduced in the anterograde direction (De Vos *et al.*, 2007). Neurofilament balance is also dysregulated in ALS-SOD1, uncovered by studies on patient-derived induced pluripotent stem cells (iPSCs), patient spinal cord motor neurons and stable motor neuron-like cell lines (Chen *et al.*, 2014; Menzies *et al.*, 2002).

1.6.2 TDP-43

In converging studies, several groups have shown that knocking out the RNA-binding protein, TDP-43, is embryonically lethal in mice (Wu *et al.*, 2010; Sephton *et al.*, 2010; Kraemer *et al.*, 2010). Similarly, inducible TDP-43 knockouts succumb to postnatal death (Chiang *et al.*, 2010), reinforcing the essential role of TDP-43 and suggesting that loss of TDP-43 may be pathogenic in ALS. Several TDP-43 mouse models have also been produced that express either WT or mutant TDP-43 at different levels, locations and time points, providing a wealth of information on a potential gain of toxic

function hypothesis (Wegorzewska and Baloh, 2011). In the majority of instances, overexpression of WT (Wils *et al.*, 2010; Xu *et al.*, 2010) or mutant TDP-43 (Stallings *et al.*, 2010; Wegorzewska *et al.*, 2009) at high levels within the nervous system of mice during development is overtly toxic, producing pathological aggregates, axonal degeneration and early lethality. Taken together, these findings suggest that both loss of normal TDP-43 function (for detailed review see Vanden Broeck *et al.* (2014)) and gain of toxic TDP-43 function may be involved in the development and progression of ALS. Although TDP-43 expression in mice produces toxicity, the majority of these studies (Wegorzewska and Baloh, 2011) failed to recapitulate the extensive TDP-43 pathology, namely, the large TDP-43-positive aggregates in the cytoplasm that are a key feature of many subtypes of ALS (Arai *et al.*, 2006; Neumann *et al.*, 2006).

Redistribution of TDP-43 to the cytoplasm was shown to be an early event in sporadic ALS pathogenesis (Giordana et al., 2010) and cytoplasmic mislocalisation of TDP-43 is required to confer neuronal toxicity (Barmada et al., 2010). Curiously, whilst TDP-43 distribution to the cytoplasm is a key event, *TARDBP* mutations are not seen to lie within the NLS (Dormann and Haass, 2011), and given the low frequency of *TARDBP* mutations in relation to the high fraction of ALS patients with TDP-43 pathology, some of which with other gene mutations (Gitcho *et al.*, 2009; Cooper-Knock *et al.*, 2012), redistribution of WT TDP-43 must be a crucial feature. TDP-43 shuttles back and forth between the nucleus and cytoplasm (Ayala *et al.*, 2008), yet is normally found predominantly in the nucleus. However, several origins of cellular stress, including oxidative and heat stress (Colombrita *et al.*, 2009), ER stress (Walker *et al.*, 2013) and osmotic stress (Dewey *et al.*, 2011), are, amongst other mechanisms (Liu *et al.*, 2015), known to cause its mislocalisation to the cytoplasm and may be important in early stages in the progression of ALS.

Following mislocalisation to the cytoplasm, TDP-43, driven by these cellular stresses, is recruited to stress granules (SGs) in cell culture experiments (Colombrita et al., 2009). SGs are dynamically assembled in response to a variety of cellular stresses and comprise densely packed mRNA and proteins, functioning to stall non-essential translation and instead focus energy on cellular survival (Figure 1.7) (Anderson and Kedersha, 2008). Interestingly, like TDP-43, many of the essential proteins required to form SGs comprise RNA binding proteins with prion-like domains (Li et al., 2013). PABP1, Ras GTPase-activating protein-binding protein 1 (G3BP1), T cell intracellular antigen 1 (TIA-1) and TIA-1 related protein (TIAR), along with others, are all found in SGs and have become markers of these structures (Anderson and Kedersha, 2006).

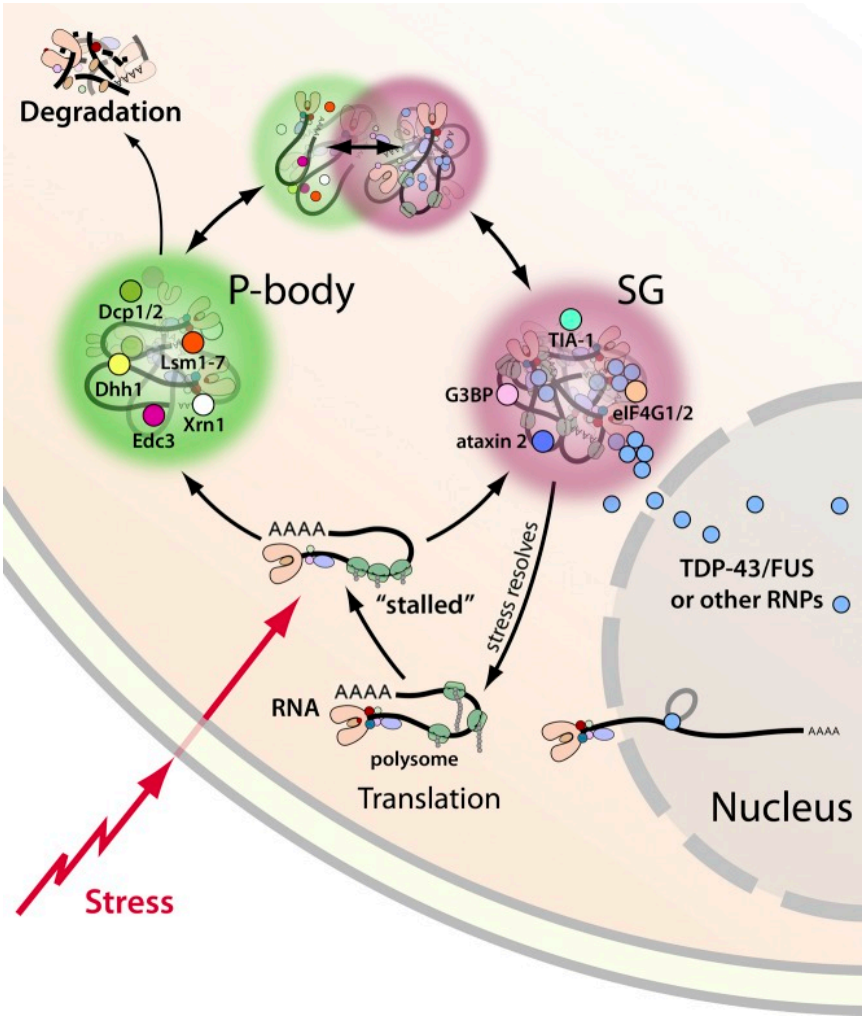

Figure 1.7. Stress granule formation and dynamics. During exposure to cellular stresses, translation of many mRNAs becomes stalled and these stalled pre-initiation complexes are directed to P bodies or stress granules (SGs). SGs, composed of several 'marker' proteins including G3BP, TIA-1, ataxin 2 and eiF-4G1/2, are highly dynamic and release pre-initiation complexes following the resolution of stress. TDP-43 and FUS may also be recruited to SGs during stress. P bodies instead have a role in targeting mRNAs for degradation. Image taken from (Li *et al.*, 2013).

However, it remains debatable as to whether SGs act as precursors to seed aggregation of TDP-43 into larger pathological inclusions in a toxic gain of SG function, or whether pathological aggregation of TDP-43 disrupts normal and protective SG function (Dewey *et al.*, 2012; Li *et al.*, 2013). Intriguingly, TDP-43-positive inclusions have also been shown to colocalise with SG markers in post-mortem ALS patient tissues (Liu-Yesucevitz *et al.*, 2010), although others did not find this to be the case (Colombrita *et al.*, 2009). Although it is not clear how aggregated TDP-43 is formed, both the ubiquitin-proteasome and autophagy systems play a role in degradation of aggregated TDP-43, with failure of these mechanisms acting to promote aggregation (Brady *et al.*, 2011; Thomas *et al.*, 2013). Furthermore, ALS-linked mutations increase

the aggregation propensity of the already aggregate-prone protein, again supporting a gain of toxic aggregate function (Johnson *et al.*, 2009).

Aside from its interactions with SGs, TDP-43 is a normal component of neuronal RNA transport granules and it has been recently demonstrated that ALS-associated TDP-43 mutants disrupt the normal mobility of these granules and may cause neuronal dysfunction, providing a mechanism through which loss of TDP-43 function may occur in the cytoplasm (Alami *et al.*, 2014; Liu-Yesucevitz *et al.*, 2014). Whilst disruptions to its normal roles in RNA metabolism in ALS have been well documented (Vanden Broeck *et al.*, 2014), Arnold *et al.* (2013) also indicate that mutant TDP-43 can gain additional function within the nucleus leading to aberrant RNA processing, which may also contribute to ALS pathophysiology. Furthermore, TDP-43 is known to regulate its own mRNA levels through an autoregulation loop (Ayala *et al.*, 2011), providing additional complication to hypotheses of loss versus gain of TDP-43 function in ALS, and indeed it is likely that an interplay of both are damaging.

1.6.3 C9orf72

Whilst C9orf72 protein remains largely uncharacterised, it has been identified through computational analysis as distant homolog of the 'differentially expressed in normal and neoplastic cells' (DENN) protein family, that have roles in membrane trafficking (Levine *et al.*, 2013; Zhang *et al.*, 2012). This is supported by the largely cytoplasmic localisation of C9orf72 protein in neurons (DeJesus-Hernandez *et al.*, 2011) and a recent study providing a direct role of the protein in endolysosomal trafficking (Farg *et al.*, 2014). Reduced levels of *C9orf72* mRNA transcript have been reported in studies on lymphoblastoid cell lines and post-mortem brain tissue from ALS-C9orf72 patients compared to healthy controls (DeJesus-Hernandez *et al.*, 2011; Gijselinck *et al.*, 2012). One mechanism proposed for this has been aberrant histone trimethylation leading to silencing of *C9orf72* (Belzil *et al.*, 2013). In addition to reductions in overall C9orf72 transcript level, expression of C9orf72 protein has been shown to be reduced in the frontal cortex of patients with the pathological repeat expansion (Waite *et al.*, 2014), which, taken together, suggests haploinsufficiency of *C9orf72* as a possible disease mechanism. Additional support for a haploinsufficiency model of C9orf72 has arisen through zebrafish and *C. elegans* models that display motor deficits following C9orf72 knockdown (Therrien *et al.*, 2013; Ciura *et al.*, 2013).

Conversely, however, knockdown of C9orf72 in mice using viral-mediated anti-sense oligonucleotides (ASOs) failed to produce any observable motor phenotype (Lagier-

Tourenne *et al.*, 2013). Additionally, other studies have provided evidence that C9orf72 mRNA expression level is not always altered between health and disease states (Cooper-Knock *et al.*, 2013; Renton *et al.*, 2011), and two more prominent features of C9orf72 pathology in ALS have instead dominated the field, namely the presence of abnormal RNA foci and dipeptide aggregates. Transcription in the sense and antisense direction of the G_4C_2 expansion produces long RNA transcripts that go on to form nuclear RNA foci in spinal cord and cortical tissue (DeJesus-Hernandez *et al.*, 2011; Zu *et al.*, 2013). As previously mentioned, RAN translation of these transcripts produces dipeptides, of which there are five possible isoforms, Pro-Arg, Pro-Ala, Gly-Ala, Gly-Arg and Gly-Pro (Mori *et al.*, 2013; Zu *et al.*, 2013). However, the toxicity associated with these pathological features of ALS-C9orf72 is still unclear. RNA foci have been shown to sequester several RNA-binding proteins, likely disrupting RNA metabolism, and cellular toxicity has been observed in cells transfected with longer repeat RNA lengths (Cooper-Knock *et al.*, 2014; Lee *et al.*, 2013). Interestingly, a mouse model expressing an 'RNA-only' form of repeat expansion showed ubiquitin-positive inclusions yet did not display any observable abnormal phenotype or cell loss (Hukema et al., 2014).

Several lines of evidence suggest a toxic role for dipeptides. Cellular production of dipeptide sequences, in the absence of the G_4C_2 RNA repeat expansions, have resulted in apoptosis in primary neurons with Gly-Ala forms (May *et al.*, 2014) and neurodegeneration in *Drosophila* models expressing arginine-rich dipeptides (Mizielinska *et al.*, 2014). In particular, Gly-Arg and Pro-Arg forms have been shown to bind and clog the nucleoli leading to nucleolar stress and cell death (Kwon *et al.*, 2014; Tao *et al.*, 2015). Additionally, expression of Gly-Ala dipeptides has been linked with increased ER stress and impaired neurite outgrowth (Zhang *et al.*, 2014). As such, it appears dipeptides are coming to the forefront of investigations into ALS-C9orf72.

1.7 ***Fused in sarcoma***

As discussed, protein aggregation and altered RNA metabolism are recurring themes in ALS, implicated across several genetic subsets. Like TDP-43, the RNA-binding protein, FUS, is linked to ALS both genetically and pathologically and has several roles in RNA metabolism. Therefore, it will be of great importance to determine the mechanisms by which FUS may be involved pathophysiologically in ALS. To begin, it is important to first understand the normal cellular roles of FUS in order to appreciate how these processes may become disrupted.

1.7.1 Normal functions of FUS

FUS is a 526 amino acid member of the FET (FUS, EWS, TAF15) family of RNA binding proteins (Crozat *et al.*, 1993) which share a high degree of homology (Hoell *et al.*, 2011). FUS has a ubiquitous expression and is predominantly localised to the nucleus (Aoki *et al.*, 2012). Its primary sequence consists of a low complexity N-terminus with domains rich in glutamine, glycine, serine and tyrosine (QGSY-rich domain) and glycine (gly-rich domain) followed by an RNA recognition motif (RRM) and a C-terminus comprising glycine-arginine-rich (RGG-rich) domains, a zinc finger (ZF) and an extreme C-terminal NLS (Figure 1.4). Significantly, this non-classical, hydrophobic proline-tyrosine NLS of FUS has previously been demonstrated as a substrate for transportin, facilitating its entry into the nucleus (Lee *et al.*, 2006).

Transcription and splicing

FUS is known to bind both single- and double- stranded DNA (Baechtold *et al.*, 1999). Recently, specific single-stranded DNA sequences in the promoter regions of a number of FUS-interacting candidate genes have been identified, which may now be thought of as putative FUS response elements. FUS affinity sequences identified included TCCCCGT, AAAGTGTC and AGGTTCTA (Tan *et al.*, 2012). Additionally, altering the levels of FUS, either by overexpression or siRNA-mediated knockdown, altered the levels of mRNA expression of these FUS transcription targets (Tan *et al.*, 2012). Although not evidenced, it is likely that the interaction of FUS with DNA is either through its ZF, a conserved region known to bind DNA, or possibly its RNA binding domains (Tan and Manley, 2009).

In addition to directly binding DNA, FUS has been shown to interact with transcription regulating proteins (Wang *et al.*, 2008) including RNA polymerases and transcription factor IID (TFIID) (Bertolotti *et al.*, 1996). TFIID is a large protein complex that upon its interaction with transcription initiation sites begins a cascade of protein recruitment to form pre-initiation complexes (PICs) (Bieniossek *et al.*, 2013). PICs then align RNA polymerase II (RNAP2) at the start site, allowing for initiation of transcription. Schwartz *et al.* (2012) have provided a scale for the interaction of FUS with RNAP2. They determined that FUS bound the C-terminal domain of RNAP2 at the site of transcription in >50% genes expressed in HEK-293 cells. This large-scale interaction of FUS with RNAP2 suggests a prominent role for FUS in transcriptional regulation. Schwartz *et al.* (2012) also demonstrated that FUS was critical for regulating the phosphorylation state of RNAP2, a feature that is linked to the progression of RNAP2 during transcription. Another mechanism by which FUS is suggested to regulate transcription comprises its

binding to the promoter antisense RNA strand, resulting in a downregulation of transcription of the coding strand (Ishigaki *et al.*, 2012). As such, disruption to this transcriptional regulation by FUS, through mutation or otherwise, could have widespread effects on cellular function. More recently, this has been demonstrated by Yang *et al.* (2014), showing that ALS-associated mutants disrupted FUS-chromatin binding and transcriptional activation by FUS. In addition, FUS has been shown to repress transcription by RNA polymerase III (RNAP3), which is responsible for the synthesis of ribosomal and small RNAs (Tan and Manley, 2010).

Transcription is not a stand-alone event but rather it is coupled to splicing (Kameoka *et al.*, 2004; Das *et al.*, 2007). Splicing is the process by which introns are removed from pre-mRNA to produce mature mRNA sequences. Further, alternative splicing provides increased sequence variation than that allowed by DNA alone. Splicing is carried out by the spliceosome, nuclear machinery comprised of protein-RNA complexes, termed small nuclear ribonucleic particles (snRNPs), and other proteins that assemble in a stepwise order on the pre-mRNA to facilitate intron removal (Will and Luhrmann, 2011). In addition to a likely role as a transcription factor, FUS has been shown to interact with a number of spliceosomal components, namely SC35, SRp75, hnRNP I and SRm160 (Meissner *et al.*, 2003) and was identified itself as a component of the spliceosome in an independent proteomic screen (Zhou *et al.*, 2002). On top of this, FUS has been shown to bind thousands of pre-mRNAs, in addition to its DNA-binding capabilities (Lagier-Tourenne *et al.*, 2012; Rogelj *et al.*, 2012), although the presence of a given consensus binding sequence is contested. Lerga *et al.* (2001) highlighted *in vitro* that FUS can bind to GGUG-containing sequences. However, in an analysis of FUS-RNA binding in mouse and human tissues, Lagier-Tourenne *et al.* (2012) instead showed the occurrence of a GUGGU sequence in ~60% RNA bound to FUS, although later found this sequence not to be necessary or sufficient for binding. Additionally, Ishigaki *et al.* (2012) and others (Zhou *et al.*, 2013) were unable to determine a consensus binding sequence in their studies, but instead suggested that secondary structure of RNA was involved.

Specifically, the *MAPT* transcript, encoding tau, has been identified as a direct target of FUS mediated splicing, with exons 3 and 10 unusually remaining included following knockdown of FUS in hippocampal neurons (Orozco *et al.*, 2012). Recently, a number of independent CLIP-seq experiments, where intracellular cross-linking of RNA and RNA-binding proteins is followed by immunoprecipitation and subsequent high-

throughput sequencing, have been performed to determine the RNA targets of FUS on a large scale (Nakaya *et al.*, 2013; Rogelj *et al.*, 2012; Lagier-Tourenne *et al.*, 2012; Zhou *et al.*, 2013; Ishigaki *et al.*, 2012). These studies have highlighted that FUS binds thousands of RNAs, preferentially to long intronic regions, further supporting its role in splicing. Indeed, loss of FUS was shown to induce splicing alterations in over 370 RNAs in embryonic mouse brain (Lagier-Tourenne *et al.*, 2012), with others also reporting alterations following knockdown of FUS, albeit using a variety of approaches (Ishigaki *et al.*, 2012; Nakaya *et al.*, 2013; Rogelj *et al.*, 2012). Interestingly, Zhou *et al.* (2013) observed that FUS is able to repress splicing of its own pre-mRNA, producing a transcript that is targeted for decay. This autoregulatory mechanism was found to be disrupted by ALS-linked mutation and has been further demonstrated in *Drosophila melanogaster* models (Machamer *et al.*, 2014). When compiled, these CLIP-seq experiments revealed that the RNA targets of FUS converge largely on pathways of neurogenesis and gene expression regulation, with genes relating to DNA damage response also enriched (for further detail see Zhou *et al.* (2014)).

The product of transcription, splicing and RNA processing events is the transcriptome, the collection of mRNAs present in a given cell or population of cells (Frith *et al.*, 2005). The FUS-regulated transcriptome is not universal and instead varies between cell types and brain regions, potentially providing an explanation for specific cell vulnerability in ALS (Fujioka *et al.*, 2013). Additionally, vast changes in the transcriptome have been identified following alterations in FUS expression levels, supporting its fundamental role in RNA metabolism. By functionally grouping differentially expressed mRNAs, van Blitterswijk *et al.* (2013b) observed altered regulation of ribosomal genes with overexpression of WT FUS, but a knockdown of FUS was instead shown to affect the expression of genes related to the spliceosome. Moreover, van Blitterswijk *et al.* (2013b) showed that the transcriptome of HEK-293 cells overexpressing ALS-linked mutant FUS (R521G or R522G) more closely resembles that of WT FUS overexpression than that produced when FUS was silenced, although the extent to which these seemingly small differences could be pathological is unknown.

FUS has also been shown to interact with the Drosha complex, involved in microRNA biogenesis (Gregory *et al.*, 2004). Specifically, Drosha acts to crop primary microRNAs to form pre-microRNAs for further processing outside of the nucleus yet the role for FUS in this process is not clear. FUS has, however, been shown to stimulate the biogenesis of a subset of microRNAs involved in neuronal function, differentiation and

synaptogenesis which may be of particular importance given the neurodegenerative nature of ALS (Morlando *et al.*, 2012). Although the scope of microRNA function still remains largely elusive, taken together with an involvement in transcription and splicing, it is obvious that FUS can have a global impact on the function of the cell.

DNA repair and genome stability

FUS knockout mice produced by disruption of exon 8 do not show survival deficits on a partially outbred background, yet these mice are ~30% smaller than WT littermates and males show complete sterility (Kuroda *et al.*, 2000). Additionally, embryonic fibroblasts from these mice, display enhanced radiation sensitivity and reduced ability of homologous pairing in extracts from the testes as a result of loss of FUS, pertaining to a role of the protein in repair following DNA damage. This sensitivity to ionising radiation was also seen at the level of the whole animal, with decreased survival following the challenge in FUS KO mice compared to WT. In a separate FUS knockout mouse model, instead produced by disruption of exon 12, mice displayed chromosomal instability and died within 16 hours of birth, indicating FUS is important for neonatal viability (Hicks *et al.*, 2000). DNA damage, specifically single- and double-strand breaks, as induced by ionising radiation, may be repaired by homologous recombination events. Given its ability to bind single and double stranded DNA, recently, FUS has been shown to be recruited to sites of DNA damage via its RGG2 domain in transfected human osteosarcoma cells (U2OS) and human embryonic kidney cells (HEK-293) (Mastrocola *et al.*, 2013). Further, it was shown that this was dependent on poly(ADP-ribose) polymerase (PARP) ADP-ribosylation, providing a supportive framework to permit the localisation of FUS and other DNA repairing proteins to these damage sites (Mastrocola *et al.*, 2013). Supporting findings from FUS KO mice, FUS was required for appropriate repair of double-strand breaks by homologous recombination, but also by non-homologous end-joining, although the mechanisms by which FUS acts in the repair of DNA are unknown (Mastrocola *et al.*, 2013). FUS may also act indirectly to modulate DNA repair via transcriptional regulation mechanisms (Wang *et al.*, 2008) and through its aforementioned role in alternate splicing of mRNAs involved in DNA damage response (Zhou *et al.*, 2014). Intriguingly, Deng *et al.* (2014) have shown that FUS is translocated to the cytoplasm following DNA damage, providing a plausible upstream mechanism by which full-length endogenous FUS may be mislocalised to the cytoplasm in ALS and other FUS-related diseases.

Subnuclear localisation of FUS

Although the nucleus of a cell does not contain membrane-bound organelles, like the cytoplasm it is emerging as a highly organised structure, with distinct subnuclear compartments acting as designated foci for transcription, RNA processing, and the biogenesis, assembly and storage of spliceosomal components. Whilst lacking defining membrane boundaries, these compartments have specific morphology, characteristic protein compositions, and are thought to be functionally specialised (for review see Sleeman and Trinkle-Mulcahy (2014) and Dundr and Misteli (2001)).

Although FUS is known to be a predominantly nuclear protein, its location within the nucleus is more ambiguous. First, FUS has been reported to be associated with survival of motor neuron (SMN) protein complexes using biochemistry (Yamazaki *et al.*, 2012; Sun *et al.*, 2015; Groen *et al.*, 2013). In the nucleus, SMN protein is localised to subnuclear bodies known as Gemini of Cajal Bodies or 'gems' (Liu and Dreyfuss, 1996). SMN protein, in addition with other members of the SMN complex, gemin proteins 2-7, has been linked to biogenesis of small nuclear ribonucleic proteins (snRNPs), critical components of the spliceosome (Fischer *et al.*, 1997; Liu *et al.*, 1997). Interestingly, mutations in the gene encoding SMN, *SMN1*, are causative of spinal muscular atrophy (SMA), a degenerative disease of lower motor neurons (Lefebvre *et al.*, 1995). However, FUS in the nucleus does not appear to be localised to gems when investigated using immunocytochemistry (Yamazaki *et al.*, 2012).

Second, FUS is a known component of the paraspeckle (Nishimoto *et al.*, 2013; Page *et al.*, 2011; Naganuma *et al.*, 2012). Named because of their proximity to nuclear splicing speckles, this subnuclear body is formed by the assembly of drosophila behaviour human splicing (DBHS) proteins, including p54nrb/NONO, PSPC1 and PSF, on the long non-coding RNA, NEAT1 (Fox *et al.*, 2002; Clemson *et al.*, 2009; Sasaki *et al.*, 2009). Whilst the function of paraspeckles remains to be fully elucidated, it is thought that they play a role in the retention of adenosine-to-inosine (A-to-I) edited transcripts and in the cellular stress response (Zhang and Carmichael, 2001; Prasanth *et al.*, 2005).

Given the limited knowledge of the normal subnuclear localisation of FUS it is not surprising that the effect of ALS-associated FUS mutations on these structures is not clear. Curiously, there are reports of reduced gem numbers in ALS-FUS patient fibroblasts, motor neurons, transgenic mouse models of ALS-FUS and stable cell lines transfected with mutant FUS (Sun *et al.*, 2015; Tsuiji *et al.*, 2013; Yamazaki *et al.*,

2012) although gem number is not reduced in sporadic ALS patients (Kariya *et al.*, 2014). Further, there is evidence to suggest that paraspeckle formation is increased in spinal motor neurons in the early stages of ALS (Nishimoto *et al.*, 2013). However, it remains to be investigated whether ALS-associated FUS mutants affect paraspeckle formation and distribution and whether this could be an important pathological mechanism in ALS and other FUSopathies.

FUS in the cytoplasm

FUS has been shown to engage in nucleo-cytoplasmic shuttling of RNA, consistent with its capacity for RNA binding (Zinszner *et al.*, 1997b) and was identified as a component of RNA transport granules isolated from mouse brain (Kanai *et al.*, 2004). Supporting a role for FUS in local translation, FUS has been found at increased levels in the dendritic spines of hippocampal neurons in mice (Belly *et al.*, 2005) and humans (Aoki *et al.*, 2012). Accompanying this, FUS was identified in a proteomic analysis of NMDA receptors, present in dendritic spines, from mouse brain extracts (Husi *et al.*, 2000). In primary cultures of mouse hippocampal neurons, translocation of FUS in an RNA-transport complex to dendritic spines occurred upon activation of metabotropic glutamate receptor 5 (mGluR5) (Fujii *et al.*, 2005). Specifically, mRNA encoding an actin-stabilising protein, Nd1-L, is associated with this RNA-transport complex (Fujii and Takumi, 2005) (Figure 1.8). The dynamic reorganization of actin, a cytoskeletal component, likely mediated through local translation of mRNAs, is required during spine remodeling (Okamoto *et al.*, 2004). Consequently, primary cultures of hippocampal neurons from FUS knockout (KO) mice (Hicks *et al.*, 2000) displaying lower levels of Nd1-L in spines, displayed abnormal dendritic spine morphology and reduced spine density (Fujii *et al.*, 2005; Fujii and Takumi, 2005), supporting a normal role of FUS in neuronal maturation and regulation of dendritic spines.

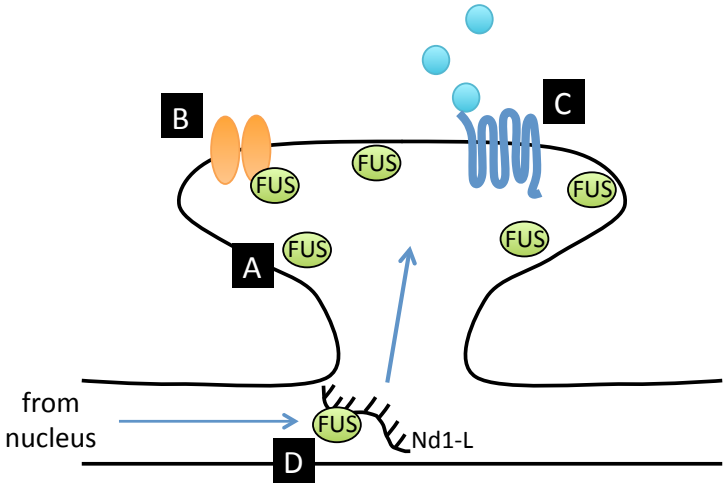

Figure 1.8. FUS is present in hippocampal dendritic spines. (A) FUS is enriched in dendritic spines. (B) FUS was identified in a screen of NMDA receptors. (C) Activation of mGluR5 receptors results in (D) translocation of RNA-complexes containing FUS and mRNA for actin stabilisation to the dendritic spine.

1.7.2 Loss of normal FUS function in disease?

Dormann *et al.* (2010) showed that ALS-linked mutations in the NLS of FUS disrupt its nuclear import, leading to mislocalisation to the cytoplasm. The crystal structure of FUS NLS bound to transportin has been solved and ALS-causing mutations are shown to fall within three main epitopes (N-terminal PGKM hydrophobic motif, central arginine-rich alpha-helix and C-terminal PY motif) that are required for this interaction with transportin (Zhang and Chook, 2012). Interestingly, in the same study, the extent to which mutation reduced the affinity of this binding was shown to correlate with the degree of cytoplasmic mislocalisation and the associated severity of patients harboring these mutations. Additionally, arginine methylation of the RGG domain adjacent to NLS has been shown to inhibit nuclear import by impairing binding of the RGG to transportin (Dormann *et al.*, 2012) which together with hyperosmolar stress (Sama *et al.*, 2013) and DNA damage (Deng *et al.*, 2014) provides another possible mechanism of redistribution of FUS without mutation.

This redistribution of FUS into the cytoplasm is thought to be a critical step in the development of FUS-related pathology and FUS depletion from the nucleus could affect the normal functions of FUS – a loss of function (LOF) hypothesis.

Although knockout of FUS in mice has been hampered with difficulties regarding viability and breeding, reducing or eliminating FUS expression in other model organisms has been instrumental in not just unraveling the normal roles of the protein but also implicating a LOF hypothesis in FUS-related neurodegeneration. Global

disruption of the *FUS* gene homologue, *Cabeza (CAZ*), in the fruit fly (*Drosophila melanogaster)* has resulted in shortened life span, reduced locomotor speed and, like the FUS knockout mouse, decreased viability (Xia *et al.*, 2012; Wang *et al.*, 2011). In their model, Wang *et al.* (2011) showed that associated phenotypes were rescued by the expression of WT Caz or human WT FUS, but not ALS-associated FUS mutants, indicating that ALS-associated mutations may lead to a loss of normal FUS function. Corroborating a LOF mechanism, knockdown of Caz specifically in neurons has been shown to be sufficient to cause a reduced synaptic branch length in presynaptic motor neuron terminals, accompanied by a reduced climbing ability of the fly (Sasayama *et al.*, 2012). This highlights that FUS is normally somehow involved in the maturation or regulation of pre-synaptic terminals.

60% knockdown of FUS in zebrafish by ASOs has also been shown to cause abnormal motor axon projections and a motor phenotype comprised of reduced escape responses to touch 48 h post-fertilisation, recapitulating findings in *Drosophila* (Kabashi *et al.*, 2011). This was rescued by co-injection of human WT but not ALS-linked mutant FUS mRNA, providing further evidence that ALS-associated mutation disrupts a physiological function of FUS in neuronal maturation and regulation at the synapse. Armstrong and Drapeau (2013) further investigated the impact of this ASO-mediated FUS knockdown, showing reductions in quantal transmission from neuromuscular junction (NMJ) synapses, leading to impaired motor activity. Again, these features were partially restored by expression of WT FUS but not ALS-linked mutant FUS, implicating LOF of FUS caused by ALS-linked mutation in disease pathogenesis. These reductions in evoked synaptic release from NMJs have also been identified in *Drosophila*, as a result of either knockdown of Caz or, conversely, expression of mutant R521C FUS (Shahidullah *et al.*, 2013). Contrastingly, Machamer *et al.* (2014) show that loss of Caz results in increases in quantal transmission at the NMJ in *Drosophila,* although it is not clear why these results differ.

Far from being fully understood, it is obvious that FUS plays a part not just post-synaptically in the regulation of dendritic spines (see Section 1.7.1), but also pre-synaptically in the maturation and function of motor neuron terminals at the NMJ. However, crucially, it remains to be seen whether the role of FUS in these processes is one of local importance in the cytoplasm, possibly acting via its RNA binding capacity, or rather that loss of FUS from the nucleus has a more global effect, resulting in

dysregulation of transcription and splicing of genes and mRNAs required for pre- and post-synaptic regulation.

1.7.3 Aggregation of FUS: Pathological or physiological?

The aggregation of proteins is a common feature associated with neurodegenerative disease (Ross and Poirier, 2004). Although cytoplasmic inclusions of mutant and/or WT FUS are seen in a proportion of patients with ALS, FTLD and other neurodegenerative diseases, the mechanisms by which these inclusions are formed and the role they play in disease is largely unknown. When the causal role for FUS in ALS was initially uncovered, Vance *et al.* (2009) noted the formation of small FUS-positive aggregates in the cytoplasm of CV-1 cells transfected with plasmid constructs expressing green fluorescent protein (GFP)-tagged R521C or R521H mutant FUS. Similarly, Kwiatkowski *et al.* (2009) also noted the formation of insoluble, cytoplasmic aggregates of GFP-tagged mutant FUS (R521G or H517Q) in transfected cell lines in their coinciding report. In addition to a potential loss of function caused by FUS depletion in the nucleus, the aggregation of these mutant variants in the cytoplasm may also contribute to the pathogenesis of disease, either through a gain of toxic function, or perhaps by a sequestration and functional disruption of essential cellular molecules by these aggregates. However, the need to understand FUS aggregation stems not just from a need to uncover its role in disease but also one of elucidating its normal cellular functions. The evolutionary conservation of domains involved in the aggregation of FUS suggests that its aggregation is physiologically relevant and that these domains are not simply deleterious.

Physiological aggregation of FUS

Several lines of evidence have pointed towards a prion-like domain within the N-terminus of FUS. The N-terminus of FUS is highly unstructured due to the prevalence of asparagine and glutamine residues, a common feature of prion domains in yeast prion proteins (Iko *et al.*, 2004; Michelitsch and Weissman, 2000; Toombs *et al.*, 2010). Additionally, FUS came 15th out of 27,879 human genome proteins in an *in silico* screen to find those most likely to contain a prion-related domain (Cushman *et al.*, 2010). Within FUS, this prion-like domain is thought to lie between N-terminus amino acids 1-239, with an additional region in the first RGG domain (amino acids 391-405) (Figure 1.4) (Cushman *et al.*, 2010). Interestingly, TDP-43 and TAF15, also implicated in ALS, have also been shown to have prion-like domains (Couthouis *et al.*, 2011). Prions are proteins which, following a conformational change, become self-templating and infectious. These misfolded proteins are responsible for a number of transmissible

spongiform encephalopathies affecting mammals, with human examples including Creutzfeldt-Jakob disease, kuru, fatal familial insomnia and Gerstmann-Staussler-Schienker syndrome (Collinge, 2001). Although FUS itself is not a prion protein; it is not known to be infectious *per se*, the presence of a prion-like domain suggests the potential of FUS to undergo conformational changes and seed aggregation.

On their own and at high concentrations, N-terminal low complexity domains of FUS are able to phase-transition into a hydrogel state shown to be composed of amyloid-like fibres upon EM (Kato *et al.*, 2012). Although recombinant WT FUS has been shown to be highly prone to aggregation *in vitro,* forming aggregates rapidly without agitation, this was dependent not only on its N-terminal prion-like domain but also on regions within the first RGG domain (Sun *et al.*, 2011). Similarly to those seen in human tissue, these *in vitro* aggregates were revealed to be filamentous under electron microscopy (EM) and were not amyloid based. Interestingly, an ALS-linked N-terminal mutation, G156E, was found to increase the aggregation propensity of FUS, although the aggregates formed by this mutation in rat hippocampal neurons were unusual in their amyloid-like nature (Nomura *et al.*, 2014).

Recently, Schwartz *et al.* (2013) have provided a distinct physiological role for the aggregation of FUS. Previously, they had determined an RNA-dependent interaction of FUS with RNAP2 (Schwartz *et al.*, 2012) but more recently have suggested a mechanism for this. Initially, multiple molecules of FUS bind along RNA, bringing the low complexity N-terminus domains of these FUS molecules closer together, enhancing their propensity to aggregate. This RNA-protein complex is then capable of seeding the aggregation of non-RNA-based FUS via protein-protein interactions of the N-terminus to form a fibrous higher-order assembly with the ability to bind the C-terminal domain of RNAP2 (Schwartz *et al.*, 2013). This has provided a compelling role for the aggregation of FUS, not just simply in disease, but also in fundamental physiological processes. Further, these readily reversible, physiological FUS interactions more than likely play an important role in the integrity of previously discussed paraspeckles and RNA transport granules.

Gain of toxic FUS function

In baker's yeast (*Saccharomyces cerevisiae*), the NLS of FUS does not result in its nuclear localisation (Ju *et al.*, 2011), making it a useful model for studying the properties of FUS in the cytoplasm. Sun *et al.* (2011) used this model to efficiently screen the cytoplasmic aggregation and toxic properties associated with mutant FUS

variants. Previously, this model was used to show a requirement of RRM2 and C-terminal domains for the aggregation and toxicity of TDP-43 and to show that ALS-linked mutations in TDP-43 exaggerated these properties (Johnson *et al.*, 2009). As with *in vitro* findings, the N-terminus of FUS, together with the RGG domain, was shown to be sufficient for aggregation in yeast (Sun *et al.*, 2011), although the cytoplasmic aggregation properties of shorter N-terminus fragments were not assessed due to their nuclear retention. Unlike TDP-43, Sun *et al.* (2011) also determined that ALS-linked mutations did not significantly affect the aggregation or toxicity of FUS compared to cytoplasmically localised WT protein. Notably, it has been seen in parallel studies that increased levels of WT FUS in the cytoplasm of yeast is toxic (Kryndushkin *et al.*, 2011; Fushimi *et al.*, 2011; Ju *et al.*, 2011; Sun *et al.*, 2011). This provides further evidence that the mislocalisation of FUS to the cytoplasm, even in full length form, is a critical first step leading to toxicity. Supporting this, the addition of a yeast-compatible NLS and uptake to the nucleus removed the toxicity associated with WT FUS (Ju *et al.*, 2011).

In addition to the phenotypes seen in *Drosophila* associated with the loss of Caz, similar phenotypes have been noted with the overexpression of human WT FUS or ALS-linked mutant variants. Overexpression of human WT FUS has resulted in reduced lifespan, locomotor impairments and a mild degenerate eye phenotypes in some (Miguel *et al.*, 2012; Xia *et al.*, 2012; Chen *et al.*, 2011; Lanson *et al.*, 2011) but, interestingly, not all (Wang *et al.*, 2011) *Drosophila* models. Similar, and sometimes more severe, phenotypes have been seen when mutant FUS variants have been overexpressed, hypothesised to be a gain of toxic function induced by mutation (Chen *et al.*, 2011; Lanson *et al.*, 2011; Xia *et al.*, 2012). Recently, however, Machamer *et al.* (2014) have provided an explanation for the increased toxicity associated with mutant forms compared to WT FUS, noting that simply the level of expression of WT or mutant FUS in the cytoplasm correlated with lethality and locomotor phenotypes, and found in previous studies that mutants were expressed at higher levels compared to WT FUS. Although Wang *et al.* (2011) did not see similar detrimental effects of FUS mutant overexpression in their hands, they report that their mutant proteins were retained in the nucleus, providing a possible explanation for these findings. Together this suggests that mislocalisation of FUS, rather than mutation is important in conveying a gain of toxic function. Similarly, Murakami *et al.* (2012) show that in *Caenorhabditis elegans*, where overexpressed mutant FUS was localised to the cytoplasm, severe motor dysfunctions were observed together with a shortened lifespan. Overexpression of WT

FUS, localised to the nucleus, was not capable of rescuing these phenotypes, opposing findings that loss of nuclear FUS function plays a role in these phenotypes.

In recent years, a number of transgenic rodent models of FUSopathy have been generated, allowing the investigation of FUS and ALS-associated mutations in higher-order systems (Table 1.2).

Table 1.2. Rodent models of FUSopathy

Species	Model	Survival	Additional features	Gain of function	Loss of function	Reference
Mouse	Homozygous knockout of FUS by exon 8 interruption	Unimpaired on partially outbred background (129svev x CD1) in specific-pathogen-free housing Rare animals survive until weaning on inbred background (129svev)	Male sterility Increased sensitivity to ionising radiation Loss of homologous DNA pairing ability *in vitro*		✓	(Kuroda *et al.*, 2000)
Mouse	Homozygous knockout of FUS* by exon 12 interruption on C57BL6 background	Death within 16 h of birth	Lymphocyte development defects B cell activation defects Chromosomal instability Primary hippocampal cultures have abnormal dendritic spine morphology and reduced spine density		✓	(Hicks *et al.*, 2000) (Fujii *et al.*, 2005)
Rat	Expression of human FUS cDNA (TRE promoter) on Sprague-Dawley background	Normal lifespan Line 20 (measured to 1 year) Line name refers to copy number	Spatial memory and learning deficits at advanced ages (1 year) Loss of neurons in frontal cortex and hippocampus at advanced ages No FUS+ inclusions Ubiquitinated inclusions at advanced ages	✓		(Huang *et al.*, 2011)

Rat	Expression of human FUS R521C cDNA (TRE promoter) on Sprague-Dawley background	<5 weeks Line 22 <10 weeks Line 16 Line name refers to copy number	Progressive paralysis onset <5 weeks Line 22, <8 weeks Line 16 Degenerating axons corticospinal tract, ventral roots, dorsal roots Loss of neurons in frontal cortex and hippocampus No FUS+ inclusions Ubiquitinated inclusions in spinal cord and brain at paralysis stages	✓(?)	✓(?)	(Huang *et al.*, 2011)
Mouse	Expression of human FUS with N-terminus V5-tag in predominantly neurons of brain from few weeks after birth using SBT	Sacrificed at 3 months	Asymptomatic Low level of FUS in cytoplasm	N/A	N/A	(Verbeeck *et al.*, 2012)
Mouse	Expression of human FUS R521C with N-terminus V5-tag in predominantly neurons of brain from few weeks after birth using SBT	Sacrificed at 3 months	Asymptomatic Increased level of FUS in cytoplasm No FUS+ aggregates	N/A	N/A	(Verbeeck *et al.*, 2012)
Mouse	Expression of human FUS ∆14 (aa.1-478) with N-terminus V5-tag in predominantly neurons of brain from few weeks after birth using SBT	Sacrificed at 3 months	Asymptomatic Pronounced level of FUS in cytoplasm Some FUS+/ubiquitin+ neuronal cytoplasmic inclusions	N/A	N/A	(Verbeeck *et al.*, 2012)
Mouse	Expression of human FUS cDNA with N-terminal HA-tag (PrP promoter) on C57BL6 background	10-13 weeks for homozygous Normal lifespan for hemizygous (measured to	Tremor at 4 weeks Hind-limb paralysis at 7-8 weeks Increased FUS in cytoplasm in brain FUS+ inclusions in spinal cord	✓		(Mitchell *et al.*, 2013)

		20 weeks)	Motor neuron loss in spinal cord			
Mouse	Expression of human FUS R521C with N-terminus FLAG-tag (Syrian hamster prion promoter)	50% N1F1 generation survived beyond 8 weeks Oldest monitored to >1 year Similar survival for subsequent generations	Motor behavioural abnormalities Low level FUS in cytoplasm motor neurons DNA damage in cortical and spinal motor neurons Loss of spinal motor neurons (55%) at 1-3 months Reduced dendritic branching Synaptic defects Transcription and splicing defects	✓(?)	✓(?)	(Qiu *et al.*, 2014)
Mouse	Expression of human FUS (CAG promoter) on C57Bl6 background	<4 weeks (Lines 629 and 638)	Gait abnormalities and grip strength reductions day 10-14 Defective neuromuscular synapses at juvenile age Increased expression of genes linked to DNA replication, recombination and repair, and regulation of cell proliferation.	✓		(Sephton *et al.*, 2014)
Mouse	Expression of human R521G FUS (CAG promoter) on C57Bl6 background	50% Line 682 <10 weeks 70% Line 673 <10 weeks	Subtle motor impairment Sociability deficits Defective neuromuscular synapses in mice with motor impairments Very few gene expression changes in spinal cord motor neurons Altered dendritic branching in spinal cord motor neurons and somatosensory cortex Reduced activity dependent FUS at synapses	✓(?)	✓(?)	(Sephton *et al.*, 2014)

* low levels of truncated FUS protein expressed. Abbreviations: CAG, cytomegalovirus immediate early enhancer-chicken β-actin hybrid; SBT, somatic brain transgenesis; Dox, Doxycline.

Overexpressing human WT FUS under the control of a prion protein (PrP) promoter in a homozygous knock-in mouse model was shown to cause a redistribution of FUS into the cytoplasm (Mitchell *et al.*, 2013). These mice developed tremor at 4 weeks, motor dysfunction by 8 weeks and rapid disease progression including paralysis by 10-13 weeks. FUS-positive structures were seen in brain and spinal cord, although these were not generally ubiquitinated and there was loss of motor neurons in the spinal cord. Neuromuscular function was also impaired in these mice. Together this highlights redistribution of WT FUS into the cytoplasm above a threshold as sufficient to cause toxicity and degeneration of motor neurons leading to motor deficiencies, although it has not been explained why these features were not seen in heterozygous mice.

More recently, others have also produced mouse models that express either WT or ALS-associated mutant FUS. Expressing low levels of WT or FUS R521C, with no FUS detected in the cytoplasm, was sufficient to cause reduced survival and defects at neuromuscular junctions that may represent early events prior to FUS mislocalisation and aggregation (Sephton *et al.*, 2014). Further, another FUS R521C model, with a low level of FUS in the cytoplasm, displayed synaptic defects and neurodegeneration (Qiu *et al.*, 2014), supporting a role for FUS in these processes.

Prior to this, Huang *et al.* (2011) had developed the first rodent models of FUSopathy. These transgenic rats overexpressed either full length human FUS or human FUS harboring the R521C mutation, a relatively common mutation in ALS-FUS patients. The mutant FUS rats developed a progressive paralysis whereas rats overexpressing human WT FUS were phenotypically normal at this age but later displayed abnormal spatial learning and memory. In both models, loss of cortical and hippocampal neurons was observed and was accompanied by loss of motor axons but not motor neurons in the mutant FUS model. No typical FUS-positive inclusions were seen in these rats, likely due to the minimal cytoplasmic redistribution of FUS that was caused by R521C mutation or WT overexpression. Neurodegeneration was accompanied by aggregates of ubiquitin only in FUS-expressing cells and glial activation in both models. Huang *et al.* (2012) also showed in a separate model that inducing the expression of human R521C FUS specifically in the neurons of the rat forebrain at postnatal day 30 resulted in a spatial learning and memory deficit and neurodegeneration in the hippocampus and cortex, preceded by neurite loss. These rats demonstrated mislocalisation of FUS to the neurites and spines to varying degrees with neurons of the entorhinal cortex, part of the temporal lobe associated with FTLD, found to show the greatest accumulations. As with previous models, although ubiquitin aggregates were seen,

these did not colocalise with FUS. This work supports findings that altered regulation of FUS is capable of producing ALS-like and FTLD-phenotypes. However, with these mice failing to display FUS aggregation in the cytoplasm, as seen in FUSopathy patients, a better model that recapitulates this crucial aspect of pathology is needed.

In day 0 mouse neonates, Verbeeck *et al.* (2012) used bilateral intracerebroventricular injection of recombinant adeno-associated virus carrying either WT or mutant human FUS cDNA (R522G or Δ14) to produce expression of these protein variants in neurons throughout the brain. This expression reached a maximum ~3 weeks after birth and continued throughout their life. No phenotypic abnormalities were detected in these mice at 3 months when animals were sacrificed. Mice expressing human WT FUS showed a nuclear localisation of FUS and failed to demonstrate any signs of toxicity caused by its overexpression at this age. Like the aforementioned rat model, mice expressing R522G FUS showed a degree of cytoplasmic mislocalisation but this was not accompanied by FUS-positive NCIs. On the other hand, mice expressing Δ14 FUS, a mutant protein thought to arise from G466VfsX14 human FUS mutation, showed the greatest degree of FUS in the cytoplasm and displayed FUS-positive NCIs in cortical neurons. However, in these mice, expression was limited to the brain. As the ALS prominently affects lower motor neurons and skeletal muscle, a more ubiquitous expression of these constructs would be preferable to model these aspects of disease.

Although providing valuable information about the progression of disease in ALS, toxic effects mediated by expressing full length forms of FUS may arise through several pathways. It is highly likely that by expressing full length forms of FUS, FUS-regulated RNA metabolism will be altered and, whilst some studies showed a degree of FUS aggregation, it is not possible to distinguish the contributions of these features to the disease process. This will be important in future models to decipher crucial pathological stages that may be pharmacologically targeted.

In summary, following mislocalisation of FUS to the cytoplasm, two simplified scenarios emerge (Figure 1.9). Loss of FUS from the nucleus can disrupt its normal nuclear roles including transcription, RNA metabolism and DNA repair, whilst gain of FUS in the cytoplasm can produce toxicity, and, importantly, there are several lines of evidence described that support each possibility. To fully appreciate the pathological mechanisms involved in the development and progression of ALS-FUS, and to potentially understand themes that may be common to ALS or other FUSopathies as a

whole, it will be key to understand what happens to FUS following its mislocalisation to the cytoplasm and how this may convey toxicity.

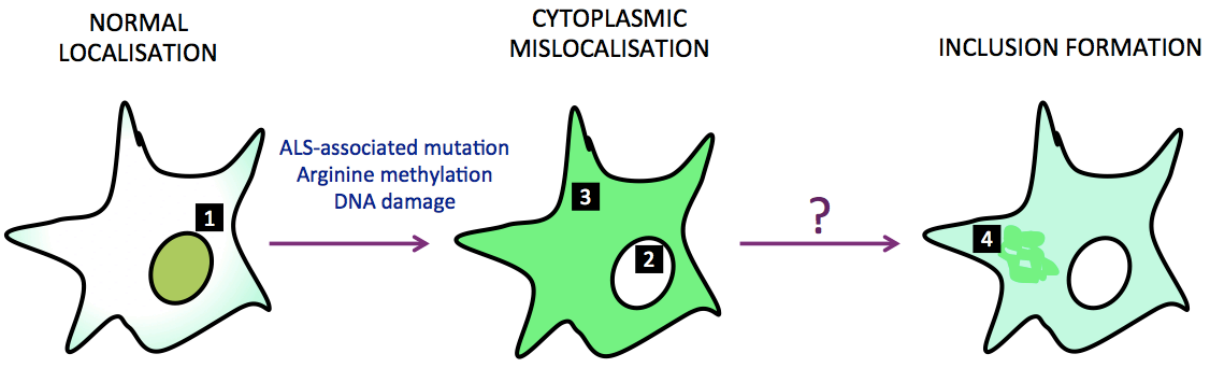

Figure 1.9. Hypotheses of the origins of toxicity in FUSopathies. (1) FUS is a predominantly nuclear protein, with evidence for increased presence at synapses and in transport granules (not shown). However, following certain pressures (purple), FUS can become largely mislocalised to the cytoplasm. Toxicity in these instances may arise from either (2) loss of normal nuclear function(s) of FUS and/or (3) toxic gain of function of FUS in the cytoplasm. (4) Additionally, large FUS-positive inclusions are formed in the cytoplasm of these patients, whilst the pathways preceding this are unknown. Finally, it remains to be seen whether these inclusions are toxic or instead represent a cytoprotective response of the cell.

Interactions of FUS aggregates in the cytoplasm

Similarly to TDP-43, mutant FUS localised to the cytoplasm as a direct result of mutation has been shown to reversibly accumulate in SGs in mammalian cell culture (Dormann *et al.*, 2010; Bosco *et al.*, 2010; Vance *et al.*, 2013). The recruitment of FUS to SGs has been shown to be dependent upon its RNA-binding domains (Bentmann *et al.*, 2012) although WT FUS is not necessary for SG formation and, unlike TDP-43, recruitment to SGs seems specific to mutant varieties. However, as is the case for TDP-43, the role for this interaction of FUS and SG proteins in ALS pathogenesis is debatable. Dormann *et al.* (2010) propose that SGs could be a precursor for the large FUS-positive inclusions seen in patients and that recruitment of FUS to these structures instigates the pathological accumulation of FUS in a gain of toxic function mechanism of the SGs themselves. However, this agglomeration of SGs has not been evidenced and as stress granules normally have a protective role, readily dissipating following the removal of stress, it is instead feasible that aggregating mutant FUS may disrupt the normal formation and/or dynamics of SGs (Baron *et al.*, 2013). Indeed, supporting this disruptive hypothesis, proteins normally localised to SGs can colocalise with FUS-positive inclusions in ALS patients (Dormann *et al.*, 2010). To understand

how FUS is aggregating within the cytoplasm in ALS it will be important to further investigate these interactions of FUS with SGs.

1.8 Aims

Even in 2015, a diagnosis of ALS remains terminal, with current pharmacotherapies failing to provide an appropriate standard of treatment. Over the past 20 years, the ongoing discovery of the genetic, pathological and clinical features of the disease has been rapid, and although several themes have surfaced, these require further research with the hope of uncovering novel therapeutic targets.

With the emergence of altered RNA metabolism as an underlying disease mechanism, and a growing body of evidence implicating RNA-binding proteins in the pathogenesis ALS, it is important to fully understand the functions of these proteins in normal and disease states.

Mutations in the gene encoding the RNA-binding protein FUS are known to cause ALS and FUS it is frequently observed in large cytoplasmic inclusions in ALS-FUS, FTLD and in certain other neurodegenerative diseases. Whilst it is thought that FUS mislocalisation to the cytoplasm represents a key stage in disease pathogenesis, relatively little is known about its interactions once in the cytoplasm and the pathways that lead to its aggregation into the large inclusions identified post-mortem within the surviving motor neurons of patients. Therefore, the first two aims of this thesis were to:

1) Explore the relationship between FUS aggregation in the cytoplasm and interactions with stress granules in the pathogenesis of disease

2) Reveal how the RNA-binding capacity of FUS affects its propensity to aggregate both *in vitro* and *in vivo*

For this, GFP-tagged mutant constructs of FUS, harbouring both ALS-associated and experimental mutations, were generated and expressed transiently in mammalian cell lines. The behaviour and interactions of these mutant proteins and their responses to various interventions, including oxidative stress, were assessed using immunocytochemistry and biochemical techniques. In addition, mice expressing a C-terminally truncated form of FUS, lacking its major RNA binding domains, were generated and characterised to determine at the level of the whole organism whether initial insult of aggregation of FUS in the cytoplasm is toxic, irrespective of primary changes to RNA metabolism that would be expected following increased expression of full length forms. These studies were complemented with the characterisation of a

second transgenic model generated through the neuronal expression of a form of cytoplasm-targeted FUS that lacked the RNA-recognition motif.

In addition to investigating the pathways that may lead to a gain of toxic function in the cytoplasm, this thesis aimed to investigate the effects that ALS-associated FUS mutants may have within the nucleus.

Loss of normal FUS function in the nucleus has also been shown to be detrimental, notably, FUS KO is lethal. Yet, whilst evidence about the physiological roles of FUS in the nucleus is increasing, the sub-nuclear localisation of FUS and the effects of ALS-associated mutations on this are not known. Therefore, this thesis also aimed to:

3) Delineate the interactions of FUS with subnuclear compartments and determine the effects of FUS mislocalisation to the cytoplasm on these interactions

For this, the location of FUS within the nucleus of cultured mammalian cells was revealed by immunocytochemical colocalisation studies with markers of known nuclear bodies and the domain requirements of FUS recruitment to these compartments was established. To ascertain how gain of FUS in the cytoplasm may affect these interactions, the localisation of FUS and marker proteins of subnuclear bodies shown to contain FUS were assessed following expression of GFP-tagged ALS-associated mutant FUS. This was also investigated in our murine model of FUSopathy and in human ALS-FUS patient tissues. In a reversal of this, we also probed the effects that a reduction in the nuclear level of FUS can have on these subnuclear bodies by using FUS-targeting small interfering RNA (siRNA).

Although the genetic background and pathology of ALS is diverse, notably, many patients have no obvious genetic component, increased understanding of individual RNA-binding proteins will not only be essential for understanding the relevant genetic subsets of the disease, but may highlight pathways common to ALS as a whole.

MATERIALS & METHODS

Unless stated otherwise, materials used for this thesis were sourced from Sigma-Aldrich.

2.1 Generation of mutant FUS cDNA constructs

In addition to driving the expression of recombinant protein-coding sequences in mammalian cell lines, expression plasmids were used to add easily detectable tags to proteins of interest. Importantly, in addition to producing tagged full-length FUS, molecular cloning methods were used to create tagged FUS proteins harboring desired ALS-linked or experimental mutations. Further, these methods were employed to create a number of truncated and chimeric proteins to investigate the roles of various domains of FUS. Although described in detail in the following sections, briefly, human cDNA was used as a template for amplification of the sequence of interest using primers designed to add specific restriction enzyme sites to each end of the sequence. These additional restriction sites allowed for orientation specific insertion of the insert fragment into the expression plasmid in later steps. Blunt ended PCR fragments were then cloned into the pCR-Blunt II-TOPO vector (Invitrogen) that permits efficient and rapid cloning. The fragment of interest was digested from this plasmid using the chosen combination of restriction enzymes. Likewise, the vector plasmid was digested with corresponding restriction enzymes. Both vector and insert fragments, now with complementary ‘sticky ends’ were purified from agarose gel and ligated together to produce an expression plasmid that, upon entering a mammalian cell, drove the expression of the tagged recombinant protein (Figure 2.1).

The following constructs were used in this thesis:

Protein	Tag	Fragment/ mutation	PCR template	Created by
FUS	N-terminal EGFP	1-359	Human cDNA	NN
	N-terminal EGFP	359-526 (to create WT)	Human cDNA	NN
	N-terminal EGFP	R522G	FUS WT in pEGFP-C1	NN
	N-terminal EGFP	1-513 (ΔNLS)	FUS WT in pEGFP-C1	NN
	N-terminal EGFP	1-466 (dRGG3)	FUS WT in pEGFP-C1	HKR
	N-terminal EGFP	ΔRRMcyt	FUS R522G in pEGFP-C1	HKR
	N-terminal EGFP	ΔRRM	FUS WT in pEGFP-C1	NN
	N-terminal EGFP	CT	FUS WT in pEGFP-C1	HKR
	N-terminal EGFP	RRM-CT	FUS WT in pEGFP-C1	TAS
	N-terminal EGFP	dRRM-RGG3	FUS ΔRRM in pEGFP-C1	TAS
	N-terminal EGFP	R518K	FUS WT in pEGFP-C1	NN
	N-terminal EGFP	R524T	FUS WT in pEGFP-C1	NN
P54nrb	N-terminal EGFP	WT	Human cDNA	TAS
TDP-43	N-terminal EGFP	WT	Human cDNA	TAS
MTAP	N-terminal FLAG	WT	Human cDNA	TAS
Chimeric Proteins				
	N-terminal EGFP	Sup35-FUS	Yeast cDNA	HKR
	N-terminal EGFP	FUS-TDP43-RRMs	Human cDNA	HKR
	N-terminal EGFP	FUS-TDP43-RRMs-3D	Human cDNA	HKR
	N-terminal EGFP	FUS-Npl3	Yeast cDNA	HKR

HKR, Hannah Kirby Robinson (author of thesis); NN, Natalia Ninkina; TAS, Tatyana Shelkovnikova

For detailed information on how these were created, including primers for amplification and restriction enzymes used see Appendix.

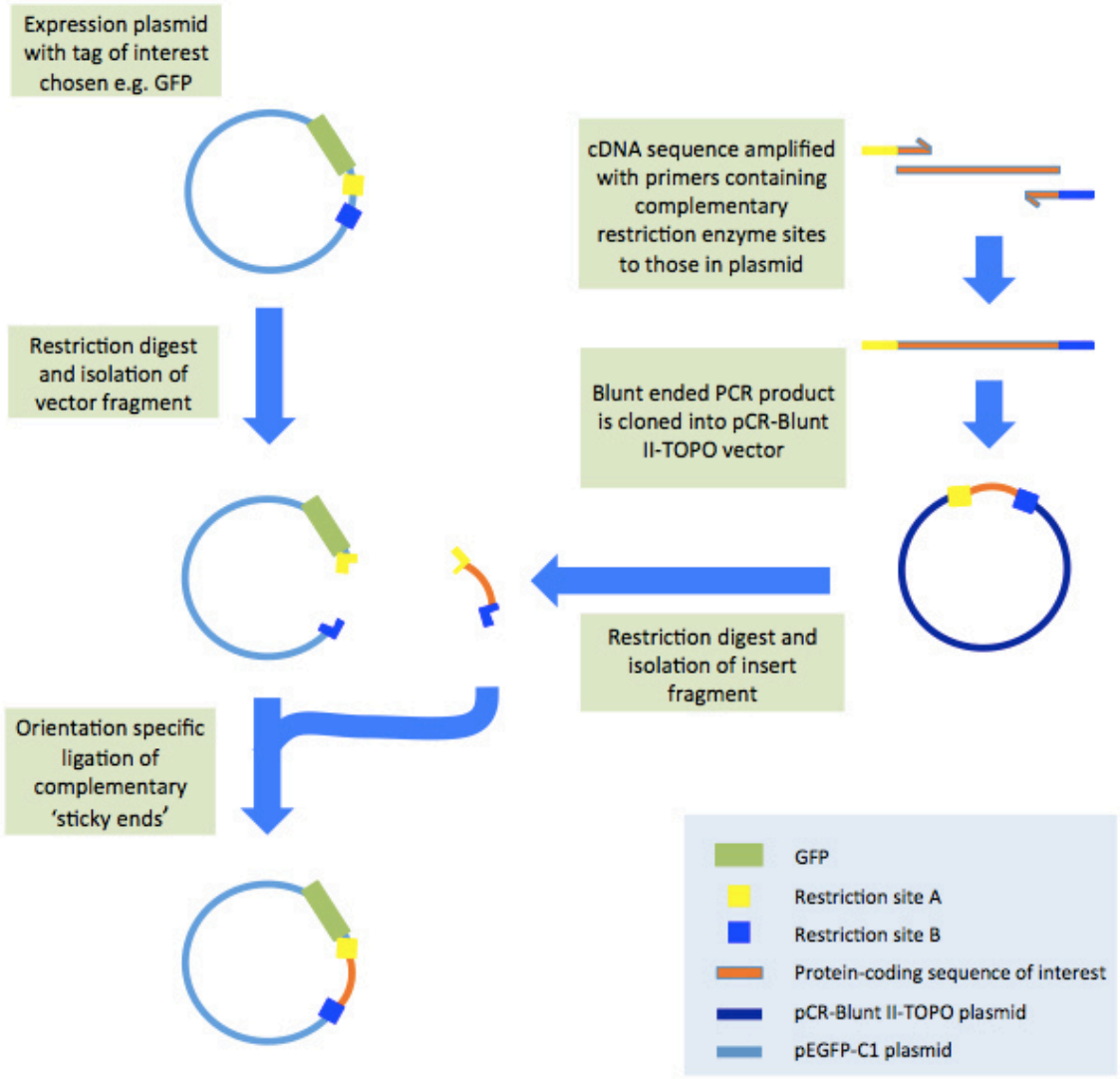

Figure 2.1. Overview of molecular cloning steps taken to create expression plasmids that drive the expression of tagged recombinant proteins of interest.

2.1.1 Expression plasmids

Sequences of interest were inserted downstream and in frame with existing tag-encoding sequences in the expression plasmid of choice. The cloning strategy for expression plasmids were designed as follows:

				Restriction sites introduced with primers during amplification of insert	
Plasmid name	Tags	Plasmid digest enzymes	Vector size produced (bp)	5' of sequence	3' of sequence
pEGFP-C1	N-terminus EGFP	XhoI/BamHI	4684	XhoI	BamHI
pFLAG-CMV4	N-terminus FLAG	HindIII/KpnI	6229	HindIII	BamHI

For expression plasmid maps and additional information including primers used for sequencing, see Appendix.

2.1.2 RNA extraction and first-strand cDNA synthesis

In some cases, human cDNA was used as a template for PCR amplification of insert fragments. For this, total RNA was isolated from cultured human neuroblastoma (SH-SY5Y) cells using the RNeasy mini kit (Qiagen) according to manufacturer's instructions. Briefly, cells were homogenized in RLT buffer, which contains a high concentration of the chaotropic agent, guanidine isothiocycanate. Together with the addition of β-mercaptoethanol, any RNases in the lysate were inactivated. The addition of ethanol then promoted the binding of RNA to a silica spin-column membrane. Following an extra DNase digestion step using the RNase-free DNase Set (Qiagen) and washing of the membrane, RNA was eluted in 50 µl RNase-free H_2O (Ambion). RNA concentration and integrity were determined using a Nanodrop 1000 Spectrophotometer (ThermoScientific). First-strand cDNA synthesis was carried out on 500 ng total RNA using SuperScript III reverse transcriptase (Invitrogen) and random hexamers (Promega) according to manufacturer's instructions.

2.1.3 PCR

Either pre-existing plasmid DNA or cDNA synthesised from total RNA was used as a template for PCR reactions. Custom synthesised primers were designed using A Plasmid Editor (ApE) v2.0.45 and Primer 3 software to amplify specific regions of

interest and to introduce mutations. In addition, primers were used to introduce restriction enzyme sites, compatible to those later required for orientation specific insertion of the sequence into the expression plasmid, both 5' and 3' to the sequence of interest.

For the production of blunt ended PCR products for cloning, DNA sequences were amplified with high fidelity AccuPrime *Pfx* SuperMix (Invitrogen). To this, 0.2 µM forward and reverse primers and ~1 ng template DNA were added in a 25 µl reaction. For a complete list of all primer sequences and corresponding amplicon sizes, see Appendix.

Typical cycling parameters:

1 cycle	95ºC for 2 min (denaturing)
44 cycles	95ºC for 15 sec (denaturing) 50-60ºC for 30 sec (annealing) 68ºC for 1 min/kb (extension)
1 cycle	68ºC for 5 min (finish all extension)
1 cycle	4ºC ∞ (storage until removed)

For PCR where the product was diagnostic rather than for further cloning, typically, PCR reactions were carried out in 50 µl reactions using the following concentrations of components:

Typical PCR reaction:	
10X Standard *Taq* reaction buffer (New England Biolabs (NEB))	1x
dNTPs (Promega)	200 µM
Forward & reverse primers	0.2 µM
Template DNA	~100 ng
Taq polymerase (NEB)	1.25 units

2.1.4 Agarose gel electrophoresis

Agarose gels were prepared using 1X TAE (40 mM Tris, 20 mM acetic acid, 1 mM EDTA), agarose and ethidium bromide. Typically, to confirm the size of either PCR products or restriction digest products, loading buffer (Finnzymes) was added to the

reaction products and the mixture then loaded into a well of a 1% agarose gel alongside 5 µl ladder (HyperLadder 1kb, Bioline). Gels were run at 140 mA until desired separation was reached. In some instances, the percentage of gel and choice of ladder were adjusted for optimal separation and identification of either small (<200 bp) or large (>3000 bp) DNA fragments. Following separation, the location of DNA fragments was visualised using UV light. For PCR reactions where the product's intended use was in molecular cloning, only a sample of the reaction was added to loading buffer and subjected to gel electrophoresis to confirm the presence of a single product of the correct size. The remaining PCR product was set aside for cloning into pCR-Blunt II-TOPO plasmid.

2.1.5 Isolation of DNA fragments

In instances where PCR could not be optimised to produce a single product, the band corresponding to the correct size fragment was isolated from agarose gel. The gel was illuminated under long-wave UV light and the required band was excised using a clean, sharp scalpel. DNA was then purified from the excised agarose using the QIAquick Gel Extraction Kit (Qiagen). DNA fragments were eluted in dH_2O. This method was also used to isolate the correctly sized fragment of interest from multiple fragments following restriction enzyme digestion of plasmids.

2.1.6 Cloning into pCR-Blunt II-TOPO vector and transformation of cells

Blunt ended PCR products, produced by amplification with AccuPrime *Pfx* SuperMix, were ligated into pCR-Blunt II-TOPO vector (Invitrogen) using the Zero Blunt TOPO PCR Cloning Kit (Invitrogen) according to manufacturer's instructions. This technology utilises the ability of DNA topoisomerase I enzyme, from *Vaccinia* virus, attached to each 3' end of the linearised pCR-Blunt II-TOPO plasmid at 5'-CCCTT-3', to produce a phosphodiester bond, ligating blunt-ended PCR product into the vector in a 5 minute reaction (Figure 2.2) (Shuman, 1994; Shuman, 1991).

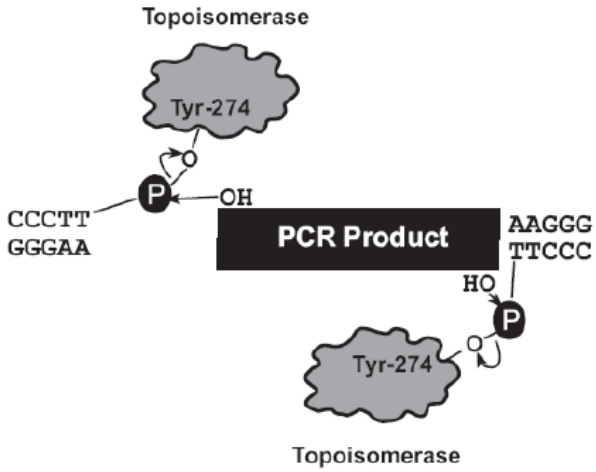

Figure 2.2. TOPO cloning ligation reaction utilises DNA topoisomerase I enzyme to introduce blunt-ended PCR products into the linearised pCR-Blunt II-TOPO vector. Upon cleavage of 5'-CCCTT-3' by topoisomerase I, energy is conserved through covalent bonding of a 3' phosphate (P) to the tyrosyl residue of the enzyme (Tyr-274). Conversely, this energy is then used for the ligation of PCR product into the vector. Image taken from the Zero Blunt TOPO PCR Cloning Kit manual (Invitrogen).

For a complete map of pCR-Blunt II TOPO vector including sequencing primers, see Appendix.

50µl aliquots of high efficiency NEB 5-alpha competent *E.Coli* (NEB) normally stored at -80ºC were defrosted on ice for 10 min prior to addition of ligation products. 2 µl of TOPO cloning reaction or T4 ligase ligation reaction was added to the competent cells, followed by further incubation on ice for 25 min. To permit uptake of plasmids by the cells, cells were subjected to heat shock at 42ºC for 30 s and incubated on ice for 2 min. 500 µl SOC medium was added and the cells then incubated at 37ºC for 1 h with shaking. Bacterial cells were pelleted at 4500 rpm for 2 min, resuspended in 50 µl SOC medium (Invitrogen) and spread onto LB agar antibiotic selection plates. Plates were incubated overnight at 37ºC.

2.1.7 Preparation of bacterial culture media

To produce Luria broth (LB) for liquid bacterial cultures, 25 g LB base (Invitrogen) was added to 1 L dH_2O. For Luria agar (LA), 1 g select agar (Invitrogen) was added per 100 ml LB. Both LB and LA were autoclaved for sterilisation. For selection of transformed cells, the desired selection antibiotic was added at a final concentration of 50 µg/ml once the media had cooled below 50°C. Ampicillin or kanamycin were frequently used as selection antibiotics. Luria agar with added antibiotics (LA+) was then set in 10 cm diameter sterile dishes. Both LA+ dishes and Luria broth with added antibiotics (LB+) were stored at 4ºC.

2.1.8 Single bacterial colony culture

Following overnight growth of colonies on antibiotic selection agar plates, single colonies were picked and grown overnight at 37ºC in 5 ml LB+ with vigorous shaking to maintain aeration.

2.1.9 Colony PCR

Colony PCR was used to quickly establish the possibility that the single colonies of transformed bacterial cells had taken up plasmid containing the desired fragment of DNA. For this, 0.5 ml overnight liquid culture was pelleted at 4500 rpm and cells were resuspended in 50 µl dH_2O. To lyse the bacterial cell membrane, samples were incubated for 10 min at 95ºC. To clear cell debris, samples were centrifuged for 10 min at 13000 rpm and the supernatant taken for subsequent PCR reactions. If the correct fragment size was observed following agarose gel electrophoresis, plasmid DNA was purified from the remaining liquid culture.

2.1.10 Purification of plasmid DNA from bacteria

Plasmid DNA was purified from overnight bacterial cultures using a ZR Plasmid Miniprep kit (Zymogen) according to manufacturer's instructions. This kit utilises an alkaline lysis protocol in combination with a spin column membrane that permits binding and washing of plasmid DNA in the presence of chaotropic salt and its subsequent elution under low salt conditions. Purified plasmid DNA was eluted in 30 µl dH_2O. The concentration of purified plasmid DNA was determined using a NanoDrop 1000 spectrophotometer (ThermoScientific).

2.1.11 Restriction enzyme digest

To further determine the likelihood of correct fragment insertion into the vector, diagnostic restriction enzyme digests were performed on purified plasmid DNA samples. To allow for variability in purity and quantity of DNA, manufacturers recommended performing digests in excess enzyme conditions. Typically, 10 units of restriction enzyme were used to digest 1 µg plasmid DNA in a 50 µl reaction, with the appropriate enzyme buffer (NEB) accounting for 10% final volume. Reactions were incubated at 37ºC for a minimum of 1 h. Agarose gel electrophoresis of digest products was performed to determine fragment sizes produced, allowing determination of correct insertion into the vector. Restriction digests were also used to isolate fragments of known DNA sequence for further use in subcloning. Following agarose gel electrophoresis, the desired fragment was isolated and purified from agarose gel.

2.1.12 Ligation

Following digestion and isolation of both vector and desired insert(s), ligation was performed using T4 DNA ligase (Invitrogen) according to manufacturer's instructions. To determine the concentration of fragments, 5 µl of each fragment was run alongside 5 µl ladder with a band pattern of known concentration on an agarose gel. Typically ligations were performed using a insert:vector molar ratio of 3:1, although this was increased for multiple insert ligations. The following formula was used to achieve this ratio:

$$\text{Insert mass required (ng)} = \frac{\text{vector mass (ng)} \times \text{insert size (kb)}}{\text{vector size (kb)}} \times \frac{\text{insert}}{\text{vector}} \text{ ratio}$$

Ligation reactions were incubated at 17ºC and slowly cooled to 4ºC overnight.

2.1.13 Sequencing

Plasmids were sequenced by the Cardiff University Sequencing Core facility using relevant primers (for details, see Appendix) to confirm correct sequence insertion and orientation. Analysis of sequences was carried out in SnapGene Viewer v1.4 (GSL Biotech) and ApE v2.0.45.

2.1.14 Frozen bacterial stocks

For long-term storage, liquid bacterial cultures transformed with plasmid containing desired sequence(s) were frozen in 25% glycerol and and maintained at -80ºC. When plasmid was required, a small sample of the frozen bacterial suspension was streaked onto an LA+ selection plate and incubated overnight at 37ºC. A single colony was then taken to produce overnight liquid cultures in LB+ media from which plasmid was isolated.

2.2 Mammalian cell culture and biochemical investigations

2.2.1 Maintenance of mammalian cell lines

Human neuroblastoma (SH-SY5Y), African green monkey kidney fibroblast-like (COS7) or human breast cancer (MCF7) cell lines were cultured in a humidified atmosphere with 5% CO_2 at 37°C in a 1:1 mixture of Dulbecco's modified Eagle's medium (Invitrogen) and Ham's F-12 nutrient mixture (Invitrogen), supplemented with 10% foetal bovine serum (Invitrogen), 1% L-glutamine (Invitrogen) and 1% penicillin and streptomycin solution (Invitrogen). The majority of *in vitro* work was performed in

SH-SY5Y cell line due to its neuronal lineage. COS7 cells were at times used for immunoprecipitation or immunofluorescence as their larger size provided more material and easier visualisation of protein interactions. MCF7 cells were used in methylation studies for paraspeckles.

2.2.2 Transfection of mammalian cell lines

24 h after splitting and plating, cells were transfected with expression plasmids or small interfering RNA (siRNA) using Lipofectamine 2000 reagent (Invitrogen) according to manufacturer's instructions. Lipofectamine is a cationic lipid which, when combined with negatively charged nucleic acid, forms a transfection complex permitting endocytosis of the expression plasmid.

2.2.3 Cell treatments

To induce stress granule formation, heat shock or sodium arsenite was used. For heat shock, cells were incubated for 1 h at 43°C. Sodium arsenite was used at a final concentration of 0.5 mM diluted in normal growth medium for 1 h. For disruption of microtubules, nocodozole was applied at a final concentration of 0.5 or 1 μM for 4 h. For translational inhibition, emetine and cycloheximide were used at final concentrations of 10 and 20 μg/ml, respectively. For transcriptional inhibition, 5 μg/ml actinomycin D (Calbiochem) or 25 μg/ml 5,6-dichloro-1-beta-D-ribofuranosylbenzimidazole (DRB) (Sigma-Aldrich) were applied for 2 h. To decrease levels of protein methylation, 5′-deoxy-5′-methylthioadenosine (MTA) was applied to SH-SY5Y cells in full medium at a final concentration of 750 μM for 24 h. For nucleolus staining living cells were exposed to 10 μg/ml of ethidium bromide for 2 h prior to fixation.

2.2.4 Knockdown of FUS with siRNA

To achieve knockdown of endogenous FUS, cells were transfected with a FUS-specific pool of siRNAs, SiGENOME SMART pool M-009497-02 (target sequences: 5′-ccuacggacagcagaguua-3′, 5′-gauuauacccaacaagcaa-3′, 5′-gaucaauccuccaugagua-3′, 5′-cgggacagcccaugauuaa-3′) (Thermo Scientific). Upon entry into the cell, this double stranded siRNA binds to the RNA-induced silencing complex (RISC). Here, the two RNA strands become separated, leaving a specific sequence-targeting activated RISC. This binds the complementary target mRNA sequence and cleaves it, reducing the pool of target mRNA and subsequently, level of the target protein itself (Elbashir *et al.*, 2001). As a control for off-target effects, non-specific scrambled siRNA sequences

(target sequence: 5′-ggacuaauaguugugcuccaauuua-3′) (Invitrogen) was used. Cells were analysed 72 h post-transfection to allow sufficient time for knockdown to take place.

2.2.5 Primary mouse hippocampal cultures

All primary hippocampal cultures were prepared by Dr Tatyana Shelkovnikova. Hippocampi were dissected from non-transgenic C57Bl6 pups at postnatal day 3. Hippocampal tissues were then digested in 0.1% trypsin in HBSS supplemented with 10 mM Hepes and 1 mM pyruvate (Invitrogen) for 40 min. To free cells, hippocampi were mechanically dissociated by several passages through a flame-polished glass pipette in Neurobasal A medium (Invitrogen) with 50 U/ml penicillin/streptomycin, 0.2% b-mercaptoethanol (Sigma), 500 mM L-glutamine and 10% horse serum (Invitrogen). Following centrifugation at 1500 rpm for 5 min, pellets were resuspended in fresh medium and plated onto poly-L-lysine-coated glass cover slips. Medium was replaced with serum-free medium containing B27 after 24 h. On DIV7, mixed neuronal-glial cultures were transfected with Lipofectamine 2000 using an adapted protocol, whereby Lipofectamine-DNA complexes were left on cells for only 1 h and replaced with normal culture medium. Cells were fixed and stained 48 h after transfection.

2.2.6 Live cell imaging

To monitor localisation and interactions of GFP-tagged FUS constructs over time, COS7 cells or SH-SY5Y cells were plated on glass-bottomed tissue culture dishes and transfected with GFP-tagged FUS mutant constructs. 24 h post-transfection, growth culture media was replaced with HEPES-buffered media (10 mM HEPES-KOH, pH 7.5) to maintain physiological pH outside a CO_2 incubator, with or without 0.5 mM sodium arsenite treatment. Still images were obtained every 8 minutes for ~4 h using a Leica TCS SP2 MP confocal microscope, equipped with an on-scope incubator with temperature control (Leica Microsystems) under a Fluotar L 63x1.4 oil objective. Live cell imaging videos were created using Leica Application Suite AF software and still images, corresponding to every 15 min, were used to create 16-frame gallery images.

2.2.7 Immunocytochemistry

Immunocytochemistry was performed to identify the cellular localisation of various proteins of interest. For this, cells were plated on 10 mm diameter round glass coverslips (VWR international) pre-treated with poly-L-lysine. Following transfection, cells were fixed with 4% paraformaldehyde (PFA) for 15 min, permeabilised in ice cold methanol for 5 min and blocked for 1 h at RT in blocking buffer (1% TritonX-100, 5%

goat serum in PBS). Cells were incubated overnight at 4ºC in primary antibodies diluted in blocking buffer (for list see Appendix). Following washes in PBS, Alexa-Fluor-conjugated secondary antibodies (anti-mouse, anti-rabbit, and/or anti-chicken, 1:1000, Invitrogen) diluted in 1% TritonX-100 in PBS were applied for 1.5 h at RT. 4',6-diamidino-2-phenylindole (DAPI) (Invitrogen), applied at a final concentration of 1 μg/ml during final washing step, was used to visualise nuclei. Cells were mounted with ImmuMOUNT (ThermoScientific) and imaged with a 100x objective using a BX61 fluorescence microscope and Cell F software (Olympus).

Fluorescence intensity measurements were performed 24 h post-transfection with GFP-tagged R522G. Following image capture using Cell F software, Image J software was used to measure fluorescence intensity in 3 non-overlapping 2.5 x 2.5 μm squares placed at random in the cell cytoplasm. From this, the mean fluorescence intensity measurement was calculated.

2.2.8 RNA-fluorescent in situ hybridisation (RNA-FISH)

RNA-FISH was used to determine the localisation of poly(A)$^+$ mRNA within cultured cells. Cells were fixed and permeabilised as for immunocytochemistry. Following this, cells were incubated in 70% ethanol for 10 min followed by 1 M Tris pH 8.0 for 5 min. Cells were then incubated in fluorescently-labelled (Cy5) oligo(dT)$_{30}$ probe, complementary to the poly(A) tail of mRNA, overnight at 37°C at a final concentration of 1 μM in hybridisation buffer (2X SSC, 25% formamide, 10% dextran sulphate, 0.005% BSA, 1 mg/ml yeast tRNA). To prevent drying in the incubator, culture vessels were placed in a sealed bag containing a fibre cloth (VWR) soaked in DEPC-treated water. Where RNA-FISH was used in combination with immunodetection of a protein, cells were exposed to primary antibodies diluted in 2X SSC, 0.1% TritonX-100 for 3 h at RT, followed by incubation with Alexa Fluor-conjugated secondary antibodies (1:1000 in 2X SSC, 0.1% TritonX-100) and DAPI. To prevent degradation of RNAs, DEPC-treated water (Ambion) was used throughout. For RNA-FISH, images were taken using BX61 microscope and processed using Cell F software.

2.2.9 Cellular fractionation

Cellular fractionation was performed to isolate detergent soluble and insoluble aggregated fractions. Cells were collected in ice cold lysis buffer (0.1% Triton X-100, protease inhibitor cocktail (Roche) in PBS) and incubated on ice for 30 min with periodic vortexing to ensure appropriate lysis. Where RNase digestion was required, RNase A was added at a final concentration of 1 mg/ml for 25 min at RT. Lysates, with

or without RNase treatment, were then centrifuged at 17000 g for 20 min. Supernatant was recovered as the soluble fraction and the pellet was recovered as the insoluble fraction. For isolation of cellular fraction enriched for granules, following lysis cells were instead centrifuged at 1000 g for 10 min to remove nuclei and then 17000 g for 20 min to remove larger aggregates and organelles. Supernatant was further subjected to centrifugation at 100000 g for 20 min to produce the granule-enriched pellet and soluble supernatant. All centrifugation steps were performed at 4°C.

2.2.10 SDS-PAGE and western blotting

Sodium dodecyl sulphate polyacrylamide gel electrophoresis (SDS-PAGE) was performed to achieve separation of proteins according to molecular weight. Pore size within polyacrylamide gel is determined by the percentage of acrylamide and bis-acrylamide. Casting SDS-PAGE gels at specific percentages allowed for optimal separation of proteins in differing molecular weight ranges. All gels were cast in two parts; a larger resolving gel of pH 8.8, topped with a smaller stacking gel of pH 6.8.

Stacking gel	6% gel
dH_2O	1.65 ml
30% Acrylamide/bis-acrylamide	0.5 ml
1.25 M Tris Base (pH 6.8)	310 µl
10% SDS	25 µl
10% APS	25 µl
TEMED	2.5 µl

Resolving gel (for 2 gels)	8% gel	10% gel	14% gel
dH2O	4.63 ml	3.97 ml	2.63 ml
30% Acrylamide/bis-acrylamide	2.67 ml	3.33 ml	4.67 ml
1.25 M Tris Base (pH 8.8)	2.5 ml	2.5 ml	2.5 ml
10% SDS	100 µl	100 µl	100 µl
10% APS	100 µl	100 µl	100 µl
TEMED	10 µl	10 µl	10 µl

Protein samples for western blotting, either monolayer cell cultures or murine tissue, were homogenised directly in 2X Laemmli gel-loading buffer and then boiled for 5 min. To remove debris, samples were centrifuged at 13000 rpm and supernatant collected and used for SDS-PAGE.

2X Laemmli gel-loading buffer:
100 mM Tris-HCl (pH 6.8)
20% glycerol
4% SDS
0.2% bromophenol blue
200 mM 2-mercaptoethanol

Equal amounts of sample in 2X Laemmli buffer were loaded into the wells of the stacking gel and were run alongside 5 µL Precision Plus Protein Dual Color standard (BioRad) to allow molecular weight to be determined. Gel electrophoresis was performed using 1X Running buffer (25 mM Tris, 200 mM glycine, 0.1% SDS) with a mini-PROTEAN 3 gel electrophoresis system (BioRad) at 200 V until the desired protein separation was reached.

For determining the presence of known proteins, western blotting was performed using protein-specific antibodies. Proteins separated in polyacrylamide gel were transferred to a polyvinylidene difluoride (PVDF) membrane (Amersham Hybond-P, GE Healthcare) using a semi dry transfer block. Briefly, following SDS-PAGE, the gel was washed in 1X transfer buffer (25 mM Tris, 150 mM glycine, 20% methanol) for 10 min. The hydrophobic PVDF membrane was prepared by rinsing in 100% methanol followed by dH_2O and then washed in 1X transfer buffer for 10 min. To transfer proteins from the gel to the membrane, the stack was arranged in the following order on the semi dry transfer block:

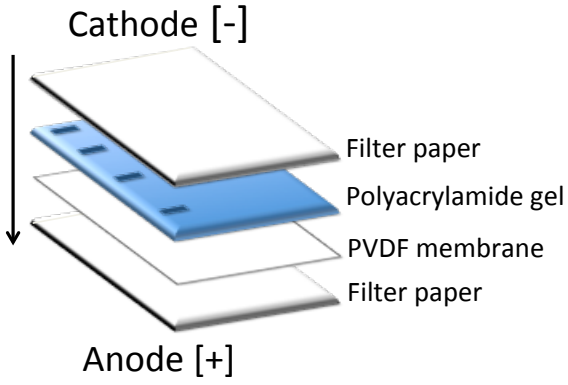

Current was applied at 50 mA for 1.5 h.

Following transfer, membranes were washed in TBS-T and blocked in 4% non-fat milk (Marvel) in TBS-T for 1 h at RT. Membranes were incubated in primary antibodies overnight at 4°C (for list see Appendix). Following washes in TBS-T, membranes were incubated in anti-mouse or anti-rabbit horseradish peroxidase-conjugated secondary antibodies (GE Healthcare, 1:3000) for 1 h at RT and washed again in TBS-T. Immunoreactivity was visualised using chemiluminescent western blotting detection reagents (ECL Prime, Amersham) according to manufacturer's instructions. All antibodies used for western blotting were diluted in 4% non-fat milk in TBS-T. As a loading control, membranes were re-probed with mouse anti-β actin primary antibody, 1:3000 (Sigma-Aldrich) for 1 h at RT followed by secondary antibody and developing steps. For quantification of western blots, band intensity after ECL reaction and exposure to film was determined using a FluoroChem Q system and Alphaview Q software (ProteinSimple).

10X TBS:
0.5 M Tris base
1.38 M NaCl
0.027 M KCl
Diluted to 1X working solution with dH_2O and the addition of 10% Electran $Tween_{20}$ (VWR) to give 1x TBS-T

2.2.11 Immunoprecipitation

Immunoprecipitation was performed to elute specific proteins of interest and bound proteins from cell culture lysates. Cells were washed in PBS 24 h post-transfection and lysed in ice cold IP buffer (1% Triton X-100 in PBS) and incubated on ice for 20 min with periodic vortexing. Lysates were centrifuged at 13000 rpm for 20 min in a cold centrifuge to pellet any remaining whole cells and cellular debris and supernatant was collected for immunoprecipitation. Input sample was taken at this point to confirm original presence of proteins in the lysate. Where required, RNase A treatment was performed at RT for 30 min. Following this, lysates were pre-incubated with either anti-GFP antibody (Protein Synthesis, clone 3A9) or anti-p54nrb antibody (Sigma-Aldrich) in IP buffer for 30 min followed by incubation with Protein A/G sepharose beads (GE Healthcare) for 2 h at 4°C with slow rotation. Alternatively, GFP-Trap agarose beads (ChromoTek) preloaded with anti-GFP antibody were used, avoiding the need to pre-incubate lysates. Beads were then washed twice in ice cold IP buffer, and bound immunocomplexes were eluted from beads by boiling for 10 min at 100°C in SDS–

PAGE loading buffer. In the case of Protein A/G sepharose beads, control samples were prepared by omitting the antibody step. To remove beads, samples were centrifuged at 2000 g for 2 min. Samples were then analysed by western blotting. For input, 10% of final IP sample was loaded.

2.2.12 Quantitative reverse transcription PCR (RT-qPCR)

RT-qPCR was used to quantify relative gene expression. Following reverse transcription of total RNA extracted from either RNA-*later* (Qiagen)-stabilised murine tissues or monolayer cell cultures, qPCR was carried out in a 20 µl reaction, combining 2 µL cDNA (1:3 dilution) with 18 µl qPCR master mix (all ThermoScientific unless stated otherwise). qPCR master mix was prepared prior to each experiment as follows:

qPCR mastermix:	For 24 wells:	Final concentration per well
10X TrueStart PCR buffer	50 µl	1X
25 mM $MgCl_2$	50 µl	2.5 mM
100 mM dNTPs	5 µl	1 mM
15X SYBR green I stock	5 µl	0.15X
50X ROX	5 µl	0.5X
100 µM gene-specific primers (Sigma-Aldrich)	5 µl	1 µM
TrueStart hot start *Taq* polymerase	3 µl	0.15 units
dH_2O	to 335 µl	

15X SYBR green I stock:	
10,000X SYBR green I nucleic acid gel stain (Invitrogen)	1 µl
DMSO	to 660 µl

Reactions were run in triplicate on an ABI StepOne real-time PCR instrument (Applied Biosystems) using the following cycle parameters:

1 cycle	95ºC for 10 min (denaturing & *Taq* activation)
40 cycles	95ºC for 15 sec (denaturing) 60ºC for 60 sec (annealing & extension)

Analysis was performed using StepOne v2.0 software (Applied Biosystems) according to the comparative C_T method (Schmittgen and Livak, 2008) using GAPDH as a reference gene. For qPCR primer sequences, see Appendix.

2.3 Transgenic mice

2.3.1 Generation of transgenic mice

In this thesis, two murine models neuronally expressing experimental forms of FUS were characterised. FUS 1-359 mice lacked the NLS and major RNA-binding domains, shown previously to be the RGG and ZF domains in an RNA-binding assay of varying domain deletion constructs (Bentmann *et al.*, 2012) (See Figure 1.4 for domain information of FUS). RRM is not a major domain required for FUS to bind RNA, which distinguishes it from canonical RRM domains (Bentmann *et al.*, 2012; Clery *et al.*, 2008; Liu *et al.*, 2012; Zinszner *et al.*, 1997b). Instead, RRM is thought to impart specificity of RNA binding (Lerga *et al.*, 2001; Zinszner *et al.*, 1997b) and to investigate this, FUS ΔRRMcyt mice, lacking RRM and harboring the R522G mutation for cytoplasmic-targeting of the protein were also characterised.

Transgenic mice expressing human FUS 1-359 under control of the Thy-1 promoter were previously generated by our laboratory, with special mention to Dr Natalia Ninkina, in collaboration with Dr Alexey Deykin at the Institute of Gene Biology, Russian Academy of Sciences. Briefly, human FUS cDNA was amplified from a plasmid containing FUS cDNA (100004335/OCAA44 g1, Source BioScience) using the following primers:

XhoI_transFUSup: 5'-AGCGGTGTTGGAACTTCGTTG-3'
transFUSdown_XhoI: 5'- AGAATTCTTACCATCAAACC-3'

This PCR fragment was cloned into pCR-Blunt II-TOPO vector and resulting plasmid was purified as described above. XhoI restriction digest was used to isolate FUS 1-359 including 9 bp of 5'UTR. This was inserted between XhoI sites of the Thy-1 promoter plasmid, 323-pTSC21k (Luthi *et al.*, 1997), resulting in insertion between exons II and IV of the Thy-1 gene. Correct orientation of insertion was confirmed by the specific pattern of fragment sizes following EcoRI restriction digest. NotI restriction digest of this plasmid was performed and the correct fragment containing FUS sequence of interest was isolated following excision and purification from agarose gel as described above. This fragment was randomly integrated into the genome following pronuclear microinjection of mouse oocytes derived from a C57Bl6/CBA mouse. Oocytes were

then transferred into a pseudopregnant female and transgenic offspring were identified by conventional PCR analysis from ear biopsies, confirming the insertion of the Thy-1 cassette (see 2.3.3). Two founders were produced and used to establish hemizygous lines F19 and F6 by backcrossing with C57Bl6 mice for >7 generations.

FUS mice expressing human FUS ΔRRMcyt mutant under control of the Thy-1 promoter were also produced by our laboratory in collaboration with Dr Alexey Deykin at the Institute of Gene Biology, Russian Academy of Sciences. XhoI restriction sites were added either end of the FUS ΔRRMcyt mutant by amplification from N-terminally GFP-tagged FUS ΔRRMcyt mutant using the following primers:

XhoI_transFUSup: 5'-AGCGGTGTTGGAACTTCGTTG-3'
hFUSdwnfullXho: 5'-GTCTCGAGTTAATACGGCCTCTCCCT-3'

Methodology from therein was the same as described for FUS 1-359 mice. Two female founders were produced but transgenic lines were unable to be established due to early deaths and a prominent tremor phenotype in TG F1 generation mice. As such, analysis of these mice was restricted because of limited availability.

For quantification of neuromuscular junctions, FUS 1-359 transgenic mice were crossed with Thy1-YFP-16 mice (The Jackson Laboratory) producing offspring which all expressed yellow fluorescent protein (YFP) under control of the Thy-1 promoter, with half of these additionally expressing FUS 1-359 protein also under control of Thy-1 promoter.

2.3.2 Animal husbandry

Mice were housed in 12 h-12 h light-dark cycles with *ad libitum* access to food and water. Mice were housed across two separate animal units with no more than 5 to a cage. All work carried out on animals was performed in accordance with the United Kingdom (Scientific Procedures) Act (1986) and European Directive EC 86/609.

2.3.3 Genotyping

Conventional PCR was used to detect the insertion of the FUS transgene (either 1-359 or ΔRRMcyt) in genomic DNA. Genomic DNA was extracted from an ear biopsy using the Wizard SV genomic DNA purification kit (Promega) according to manufacturer's instructions. The PCR reaction was set up as described above.

FUS forwards: 5'-TCTTTGTGCAAGGCCTGGGT-3'
FUS reverse: 5'-AGAAGCAAGACCTCTGCAGAG-3'

Cycling parameters:

1 cycle	94ºC for 2 min (denaturing)
30 cycles	94ºC for 15 sec (denaturing) 58ºC for 30 sec (annealing) 68ºC for 40 sec (extension)
1 cycle	68ºC for 5 min (finish all extension)
1 cycle	4ºC ∞ (storage until removed)

To permit the distinction between mice expressing the transgene in a hemizygous or homozygous manner, i.e. the number of copies of the transgene, quantitative PCR (qPCR) was performed by Dr Natalia Ninkina. This was carried out in a 20 µl reaction, combining 2 uL genomic DNA with 18 ul freshly prepared qPCR master mix, as described above.

2.3.4 Behavioural testing

Gait analysis

Mice were trained to run along a narrow ambiently lit Perspex corridor into a darkened area where they received a cereal reward. For each run, the floor of the corridor was lined with removable white paper. Blue and red inks (Pelikan) were used to cover the hind and forelimbs, respectively, of each mouse immediately prior to the trial run, allowing for the placement of these limbs during the run to be assessed.

2.4 Histology

2.4.1 Fixation of tissues

Mice were sacrificed either by Schedule 1 method or were perfused with 4% PFA in PBS (pH 7.4). For perfusion, mice were given a lethal intraperitoneal injection of sodium pentobarbital (Euthetal, Merial) and transcardially perfused with an ice cold PBS pre-wash followed by 4% PFA in PBS. Tissues were dissected and collected into 4% PFA in PBS. Duration of fixation was adjusted for the tissue type:

Brain	4% PFA in PBS overnight at 4 °C
Spinal cord	4% PFA in PBS overnight at 4 °C

Gastrocnemius	4% PFA in PBS 30 min at RT

Fixed tissues were then processed and embedded for either paraffin or frozen sections.

2.4.2 Preparation of paraffin sections

PFA-fixed samples were dehydrated and then cleared by passage through the following series:

PBS	15 min (x4)
70% ethanol	3 h
95% ethanol	5 min (x3)
100% ethanol	40 min
1:1 ethanol:chloroform	30 min
chloroform	60 min
chloroform	Overnight (4ºC)

Following clearing in chloroform, tissues were infiltrated with molten paraffin wax (ThermoScientific) at 60ºC for 3 h. Tissues were then oriented in stainless steel moulds, surrounded with molten paraffin wax and left to set on a cold plate. 8 µm sections were cut from paraffin-embedded tissues using a microtome (Leica). Sections were floated on dH_2O at 40ºC and collected onto polysine microscope slides. Sections were left to dry overnight prior to further applications. For stereological quantification, serial sections were taken and arranged in the following manner:

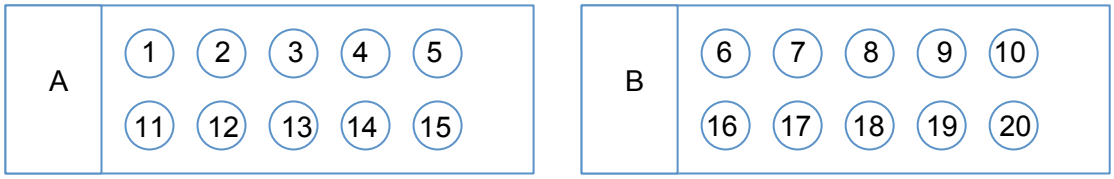

This produced two sets of slides, A and B, with set B acting as a backup for repetition or permitting separate staining of the same region of tissue.

2.4.3 Preparation of frozen sections

PFA-fixed samples were cryoprotected by passage through a gradient of sucrose solutions (10-30% sucrose in PBS) at 4°C until tissues sank. Following infiltration of

sucrose, tissues were embedded in optimal cutting temperature (OCT) compound (ThermoScientific) in removable plastic moulds (VWR International) and flash-frozen on a 1:1 slurry of ethanol and dry ice. For quantification of neuromuscular junctions in gastrocnemius muscle, 35 µm longitudinal sections of OCT-embedded muscle were cut on a cryostat (Leica CM1850, Leica Biosystems) set to -20°C and transferred directly onto polysine-coated microscope slides (ThermoScientific). Sections were left to dry overnight prior to further applications or long term storage at –80°C.

2.4.4 Human tissue samples

For assessment of paraspeckle protein localisation in human patient tissues, human spinal cord paraffin sections from clinically and histopathologically characterised disease and control cases were obtained from the MRC London Neurodegenerative Diseases Brain Bank (Institute of Psychiatry, King's College, London). Consent was obtained from all subjects for autopsy, histopathological assessment and research in accordance with local and national Ethics Committee approved donation. Histological experiments performed on human tissue samples were carried out by Dr Tatyana Shelkovnikova.

2.4.5 Cresyl violet staining

For visualisation and quantification of neuronal populations, 8 µm paraffin sections of mouse brain and spinal cord were stained with cresyl violet. Using this technique, motor neurons were identified by their distinctive staining pattern comprising of dark nucleolar staining and pale pink cytoplasm. First, sections were dewaxed in xylene and brought to water through a series of decreasing ethanol percentage. Once brought to water, samples were stained with 0.5% cresyl violet acetate in dH_2O for 20 min. Staining was differentiated and tissues dehydrated through a series of increasing ethanol percentage followed by clearing in xylene prior to mounting in DPX mounting medium (RA Lamb).

For stereological quantification of motor neurons in brainstem nuclei or ventral horns of spinal cord, serially sectioned paraffin sections were arranged as described above and a single set stained with cresyl violet. Motor neurons with visible nucleoli were counted in every 10^{th} section at 40x magnification either over a 1 mm distance of ventral horn spinal cord or over the total length of a coronally sectioned brainstem nucleus.

2.4.6 Haematoxylin and eosin

Paraffin embedded cross-sections of mouse gastrocnemius muscle were dewaxed in xylene and brought to water through a series of decreasing ethanol percentage. Sections were incubated in Gill's haematoxylin (Leica) for 5 min and excess staining was removed in dH_2O followed by 30 s incubation in acidified ethanol (1% glacial acetic acid in ethanol). Following washing in dH_2O, sections were incubated in 1% eosin for 5 min followed by further washing, dehydration to xylene and mounting in DPX mounting medium.

2.5 Immunohistochemistry

2.5.1 Standard immunohistochemistry

For determining the location of specific proteins in mammalian tissue samples, 8 µm paraffin embedded sections were dewaxed in xylene and rehydrated through a series of decreasing ethanol percentage. Antigen retrieval was then performed using microwave irradiation of tissues in 10 mM sodium citrate (pH 6). Following cooling, background oxidase activity in the tissue was quenched using 3% hydrogen peroxide in methanol at 4°C for 30 min. Tissues were blocked for 30 min at RT in 10% goat serum/ 0.1% tween 20 in PBS. Primary antibodies were applied for either 1.5 h at RT or overnight at 4°C. Following washes with PBS, anti-mouse or anti-rabbit biotinylated secondary antibodies (Vector Labs) diluted 1:1000 in 0.1% tween in PBS were applied for 1 h at RT. Tissues were washed in PBS and avidin-biotin HRP complexes (VECTASTAIN ABC kit, Vector labs) were applied for 45 min. After washing, 3,3'-diaminobenzidine (DAB) at a final concentration of 10 mg/ml was used as a substrate for HRP and applied until a dark brown pigment developed, usually between 5-7 min. Following DAB, tissues were washed in dH_2O and dehydrated through a series of increasing ethanol percentage before being cleared in xylene and mounted in DPX mounting medium.

2.5.2 Fluorescent immunohistochemistry

Fluorescent immunohistochemistry was performed largely in instances where the localisation of two or more proteins at the same time in the same tissue sample was required. For this, 8 µm paraffin embedded sections were prepared in the same way as those used for standard DAB immunohistochemistry, minus quenching of background oxidases. Following incubation with primary antibodies and washes in PBS, Alexa fluor-conjugated secondary antibodies (1:1000 dilution in 0.1% tween 20 in PBS), anti-mouse or anti-rabbit, were applied for 1 h at RT. Following washes, DAPI stain at a

final concentration of 1 μg/ml was applied for 5 min. Tissues were finally washed in dH_2O and mounted in ImmuMOUNT.

For proteinase K treatment, the proteinase K enzyme (Fermentas) was diluted in Tris buffer (10 mM Tris-HCl, pH 7.5, 5 mM EDTA) to a final concentration of 200 μg/ml. Sections were dewaxed, rehydrated, washed with PBS, and incubated in proteinase K solution for 1 h at 37ºC in a humidified chamber. After several thorough washes, anti-FUS staining and DAPI staining were performed as above.

For quantification of neuromuscular junctions, 35 μm frozen sections of gastrocnemius muscle were washed in PBS and incubated in blocking solution (0.4% tween 20, 10% goat serum in PBS) at RT for 1 h. To fluorescently label acetyl choline receptors present at the neuromuscular junction, sections were then exposed to Alexa 647-conjugated alpha-bungarotoxin (1:1000, ThermoScientific) diluted in blocking solution for 1 h at RT. Following washes in PBS, sections were mounted in Immumount and left to dry. Images were taken using a laser scanning confocal DM6000B microscope (Leica Microsystems) and processed using the Leica confocal software.

2.6 Statistics

Statistical analysis was performed using IBM SPSS Statistics software (IBM). Data were tested for normality of distribution using the Shapiro-Wilk test, where $p>0.05$ indicated normal distribution. Parametric testing was used when the assumption of normality was met and the size of data groups was sufficiently large. These included the Student's t test for determining whether two groups were significantly different from each other, and analysis of Variance (ANOVA) with *post-hoc* testing for comparing three or more groups. Where the assumption of normality could not be met, often due to smaller sample size, the non-parametric equivalents of these tests were performed. Non-parametric Mann-Whitney test was used for comparing two groups and the non-parametric Kruksal-Wallis test was performed for three or more groups. Significance was assigned to p-values less than or equal to 0.05 ($p<0.05$), where rejection of a true null hypothesis, that is that two groups are not significantly different from each other, (type I error) occurs at a frequency of <5%.

Results I:

EXPRESSION OF RNA-BINDING-COMPROMISED FORMS OF HUMAN FUS IN THE MURINE NERVOUS SYSTEM

3.1 Declaration and contributions

Data included within this chapter have been published within the following open access articles:

Shelkovnikova TA, Peters OM, Deykin AV, Connor-Robson N, **Robinson HK**, Ustyugov AA, Bachurin SO, Ermolkevich TG, Goldman IL, Sadchikova ER, Kovrazhkina EA, Skvortsova VI, Ling SC, Da Cruz S, Parone PA, Buchman VL, Ninkina NN. Fused in sarcoma (FUS) protein lacking nuclear localization signal (NLS) and major RNA-binding motifs triggers proteinopathy and severe motor phenotype in transgenic mice. *J Biol Chem*. (2013) Aug 30;288(35):25266-74.

Robinson HK, Deykin AV, Bronovitsky EV, Ovchinnikov RK, Ustyugov AA, Shelkovnikova TA, Kukharsky MS, Ermolkevich TG, Goldman IL, Sadchikova ER, Kovrazhkina EA, Bachurin SO, Buchman VL, Ninkina NN. Early lethality and neuronal proteinopathy in mice expressing cytoplasm-targeted FUS that lacks the RNA recognition motif. *Amyotroph. Lateral Scler. & Frontotemp. Demen.* (2015). May 20:1-8.

3.2 Overview: Part I

In the General Introduction it was discussed that murine models of FUSopathy produced to date have largely focused on overexpressing either WT FUS or FUS carrying ALS-associated missense mutations, with neurodegenerative phenotypes noted to varying extents. However, many of these models have not been able to recapitulate the aggregation of FUS into large inclusions that is widespread in human ALS-FUS patients. Furthermore, expressing full length RNA-binding-competent forms of human FUS may cause toxicity by disrupting RNA metabolism homeostasis through aberrant RNA interactions produced by the exogenous protein. Given that there is conflicting evidence surrounding the pathological origins of FUS toxicity in ALS-FUS patients, we sought to investigate the effects that an initial insult of FUS aggregation, independent of primary disruption to RNA metabolism homeostasis, may have on the common tissue targets of ALS. Therefore, following our preliminary observations in cell culture, we generated, in collaboration with colleagues at the Institute of Gene Biology, Russian Academy of Sciences, a novel murine model of FUS aggregation through neuronal expression of a C-terminally truncated form of human FUS. This protein lacked major RNA-binding domains and the NLS (FUS 1-359), compromising its interactions with RNA. The first half of this chapter focused on the behavioural,

histological and biochemical analyses of these mice and the subsequent insights into FUS pathology that arose.

3.3 Results: Part I

3.3.1 Aggregation of FUS mutants in the cytoplasm of SH-SY5Y cells

To first investigate the aggregation propensity of FUS isoforms associated with varying capacity for RNA interactions, a series of mutant FUS constructs, each tagged with a widely used reporter, GFP, to aid visualisation were produced through molecular cloning techniques and expressed transiently in human neuroblastoma (SH-SY5Y) cells (Figure 3.1A). GFP tags were placed at the N-terminus as this has previously been validated as a mechanism of modeling FUS localisation, whereas adding an GFP tag at the C-terminus has been shown itself to alter localisation of the protein (Kino *et al.*, 2011). In addition to endogenous full length FUS (WT FUS) protein, ALS-linked mutant proteins were created, harboring either the missense mutation, R522G, or the proposed protein product of the G466VfsX14 mutation that is thought to result in a C-terminal truncation leaving only amino acids 1-466 (DeJesus-Hernandez *et al.*, 2010). To investigate the aggregation of isoforms with proposed disruption to their RNA-binding capacity, additional experimental mutants were created, lacking either NLS (FUS 1-513), NLS, ZF and RGG domains (FUS 1-359), or lacking simply the RRM domain in conjunction with the R522G mutation to render the protein cytoplasmic (FUS ΔRRMcyt). Indeed, deletion of NLS, RGG and ZF domains in even a slightly longer FUS mutant construct (FUS 1-375) was previously shown to lack RNA-binding capacity (Bentmann *et al.*, 2012). Western blotting of whole cell lysates from human neuroblastoma (SH-SY5Y) cells transfected with these expression plasmids using an anti-GFP antibody confirmed that the appropriate sized proteins were being expressed comparably in these cells (Figure 3.1B).

As expected, GFP-tagged WT FUS maintained a nuclear localisation in these cells (Figure 3.1D). Early after transfection, between 4 and 12 h, ALS-associated mutant R522G, ΔNLS mutant 1-513, and cytoplasmic FUS lacking RRM domain all displayed a diffuse distribution in the cytoplasm (Figure 3.1C). This was also seen at later times in cells expressing low levels of the protein. However, even at this early stage, FUS 1-359, lacking NLS, RGG domains and ZF, showed the formation of distinct small puncta in the cytoplasm (Figure 3.1C). By 36 h post-transfection, mutant FUS constructs had formed granule-like aggregates in the cytoplasm to varying extents (Figure 3.1D). However, whilst mutants 1-513, R522G, 1-466 all showed the formation of similar

structures, the pattern of FUS 1-359 was distinctive. In SH-SY5Y cells transfected with FUS 1-359, large juxtanuclear aggregates formed that appeared more similar to the large inclusions seen in ALS-FUS patient tissues. Interestingly, these were also seen in rarer instances in cells transfected with another RNA-binding-compromised form of FUS, FUS ΔRRMcyt (Figure 3.1D). Therefore, we sought to determine whether an initial insult of FUS aggregation, irrespective of introducing aberrant interactions with RNA, was sufficient to produce features of ALS pathology *in vivo* (Figure 3.2A).

3.3.2 Expression of human FUS 1-359 in the murine nervous system

Thy-1 promoter was chosen to express FUS 1-359 in these mice as this produces a neuronal expression pattern that has been used successfully in several other models (McGoldrick *et al.*, 2013). Biochemical analysis by western blot confirmed that the C-terminally truncated FUS 1-359 protein was expressed in the spinal cord, brainstem and cortex of TG but not non-transgenic, herein referred to as 'WT', littermates (Figure 3.2B). Tissues were taken from 4 month old F19 hemizygous TG or WT mice. This shorter human truncated protein displayed a molecular weight of ~55 kDa compared to the larger full length endogenous protein at ~70 kDa, making it easily distinguishable. Both forms were readily detected by an antibody to the N-terminus of FUS, and in the neural tissues of transgenic mice FUS 1-359 was expressed at a low level compared to endogenous full length FUS (Figure 3.2B). Using an antibody that specifically detected human FUS, hemizygous F19 mice were shown to express FUS 1-359 protein at a higher level compared to hemizygous mice from a second line, also expressing FUS 1-359 (F6) (Figure 3.2C).

3.3.3 Phenotype, behaviour and survival

FUS 1-359 F19 hemizygous mice were indistinguishable from WT littermates until around 2.5-4.5 months when they began to develop an obvious motor phenotype. An initial limb paresis, most often beginning asymmetrically in the hind limbs, progressed rapidly leading to complete limb paralysis (Figure 3.2D). This limb weakness was easily distinguished in gait analysis traces of these symptomatic mice compared to WT littermates (Figure 3.2E). This short window of 'end-stage' disease lasted no more than 2 weeks, during which mice became emaciated and dehydrated, eventually losing their self-righting reflexes, resulting in reduced survival of these mice in two separate cohorts (Figure 3.2F and 3.6C).

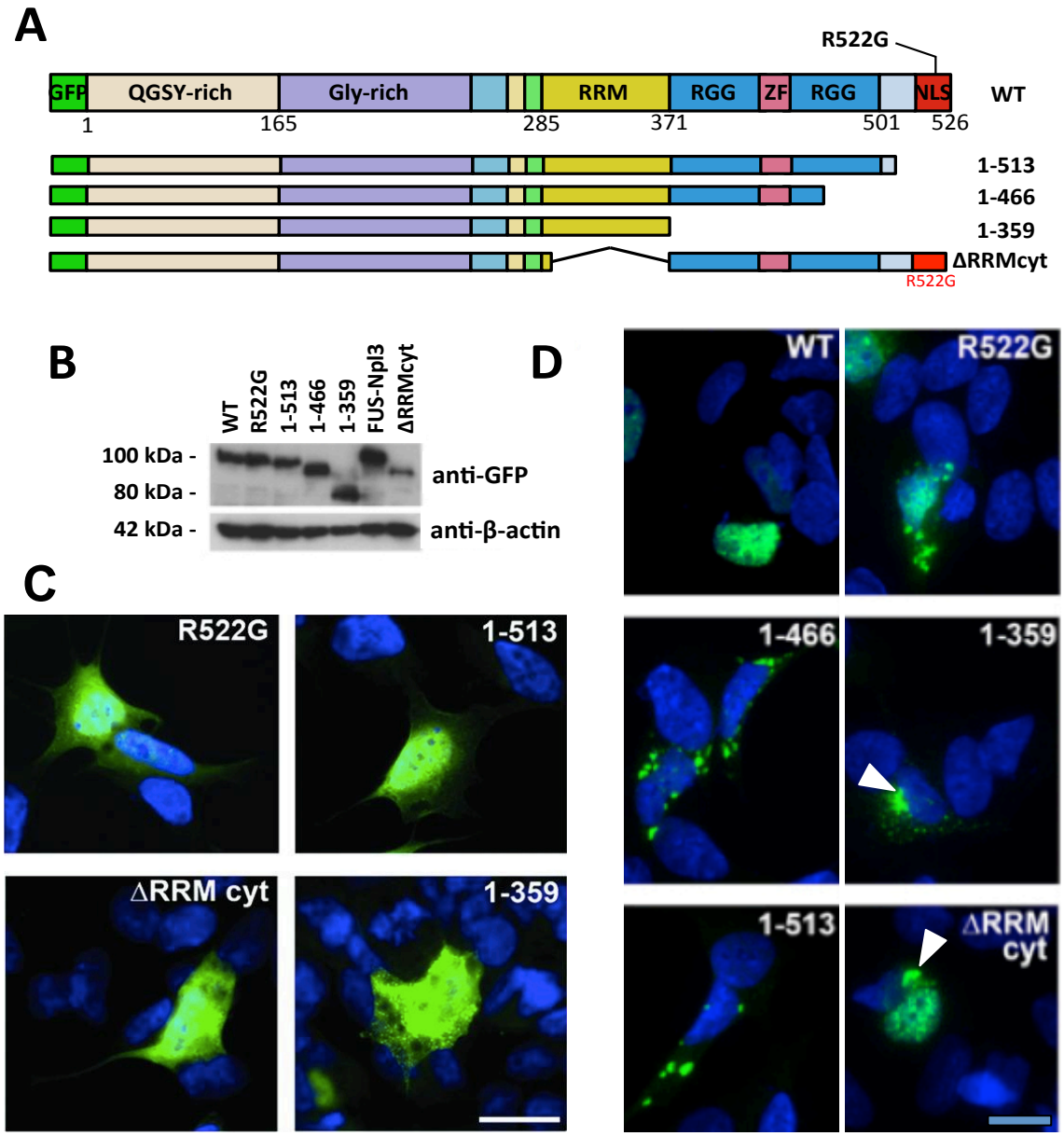

Figure 3.1. Mutant FUS constructs N-terminally tagged with GFP aggregate over time in the cytoplasm of SH-SY5Y cells. (A) Domain map of mutant FUS constructs used. The single thin line denotes deletion of this region in the ΔRRMcyt construct. (B) Western blot of total cellular lysates 24 h post-transfection with expression plasmids using anti-GFP antibody and reprobing with anti-β-actin antibody. (C) Early after transfection (4-12 h), R522G, 1-513 and ΔRRMcyt mutant FUS proteins showed a diffuse distribution, whereas even at this early stage, FUS 1-359 formed very small granular structures. (D) The degree of aggregation in the cytoplasm of FUS mutants was greater 36 h post-transfection. Unlike other mutants, FUS 1-359 and in FUS ΔRRMcyt formed large and compact juxtanuclear structures (arrowheads). Green, GFP fluorescence; Blue, DAPI. Scale bars all panels; 15 μm. These data were produced by Dr. Tatyana Shelkovnikova and Dr. Natalia Ninkina. At least 3 biological replicates were performed and representative images are shown.

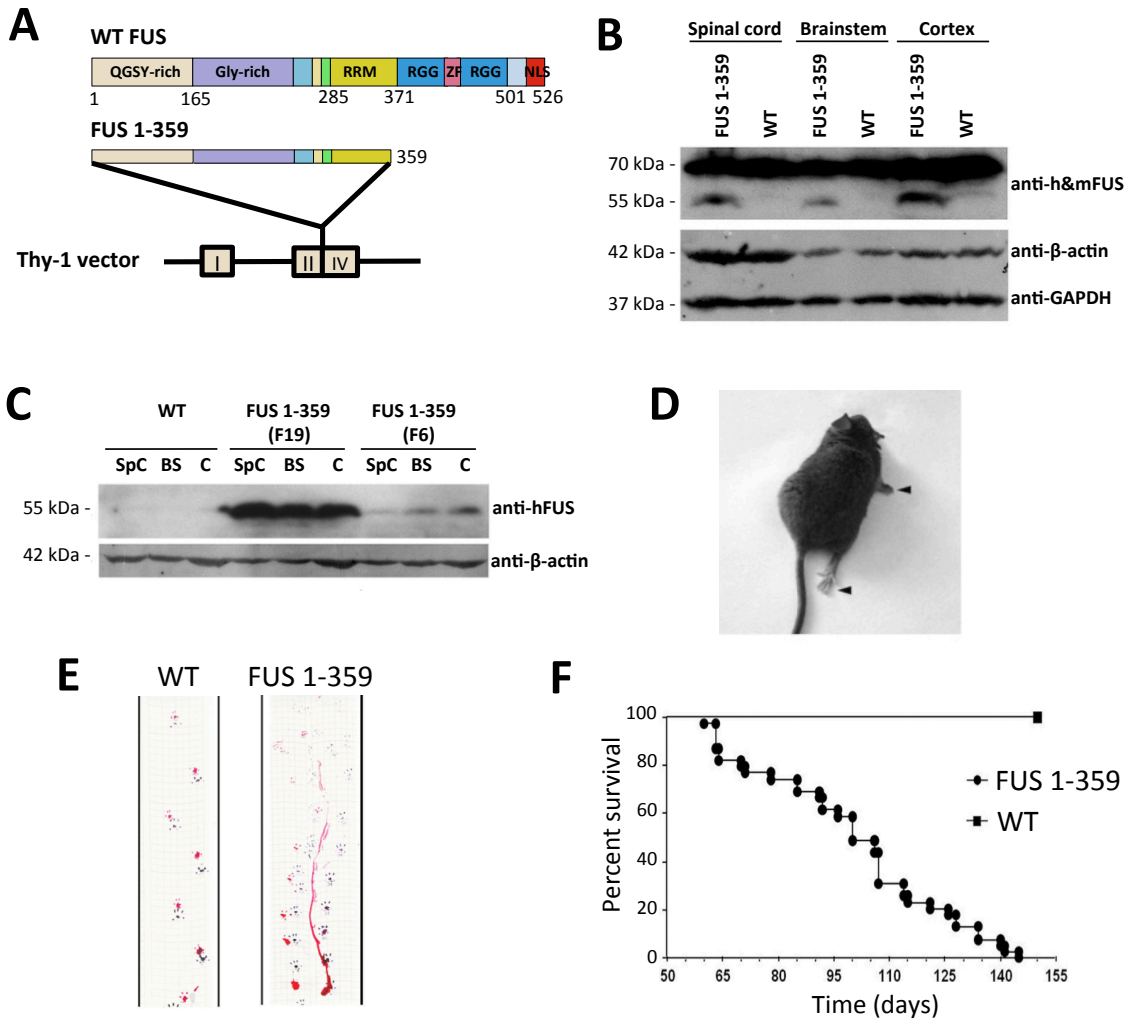

Figure 3.2. Neuronal expression of human FUS 1-359 results in paralysis and reduced survival. (A) A truncated form of WT human FUS (FUS 1-359) is inserted between exons II and IV of Thy-1 vector resulting in neuronal expression of the transgene. (B) Human FUS 1-359, with a molecular weight of 55 kDa, is expressed at a comparatively lower level to endogenous FUS, with a molecular weight of 70 kDa, in FUS 1-359 TG (F19) mice and is absent in non-transgenic (WT) littermates as detected by an antibody recognising both endogenous and human mutant FUS (anti-h&mFUS). (C) FUS 1-359 mutant is expressed at a higher level in TG F19 than in TG F6 mice as detected by an antibody recognising only human FUS (anti-hFUS). All tissue samples were taken from 4 month old hemizygous mice. (D) Symptomatic-stage FUS 1-359 TG F19 mouse displaying hind and forelimb paralysis (arrowheads). (E) Gait analysis trace showing altered gait of symptomatic FUS 1-359 TG F19 mouse compared to WT littermate. Blue, forelimbs; Red, hindlimbs. (F) FUS 1-359 FUS TG F19 mice show reduced survival compared to WT mice. These data were generated by Dr. Owen Peters and Dr. Tatyana Shelkovnikova.

On the other hand, FUS 1-359 F6 hemizygous mice, expressing low levels of the transgene, did not display any obvious signs of muscle weakness or paralysis throughout their lifetime. FUS-positive inclusions were only seen in homozygous, aged FUS 1-359 F6 mice, and these were rare compared to those in hemizygous F19 mice (Figure 3.3H). For these reasons, the higher expressing hemizygous F19 TG mice were focused upon for the remainder of analysis and will herein be referred to as FUS 1-359 TG mice.

3.3.4 Proteinopathy in the cytoplasm

To determine whether any FUS-positive structures were present in these TG mice, standard immunohistochemistry was performed on paraffin sections utilising an antibody that recognises the N-terminus of both human and mouse FUS. As expected, FUS maintained a predominantly nuclear localisation in cells of the spinal cord, brainstem and cortex in WT animals (Figure 3.3A-D). However, in end-stage FUS 1-359 TG mice displaying paralysis, prominent FUS staining was observed in the cytoplasm and multiple FUS-positive inclusions were seen, predominantly in the lower motor neurons of the spinal cord and brainstem (Figure 3.3A', B'). These were mainly found in the cytoplasm of these cells although in some populations, nuclear inclusions were observed (Figure 3.3A').

In brainstem neuronal tracts, FUS was redistributed to the axons of these neurons, where multiple spheroids formed (Figure 3.3B',C'). Although observed less frequently, these TG mice at the end-stage of disease also displayed FUS-positive inclusions in cortical neurons (Figure 3.3D'). These findings were recapitulated using an antibody that recognised only human forms of FUS, showing that FUS 1-359 indeed formed these inclusions (Figure 3.3E-G). As with inclusions seen in human ALS patients, these inclusions were not amyloid in nature, indicated by their inability to be stained with either thioflavin S or Congo red (data not shown). These FUS-positive inclusions were also shown to persist following treatment of paraffin embedded tissues with proteinase K (Figure 3.4A), a feature also associated with inclusions in other neurodegenerative diseases (Neumann *et al.*, 2002). As ubiquitinated inclusions are a key feature of ALS, symptomatic FUS 1-359 TG mice were also screened for the presence of these structures. Standard immunohistochemistry with anti-ubiquitin antibodies detected a number of ubiquitin-positive inclusions throughout the neural tissue of these TG mice, although these were seen less frequently compared to FUS-positive inclusions (Figure 3.4B). To determine whether FUS-positive inclusions were ubiquitinated, fluorescent co-localisation studies were performed with anti-FUS and anti-ubiquitin antibodies.

FUS-positive inclusions were differentially positive for ubiquitin, with only a fraction of FUS-positive inclusions ubiquitinated and in some instances, non-overlapping FUS- or ubiquitin-positive aggregates were seen in the same cell (Figure 3.4C), similarly to what is known for human ALS-FUS patients.

In several other neurodegenerative diseases, misfolded proteins of interest, for example α-synuclein in Parkinson's disease and tau in Alzheimer's disease, are able to seed aggregation of endogenous soluble forms, disrupting their normal functions (Luk *et al.*, 2009; Clavaguera *et al.*, 2013). To determine whether similar processes may also be involved in our FUS 1-359 model of FUSopathy, we investigated whether human FUS 1-359 aggregates were able to recruit endogenous FUS. This was done using FUS antibodies recognising epitopes within the C-terminus (absent in FUS 1-359 and recognising only endogenous FUS) or N-terminus (common to both) in fluorescent immunohistochemistry experiments (Figure 3.4D, D'). This double fluorescent labelling showed that in some cells, nuclear FUS 1-359 aggregates in these mice were also positive for endogenous mouse FUS (Figure 3.4D'). Using an antibody that recognises only mouse endogenous FUS, cytoplasmic inclusions were identified in the nucleus of some cells and in rare cases the cytoplasm (Figure 3.4E, E', E"), demonstrating that endogenous FUS was indeed sequestered into abnormal structures.

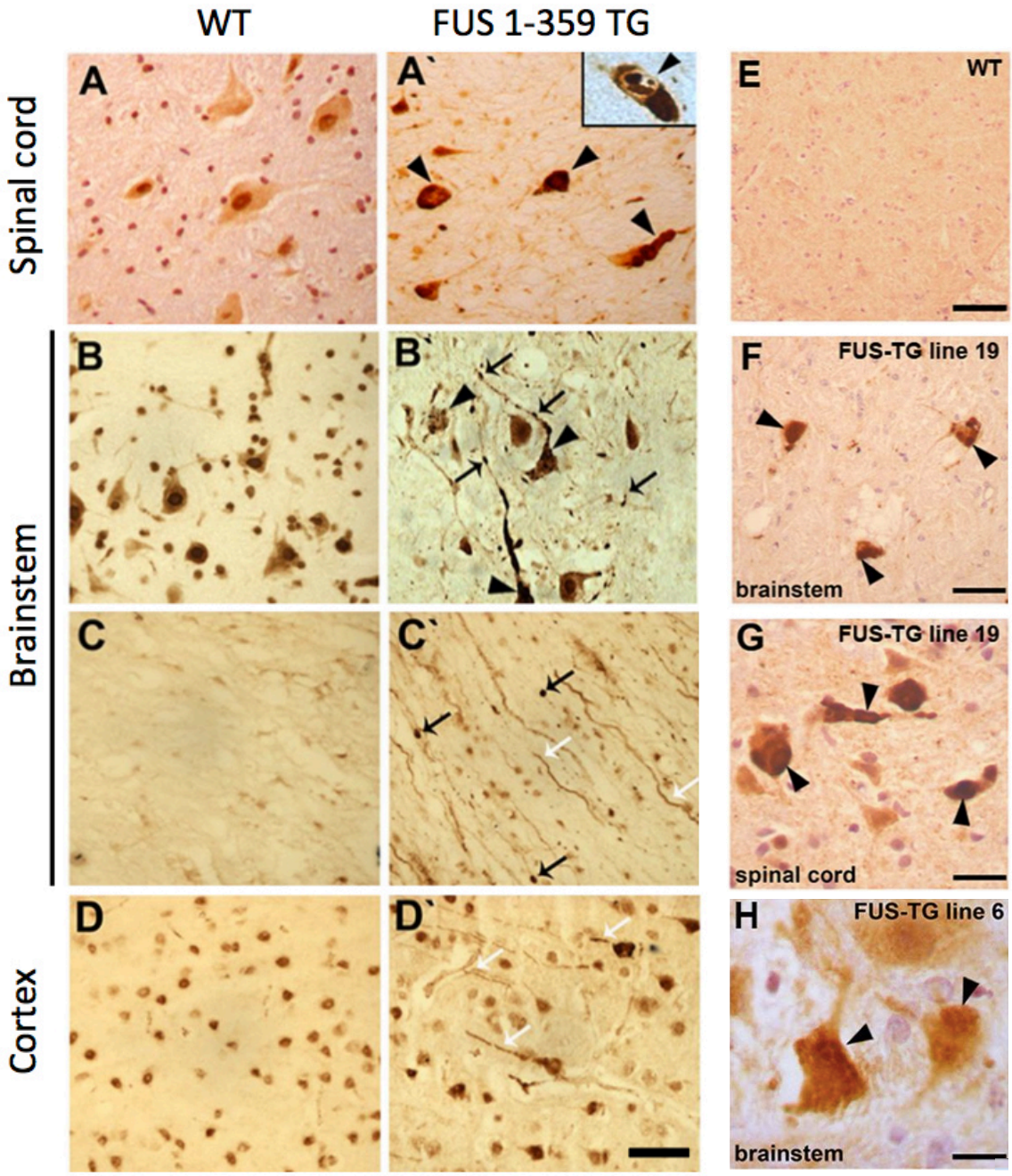

Figure 3.3. FUS 1-539 proteinopathy in the murine nervous system. Representative images following standard immunohistochemistry using antibodies recognising both mouse and human FUS (A-D) or human FUS alone (A'-D' and E). Symptomatic FUS 1-359 TG mice displayed prominent cytoplasmic (arrowheads), and sometimes nuclear (inset), inclusions in (A',G) cells of the anterior horn of the spinal cord and (B',F) brainstem. (A-C) On the other hand, WT mice displayed a prominent nuclear localisation of FUS in these cells. (B',C') FUS 1-359 TG mice also displayed redistribution of FUS into axons (white arrows) of neuronal brainstem tracts where it formed spheroids (black arrows). (D-D') Similar redistribution of FUS was also seen in cortical neurons (D'), whereas localisation remained nuclear in WT cortical neurons (D). (H) Example of FUS staining and formation of inclusion structures in FUS TG F6 mice. Scale bars; A-F, 50 µm; G, 30 µm; H, 15 µm. At least 3 transgenic mice and 3 WT mice were analysed and representative images shown.

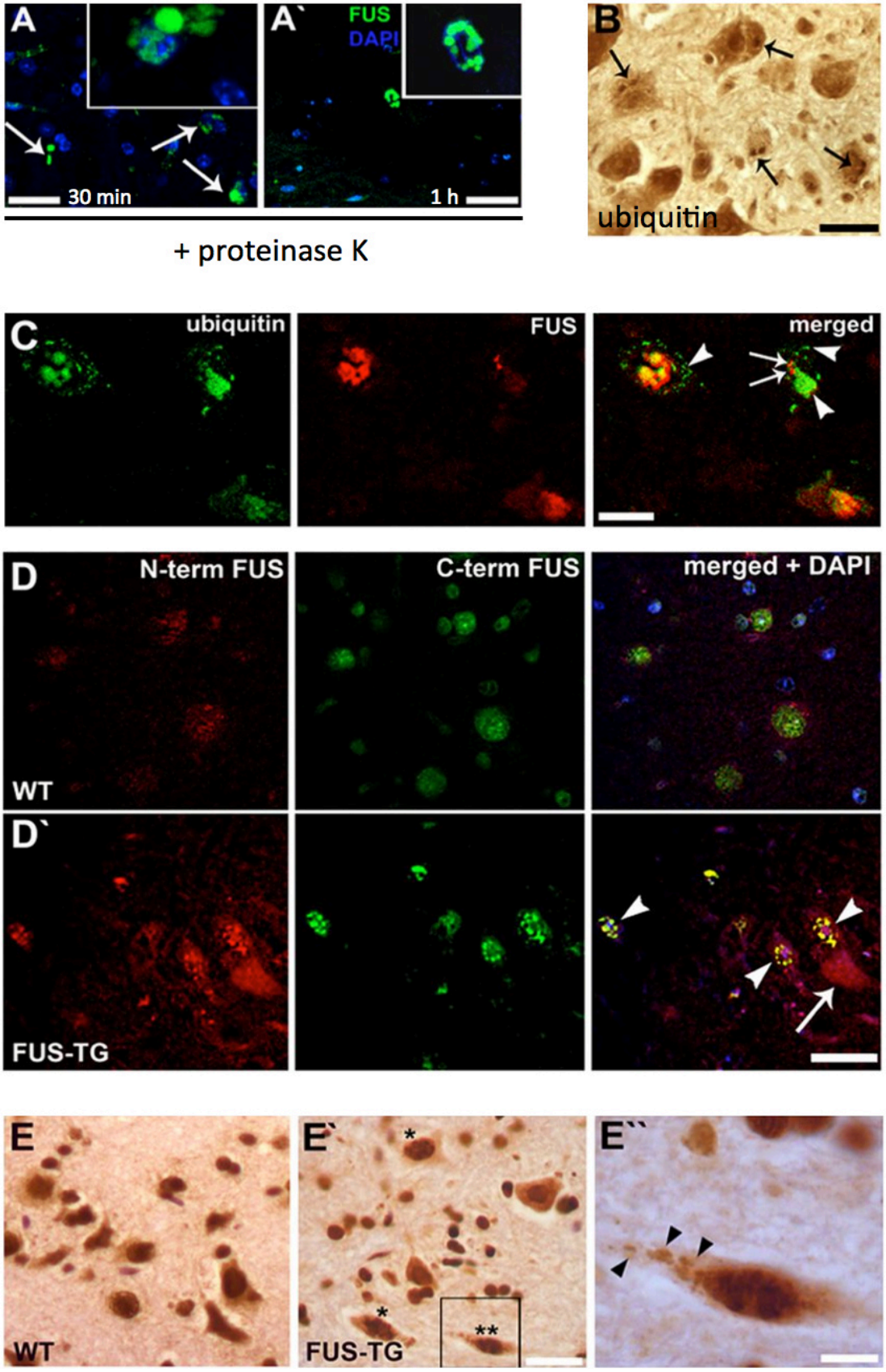
A
30 min
A`
FUS
DAPI
1 h
+ proteinase K
B
ubiquitin
C
ubiquitin
FUS
merged
D
N-term FUS
C-term FUS
merged + DAPI
WT
D`
FUS-TG
E
WT
E`
*
*
**
FUS-TG
E``

Previous page:

Figure 3.4. Characterisation of FUS 1-359 inclusions. FUS 1-359 inclusions in symptomatic TG mice remained present following 200 μg/ml proteinase K treatment of paraffin sections for (A) 30 min or (A') 1 h. (B) Ubiquitin-positive inclusions were also seen in these mice following standard immunohistochemistry. (C) Using fluorescent immunohistochemistry, approximately half of FUS-positive structures were shown to be positive for ubiquitin (arrowheads), whilst some ubiquitin-positive, FUS-negative structures were also seen (arrows). (D-D') Immunoreactivity to endogenous full length FUS detected using an antibody recognising the C-terminus of FUS. Endogenous FUS was redistributed from its normal localisation shown in WT tissues (D) to nuclear inclusions of FUS 1-359 (arrowheads) but was not recruited to cytoplasmic inclusions (arrow) in ventral spinal cord of FUS 1-359 TG (D'). (E-E'') Recruitment of full length FUS to cytoplasmic inclusions (arrowheads) was also seen in FUS 1-359 TG (E', enlarged E'') but not WT mice (E) using standard immunohistochemistry with an antibody that recognises only mouse FUS in the nucleus (*) or cytoplasm (**). Scale bars; A and A′, 50 μm; B–E′, 30 μm; E″, 10 μm. These data were produced by Dr. Tatyana Shelkovnikova. At least 3 transgenic mice and 3 WT mice were analysed and representative images shown.

3.3.5 Effect of FUS 1-359 expression on spinal cord LMNs

In ALS, in addition to the formation of proteinaceous inclusions, prominent loss of motor neurons occurs in the anterior/ventral horn of the spinal cord. Having observed the formation of FUS-positive inclusions in these mice, whether the neuronal expression of FUS 1-359 was sufficient to cause a loss of motor neurons in anterior horn of spinal cord was investigated. For this, motor neurons in the anterior horn across 1 mm of lumbar spinal cord length were quantified using a stereological counting technique performed on cresyl violet stained paraffin sections. The number of motor neurons (MNs) in lumbar spinal cord in symptomatic FUS TG mice was prominently reduced compared to the number of MNs across the same distance in WT littermates and pre-symptomatic mice (Figure 3.5B). In symptomatic FUS TG mice, surviving motor neurons in this region also displayed signs of damage, including chromatolysis, and visible shrinkage, although this was not quantified (Figure 3.5A).

3.3.6 Effect of FUS 1-359 expression on skeletal muscle and its innervation

Because end-stage TG mice rapidly developed an observable paralysis, skeletal limb muscles and any changes to their innervation caused by the expression of this C-terminally truncated FUS mutant were investigated. As paralysis largely affected the hind limbs of these mice, this region was the focus of investigation. Gastrocnemius muscles of end-stage FUS 1-359 TG mice with hind limb paralysis were atrophied compared to healthy WT littermates, observed following dissection and weighing of the whole muscle (Figure 3.6A). Muscle fibres also appeared damaged following haematoxylin and eosin staining of gastrocnemius cross sections (Figure 3.6B).

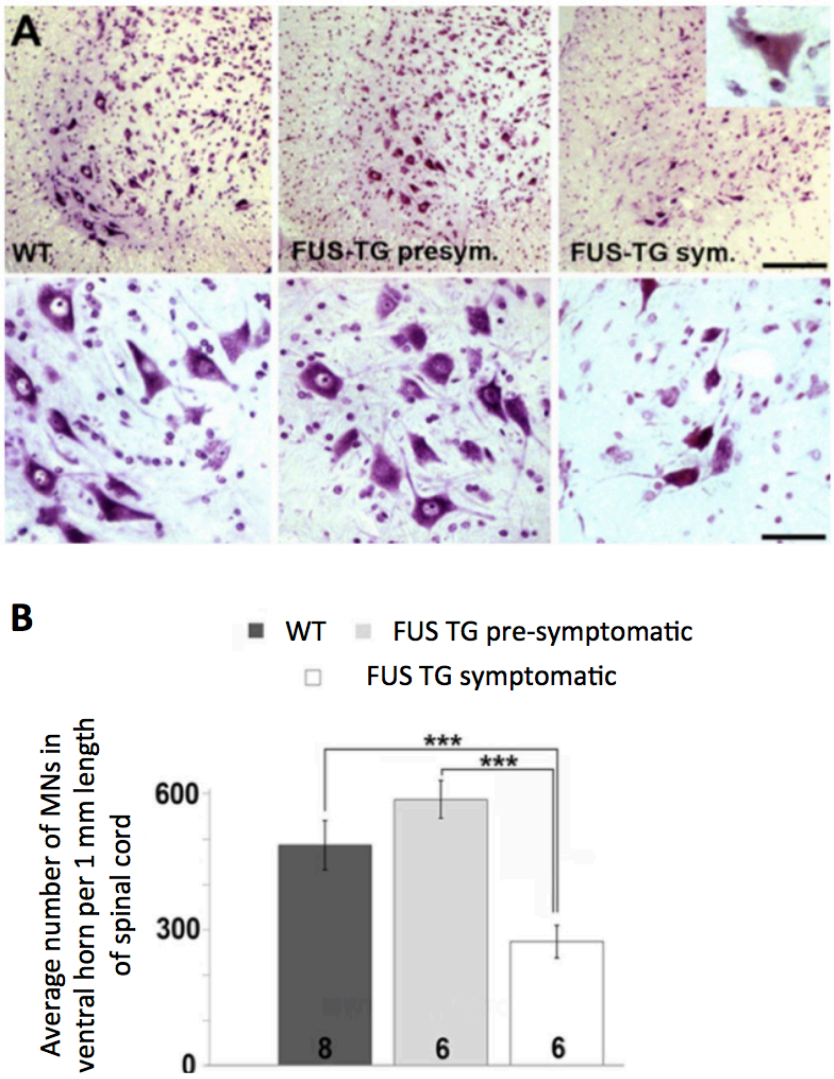

Figure 3.5. Symptomatic FUS 1-359 TG mice display motor neuron loss in the ventral horn of spinal cord. (A) Representative images of cresyl violet stained ventral spinal cord from WT, pre-symptomatic and symptomatic mice, with higher magnification shown in lower panel. Surviving motor neurons of symptomatic mice display signs of degeneration including chromolysis and shrinking (inset). (B) Quantification (mean±S.E.M) of MNs in ventral horn per 1 mm of lumbar (L4-L6) spinal cord tissue in WT, pre-symptomatic and symptomatic mice. Numbers of animals for each group are indicated at the base of each bar. ***, $p<0.001$, Mann-Whitney test. Scale bars; A (upper), 100 μm; A (lower), 30 μm.

Neuromuscular innervation was also investigated in these mice. As immunostaining of axon terminals using a combination of anti-synaptophysin and anti-neurofilament-M antibodies was previously challenging, with antibodies having to be used at very high concentrations, we chose to cross these FUS 1-359 TG mice with a line of mice (thy-1-YFP-16) where axons are fluorescently labelled with yellow fluorescent protein expressed in neurons under control of a Thy-1 promoter. By then counter staining gastrocnemius sections with fluorescently-labelled-α-bungarotoxin, which binds selectively to acetyl choline receptors present at the NMJ, the extent to which each NMJ is innervated can easily be established by observing the degree of overlap (Figure 3.6D). Mice expressing YFP showed similar survival to those on a pure C57/Bl6 background and expression of YFP was, alone, not sufficient to elicit degeneration of axon terminals, enabling the use of these mice to investigate our degenerative FUS 1-359 phenotype without confound (Figure 3.6C, D). To investigate the influence of both the stage of progression (i.e. preceding or following the onset of paralysis) and age on NMJ innervation, quantification of NMJs was performed on WT mice and TG mice with (symptomatic) or without (pre-symptomatic) paralysis across a range of ages (2-5 months old). No significant differences in NMJ innervation were identified between mice of different age groupings when collapsed across stage of progression/genotype ($p>0.05$, Kruksal-Wallis test). However, differences in NMJ innervation were observed between mice grouped by their stage of progression/genotype ($p<0.05$, Kruksal-Wallis test). Indeed, TG mice displaying paralysis (symptomatic) displayed a significant reduction in NMJ innervation compared to WT or non-symptomatic stage TG mice ($p<0.05$, Mann Whitney test) (Figure 3.6D, E). Whilst for this analysis percentage NMJ innervation was averaged across hind limbs, in the majority of cases, as with in humans, paralysis developed asymmetrically in these mice. Further analysis of symptomatic stage TG mice revealed that, somewhat surprisingly, in addition to the loss of innervation in the affected 'paralysed' limb ($p<0.05$, Mann Whitney test), the corresponding limb showing no outward signs of paralysis or weakness also showed significant reductions in percentage NMJ innervation compared to WT mice ($p<0.05$, Mann Whitney test), although there remained a small but significant difference between these two states (Figure 3.6F).

Analysis of the sciatic nerve, which innervates the lower limb, was performed by lab member, Dr Owen Peters. This showed that only symptomatic FUS TG mice displayed significant loss of, and damage to, myelinated axons compared to WT littermates (Figure 3.7A, B, C). In additional experiments performed by Dr Owen Peters, dorsal

(sensory) roots showed less damage compared to the extensive damage to ventral (motor) roots in symptomatic stage mice (Figure 3.7A).

3.3.7 Effect of FUS 1-359 expression on brainstem motor nuclei

Although cytoplasmic FUS-positive inclusions were previously observed in the brainstem tracts of these mice (Figure 3.3C'), whether inclusions were also present in the cells of brainstem motor nuclei and whether there was any associated loss of motor neurons in these regions, was also investigated. Indeed, prominent FUS-positive inclusions were detected in the facial and motor trigeminal nuclei using standard immunohistochemistry with an anti-FUS antibody (Figure 3.8A). Loss of motor neurons from these nuclei was also observed following immunofluorescent labelling of neurons with neurospecific marker NeuN (Figure 3.8B) and quantified by stereological counting of neurons on cresyl violet stained paraffin sections (Figure 3.8C, D). A significantly reduced number of motor neurons was seen in facial (1518 ± 71.2), motor trigeminal (272 ± 45.8) and hypoglossal (1102 ± 51.6) nuclei in symptomatic FUS TG mice compared to WT littermates (1956 ± 88.0, 685 ± 43.6, 1743 ± 80.3, respectively). Interestingly, the abducens nucleus was spared in these mice and the total number of motor neurons within this nucleus in TG mice (167 ± 16.6) was not significantly different to that of WT littermates (154 ± 19.5). Surviving motor neurons within affected brainstem motor nuclei also showed morphological signs of damage on cresyl violet stained sections including, in some cases, vacuolisation of the cytoplasm (Figure 3.8D'-F'). In sagittal brainstem sections taken from pre-symptomatic mice, the expression of human FUS 1-359 was similar across abducens and facial nuclei (Figure 3.8G) and facial and hypoglossal nuclei (Figure 3.8H).

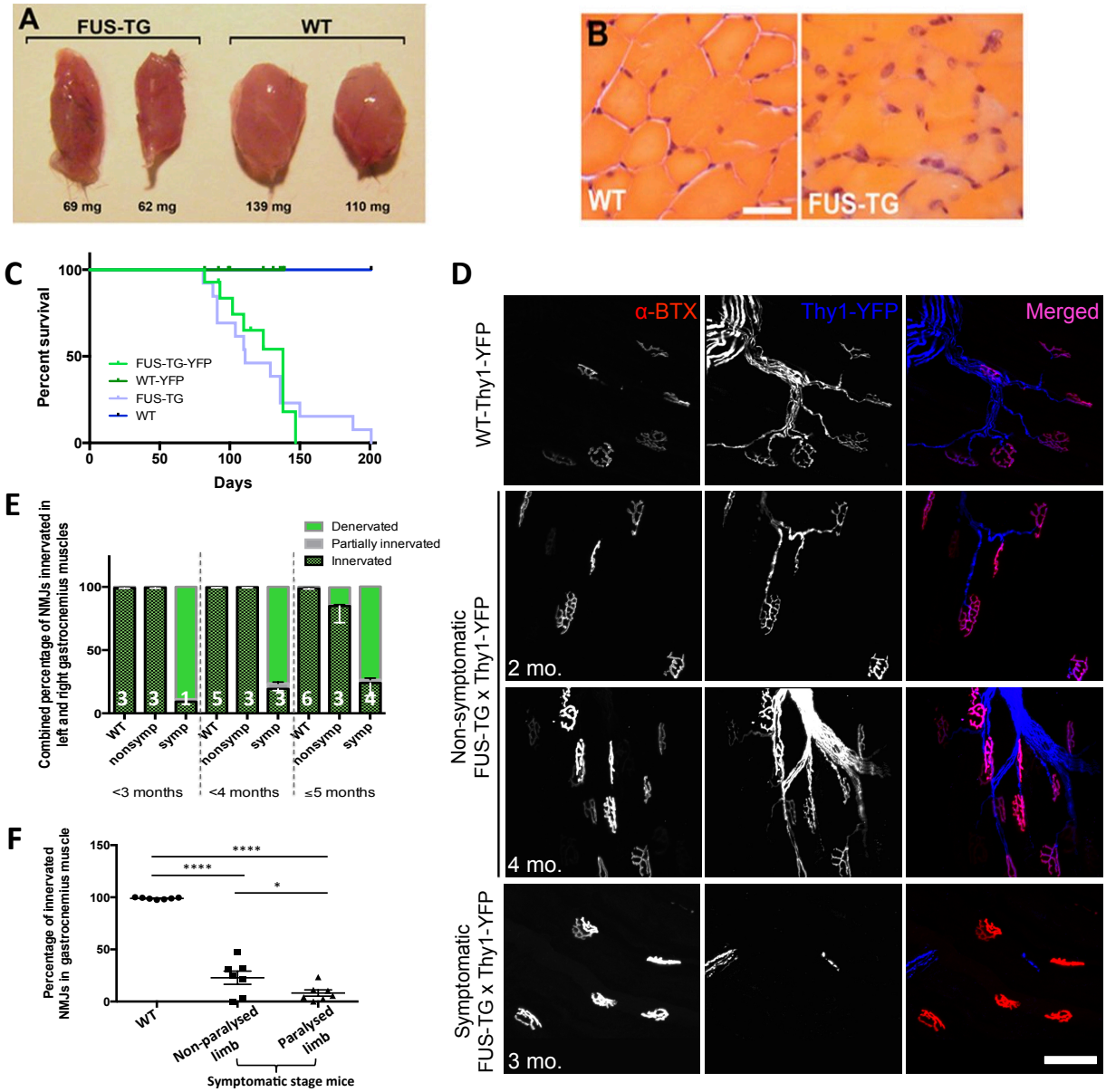

Figure 3.6. Symptomatic FUS 1-359 TG mice display muscular atrophy and loss of muscular innervation. (A) Representative whole gastrocnemius muscles taken from a symptomatic-stage FUS 1-359 TG and an age-matched WT mouse. (B) Cross-sections of gastrocnemius stained with haematoxylin and eosin reveal damage to muscle fibres in FUS 1-359 TG mice displaying paralysis. (C) FUS TG mice crossed with Thy-1-YFP-expressing mice to investigate NMJ innervation displayed similar survival compared to those not expressing YFP. Instances where mice were removed for NMJ analysis are indicated as points on the line. (D) Denervation of NMJs was apparent in FUS TGxThy-1-YFP mice at symptomatic stage of disease using fluorescently labelled α-bungarotoxin to stain acetylcholine receptors at the NMJ and neuronally-expressed YFP (blue). (E) The percentage of NMJs in gastrocnemius that were denervated, partially denervated or innervated was determined in WT-Thy-1-YFP (WT) mice and in FUS-TGxThy-1-YFP mice with (symp) or without (nonsymp) signs of limb weakness or paralysis. Bar chart shows mean of percentage of NMJs innervated/denervated/partially innervated ± S.E.M for percentage innervation. 500 NMJs per gastrocnemius muscle were classified and averaged across limbs for each mouse. There was a significant effect of genotype/stage of progression on NMJ innervation ($p<0.05$, Kruksal-Wallis test). NMJ innervation was significantly reduced in symp mice compared to either WT mice or nonsymp mice ($p<0.05$, Mann Whitney test). Collapsing across genotype/stage of progression revealed that there were no significant differences in NMJ innervation between mice in different age groupings ($p>0.05$, Kruksal-Wallis test). Number of animals per group are indicated at the base of each bar. (F) Analysis of NMJs in asymmetrically affected mice (n=7) revealed that although paralysed limbs displayed a significant reduction in innervation of NMJs compared to non-paralysed limbs ($p<0.5$, Mann Whitney test) both non-paralysed and paralysed gastrocnemius muscles in these mice showed significant reductions in innervation compared to WT limbs (both $p<0.0001$, Mann Whitney tests). Scale bar all panels; 50 µm.

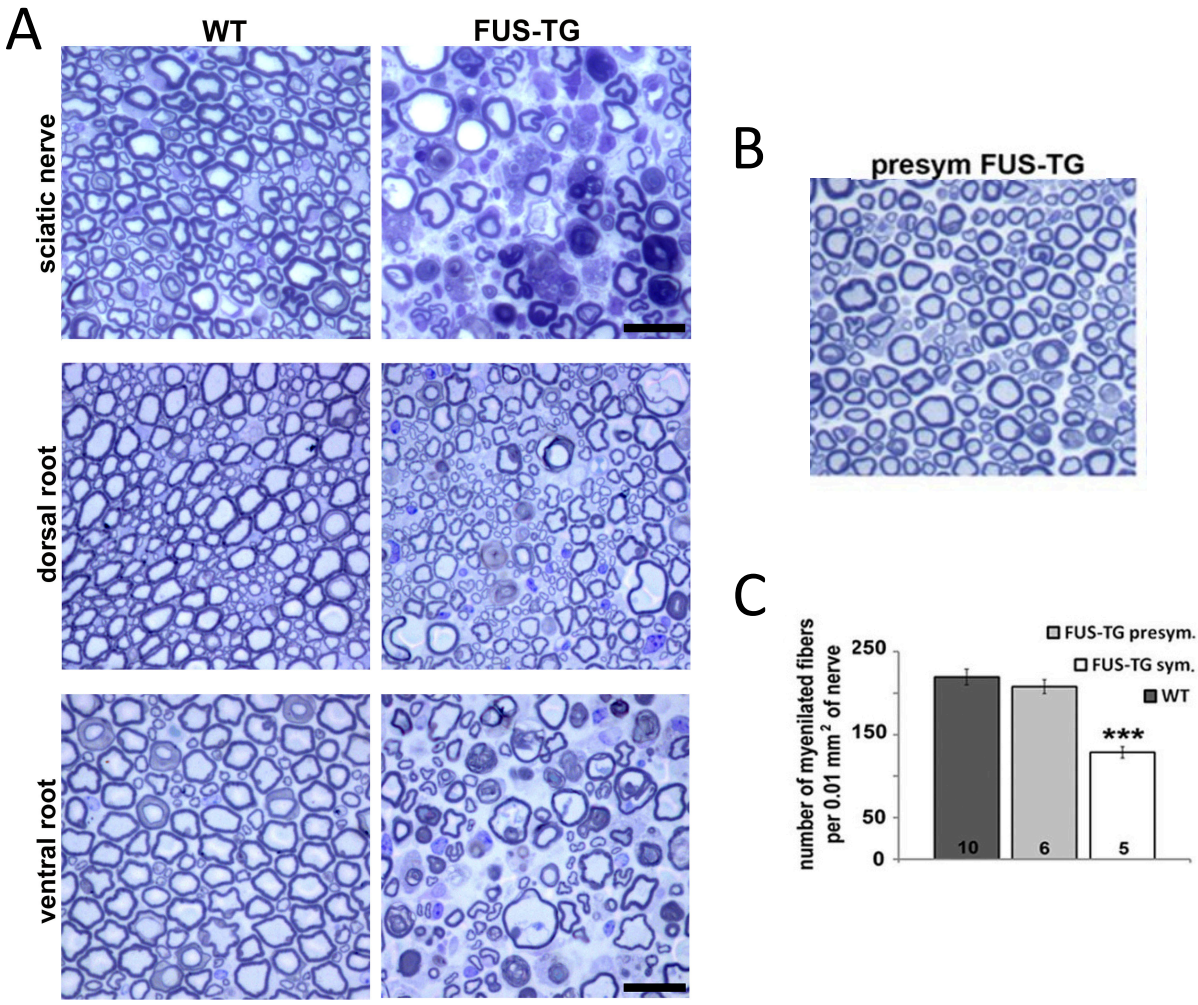

Figure 3.7. Damage and loss of myelinated axons in symptomatic stage FUS 1-359 mice. (A) Semi-thin toluidine blue stained sections of sciatic nerve revealed prominent damage and demyelination of axons in FUS TG mice at the symptomatic, end stage of disease compared to pre-symptomatic and WT mice. (B) Quantitative analysis of semi-thin sections revealed that the number of myelinated fibres per 0.01 mm^2 sciatic nerve was significantly reduced in symptomatic, but not pre-symptomatic, FUS TG mice compared to WT mice. N numbers used for quantification are displayed at the base of each bar and bars represent mean±S.E.M. ***, $p<0.001$, Mann Whitney test. Scale bars; C–E, 30 µm. Panels A and B were produced by Dr Owen Peters.

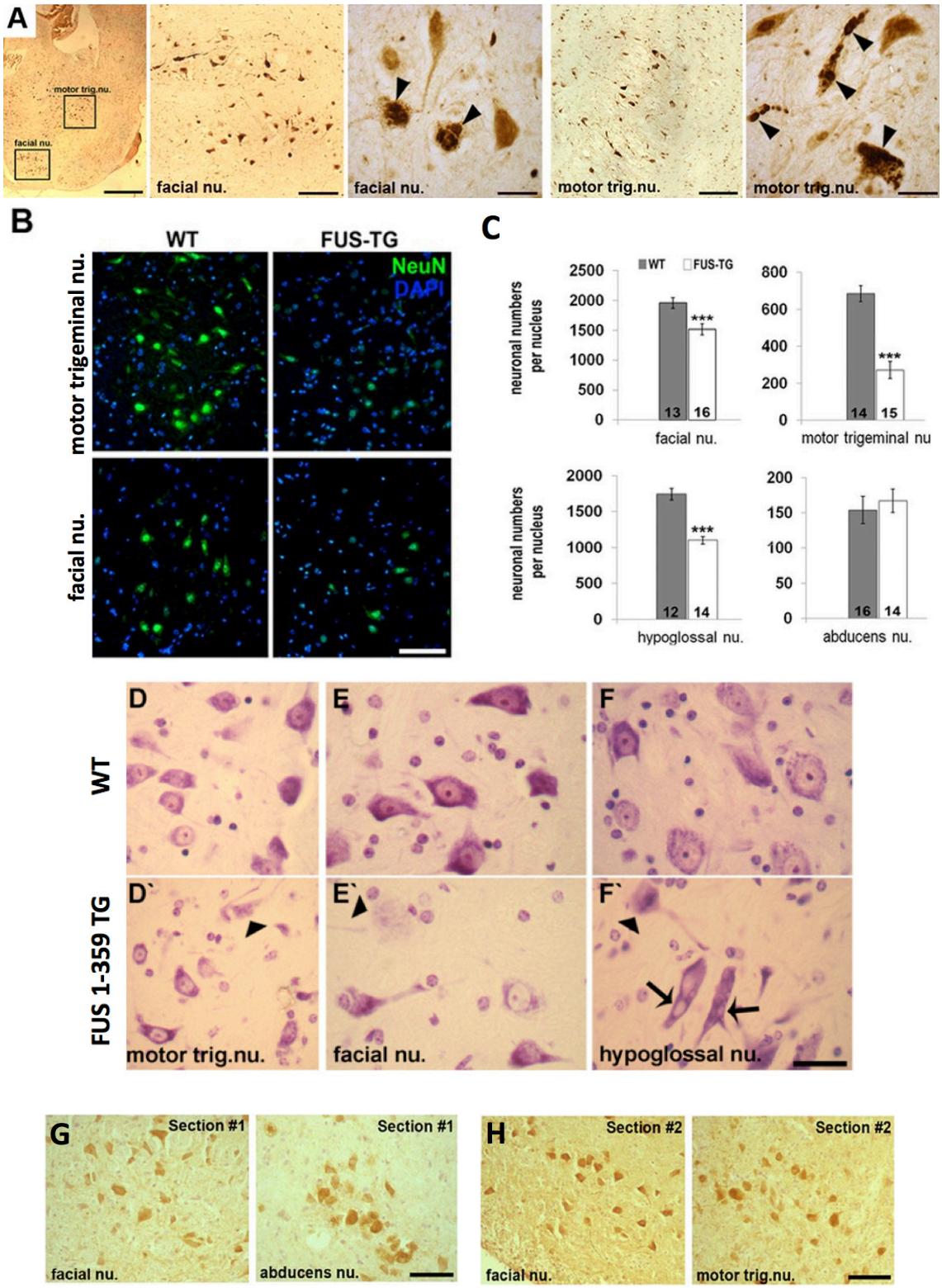

Figure 3.8. FUS pathology and loss of motor neurons in brainstem motor nuclei in symptomatic FUS 1-359 TG mice. (A) Standard immunohistochemistry of a sagittal brainstem section of FUS 1-359 symptomatic mice using anti-FUS antibody revealed the presence of FUS-positive inclusions (arrowheads) in facial and motor trigeminal nuclei. Low and high magnification images are shown. (B) Representative fluorescent immunohistochemistry with neuronal marker, NeuN, shows loss of neurons in facial and motor trigeminal nuclei in symptomatic FUS TG mice compared to WT mice. (C) Quantitative analysis of the number of surviving motor neurons in entire brainstem motor nuclei following stereological counts in symptomatic FUS TG mice compared to age-matched WT mice. Quantification was performed on cresyl violet stained

paraffin sections. N numbers for each group are indicated at the base of each bar and bars represent mean±S.E.M. ***, p<0.001, Mann Whitney test. (D-F') Representative cresyl violet stained paraffin sections show loss and damage (arrowheads) to motor neurons in motor trigeminal (D,D'), facial (E,E') and hypoglossal (F,F') nuclei in symptomatic FUS TG (D'-F') compared to WT mice (D-F). Vacuolization of the cytoplasm of motor neurons can also be seen in these TG mice (arrows). (G-H) Standard immunohistochemistry using an antibody recognising human FUS alone revealed that in pre-symptomatic mice, the levels of FUS in the cytoplasm of motor neurons were similar between nuclei in sections comprising facial and abducens nuclei (G) or facial and motor trigeminal nuclei (H). Scale bars: A, 250 µm for general plane image, 50 µm for images of entire nuclei, and 15 µm for increased magnification images; B, 75 µm; D-F, 20 µm; G-H, 50 µm.

3.3.8 Neuroinflammation in FUS 1-359 TG mice

Prominent reactive astrogliosis was observed in the spinal cord of symptomatic FUS 1-359 TG mice, as visualised by increased reactivity to glial fibrillary acidic protein (GFAP) in immunohistochemically stained sections (Figure 3.9A', A'') compared to WT littermates (Figure 3.9A). This increase in GFAP in symptomatic FUS-TG mice was also detected by western blot analysis of spinal cord homogenates using anti-GFAP antibodies (Figure 3.9B). Microgliosis was also seen in symptomatic FUS TG mice (Figure 3.9D) but not WT littermates (Figure 3.9C), as indicated by staining with *R. communis* agglutinin I (RCAI), a lectin which is known to specifically detect CNS microglia (Mannoji *et al.*, 1986; Colton *et al.*, 1992). Although these glial events were prominent in spinal cord, they were seen to a much lesser extent in brainstem neuronal populations. This was evidenced by performing immunostaining on two adjacent sections of brainstem at the level of the hypoglossal nucleus (Figure 3.9E,F). By staining one section with NeuN and GFAP, it can be seen that there is limited astrogliosis accompanied by a loss of neurons in this region, whilst staining the adjacent section with RCAI, there is also no evidence of microgliosis in this nuclear region. However, it can be noted that there is prominent astro- and micro-gliosis in adjacent brainstem regions (Figure 3.9E,F).

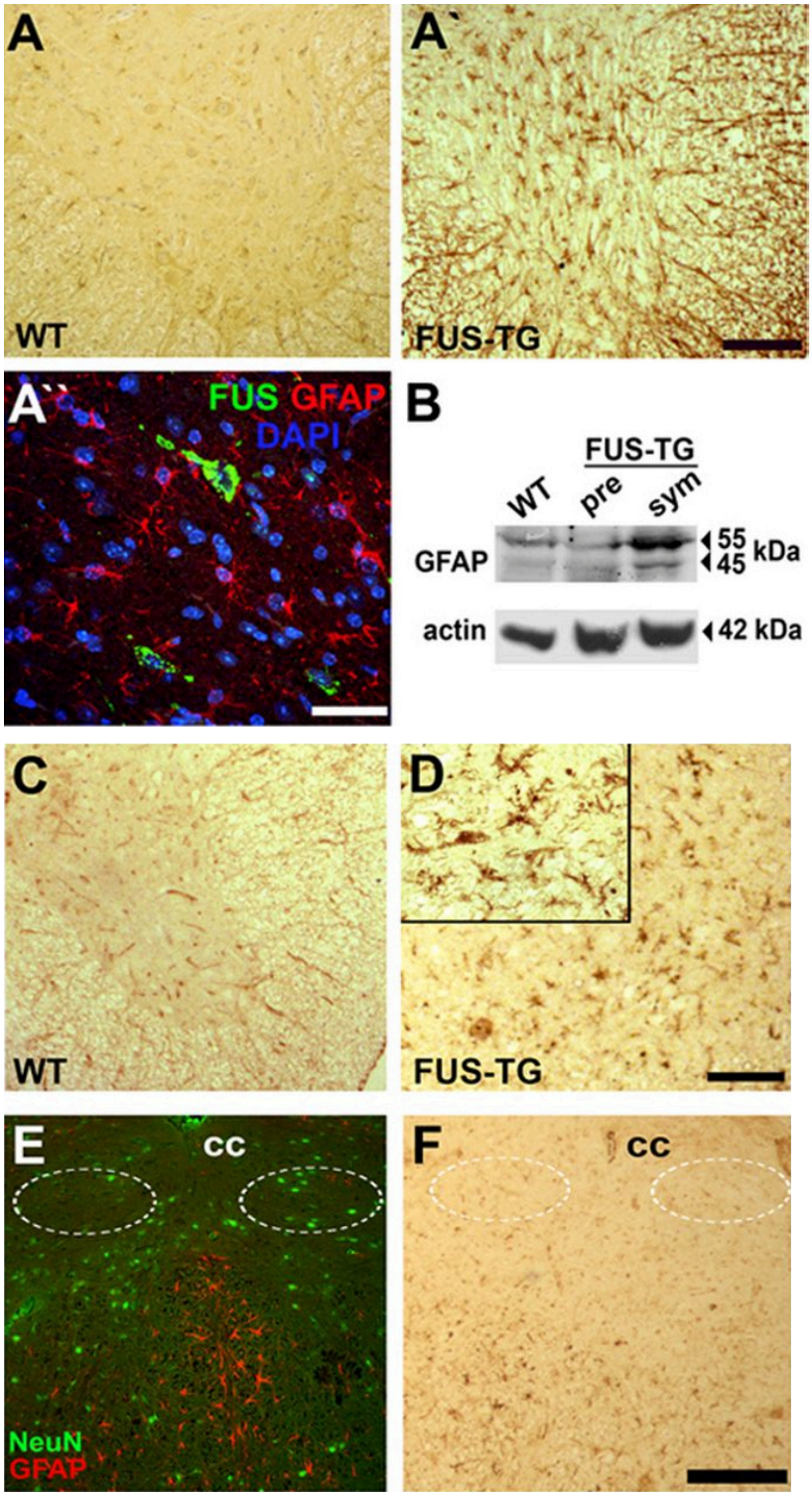

Figure 3.9. Symptomatic FUS 1-359 TG mice display prominent neuroinflammation in the nervous system. (A) Immunohistochemistry reveals marked reactive astrogliosis detected with anti-GFAP antibody in the spinal cord of (A',A'') symptomatic FUS TG but not (A) WT littermates. (B) Homogenates of spinal cord show elevated levels of GFAP protein in symptomatic FUS TG mice compared to pre-symptomatic and WT mice detected by western blot. (C-D) Immunohistochemistry with R. communis agglutinin I (RCAI) in sections of spinal cord revealed microgliosis in symptomatic FUS 1-359 TG mice (D, inset, increased magnification), compared to WT littermates (C). (E-F) Limited astrogliosis is seen in brainstem motor nuclei. Staining two adjacent sections with either NeuN and GFAP (E) or RCAI (F) showed relatively little astrogliosis or microgliosis within hypoglossal nuclei (circled), although these were seen in surrounding areas. Cc; central canal. Scale bars: A, A′, C and D, 100 μm; A″, 50 μm; E and F, 75 μm. At least 3 transgenic mice and 3 WT mice were analysed and representative images shown.

3.4 Discussion: Part I

Perhaps one of the largest difficulties in understanding the mechanisms by which dysregulation of FUS can cause toxicity has been in trying to decipher between the effects caused by its aggregation in the cytoplasm and those caused as a result of altered RNA metabolism. Although there have been overexpression models produced (Mitchell *et al.*, 2013; Huang *et al.*, 2011), suggesting that excess FUS can indeed have a gain of toxic effect, it has not been made clear in these instances whether this is caused by toxic FUS in the cytoplasm or instead by augmenting the activities of FUS in the nucleus, perhaps altering processes such as transcription, splicing and RNA metabolism. Notably, these models have failed to recapitulate the formation of FUS-positive inclusions to the same extent as seen in human disease.

Here, a model of FUSopathy was developed by expressing an RNA-binding-compromised form of FUS, lacking NLS, RGG and ZF domains, in the murine nervous system. In cultured SH-SY5Y cells, this C-terminally truncated form of FUS, N-terminally tagged with GFP, readily aggregated, forming large juxtanuclear structures, although the nature of these structures and their involvement with toxicity remains to be investigated. By removing crucial RNA-binding domains of FUS, the effects of FUS aggregation were investigated independently of primary changes to RNA metabolism that may be directly induced in other models through expression of full length forms of the protein. However, it must be mentioned that later changes to RNA metabolism may arise, perhaps for example through disruption of endogenous FUS. This neuronal expression of FUS 1-359 protein, at a lower level than that of endogenous FUS, was sufficient to result in a severe motor phenotype in these hemizygous F19 mice that was in line with the progression of human ALS when the comparatively shorter lifespan of the mouse is taken into account. Further, several signs of ALS-like pathology were observed.

In hemizygous symptomatic FUS TG F19 mice, significant degeneration and loss of motor neurons was seen in both the anterior horn of the spinal cord and in specific brainstem motor nuclei. In ALS, oculomotor nuclei, controlling eye movements, are spared (Reiner *et al.*, 1995). This was also apparent in these FUS 1-359 TG mice, with no signs of motor neuron loss or degeneration in abducens nucleus, perhaps reflecting a decreased sensitivity to FUS aggregation of this neuronal population. In the anterior horn of the spinal cord of these mice, prominent reactive astrogliosis and microgliosis were detected, again recapitulating responses commonly seen to accompany motor neuron degeneration that are evident in ALS patient spinal cord and brain post-mortem

(Schiffer *et al.*, 1996; Nagy *et al.*, 1994). Similarly to brainstem motor nuclei, susceptibility of different neuronal populations to FUS aggregation was also seen between motor and sensory neurons, with the most extreme disturbances localised to the motor system, exemplified by the extensive damage to ventral root fibres over dorsal root sensory fibres. Further, these mice demonstrated NMJ denervation and muscular atrophy of gastrocnemius muscles that contributed to the development of paralysis, although the initial targets of FUS 1-359 aggregation in this instance remain unknown. Further analysis of this model could reveal important information with respect to progression of neurological disease associated with FUS protein aggregation.

Together, this suggests that aggregation of FUS, in the absence of the direct effect of pathogenic protein on RNA metabolism that may otherwise be driven by expressing RNA-binding-competent full length forms, is sufficient to produce toxicity. This supports a gain of toxic FUS function hypothesis. However, unexpectedly, FUS 1-359 was also able to form nuclear aggregates. Removing the NLS of FUS has been shown to result in mislocalisation to the cytoplasm in cultured cells by ourselves and others (Dormann *et al.*, 2010), and so, it is not understood why nuclear inclusions of an NLS-deficient FUS mutant would form. Perhaps, in these cells, interactions of mutant FUS with endogenous FUS could be responsible for the import of FUS which lacks the NLS into the cytoplasm. Additionally, it remains to be investigated how FUS import mechanisms are affected by the expression of this ectopic protein.

Given it was demonstrated that endogenous FUS may also be recruited to these FUS 1-359 inclusions in the nucleus and cytoplasm, however, loss of normal FUS function, perhaps downstream of FUS aggregation in the cytoplasm, cannot be excluded as a pathological contributor to the progression of FUSopathy. It will be interesting to investigate the mechanisms by which FUS 1-359 is aggregating in the cytoplasm and to determine whether this may be physiologically relevant for ALS-associated mutant forms.

3.5 Overview: Part II

To further investigate the effects of expressing FUS with compromised RNA-binding domains in a whole organism system, another mouse model was created, expressing ΔRRM FUS, targeted to the cytoplasm. This mutant, like FUS 1-359, was shown *in vitro* to form large juxtanuclear structures, albeit to a lesser frequency than FUS 1-359,

although the toxic effects associated with expressing this RNA-binding compromised form of FUS were not known.

Whilst the presence of a consensus binding sequence for FUS is disputed (Iko *et al.*, 2004; Ishigaki *et al.*, 2012; Lagier-Tourenne *et al.*, 2012), specificity of its RNA-binding is thought to arise from the cooperation of the RRM domain with the less structurally complex RGG domains (Lerga *et al.*, 2001; Zinszner *et al.*, 1997b). Unlike C-terminus RGG and ZF domains, which were absent in the previous transgene, the RRM domain, though thought to impart specificity, is not a major domain required for FUS to bind RNA, which distinguishes it from canonical RRM domains (Bentmann *et al.*, 2012; Clery *et al.*, 2008; Liu *et al.*, 2012; Zinszner *et al.*, 1997b). As such, we investigated the toxicity related to introducing this form of FUS with reduced specificity of RNA-binding.

Although expression of this mutant in mice resulted in a severe neurological phenotype, preventing the development of a transgenic line of these mice, this phenotype warranted further investigation. The second half of this chapter was therefore focused on the characterisation of the tissues that were available from the F1 generation of hemizygous mice that were produced.

3.6 Results: Part II

3.6.1 Phenotype, behaviour and survival

Two transgenic female founders were generated and mated with C57/Bl6 males to produce offspring expressing a modified isoform of human FUS, ΔRRMcyt, which lacked amino acids 300-360 and harbored the cytoplasm-targeting mutation, R522G, under the control of a Thy-1 neuronal promoter (Figure 3.10A). The first female founder produced 5 litters and the transgene displayed a Mendelian pattern of inheritance. All transgenic FUS ΔRRMcyt offspring were substantially smaller (~30% weight decrease) than WT littermates and exhibited very early lethality, with mice moribund at a mean age of 20 ± 1 days (n=17) (Figure 3.10B). Approximately 25% died suddenly, prior to the observation of any additional phenotype(s). Interestingly, however, the remainder of these mice developed pronounced tremor on average 2 days prior to death, with the survival duration following tremor onset never exceeding more than 5 days. Tremor was constant and vigorous, affecting the whole body and was not confined to the limbs. Likely as a direct result of tremor, mice displayed a lack of balance, however, they were able to move around the cage freely and signs of limb paralysis were not observed. Because of the rapid nature of disease progression in these mice, we were

unable to perform additional quantitative behavioural analyses. Although further breeding and production of TG lines was not possible as mice died prior to sexual maturation, we endeavored to characterise transgene expression and the associated pathology in this F1 generation. It is important to note that a second female founder gave four litters, which yielded two transgenic offspring. Again, both of these mice also died at the age of 3 weeks, with one developing a visually identical tremor to those from the initial founder.

3.6.2 Expression of FUS ΔRRMcyt transgene in mice

RNA samples extracted from tissues of TG mice sacrificed at moribund stage in parallel with WT littermates were used to determine the level of transgene expression in the brain and spinal cord in these mice. qPCR with a primer pair that detected both endogenous mouse FUS and the human ΔRRMcyt mutant FUS, showed that global FUS expression in the brain (9.8 ± 0.77 fold) and spinal cord (18.1 ± 2.07 fold) was significantly increased in TG mice compared to WT littermates (Figure 3.10C). As endogenous mouse FUS expression was not significantly altered from WT littermates in brain or spinal cord of TG mice, the increase in FUS RNA can be attributed directly to the expression of the transgene (Figure 3.10C). Further, expression of human ΔRRMcyt FUS protein was confirmed by western blotting of brain tissue with an antibody specifically recognising human FUS (Figure 3.10D). Using an antibody recognising both human and mouse isoforms, it was shown that FUS ΔRRMcyt protein is not massively accumulated in the brain of transgenic mice, having reduced band intensity compared to endogenous mouse FUS (Figure 3.10D). To confirm band identification in these western blots, a blot previously exposed to only anti-hFUS antibodies was reprobed with antibodies detecting human and mouse FUS (Figure 3.10E). Indeed, with reprobing, the endogenous mouse FUS band appeared in TG sample above the previously revealed FUS ΔRRMcyt band, confirming our banding pattern.

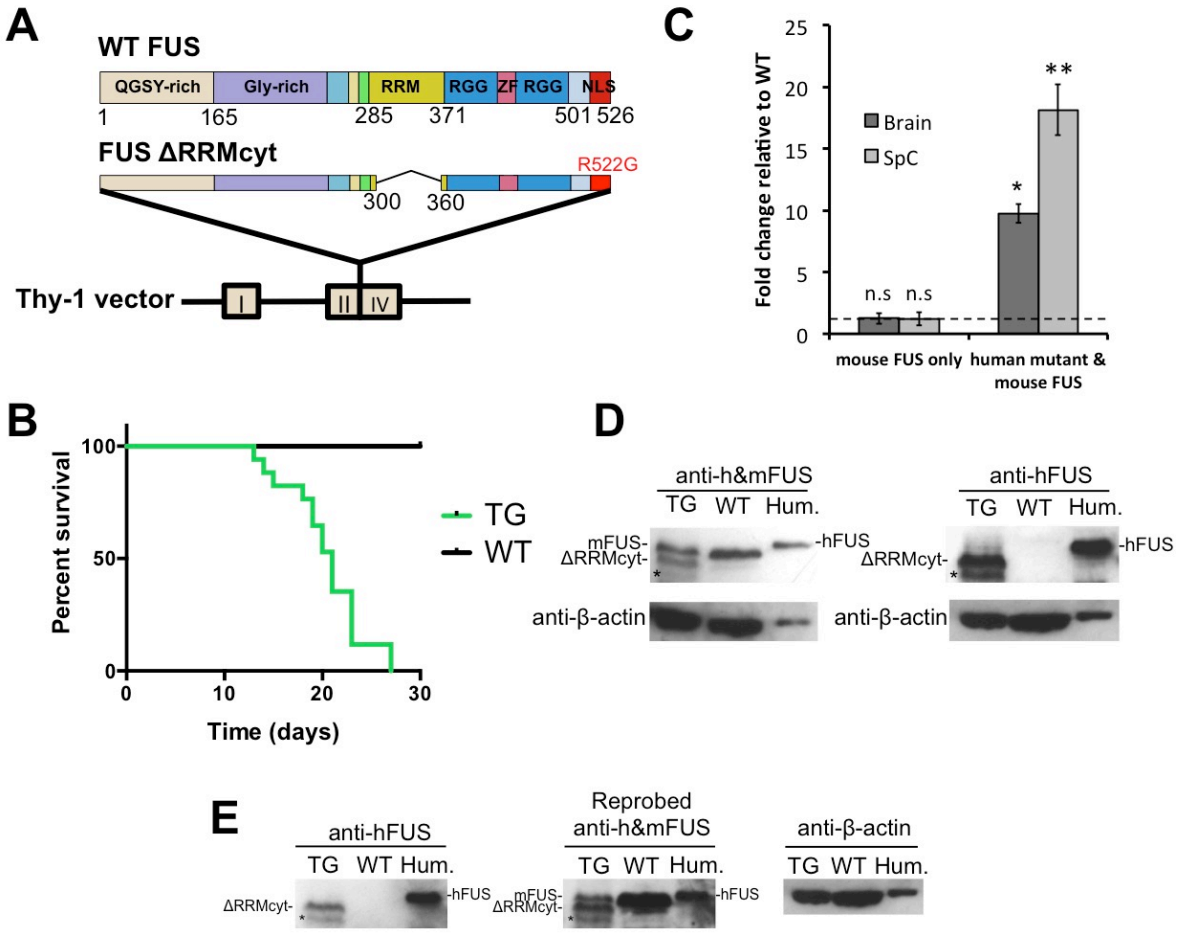

Figure 3.10. Neuronal expression of cytoplasm-targeted FUS lacking RNA-recognition motif causes early lethality in mice. (A) Map of the DNA fragment used for pronuclear microinjection. Human FUS lacking RRM domain and targeted to the cytoplasm by the ALS-associated R522G mutation was inserted between exons II and IV of the Thy-1 gene. (B) Survival plot of the F1 generation of mice used in this study which originated from the initial founder. TG mice were either found dead or were sacrificed at moribund stage (TG, n=17; WT, n=18). (C) The bar chart shows the mean±S.E.M of FUS mRNA expression levels in the brain and spinal cord of moribund TG mice expressed as fold change from WT littermates (*p<0.05, **p<0.001, n=3, Mann-Whitney test). The dashed line indicates the relative WT baseline of 1. No significant difference in endogenous mouse FUS mRNA expression was found between TG and WT littermates in either the brain or spinal cord (p>0.05, n=3, Mann-Whitney test). (D) Expression of FUS protein in brain tissues from TG and WT mice, recognised with antibodies against either human FUS (hFUS) or human and mouse FUS (h&mFUS). Cell lysates from the human neuroblastoma cell line, SH-SY5Y, were included as a positive control for endogenous human FUS. (E) Reprobing western membrane previously exposed to anti-hFUS with anti-h&mFUS confirmed the distinction between human or mouse FUS proteins. Blots were reprobed for β-actin as a loading control. Asterisk indicates presence of a nonspecific band.

3.6.3 Proteinopathy in the cytoplasm

To determine the pattern of cellular FUS localisation, immunohistochemistry was performed on brains taken post-mortem from TG mice in conjunction with those from age-matched WT littermates. Indeed, by using a monoclonal antibody that detects both endogenous mouse FUS and the human mutant FUS, prominent staining was observed in the cytoplasm of the cortex and brainstem cells of TG mice expressing the human FUS ΔRRMcyt but not in WT mice where endogenous FUS was predominantly localised to the nucleus (Figure 3.11A). In most instances, FUS that was redistributed into the cytoplasm displayed a granule-like appearance, although frequently, round, dense inclusions, highly immunoreactive to FUS antibodies and resembling the pathological FUS inclusions seen in the neurons of ALS patients, were also observed, typically one per cell. This redistribution into the cytoplasm and pattern of FUS accumulation in TG mice was also confirmed using immunofluorescent staining of sections co-stained with the nuclear dye, DAPI (Figure 3.11B). The same pattern of FUS staining was also revealed by immunohistochemistry with a different antibody, this time polyclonal, also recognising mouse and human FUS (Figure 3.11C). Co-staining with a neuronal marker, NeuN, demonstrated that mislocalisation of FUS occurred in a large fraction of cortical neurons (Figure 3.11C). In cells with prominent cytoplasmic localisation of FUS, the nucleus often appeared depleted of this protein (Figure 3.11, 3.12B). However, upon staining with an antibody specifically recognising mouse FUS, we observed that the majority of cells maintained a nuclear localisation of endogenous FUS, not dissimilar from WT littermates (Figure 3.12A). Moreover, cytoplasmic inclusions positive for endogenous mouse FUS were rare (Figure 3.12A, inset). Taken together with the unaltered expression of endogenous FUS RNA, this suggests that endogenous FUS was affected to a minimal degree. Surprisingly, immunoreactivity of FUS in the cytoplasm of cerebellar Purkinje cells was comparatively weak (Figure 3.11A), although was detected more readily using an antibody highly specific to human FUS (Figure 3.12B). In these cells, FUS staining was predominantly nuclear and no FUS-positive inclusions or granule-like accumulations were observed (Figure 3.12A). In some rare instances, large FUS-positive inclusions were also found to be ubiquitinated (Figure 3.13). In addition to upper motor neurons in the cortex and brainstem motor nuclei, lower motor neurons in the spinal cord are also a key site of pathology in ALS, including FUS-ALS (Blair *et al.*, 2010). However, all samples for histological analysis of FUS ΔRRMcyt mice were collected post-mortem and spinal cord tissues suffered from significant structural damage, preventing proper examination of FUS proteinopathy.

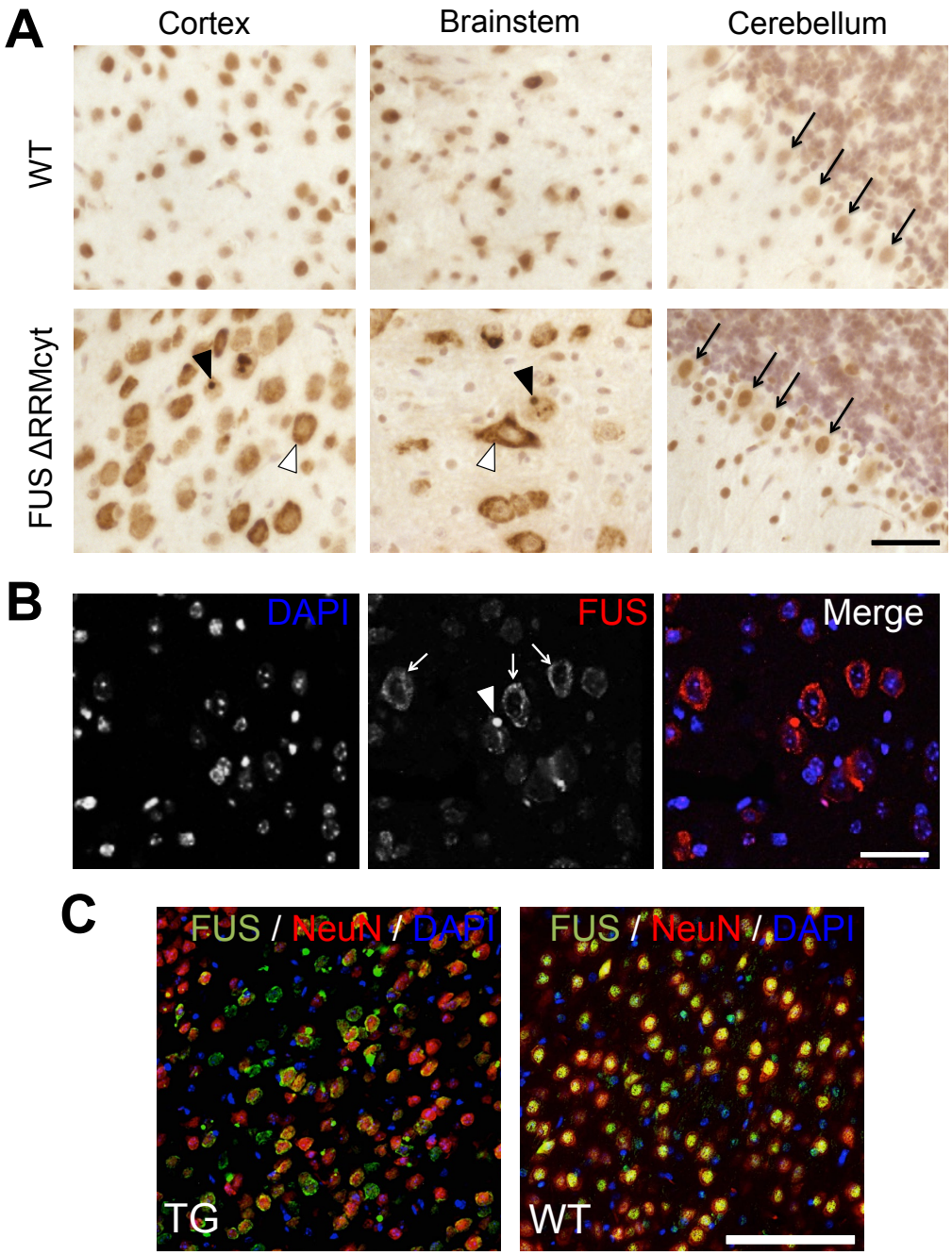

Figure 3.11. FUS mislocalisation in cortical and brainstem neuronal populations in FUS ΔRRMcyt mice. Mouse brain sections were immunostained with a mouse monoclonal antibody detecting both human mutant and mouse endogenous FUS proteins. (A) Cells of the cortex and brainstem in TG mice displayed prominent FUS immunoreactivity in the cytoplasm (white arrowheads). Large FUS-positive, round inclusions were also frequently observed in the cytoplasm of these cells (black arrowheads). Purkinje cells of the cerebellum (black arrows), however, displayed only very slight staining in the cytoplasm. In WT mice, the cellular localisation of FUS is predominantly nuclear. (B) Immunofluorescent staining for FUS and DAPI counterstaining of cell nuclei revealed a granular pattern (white arrows) and the presence of FUS-positive inclusions (white arrowhead) in the cytoplasm of cortical cells. (C) Double immunofluorescent staining for FUS and the neuronal nuclear marker, NeuN, demonstrated that cytoplasmic mislocalisation of FUS is widespread in cortical neurons of TG mice. Scale bars; A-B, 25 µm; C, 100 µm.

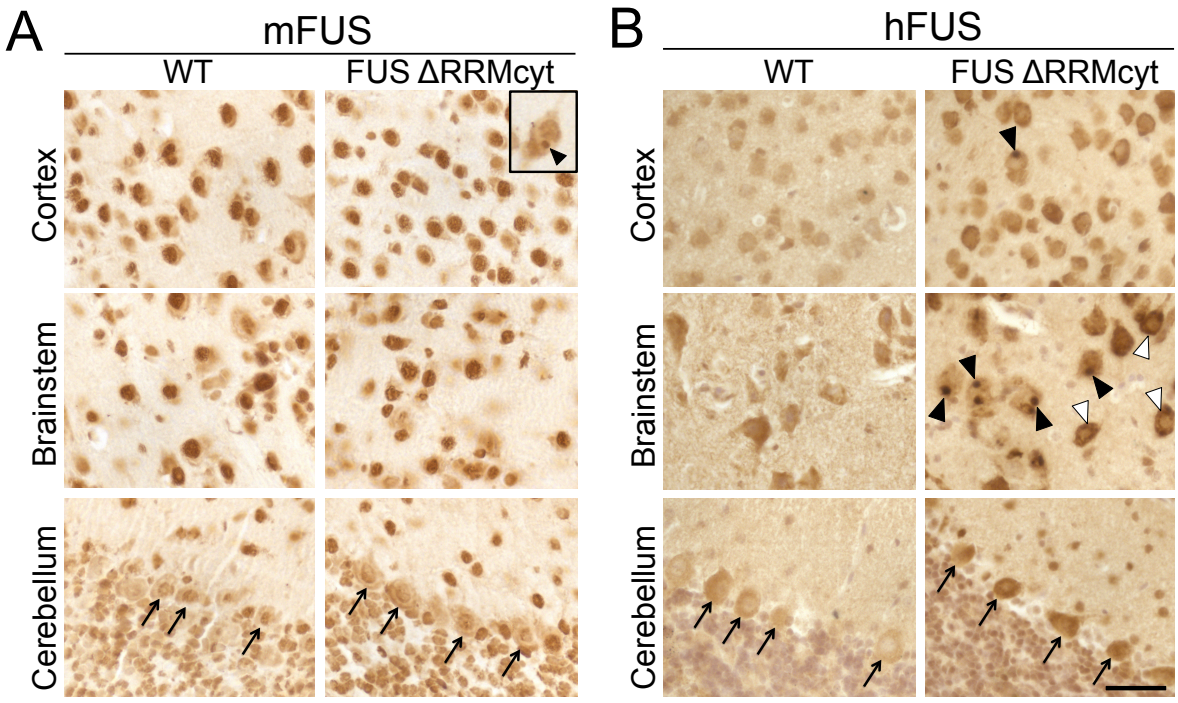

Figure 3.12. Localisation of mouse and human FUS in FUS ΔRRMcyt mice. (A) Brain sections immunostained with an antibody that recognises only mouse FUS (mFUS). Endogenous mouse FUS displays a predominantly nuclear localisation in the cortex, brainstem and cerebellar Purkinje cells in WT littermates. This pattern of FUS localisation is similar in mice expressing human FUS ΔRRMcyt, although in very rare instances, cytoplasmic inclusions positive for endogenous mouse FUS were observed (inset). (B) Brain sections immunostained with antibody that recognises only human FUS (hFUS). Immunostaining is prominent in the cytoplasm of cells of the cortex and brainstem (white arrowheads) of FUS ΔRRMcyt mice, with large hFUS-positive inclusions observed frequently in these cells (black arrowheads). Staining in the cytoplasm of cerebellar Purkinje cells (arrows) was comparatively weak. Non-specific background levels of hFUS staining are depicted in WT littermates. Scale bars; all panels, 25 μm.

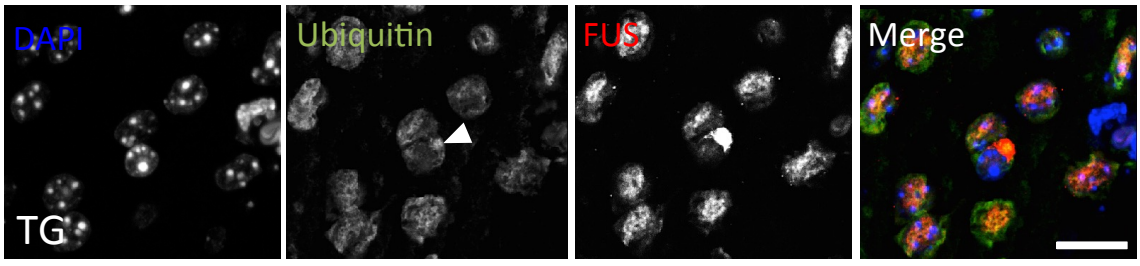

Figure 3.13. Ubiquitin staining in FUS ΔRRMcyt mice. Double immunofluorescent staining of mouse brain sections with a rabbit polyclonal antibody detecting both human mutant and mouse endogenous FUS proteins, and mouse monoclonal anti-ubiquitin antibody. Some FUS-positive inclusions (arrowhead) displayed immunoreactivity to ubiquitin. Scale bars; 15 μm.

3.6.4 Effect of FUS ΔRRMcyt expression on neuronal populations

Although quantitative analysis was not carried out due to limited tissue availability, mice expressing FUS ΔRRMcyt did not display any obvious loss of motor neurons in motor trigeminal, facial or hypoglossal brainstem motor nuclei upon histological analysis. Additionally, no changes to the morphology or size of motor neurons in these nuclei were apparent compared to WT (Figure 3.14A). Additionally, standard immunohistochemistry with anti-GFAP or RCAI antibodies failed to reveal any indication of astro- or microgliosis, respectively, in these regions (Figure 3.14B and data not shown).

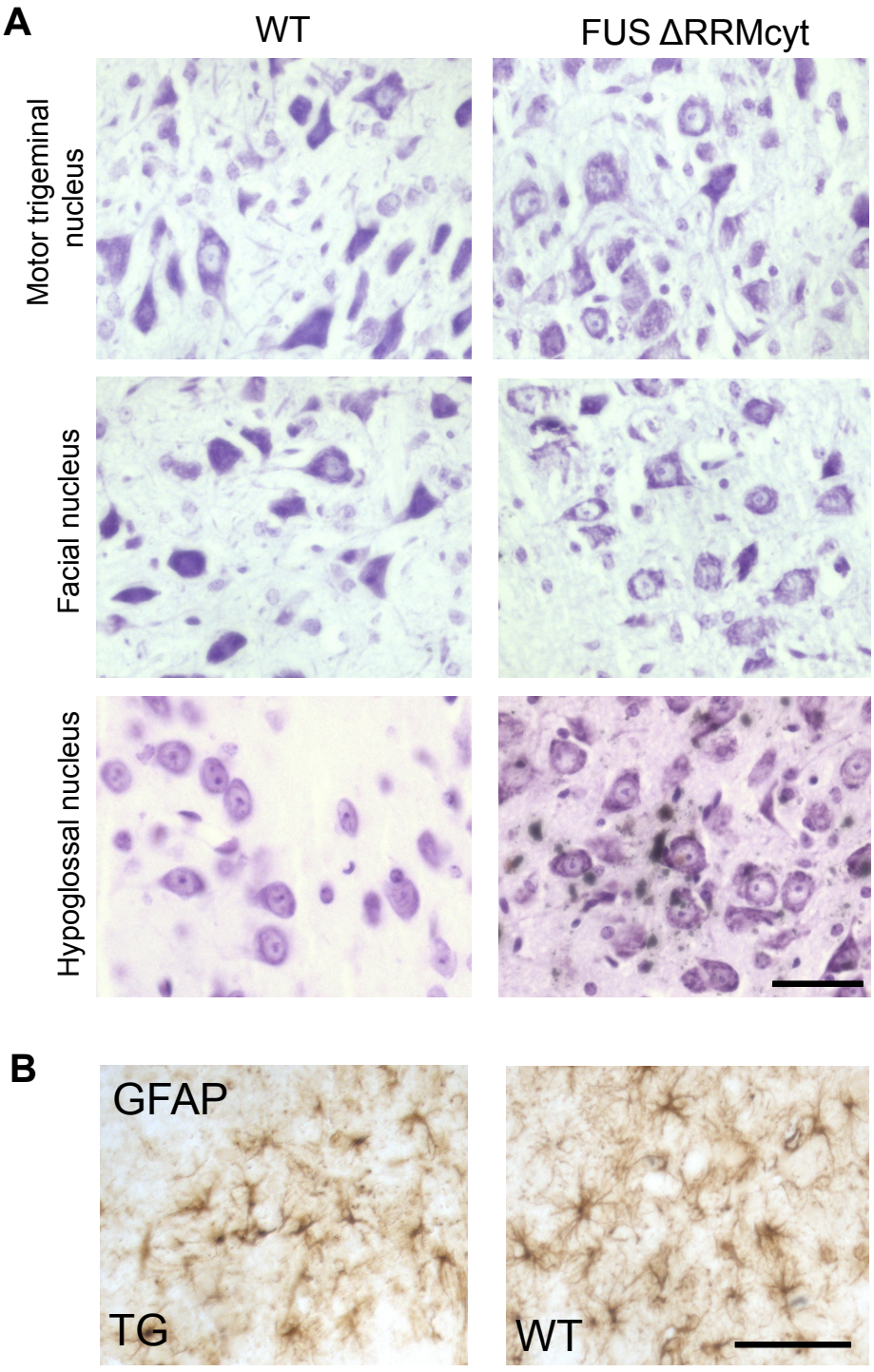

Figure 3.14. Brainstem motor nuclei of FUS ΔRRMcyt mice do not display obvious signs of neurodegeneration. (A) Motor trigeminal, facial and hypoglossal nuclei in TG and WT mice were stained with cresyl violet to permit identification of motor neurons. No morphological differences were identified in TG mice compared with WT littermates. (B) Immunoreactivity to glial fibrillary acidic protein (GFAP) and morphology of astrocytes are indistinguishable between FUS ΔRRMcyt mice and WT littermates. Representative images shown. Scale bars; A, 25 μm; B, 50 μm.

3.7 Discussion: Part II

Neuronal expression of FUS lacking its RRM domain and targeted to the cytoplasm caused an abundant FUS pathology, a severe tremor phenotype and juvenile lethality in these transgenic mice. Although analysis of this F1 generation was restricted compared to that of FUS 1-359 mice, given that they died suddenly a few weeks after birth and that collection of tissues in many instances was post-mortem, we were able to successfully investigate the pattern of FUS pathology in brain and brainstem areas.

In transgenic FUS ΔRRMcyt mice, dramatic mislocalisation of FUS to the cytoplasm of neuronal cells was detected in the cortex and in the brainstem. The occurrence of large, FUS-positive cytoplasmic inclusions in many of these cells was also seen, reminiscent of those observed in patients' neurons and in FUS 1-359 mice. Although not quantified, interestingly, the extent of FUS pathology appeared greater in these mice compared to that seen in FUS 1-359 transgenics, with inclusions visibly more prevalent. However, in FUS ΔRRMcyt animals, unlike FUS 1-359 mice, immunostaining with mouse specific antibodies showed that endogenous mouse FUS maintained its nuclear localisation and did not appear depleted compared to WT littermates. Indeed, endogenous FUS was very rarely included in human FUS-positive inclusions in the cytoplasm. Perhaps endogenous FUS has reduced affinity to FUS ΔRRMcyt isoform than FUS 1-359 isoform resulting in its limited recruitment, or, moreover, perhaps recruitment of endogenous FUS to cytoplasmic structures represents a later stage of FUSopathy, which these mice did not reach, giving insights into the progression of FUSopathy.

Despite a prominent proteinopathy, tremor and an early onset lethality caused by expression of FUS ΔRRMcyt in the cytoplasm, we were not able to detect any signs of neurodegeneration or accompanying inflammatory glial response within either the cortex or brainstem motor nuclei that are commonly affected in ALS. In a recent murine model where wild-type human FUS was overexpressed, homozygous mice also developed a visually similar early-onset tremor, in this case progressing into to limb paralysis and lethality at a young, although significantly older, age than in FUS ΔRRMcyt mice. Interestingly, although FUS-positive inclusions were widespread, loss of neuronal populations and neuroinflammatory response were not found in the brain of these mice (Mitchell *et al.*, 2013), which is consistent with our observations.

The origins of pronounced tremor in these mice were not obvious. Though FUS mutation and/or pathology has been associated with cases of essential tremor (Merner *et al.*, 2012; Rajput *et al.*, 2014; Wu *et al.*, 2013; Zheng *et al.*, 2013) and cerebellar ataxias (Doi *et al.*, 2010), we observed no signs of overt FUS pathology in cerebellar Purkinje cells, common targets of these disorders in humans (Xia *et al.*, 2013) and mouse models (Sarna and Hawkes, 2011; Sawada *et al.*, 2009). However, whilst FUS did not appear to be redistributed in these cells upon histological analysis, functional alterations to these cells cannot be ruled out.

It is feasible that the interactions of FUS with RNAs were altered in cells expressing this modified protein. As the RRM domain is proposed to impart specificity, one would expect an increase in non-specific RNA interactions for this isoform of FUS. Therefore, in addition to a deleterious effect on function or metabolism of normal RNA targets of FUS, this isoform might have become engaged in interactions with, and compromise the normal functions of, novel RNA targets. Both of these mechanisms might have contributed to the development of the severe early onset phenotype observed in these transgenic mice.

Although it was not possible to determine exact mechanism by which severe pathology developed in this model, it is tempting to hypothesise that the very early death of FUS ΔRRMcyt mice before or soon after developing tremor but prior to the potential onset of any motor symptoms reflects dramatic changes to intracellular regulatory/signaling processes that make neurons throughout the nervous system dysfunctional before any structural damage to these cells becomes evident. Such systemic dysregulation could have an insurmountable effect on bodily functions, for example by causing dysregulation of respiratory control, leading to death of the animal before changes more typical to ALS pathology occur in motor neurons.

Taken together with our previous model of FUSopathy (FUS 1-359 mice), these data further support the notion that expression of cytoplasmically mislocalised FUS with compromised RNA-binding capacity causes particularly prominent and harmful FUS pathology in the mouse nervous system.

Results II:
Aggregation of mutant FUS in the cytoplasm: Interactions with stress-induced stress granules

4.1 Declaration

Data included within this chapter have been published within the following open access article:

Shelkovnikova TA, Robinson HK, Connor-Robson N, Buchman VL. Recruitment into stress granules prevents irreversible aggregation of FUS protein mislocalized to the cytoplasm. Cell Cycle. 2013 Oct 1;12(19):3194-202.

4.2 Overview

In the previous chapter, the effect of expressing FUS with compromised RNA-binding capacity in the murine nervous system was investigated using two transgenic models. In both instances, this caused pronounced effects on animal physiology with reduced survival and the formation of pathological FUS-positive inclusions. The severe phenotype associated with expression of a C-terminally truncated FUS isoform, FUS 1-359, that lacked major RNA-binding domains, giving rise to several ALS-like signs, suggested that aggregation of FUS in the cytoplasm is a primary insult sufficient to confer pathology in the absence of initial widespread disruption to RNA metabolism homeostasis that may otherwise occur when expressing full length forms. However, the pathways through which this isoform of FUS that was mislocalised to the cytoplasm aggregated to form large FUS-positive inclusions, and the nature of these inclusions were not clear. Following stress insult, FUS mutants which have been mislocalised to the cytoplasm have been shown to interact with SGs (Bosco *et al.*, 2010; Dormann *et al.*, 2010; Vance *et al.*, 2013), yet as FUS 1-359 lacks major RNA-binding domains and RNA-binding is thought to be required for SG interactions (Bentmann *et al.*, 2012), it was unclear whether this isoform would act in a similar manner. Therefore, the aim of this chapter was to investigate the aggregation pathways of FUS 1-359 and the relationship of this isoform with SGs in the cytoplasm under basal and stress conditions to determine, *in vitro*, how large FUS-positive inclusions seen in our FUS 1-359 transgenic model may be formed, and to elucidate the role of cytoplasmic FUS recruitment to SGs.

4.3 Results

4.3.1 Aggregation of FUS 1-359 in the cytoplasm of SH-SY5Y cells

In the previous chapter, it was shown that GFP-tagged FUS 1-359 aggregated over time in the cytoplasm of SH-SY5Y cells, producing large juxtanuclear aggregates. Live cell imaging of this construct revealed that these large structures were formed by the agglomeration of small FUS 1-359 precursor aggregates over time (Figure 4.1A).

These large juxtanuclear structures were not uncommon in these cells and at 24 h they are seen in >40% of transfected SH-SY5Y cells, while some degree of aggregation was seen in ~60% of these cells (Figure 4.1B).

4.3.2 Characterisation of large juxtanuclear structures formed by FUS 1-359

Lysosomes are membrane enveloped organelles containing acid hydrolases acting to degrade damaged and unwanted proteins in the cytoplasm. These structures are often located in the juxtanuclear region where they are formed from the fusion of endosomes arising from the cellular membrane and Golgi vesicles containing digestive enzymes (Luzio *et al.*, 2007). Considering this, immunoreactivity of FUS 1-359 structures to endosomal and lysosomal markers was tested to determine whether FUS was targeted to these areas. Large juxtanuclear structures of FUS 1-359 were, however, negative for markers of endosomal and lysosomal compartments, LAMP-1 and LAMP-2 (Figure 4.2A).

Instead, these structures displayed features typical of aggresomes. Aggresomes are also found in a juxtanuclear location where they are organised around microtubule organising centres (MTOCs) (Garcia-Mata *et al.*, 1999). They are formed by the retrograde trafficking of small aggregates along microtubules and it is hypothesised that this condensation of aggregates may act to facilitate targeting of these proteins to autophagic degradation pathways (Kopito, 2000). As with aggresomes (Bolhuis and Richter-Landsberg, 2010; Oakley, 1995), FUS 1-359 juxtanuclear structures were positive for chaperone protein, HSP-27 (Figure 4.2B) and were organised around MTOCs as visualised with an antibody to gamma-tubulin, a marker of this region (Figure 4.2C). Like aggresomes (Johnston *et al.*, 1998), large FUS 1-359 structures were surrounded by a cage of redistributed intermediate filament, vimentin (Figure 4.2D). Disruption of microtubules with nocodozole, that prevents the formation of aggresomes (Vasquez *et al.*, 1997), also prevented the formation of these FUS-positive structures (Figure 4.2E).

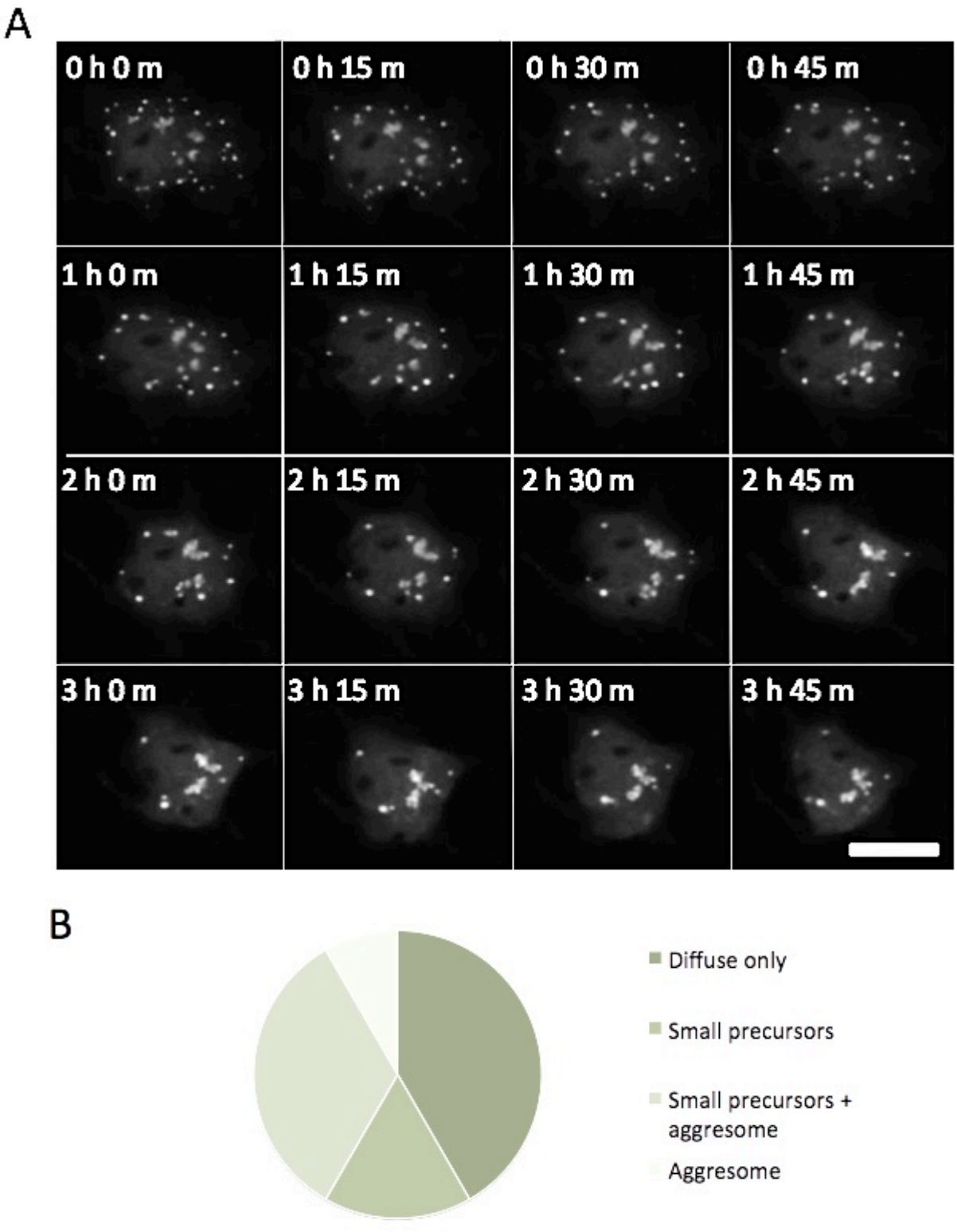

Figure 4.1. Small aggregates of FUS 1-359 mutant coalesce over time to form large juxtanuclear structures. (A) Stills from live cell imaging of SH-SY5Y cell transfected with GFP-tagged FUS 1-359 beginning 24 h post transfection. (B) These large aggresome structures are seen in >40% SH-SY5Y cells at 24 h post-transfection with FUS 1-359 and some degree of aggregation is seen in ~60% cells. Scale bar; 25 µm.

4.3.3 Interaction between FUS mutants and SG marker proteins

Whilst FUS 1-359 was shown to form aggresomes, ALS-related mutant R522G and NLS deletion mutant 1-513 were instead shown to colocalise with markers of SGs, TIAR and G3BP1, in naïve cells without the addition of exogenous stress (Figure 4.3). Contrastingly, FUS 1-359 aggregates did not colocalise with occasional SG marker-positive structures seen in these cells (Figure 4.3). Emetine, a polysome stabiliser, is known to cause the disassembly of SGs (Kedersha *et al.*, 2000). Treatment of cells transfected with FUS R522G with emetine was sufficient to prevent the formation of FUS R522G foci. However, emetine treatment was not able to prevent the aggregation of FUS 1-359 (Figure 4.4).

To induce SG formation, transfected cells were treated with 0.5 mM sodium arsenite for one hour or subjected cells to heat shock at 43°C for one hour. Whilst cytoplasmically localised FUS mutants, R522G, 1-513 and ΔRRMcyt are recruited to SGs induced by both methods, FUS 1-359 aggregates did not colocalise with SGs in either case (Figure 4.5). As expected, WT FUS remained nuclear and was not recruited into SGs (Figure 4.5A). Again, disruption of induced SGs with emetine or cycloheximide, also known to cause disruption of SGs by a similar mechanism to that of emetine (Kedersha *et al.*, 2000), was sufficient to prevent the presence of ALS-linked R522G FUS foci but not the presence of FUS 1-359 aggregates (Figure 4.6). Together with previous data, this confirms that FUS 1-359, lacking NLS, RGG and ZF domains is not capable of being recruited into SGs but forms small aggregates which are not easily dissipated and instead go on to form aggresomes.

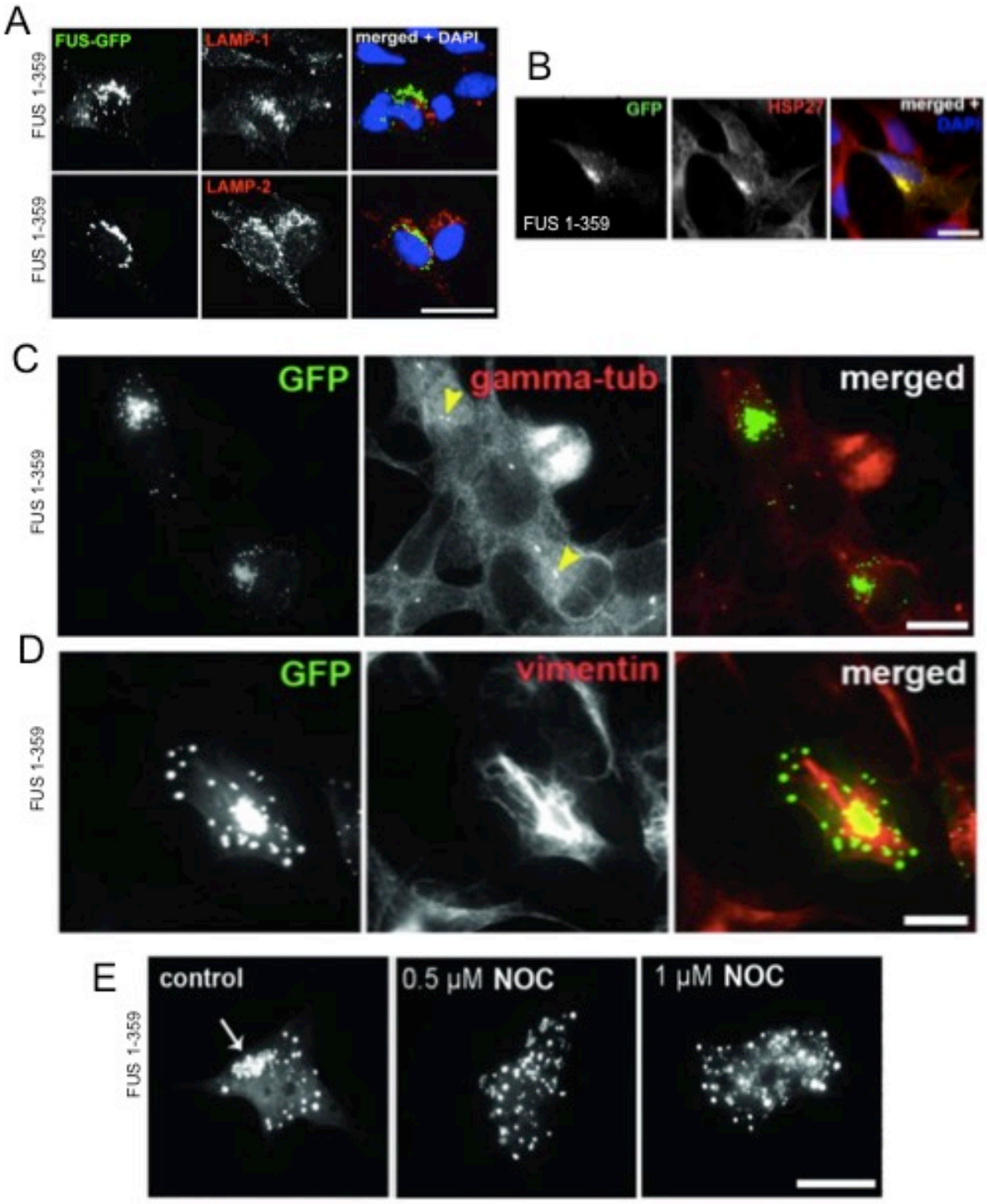

Figure 4.2. Large juxtanuclear structures formed by FUS 1-359 in SH-SY5Y cells display features typical of aggresomes. (A) Large juxtanuclear agglomerations of FUS 1-359 do not colocalise with LAMP-1 or LAMP-2, markers of endosome and lysosome compartments but are positive for the chaperone protein, HSP-27 (B) These structures are formed around microtubule organising centres, as highlighted by anti-gamma tubulin antibody (yellow arrowheads) (C), and are surrounded by a 'vimentin cage' (D). (E) Additionally, formation of these large juxtanuclear structures (arrow) is prevented by disrupting microtubules with nocodozole (0.5 μM or 1 μM). Scale bars; A, 20 μm; B-E, 15 μm. At least 3 biological replicates were performed and representative images are shown.

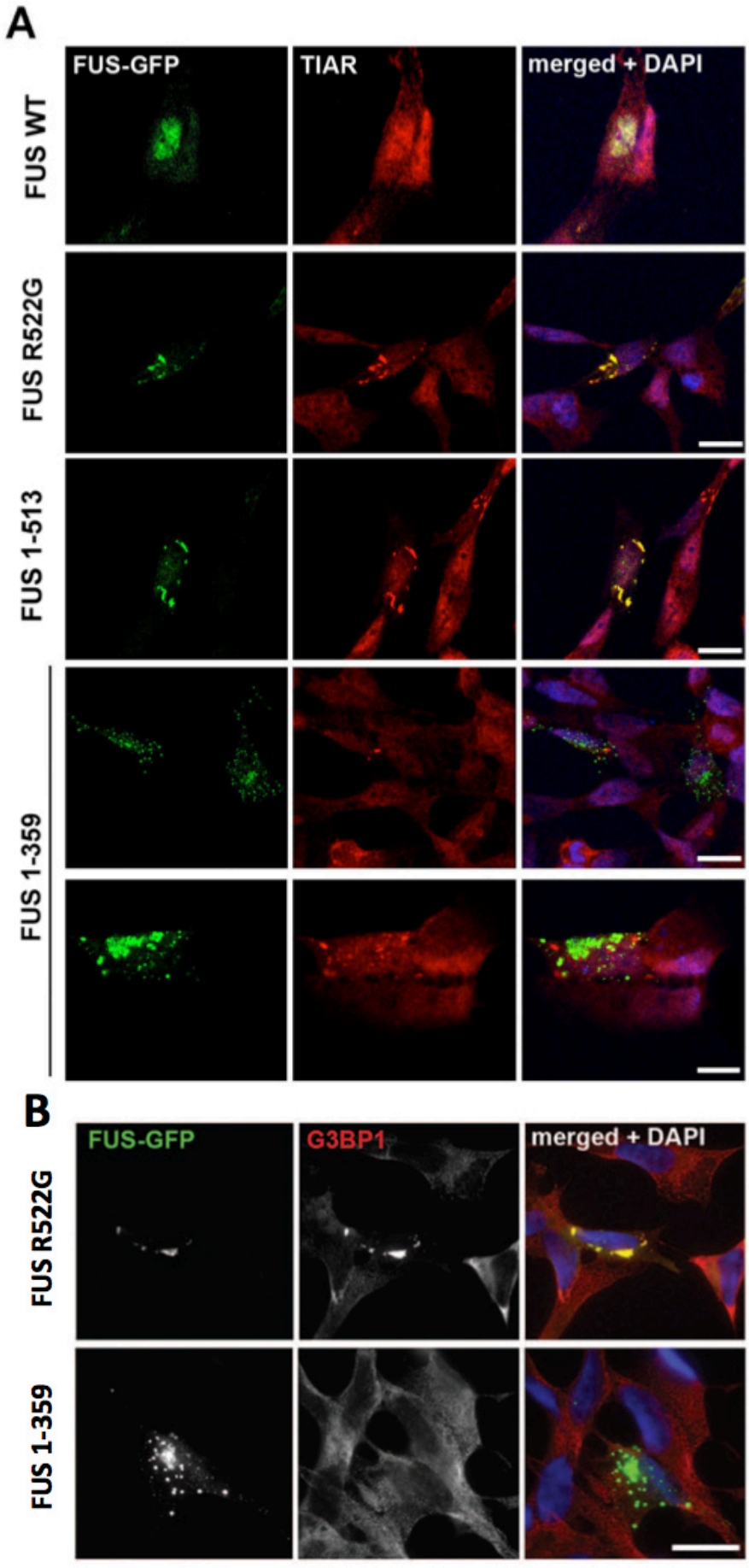
A
FUS-GFP
TIAR
merged + DAPI
FUS WT
FUS R522G
FUS 1-513
FUS 1-359
B
FUS-GFP
G3BP1
merged + DAPI
FUS R522G
FUS 1-359

Figure 4.3. C-terminally truncated FUS mutant 1-359 is not recruited into SGs in naïve cells. Aggregates of ALS-linked FUS mutants R522G and 1-513, but not the C-terminal truncation 1-359, may colocalise with SG markers TIAR (A) or G3BP1 (B) in naïve SH-SY5Y cells. Scale bars; 15 μm. At least 3 biological replicates were performed and representative images are shown.

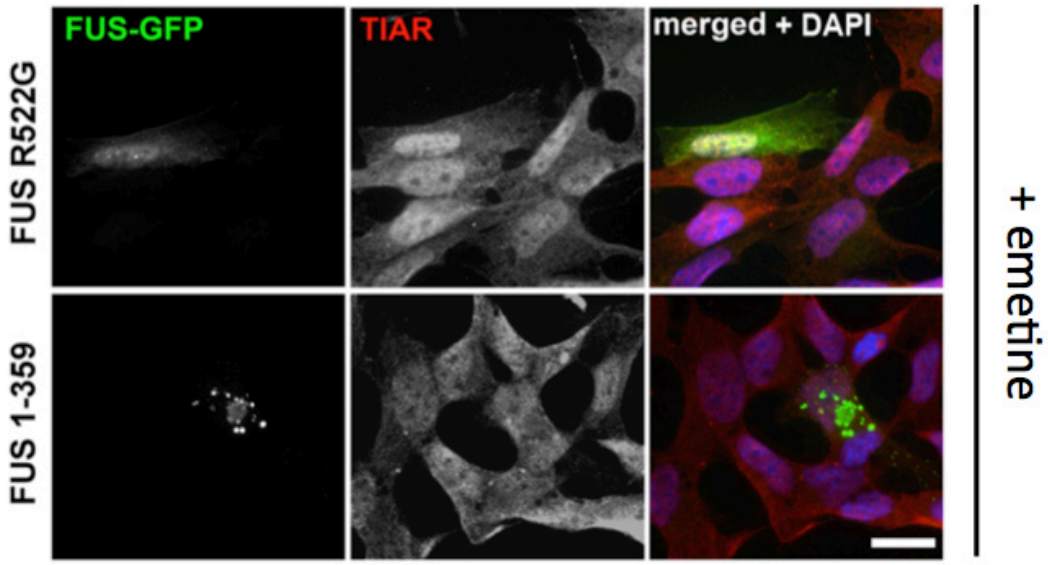

Figure 4.4. Disruption of SG formation is not sufficient to prevent the aggregation of FUS 1-359 into large juxtanuclear structures. SH-SY5Y cells were treated with emetine (10 μg/ml) to prevent SG formation. Anti-TIAR staining was used to confirm that no SGs were formed. Scale bar; 15 μm. At least 3 biological replicates were performed and representative images are shown.

4.3.4 RNA-binding dependency of FUS recruitment to SGs

To confirm that the recruitment of cytoplasmic FUS to SGs is indeed dependent upon the RNA-binding abilities of FUS, as is suggested by the inability of FUS 1-359, lacking crucial RNA-binding domains, to be recruited to these structures, a fusion protein was created to reinstate additional RNA-binding domains. This fusion protein was created through the addition of two RRMs, taken from the functionally similar human RNA-binding protein, TDP-43, to the C-terminus of FUS 1-359 (FUS-1-359-TDP). An RNA-binding deficient form of this fusion protein (FUS-1-359-TDP3D) was also created by inserting three missense mutations L106D, V108D and L111D (corresponding to positions in full length TDP-43) within the first RRM domain of TDP-43, which has previously been shown to severely disrupt the RNA-binding capacity of TDP-43 (Buratti and Baralle, 2001) (Figure 4.7A). These fusion constructs were expressed at a level comparable to that of FUS 1-359 in SH-SY5Y cells as detected by western blot of total cellular lysates 24 h post-transfection using an antibody recognising GFP (Figure 4.7B). As expected, the addition of RNA-binding competent RRM domains to FUS 1-359, but not those with RNA-binding disrupting mutations, was sufficient to prevent the aggregation of these proteins into large aggresome structures (Figure 4.7C) and permit their recruitment into sodium arsenite-induced SGs (Figure 4.7D).

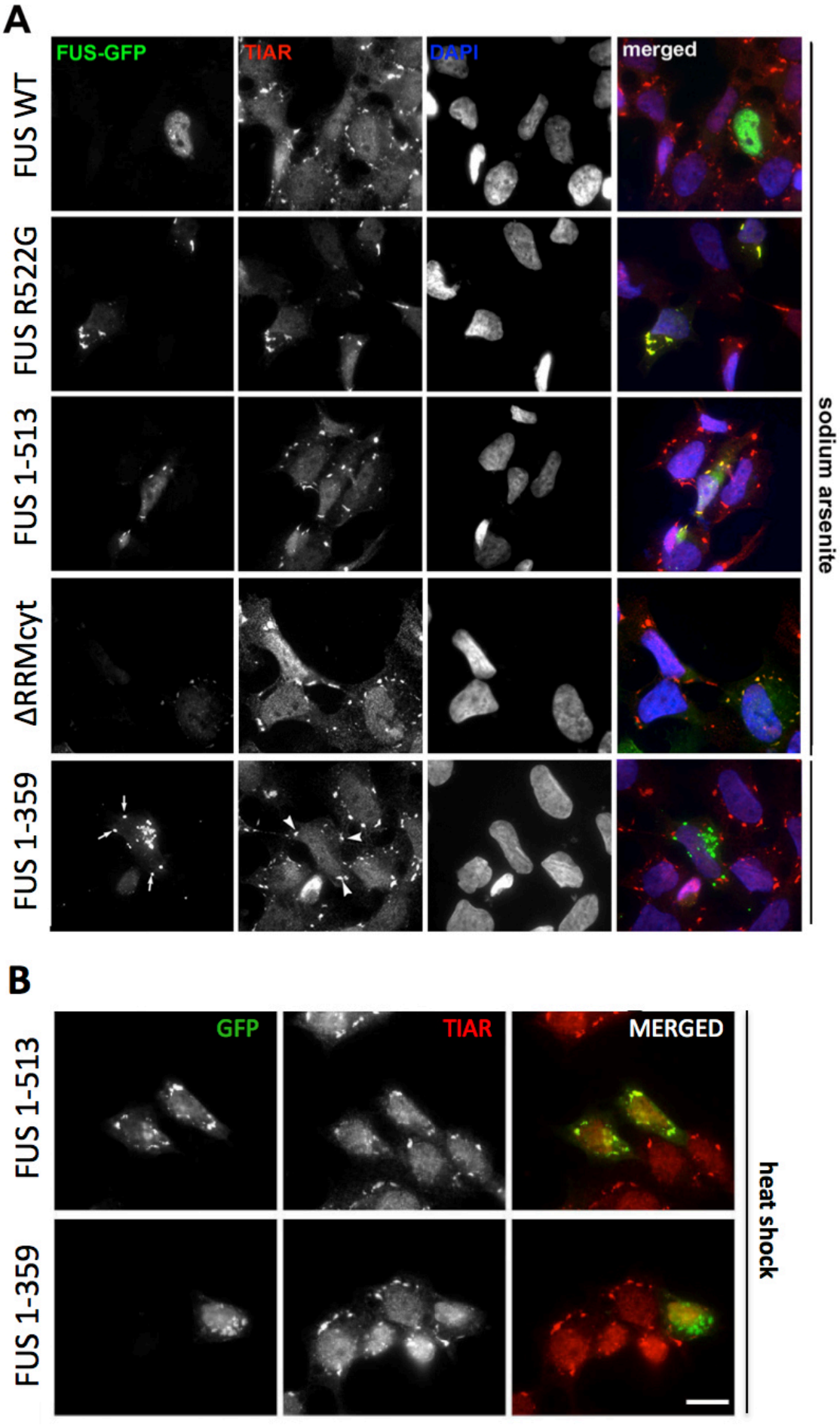
A
FUS-GFP
TIAR
DAPI
merged
FUS WT
FUS R522G
FUS 1-513
ΔRRMcyt
FUS 1-359
sodium arsenite
B
GFP
TIAR
MERGED
FUS 1-513
FUS 1-359
heat shock

Previous page:

Figure 4.5. FUS 1-359 is not recruited into bona fide, induced SGs. FUS mutants, R522G, 1-513 and ΔRRMcyt, but not C-terminal truncation mutant, FUS 1-359, are recruited into SGs, as visualised by anti-TIAR antibody, upon the induction of SG formation by either 0.5 μM sodium arsenite treatment (A) or heat shock at 43°C for 1 h (B). Arrows, FUS granules; Arrowheads, SGs. Scale bar for all panels; 15 μm. At least 3 biological replicates were performed and representative images are shown.

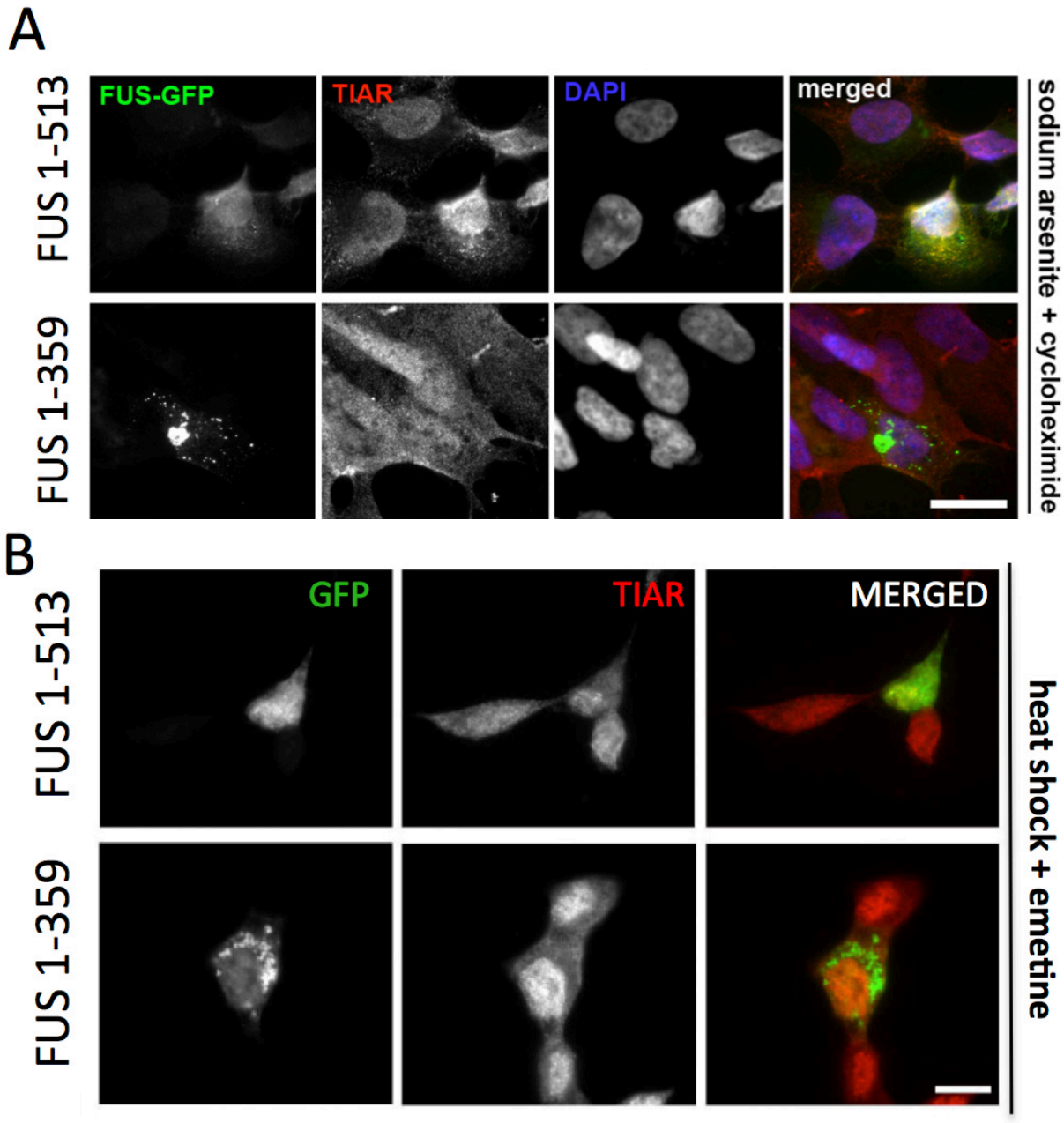

Figure 4.6. Induction of SG formation is prevented by translational inhibitors, yet this is not sufficient to prevent the formation of FUS 1-359 aggregates. Treatment with either cycloheximide (A) or emetine (B) was sufficient to disrupt induction of SG formation and the recruitment of FUS 1-513 to these structures although large FUS 1-359 structures persisted. Anti-TIAR staining was used to confirm the absence of SGs under these conditions. Scale bars; 15 μm. At least 3 biological replicates were performed and representative images are shown.

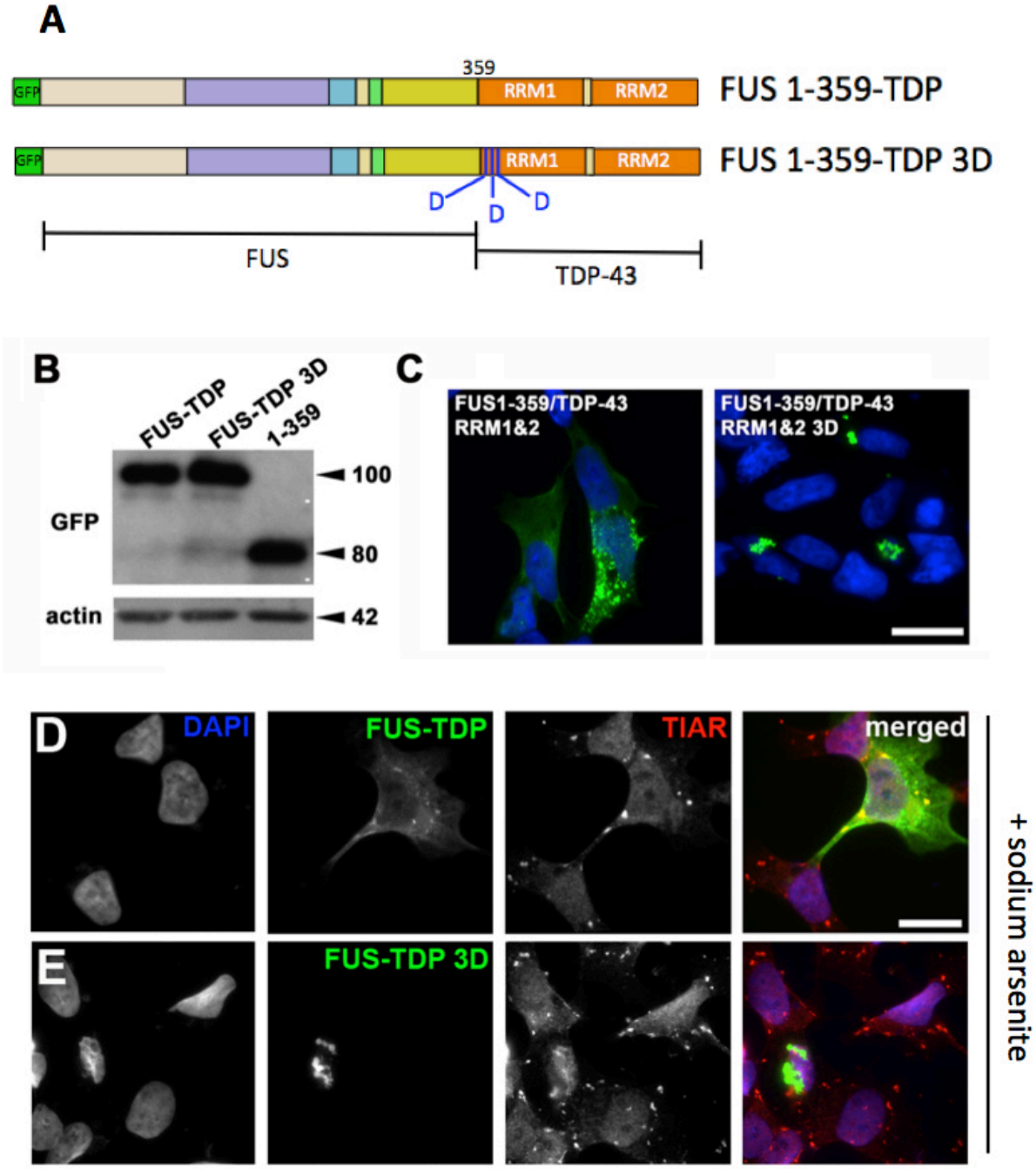

Figure 4.7. Addition of functional RNA-binding domains from TDP-43 prevents formation of large aggregates and restores recruitment of FUS 1-359 to induced SGs. (A) RRM domains from TDP-43 were added to the C-terminus of FUS 1-359. Fusion construct FUS 1-359-TDP 3D harbored 3 asparagine missense mutations (blue) to disrupt the RNA-binding capacity of the TDP-43 domains. (B) Fusion constructs were expressed at comparative levels as demonstrated by western blot from transfected SH-SY5Y cells using anti-GFP antibody. Membranes were reprobed with anti-β-actin antibody to confirm equal loading. In all cells analysed, the addition of RRM domains (C,D), but not those harboring functionally disruptive mutations (C,E), from TDP-43 was sufficient to prevent the agglomeration of FUS 1-359 into larger structures (C) and permitted the recruitment of this fusion protein to sodium arsenite-induced SGs (D,E). Scale bars; 15 μm. At least 3 biological replicates were performed and representative images are shown.

4.3.5 Ability of FUS 1-359 to seed aggregation

In the previous chapter, large inclusions of FUS 1-359 were shown to sequester endogenous FUS in transgenic mice, highlighting a potential seeding mechanism of this FUS isoform. To investigate this further, it was probed *in vitro* whether FUS 1-359 was able to seed the aggregation of other FUS forms, importantly, endogenous FUS from the nucleus. FUS 1-359 was co-expressed with either R522G or WT FUS in SH-SY5Y cells. Similarly to immunohistochemical studies in our transgenic mice, an antibody to the C-terminus of FUS was used to detect the localisation of other FUS forms independent of FUS 1-359, which is not recognised by this antibody (Figure 4.8A). When coexpressed with FUS 1-359, R522G and WT FUS were both recruited to FUS 1-359 foci (Figure 4.8B). Recruitment of endogenous FUS to FUS 1-359 aggregates was also detected although rarely and in small number (~5%) of foci (Figure 4.8B).

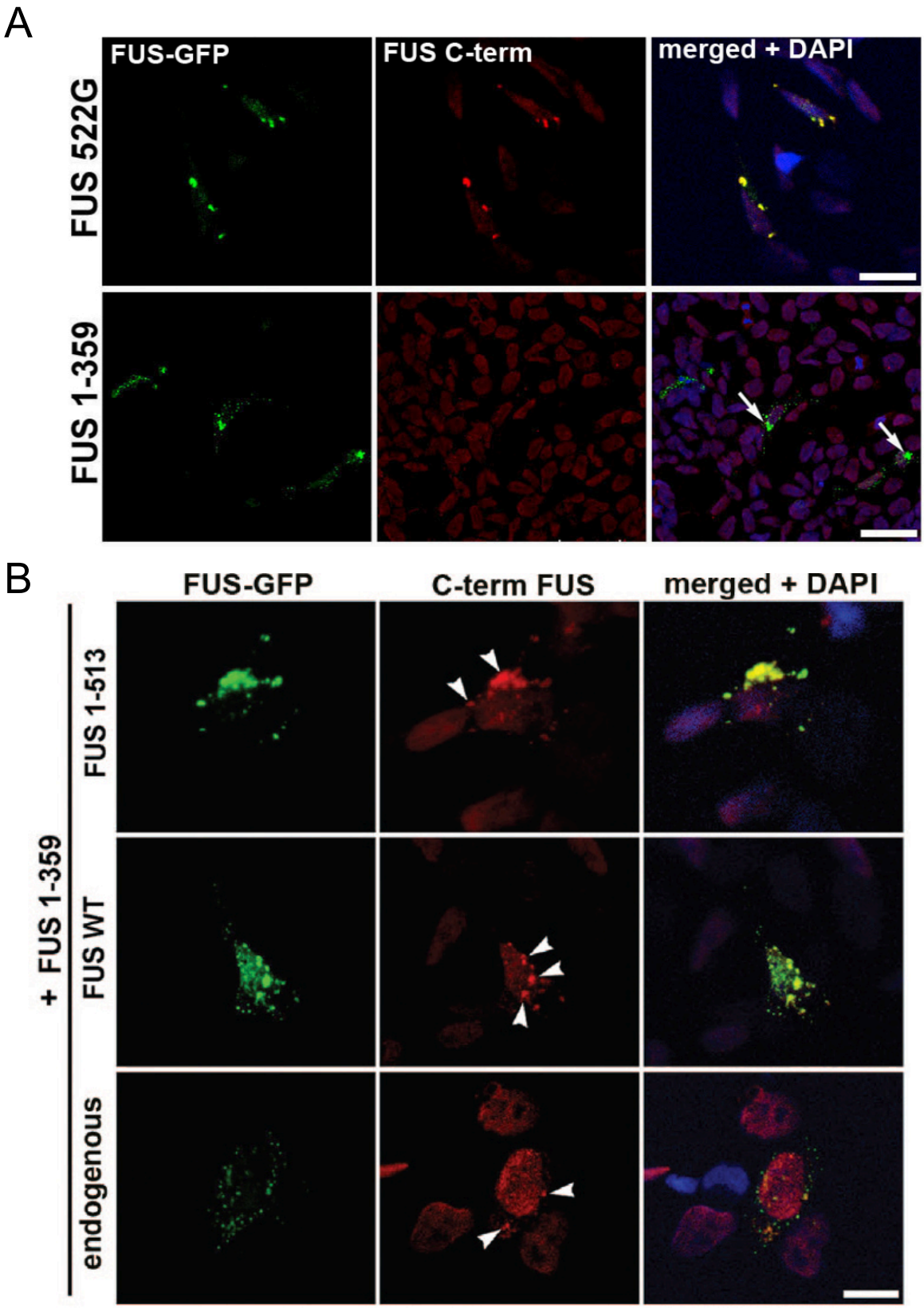

Figure 4.8. FUS 1-359 is capable of seeding aggregation. (A) An antibody to C-terminus of FUS recognises other FUS variants but not FUS 1-359 lacking C-terminal domains (arrows). (B) FUS 1-513, WT FUS and endogenous FUS may all recruited into FUS 1-359 foci following co-transfection. Arrowheads; localisation of FUS independent of FUS 1-359. Scale bars; A (upper panel), 35 μm; A (lower panel), 45 μm; B, 15 μm. At least 3 biological replicates were performed and representative images are shown. Data generated by Dr. Tatyana Shelkovnikova.

4.4 Discussion

Cytoplasmically localised ALS-linked FUS mutant, R522G, was recruited to cytoplasmic structures positive for SG markers both in cells stressed by externally applied factors (heat shock, sodium arsenite) and untreated cells, potentially stressed by overexpression of the protein itself. This agrees with findings by others that suggest ALS-associated FUS variants in the cytoplasm can be incorporated into SGs induced by stressful cellular conditions (Vance *et al.*, 2013; Bosco *et al.*, 2010). This recruitment pattern was also seen with other cytoplasmically localised FUS variants, namely FUS 1-513, which lacks the NLS, and ΔRRMcyt, a cytoplasmically targeted FUS variant with deleted RRM domain. However, the recruitment of WT FUS to induced SGs was not observed, recapitulating findings that a cytoplasmic localisation of FUS is key for recruitment to these structures (Dormann *et al.*, 2010). In 2012, Bentmann *et al.* (2012) suggested that the major domains required for recruitment of FUS to SGs were the RGG and ZF domains and that the RRM was involved to a limited extent. Here, cytoplasmic FUS lacking the RRM domain was able to be recruited into SG marker-positive structures, supporting that this domain is not necessary for this process, however, the degree to which deletion of this domain affects the dynamics of recruitment to these structures remains unknown.

Supporting a previously suggested definite role for RGG and ZF domains in recruitment to SGs, FUS lacking NLS, RGG and ZF domains, unlike other FUS variants studied, was not recruited to SG marker-positive structures in naïve or exogenously stressed cells. Although proper SGs form in these cells in response to exogenous stresses, these SGs were negative for FUS 1-359. Instead, this FUS variant, with compromised RNA-binding, formed foci clearly distinct from SGs.

Dormann *et al.* (2010) have previously suggested that SGs may be precursors to the large cytoplasmic FUS-positive inclusions seen in ALS and FTLD patients. However, at no point during our experiments was the agglomeration of FUS-positive SGs into larger structures detected. The RNA-binding capacity of FUS 1-359 is severely compromised given the removal of its major RNA-binding domains - the RGG, ZF and NLS domains. Supporting this, others have previously shown that even a slightly longer FUS 1-375 construct, also lacking these domains failed to bind either UG_{12} or CCUC RNA probes *in vitro* (Bentmann *et al.*, 2012). Given this diminished capacity, FUS 1-359 was unable to be recruited to SG marker-positive structures and was accompanied by a prominent and extreme aggregation of the protein. Over time, small dot-like aggregates of FUS 1-

359, unable to be recruited into these structures, instead came together to form large juxtanuclear structures with features typical of aggresomes.

Additionally, restoration of RNA-binding ability of FUS 1-359, through the generation of FUS-fusion proteins, restored its recruitment to proper, inducible SGs, preventing its irreversible aggregation into large aggresome structures. This supports evidence provided by others that recruitment into bona fide SGs is dependent on the ability of FUS to bind RNA (Daigle *et al.*, 2013). Taken together, these findings suggest that rather than SGs being maladaptive and pathogenic precursors to the formation of inclusions, they instead prevent irreversible aggregation in the cytoplasm of stressed cells of FUS variants capable of binding to target RNA. This is likely a cytoprotective response of SGs.

In ALS and FTLD, the appropriate protective response by SGs may be somehow disrupted and failure of SGs to sequester cytoplasmically mislocalised FUS, even forms with the intact ability to bind RNA, might lead to their irreversible aggregation. Perhaps even if disruption of SG function was transient, the initial aggregation of FUS outside of SGs could promote the seeding of larger FUS structures through a prion-like mechanism even following the restoration of SG function. The precise circumstances and mechanisms through which ALS-associated forms of RNA-binding competent FUS may aggregate aside from their sequestration into stress-induced SGs remain to be determined, but investigation of these pathways could provide improved understanding of how large FUS inclusions may be formed in FUSopathies.

Results III:

Stress granule-independent aggregation of ALS-associated FUS mutants

5.1 Declaration

Data included within this chapter have been published within the following open access article:

Shelkovnikova TA, **Robinson HK**, Southcombe JA, Ninkina N, Buchman VL. Multistep process of FUS aggregation in the cell cytoplasm involves RNA-dependent and RNA-independent mechanisms. Hum Mol Genet (2014) Oct 1;23(19):5211-26

5.2 Overview

In the previous two chapters, it was shown that experimentally truncated FUS, with reduced ability to bind target RNAs due to the lack of major RNA binding domains, was unable to be sequestered into induced stress granules and, instead, aggregated to form large pathological inclusions, both in mice and cell culture, reminiscent of inclusions formed in ALS patient tissues. At the same time, it was observed that FUS variants carrying ALS-associated mutations and with intact RNA binding domains, readily associated with stress-induced stress granules, a feature also replicated by others (Baron *et al.*, 2013; Bosco *et al.*, 2010; Dormann *et al.*, 2010). However, how ALS-linked FUS variants interacting with physiological RNP granules may give rise to pathological FUS inclusions was not clear. Indeed, it was not known whether the downstream aggregation of these FUS variants capable of entering physiological RNA granules may be similar to the mechanism of inclusion formation for RNA-binding incompetent forms of FUS. Given that understanding the pathways of FUS aggregation into pathological inclusions may be therapeutically relevant for patients with FUS pathology, we sought to characterise the aggregation of ALS-associated forms of FUS in the cytoplasm and determine how these structures may transform in response to cellular stress and attenuated transcription.

5.3 Results

5.3.1 Cytoplasmic FUS spontaneously aggregates in cultured cells in a concentration-dependent manner

As previously demonstrated, GFP-tagged FUS harboring a common ALS-associated mutation, R522G, disrupting its NLS, accumulated in the cytoplasm of cultured neuroblastoma cells where it had the ability to form large granules (Figure 3.1). This was also seen for other FUS variants including FUS 1-466 and FUS 1-513 (Figure 3.1). Detailed characterisation of this phenomenon in both neuroblastoma cells and neurons from primary hippocampal cultures revealed that FUS R522G in the cytoplasm appeared either diffuse (Figure 5.1A) or as one of several accumulated forms,

including small granules (*FUS granules*, FGs) (Figure 5.1B), which further coalesced into clusters of granules (Figure 5.1C) and finally formed aforementioned larger granules (Figure 5.1D). This accumulation of diffuse FUS R522G into these granular forms occurred after a certain concentration threshold was reached, shown by fluorescence intensity measures for GFP in cells expressing either form (Figure 5.1E). Of cells containing accumulated forms of FUS, cells with FGs were most frequent, with clusters of granules and large aggregates less common (Figure 5.1F). As clusters of granules were immediate precursors to larger granules and represented the same structure, these two categories were combined for clarity into *FUS aggregates* (FAs).

High resolution confocal microscopy was performed to determine structural differences between these FAs appearing in naïve cells that highly expressed FUS R522G, and the R522G-positive bona fide SGs induced by sodium arsenite seen in cells expressing low levels of the GFP-tagged protein. Under high magnification, induced SGs were distinct and compact structures, whereas similarly-sized FAs formed by accumulated FUS were non-compact, irregularly shaped accumulations of small round granules (Figure 5.2). Differences in the dynamics of these two structures were also noted. Where further fusion of mature SGs is not typical, this was a common feature for FAs, often coalescing to form larger FAs (Figure 5.1D), as visualised with live cell imaging of transfected cells (data not shown). Additionally, FGs, the precursors to FAs, persist for several hours in cell culture, as evidenced by the great proportion of cells bearing these structures after 24 h, whereas the formation of SGs following sodium arsenite or heat shock induction is rapid, beginning within 10 min and reaching peak formation after 20-30 min (Zhang *et al.*, 2011). Immunocytochemistry for SG markers, TIAR and G3B1 (Figure 5.3A,B), revealed that a fraction of FAs were not positive for these proteins, and although this fraction was not quantified, the formation of SG-marker negative FAs suggests that these proteins are not essential for the integrity of FAs. Again, another protein usually seen within SGs, the ribosomal protein S6 (Kimball *et al.*, 2003), was not seen in FGs or FAs, confirming that stalled pre-initiation complexes were not major components of these FUS structures (Figure 5.3C). Together with this, P-bodies, involved in mRNA processing and turnover (Kedersha and Anderson, 2007), which are normally docked to induced SGs in neuroblastoma cells (Figure 5.4B,C), as visualised with anti-Dcp1a staining, were not docked to FAs (Figure 5.4A).

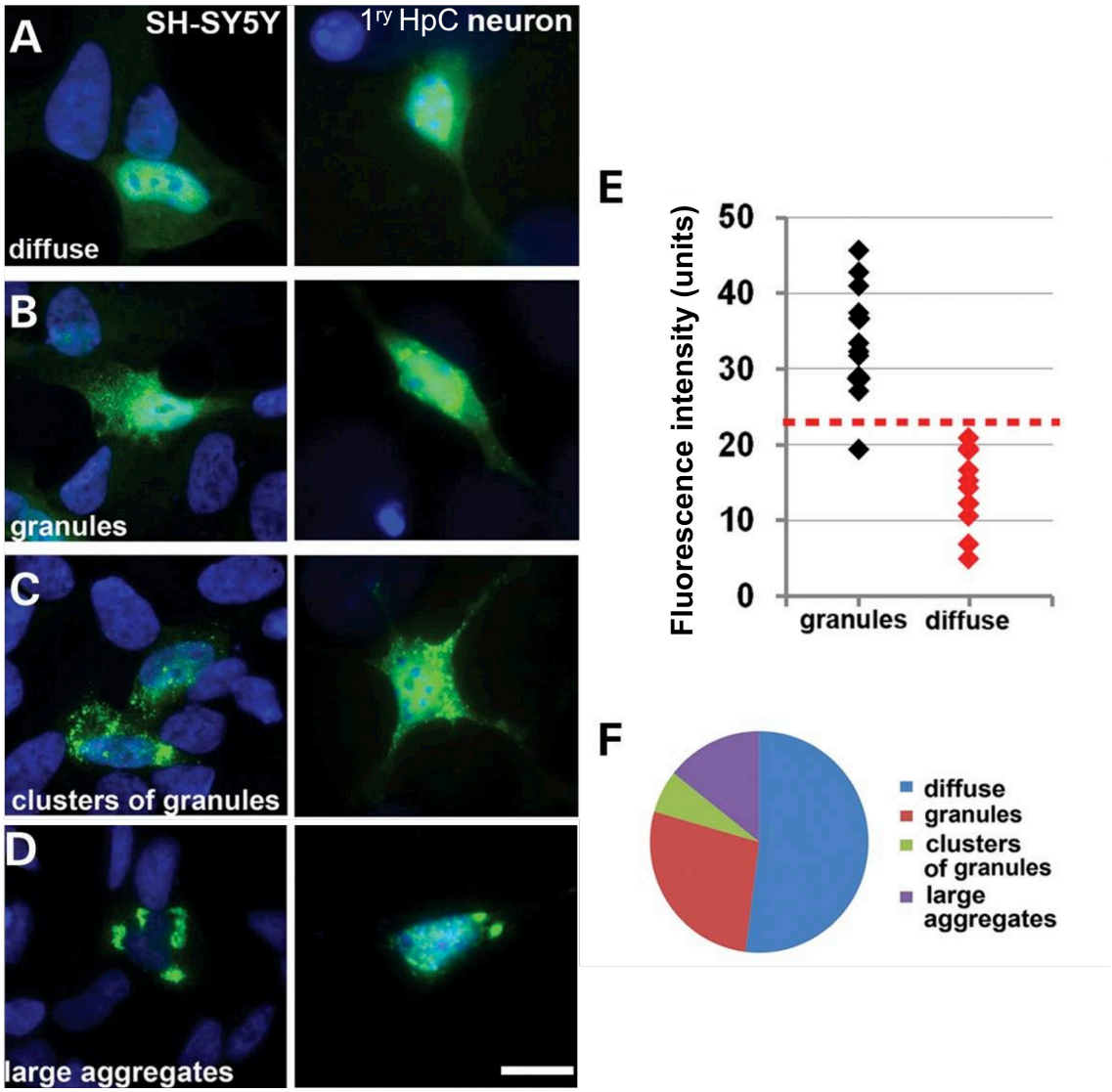

Figure 5.1. ALS-associated mutant FUS R522G accumulated in the cytoplasm and formed granule-like aggregates in a concentration-dependent manner. SH-SY5Y cells cells or primary hippocampal neurons were transfected with GFP-tagged FUS R522G. The protein either displayed diffuse distribution (A) or was found in multiple granule-like microaggregates (B) that in some cells formed clusters (C) or large compact aggregates (D). (E) Aggregation of FUS in the cytoplasm was concentration dependent. Arbitrary units of fluorescence intensity measures from the cytoplasm of individual cells 24 h after transfection with GFP-tagged FUS R522G with diffuse only distribution or with already formed granules are plotted. Red dotted line indicates maximum fluorescence intensity at which diffuse staining was observed for the FUS R522G mutant. (F) Proportion of cells with each type of FUS R522G distribution in the population of expressing cells. Scale bars; 10 μm.

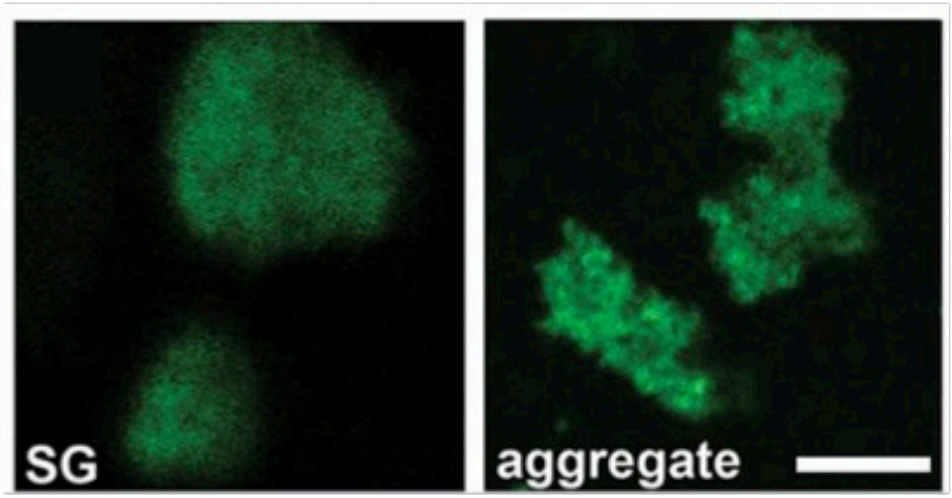

Figure 5.2. High magnification confocal imaging of FUS-positive structures. High magnification confocal maximum projection images of FUS R522G-positive SGs formed in low-expressing COS7 cells upon sodium arsenite treatment (left panel) versus similarly-sized FAs formed by the same protein in naïve COS7 cells (right panel). Scale bar; 2 μm.

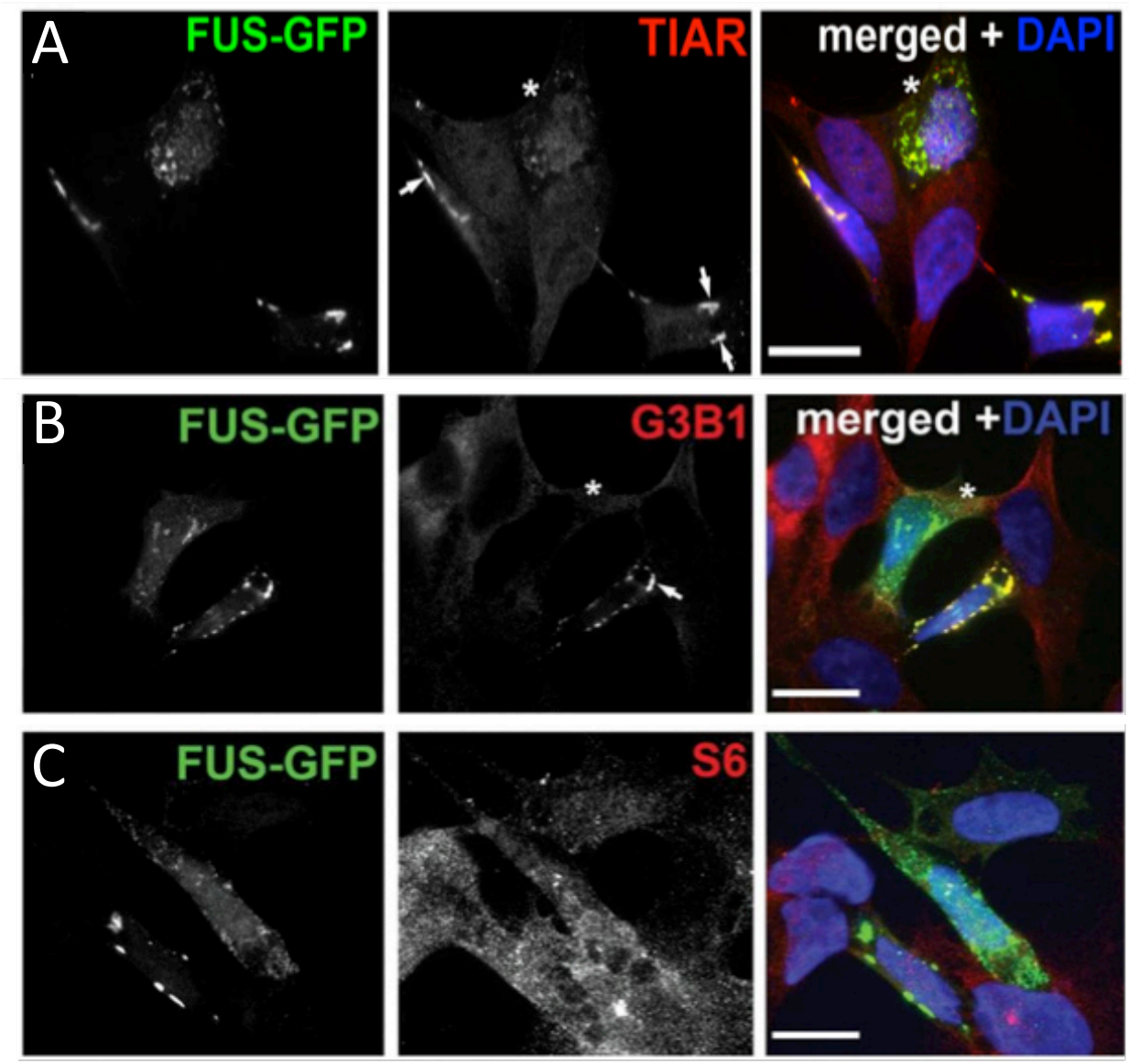

Figure 5.3. FAs display several differences to stress-induced SGs that contain FUS. (A) Some FAs were strongly positive for a SG marker TIAR (arrows), whereas a fraction of FAs displayed only weak or no TIAR immunoreactivity (cell marked with an asterisk). (B) Only a fraction of FAs formed in naïve SH-SY5Y cells were positive for the SG marker, G3B1 (arrow), while other FAs did not contain this protein (cell marked with an asterisk). (C) Ribosomal protein S6 was not accumulated in FGs or FAs. Scale bars; 10 μm.

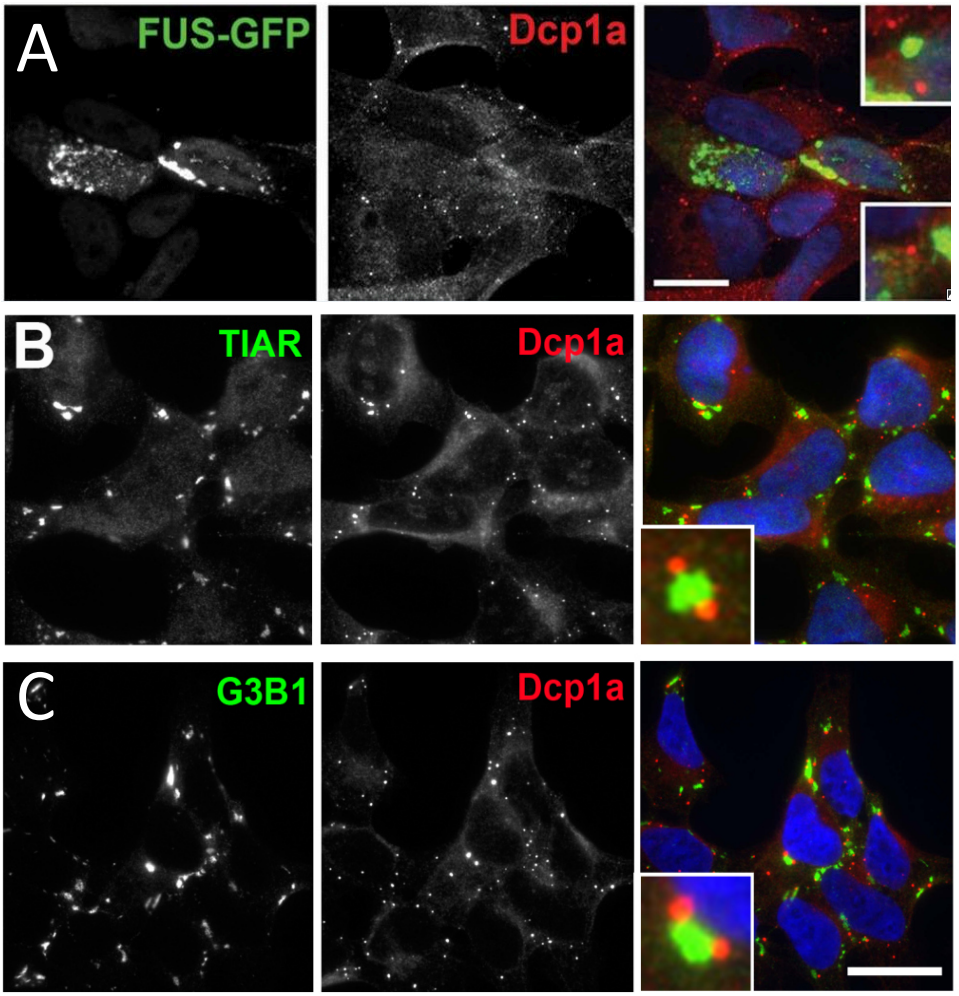

Figure 5.4. P body localisation in SH-SY5Y cells expressing FUS R522G. (A) In SH-SY5Y cells expressing FUS R522G, P bodies visualised with anti-Dcp1a antibody did not occur next to FAs. (B,C) In untransfected sodium arsenite-stressed SH-SY5Y cells, P bodies are located in the immediate vicinity of SGs visualised with anti-TIAR (B) or anti-G3B1 antibodies (C). Scale bars; 10 µm.

5.3.2 RNA is an important structural component of FAs required for their integrity and sequestration of SG-associated proteins

Whilst the above data suggested that FAs were distinct from SGs, a significant proportion of FAs displayed immunoreactivity for SG markers (Figure 5.3B). To determine whether this could be due to secondary recruitment of SG proteins via RNA molecules trapped within FAs by RNA-binding competent FUS, it was first shown that mature RNA transcripts are components of FAs. This was determined using *in situ* hybridisation with a fluorescently labelled oligo(dT) probe that bound to poly(A)$^+$ mRNA (Figure 5.5A). Secondly, following mild methanol fixation of transfected cells, RNase A digestion was sufficient to remove TIAR staining of all FAs (Figure 5.5B, C). However, under the same treatment, sodium arsenite-induced SGs could still be detected with anti-TIAR antibodies (Figure 5.5D). Together this suggested that TIAR was weakly associated with FAs via an RNA interaction, possibly on the surface of FAs, that can readily be removed by RNase treatment even after mild fixation. Contrastingly, TIAR, an integral component of SGs, was not removed following RNase after methanol fixation, highlighting that TIAR may be fixed within the SGs as opposed to secondarily bound. However, as other explanations for these data are possible (perhaps relative abundance of FUS and TIAR is important in the fixing and sensitivity to RNase), this possibility needs to be further investigated in the future.

Although TIAR staining was removed following RNase treatment post-fixation, FAs themselves persisted (Figure 5.5C, D). By isolating Triton-X-100 soluble and insoluble fractions from naïve cells expressing GFP-tagged FUS R522G, it was shown, as expected, that FUS R522G accumulated over time in this insoluble fraction (Figure 5.6A). To further assess the role of RNA in FAs we sought to determine how the distribution of FUS between soluble and insoluble fractions changed following RNase A treatment. Upon RNase A treatment of lysates, a profound shift of the protein towards the soluble fraction was observed (Figure 5.6B, C). Note that in this instance, cells were not fixed prior to RNase treatment. Furthermore, and replicating immunocytochemical findings, the insoluble fraction was weakly positive to TIAR staining, which was removed following RNase treatment (Figure 5.5D).

We sought to determine the source of the RNA that was required for FA integrity by quantifying the fraction of cells containing FAs following inhibition of either translation with emetine or transcription with actinomycin D. Treatment with emetine, which stalls pre-initiation complexes, reduced the proportion of cells with FAs and inhibition of transcription with actinomycin D, had a similar effect (Figure 5.6E). Together, this

suggested that transcripts running off polysomes, blocked by emetine, and newly synthesised transcripts, reduced by actinomycin D, contribute to integrity of FAs.

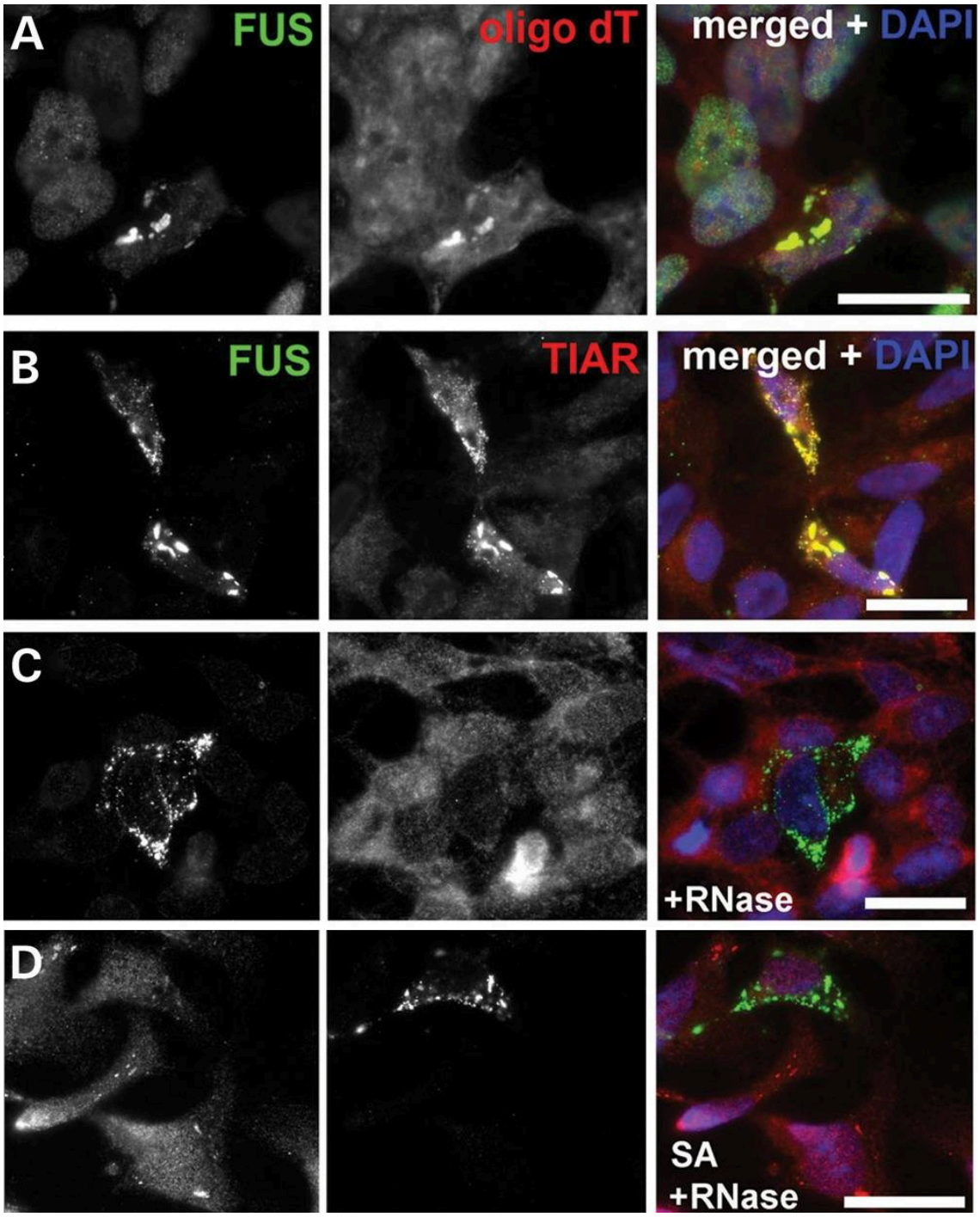

Figure 5.5. Poly(A)$^+$ mRNA is incorporated into FAs and recruitment of SG protein, TIAR to these structures is RNase-sensitive. FAs formed by FUS R522G in SH-SY5Y cells were enriched in poly(A)$^+$ mRNA as revealed by RNA-FISH with fluorescently labeled oligo(dT) probe. (B–D) Some FAs were strongly positive for TIAR (B), but this protein was removed from all aggregates by RNase treatment on cover slips following mild methanol fixation (C) while sodium arsenite-induced SGs remained TIAR positive following this treatment (D). Scale bars; 15 μm.

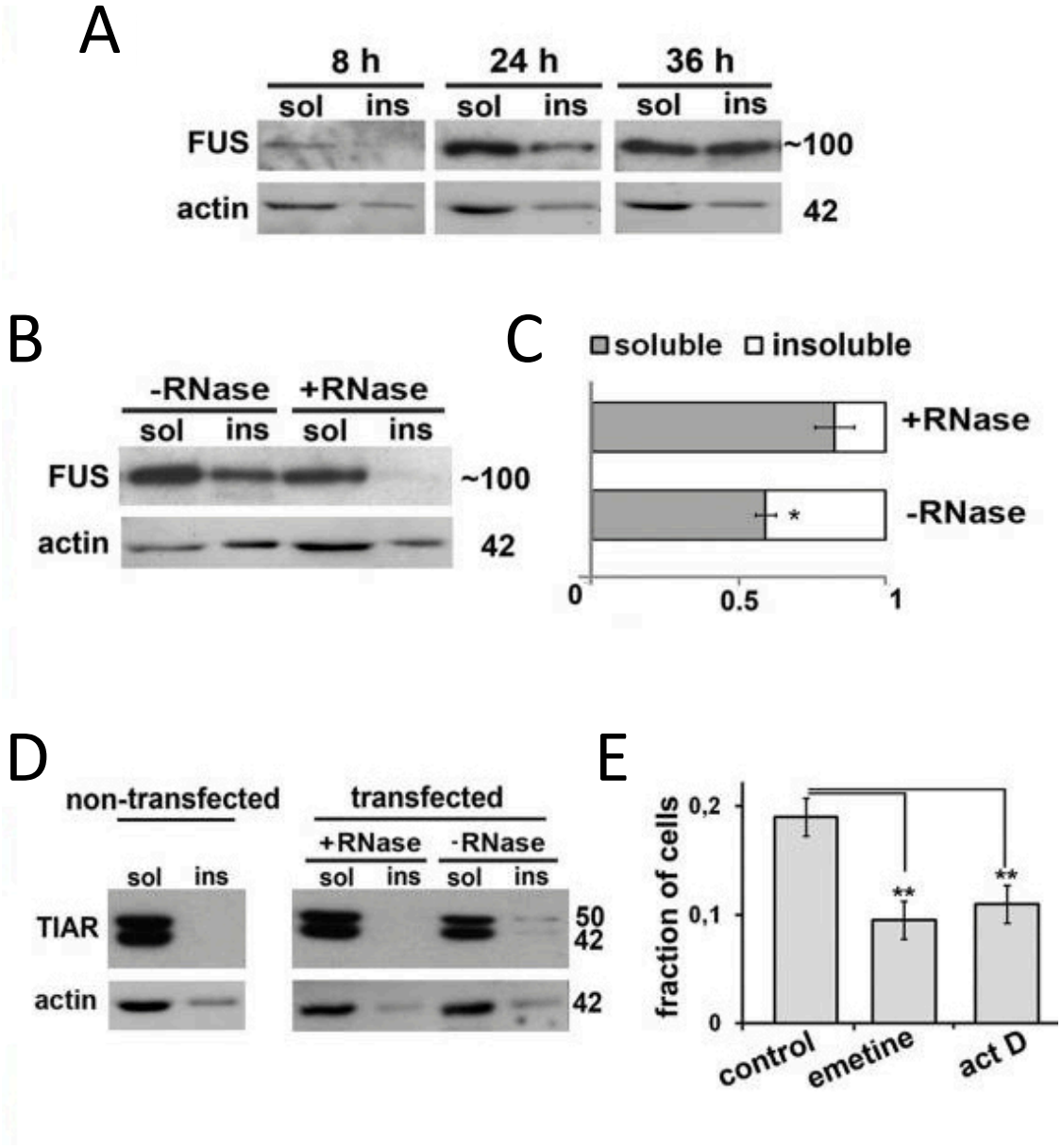

Figure 5.6. RNA is important for the integrity of FAs. (A) Western blots show that FUS R522G progressively accumulated in Triton X-100 insoluble (ins) fraction of transfected SH-SY5Y cells. (B) RNase treatment of cell lysates prior to fractionation shifted GFP-tagged FUS R522G protein to the soluble (sol) fraction. Equal proportions of soluble and aggregated fractions were analysed on western blots. (C) Quantification of B. (D) TIAR was found only in soluble fraction in non-transfected cells, was partially recruited into insoluble fraction in cells expressing FUS R522G but could be re-solubilised by digestion of lysates with RNase A prior to fractionation. (E) Treatment with a translational inhibitor, emetine, or a global transcriptional repressor, actinomycin D (act D), for 2 h resulted in disintegration of a significant proportion of FAs and, consequently, a reduction in the fraction of transfected cells bearing these structures. For western blots, sizes of proteins (in kDa) are shown. Bar charts in C and H show means ± S.E.M, *$p < 0.05$, ** $p < 0.01$.

5.3.3 N-terminal prion-like domain and the ability to bind to a specific pool of RNAs are both required for FUS aggregation in the cell cytoplasm

As well as the integrity of FAs elicited by interactions with RNA arising from RNA-binding domains of FUS, we wondered how the prion-like N-terminus of the protein might contribute to this aggregation, for example, whether it could have important roles in the formation or perhaps even growth of FAs. Removing the N-terminus domain from FUS R522G, giving rise to the truncated FUS proteins, CT or CT-RRM (Figure 5.7A), resulted in loss of visible aggregation of the protein in the cell cytoplasm (Figure 5.7B, C) and its disappearance from the insoluble fraction (Figure 5.7D). Addition of a known prion domain from the yeast protein, Sup35, to the N-terminus of FUS CT fragment was sufficient to restore this aggregation capacity (Figure 5.7B, D). To determine whether various pools of RNA were sufficient for FUS aggregation, the major RNA-binding domains of FUS were replaced with non-homologous RNA recognition motifs from functionally similar human TDP-43 protein or an evolutionarily distant yeast protein Npl3 (Figure 5.7A). In SH-SY5Y cells, FUS-TDP-43 chimeric protein formed structures resembling those formed by FUS R522G and was present in the insoluble fraction (Figure 5.7B, C). Contrastingly, FUS-Npl3 chimeric protein was only observed in the soluble fraction and displayed diffuse staining, irrespective of its expression level (Figure 5.7B, C). This suggests that FUS aggregation within the cytoplasm requires both the prion-like activity of the N-terminus but also interactions with a specific pool of RNAs, although the exact nature of these RNAs remain to be determined. Note, the contribution of potential protein-protein interactions arising from these RNA-interacting domains is unknown.

5.3.4 FGs are a novel type of RNA granule

Next, we sought to further characterise the early precursor structures, FGs, to ascertain whether these may be nucleated by existing RNP granules known to contain FUS or whether they represent a separate entity yet to be described. Upon high resolution microscopy, FGs were shown to be relatively uniform, round structures of approximately 150-200 nm diameter (Figure 5.8A). Therefore, comparison was carried out between FGs and a similarly sized (100-200 nm) granule observed in neurons and known to contain FUS, the kinesin-associated RNA transport granule (Kanai *et al.*, 2004). These transport granules are detergent-resistant and sensitive to RNase, so the following experiments were performed to see whether FGs also displayed similar features.

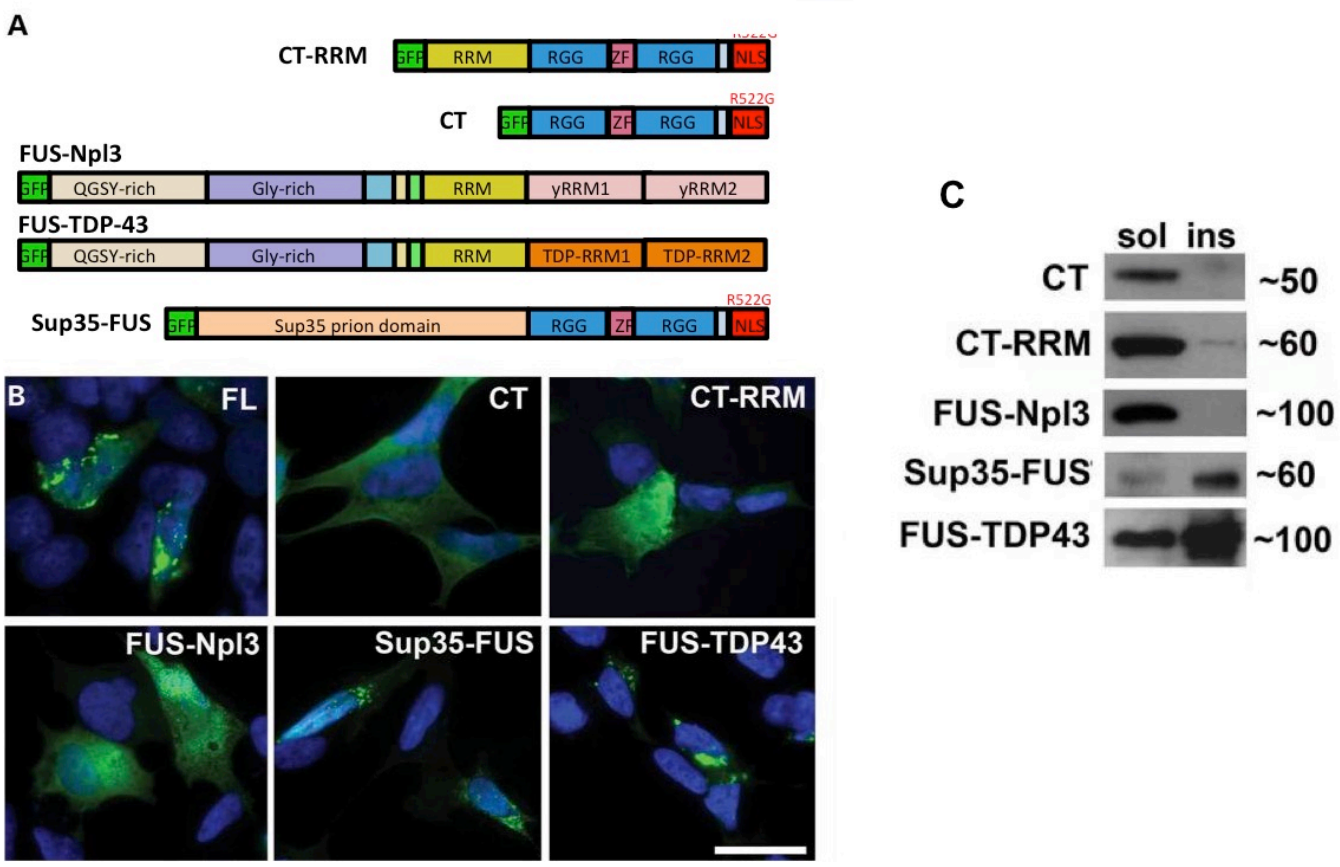

Figure 5.7. N-terminus prion-like domains and the ability to bind a specific pool of RNAs are both essential for FA formation. (A) Schematic representation of GFP-tagged experimental FUS constructs used. N-terminal domains of FUS were removed from CT-RRM and CT fragments, whereas in FUS-Npl3 and FUS-TDP-43 the major RNA-binding domains within the C-terminus were replaced with ectopic RRM domains from either yeast Npl3 protein or TDP-43 protein, respectively. In Sup-35-FUS, the N-terminus domains of FUS were replaced with the prion domain (amino acids 1-125) of yeast protein, Sup35. (B) Sup35-FUS and FUS-TDP43 were able to recapitulate the formation of aggregates as seen in full length FUS with R522G mutation (FL), yet only diffuse distribution was seen for CT, CT-RRM and FUS-Npl3. (C) Western blot analysis of proteins in fractionated lysates of transfected cells with anti-GFP antibody demonstrated that FUS-TDP-43 and Sup-35-FUS are recovered in Triton X-100 insoluble fraction, while CT, CT-RRM and FUS-Npl3 are almost wholly soluble. Scale bar; 15 μm.

A fraction of cellular lysate from cells transfected with either FUS R522G or 1-466 (dRGG3) that was enriched for FGs and depleted of FAs was isolated using a differential centrifugation protocol commonly used for preparation of RNA transport granule-enriched fraction. RNase treatment of lysates prior to fractionation resulted in a shift of the FUS proteins from particulate pellet to soluble supernatant fractions (Figure 5.8B, D). Fragile X mental retardation protein (FMRP), a component of RNA granules, was used as a marker of RNA granules and was also efficiently dissipated following RNase treatment (Figure 5.8B), suggesting that RNAs are required for structural integrity of both types of granules. Similarly to experiments performed on FAs, treatment of transfected cells with emetine or actinomycin D were used to gauge the source of RNA required for integrity of FGs. Whist FGs also displayed a shift to the soluble fraction occurred following actinomycin D (Figure 5.8D), unlike FAs, FGs persisted following emetine treatment (Figure 5.8C). This suggested that FGs are most likely nucleated on newly synthesised transcripts exiting the nucleus.

Immunocytochemistry with known markers for endogenous RNA transport granules was also performed to further investigate the possibility that FGs represented these structures. No overlap was seen between FGs and FMRP, a component of neuronal RNA granules (Figure 5.8E). Additionally, only partial overlap was observed for FGs with DEAD box helicase 5 (DDX5), also a common constituent of neuronal RNA transport granules (Kanai *et al.*, 2004) (Figure 5.8F). Along with this, FAs were strongly positive for DDX5, whereas sodium arsenite-induced SGs were negative (Figure 5.9), providing a distinguishing marker between these two structures and also providing further evidence for FGs being precursors of FAs. Considering these findings together, it was concluded that FGs represented a novel RNP granule, which also had the ability to sequester some proteins that are constituents of physiological neuronal RNP structures.

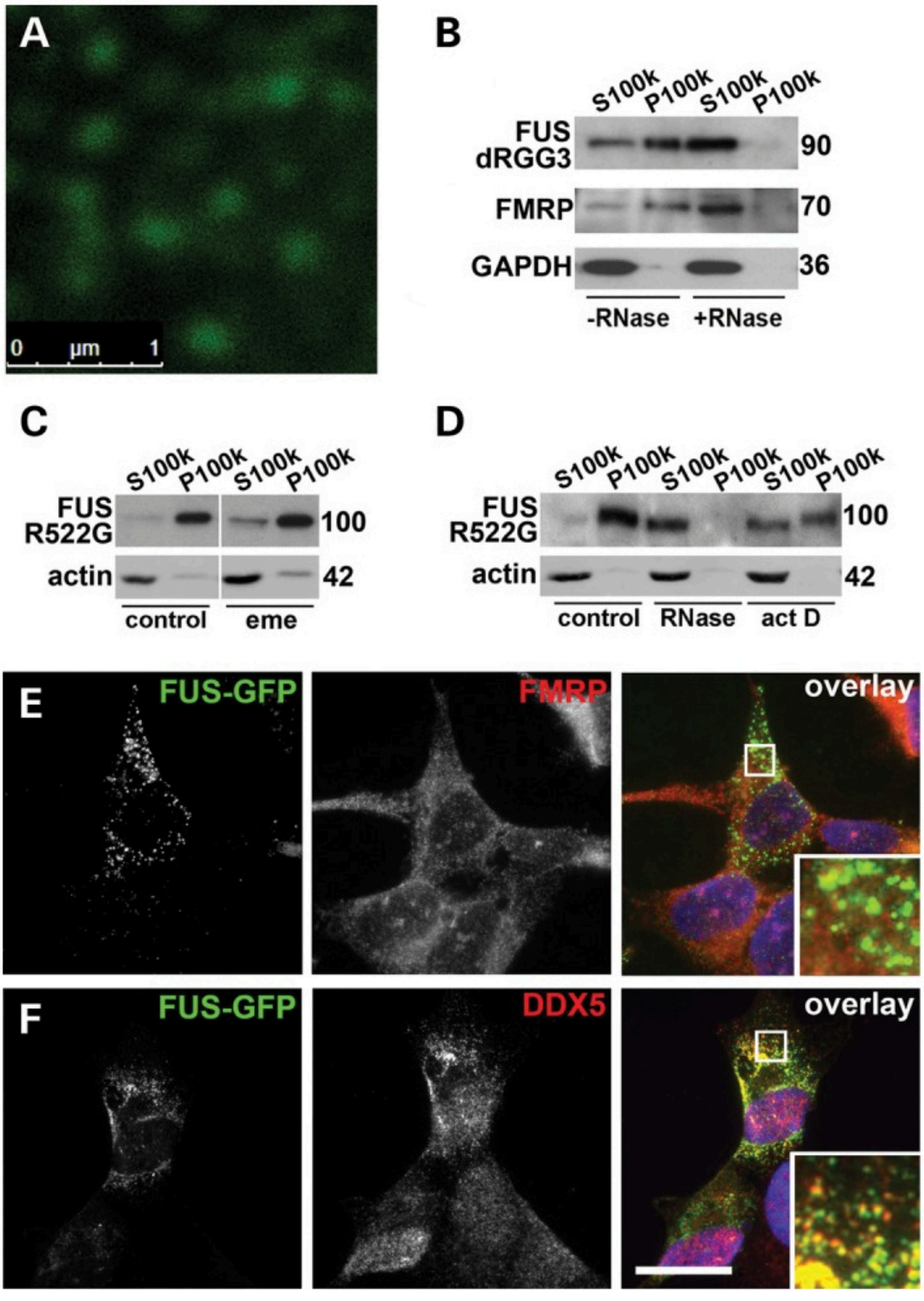
A
0 µm 1
B
S100k P100k S100k P100k
FUS dRGG3
FMRP
GAPDH
90
70
36
-RNase +RNase
C
S100k P100k S100k P100k
FUS R522G
actin
100
42
control eme
D
S100k P100k S100k P100k S100k P100k
FUS R522G
actin
100
42
control RNase act D
E
FUS-GFP
FMRP
overlay
F
FUS-GFP
DDX5
overlay

Previous page:

Figure 5.8. FGs were assembled on newly synthesised RNA and shared some, but not other, features of RNA transport granules. (A) High-magnification confocal image of FGs formed by GFP-tagged FUS R522G in the cytoplasm of SH-SY5Y cells. (B) FGs were RNase-sensitive. Western blot of proteins from a granule-enriched fraction (P100K) and soluble (S100K) fraction isolated in the presence or absence of RNase A from cells transfected with GFP-tagged FUS 1-466 (dRGG3). The membrane was reprobed with antibodies against FMRP, a core protein of neuronal RNA transport granules, and soluble GAPDH protein. (C, D) Novel transcripts but not mRNAs from polysomes contributed to the stability of FGs. SH-SY5Y cells expressing GFP-tagged FUS R522G, were treated with translational elongation inhibitor, emetine (C) or transcriptional inhibitor, actinomycin D (D) for 2 h prior to lysis and fractionation to granule-enriched (100 000 g pellet, P100k) and soluble (100 000 g supernatant, S100k) fractions. RNase A-treated sample was processed in parallel as an internal positive control. (E) FGs were negative for FMRP. (F) A a subset of FGs were DDX5-positive. In (B–D), three times more P100k fraction relative to S100k fraction was loaded; for western blots, sizes of proteins (in kDa) are shown. Scale bars; 15 μm.

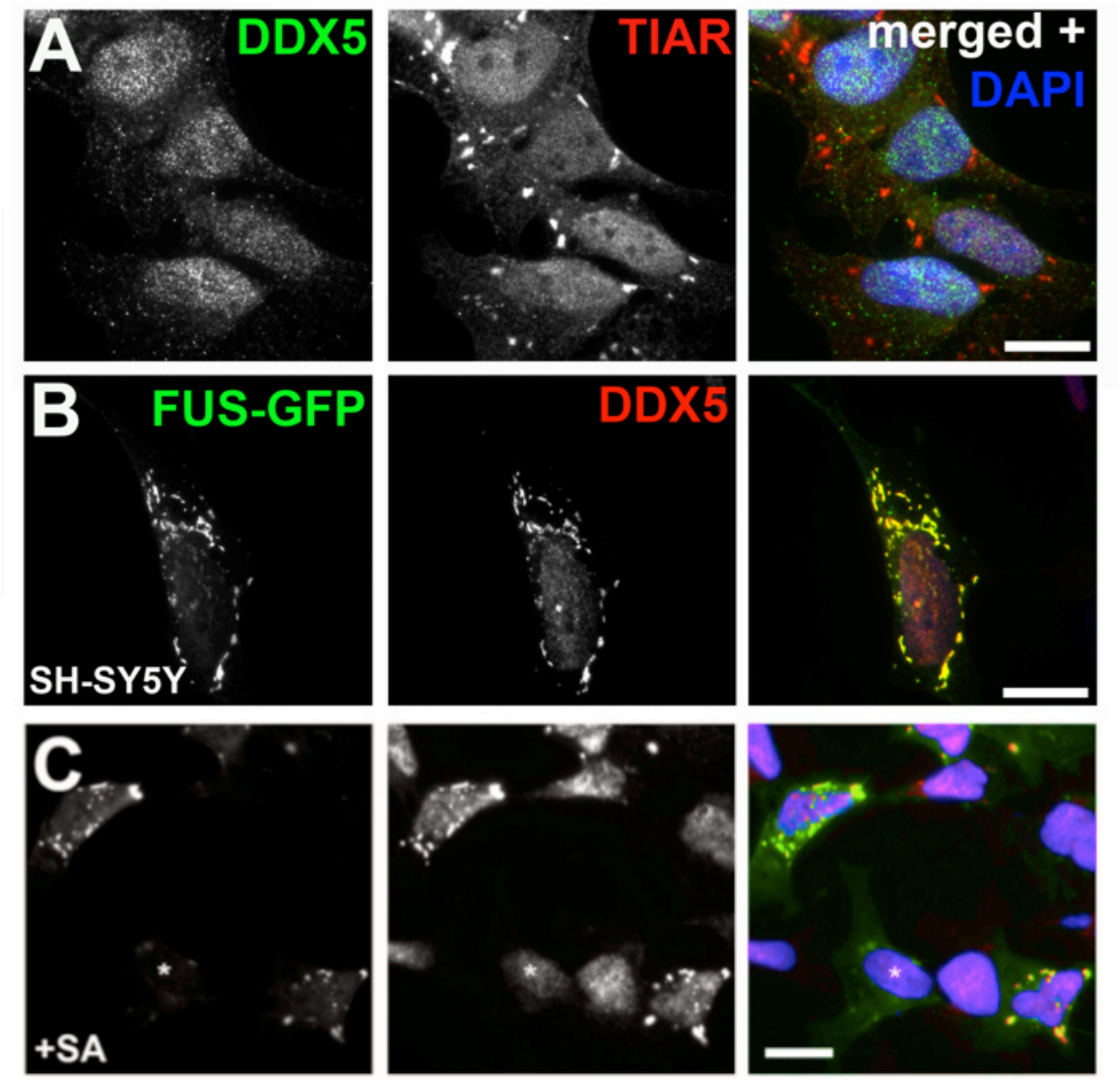

Figure 5.9. DDX5 can be used as a selective marker of FAs, distinguishing them from induced SGs. (A) In SH-SY5Y cells, DDX5 was not recruited to sodium arsenite-induced SGs as revealed by co-staining with anti-DDX5 and anti-TIAR antibodies. (B) FAs formed in SH-SY5Y cells expressing GFP-tagged FUS R522G were strongly positive for DDX5. (C) In cells with a low level of FUS and lacking FGs/FAs, sodium arsenite treatment induced formation of FUS-positive SGs that were negative for DDX5 (cell marked with an asterisk). Scale bars; 10 μm.

5.3.5 FAs disrupt formation of stress granules and P-bodies

In conditions of cellular stress, the level of free mRNA is dramatically increased as polysomes are dissociated and mRNA transcripts are run off (Kedersha *et al.*, 2000; Bounedjah *et al.*, 2014). As it was demonstrated that RNA is required for the formation and integrity of FAs, we predicted that conditions of cellular stress would favour FA assembly. Using live cell imaging, the response of FGs to sodium arsenite-induced stress was monitored over time. As predicted, following stress insult, FGs rapidly clustered and assembled into FAs, occurring on a much shorter timescale than transition from FGs into FAs in naïve cells, normally taking several hours to develop (Figure 5.10A and data not shown). As FAs indeed developed in a fraction of naïve cells (Figure 5.1D, F), it could indicate that a stress response had been initiated in this subpopulation. Supporting this, in cells with only FGs the level of phosphorylated eIF2α, a reliable marker of stress, was the same as in untransfected cells but was markedly higher in the majority of cells with FAs (Figure 5.10B, C).

To determine whether this recruitment of RNA and SG proteins into FAs may disrupt the formation of SGs, the ability of cells to form stress-induced SGs was compared in cells expressing either diffuse FUS or FAs. Cells expressing diffuse FUS formed typical SGs strongly positive for G3BP1, which sequestered FUS, following sodium arsenite treatment (Figure 5.11A, asterisk, 5.12). On the other hand, those with pre-formed FAs or FGs generally failed to form SGs (Figure 5.11A, double asterisk) or displayed reduced SGs per cell compared to those formed in cells with diffuse FUS (Figure 5.11C).

It is also possible that FAs disrupt the formation of other RNP structures, including P-bodies. P-bodies were abundant in SH-SY5Y cells (Figure 5.4) yet in cells displaying FGs or FAs, P-bodies were lost, with the majority of these cells displaying fewer than two P-bodies and often none at all (Figure 5.11D). Furthermore, FAs displayed differential immunoreactivity to P-body protein, Dcp1a, (Figure 5.11B) suggesting that FAs can disrupt P-body formation not only by RNA sequestration but by depletion of local pools of P-body protein components, e.g. Dcp1a.

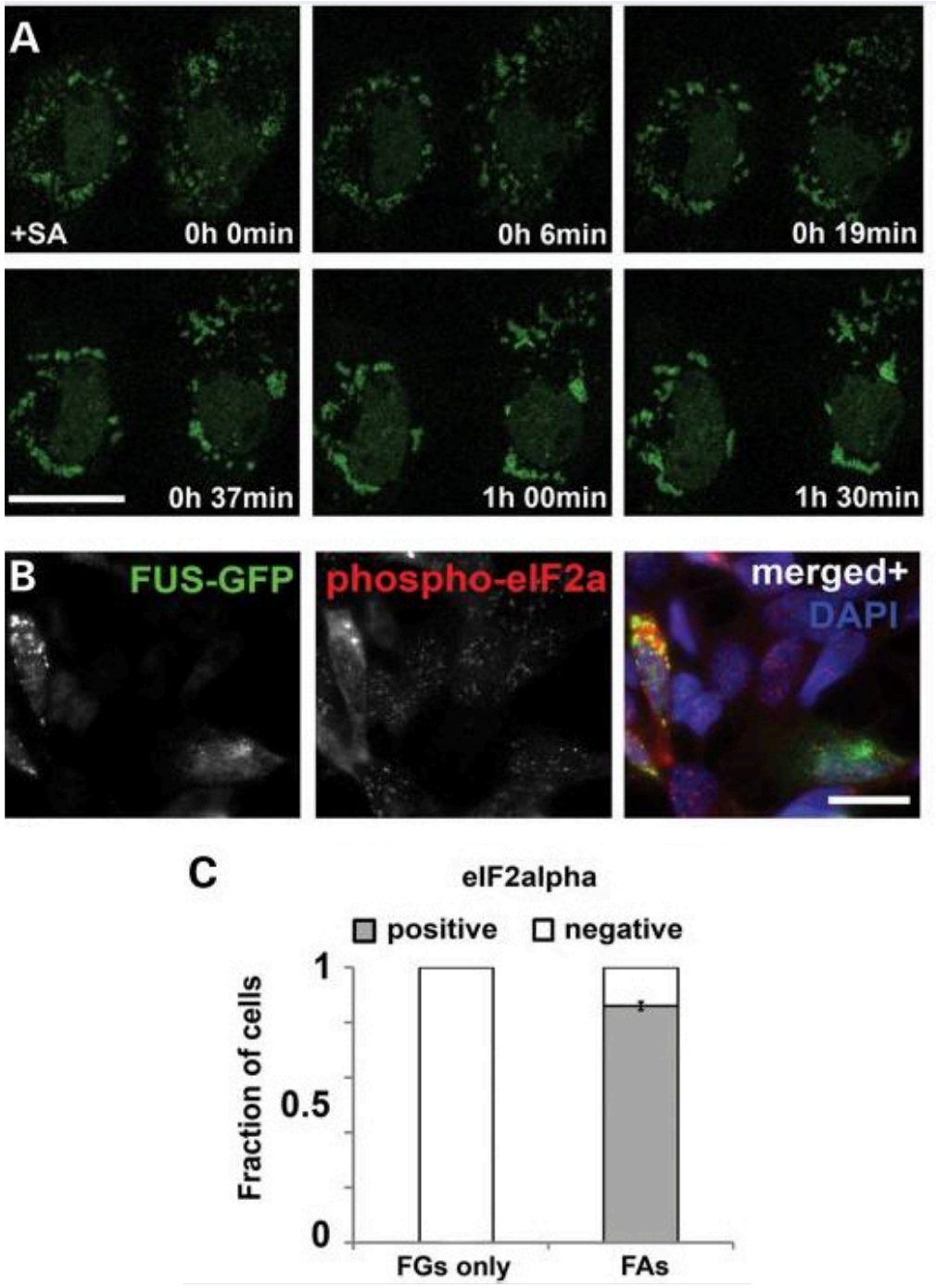

Figure 5.10. Cellular stress promoted the formation of FAs. (A) Live cell imaging revealed rapid assembly of FGs into FAs in cells subjected to sodium arsenite (SA) within 1.5 h. (B and C) The majority of naïve cells with FAs displayed elevated levels phospho-eIF2alpha, a marker of activated cellular stress response, while levels of this protein were unaltered in cells with FGs only. Bar chart shows means ± S.E.M, Scale bars; 10 µm.

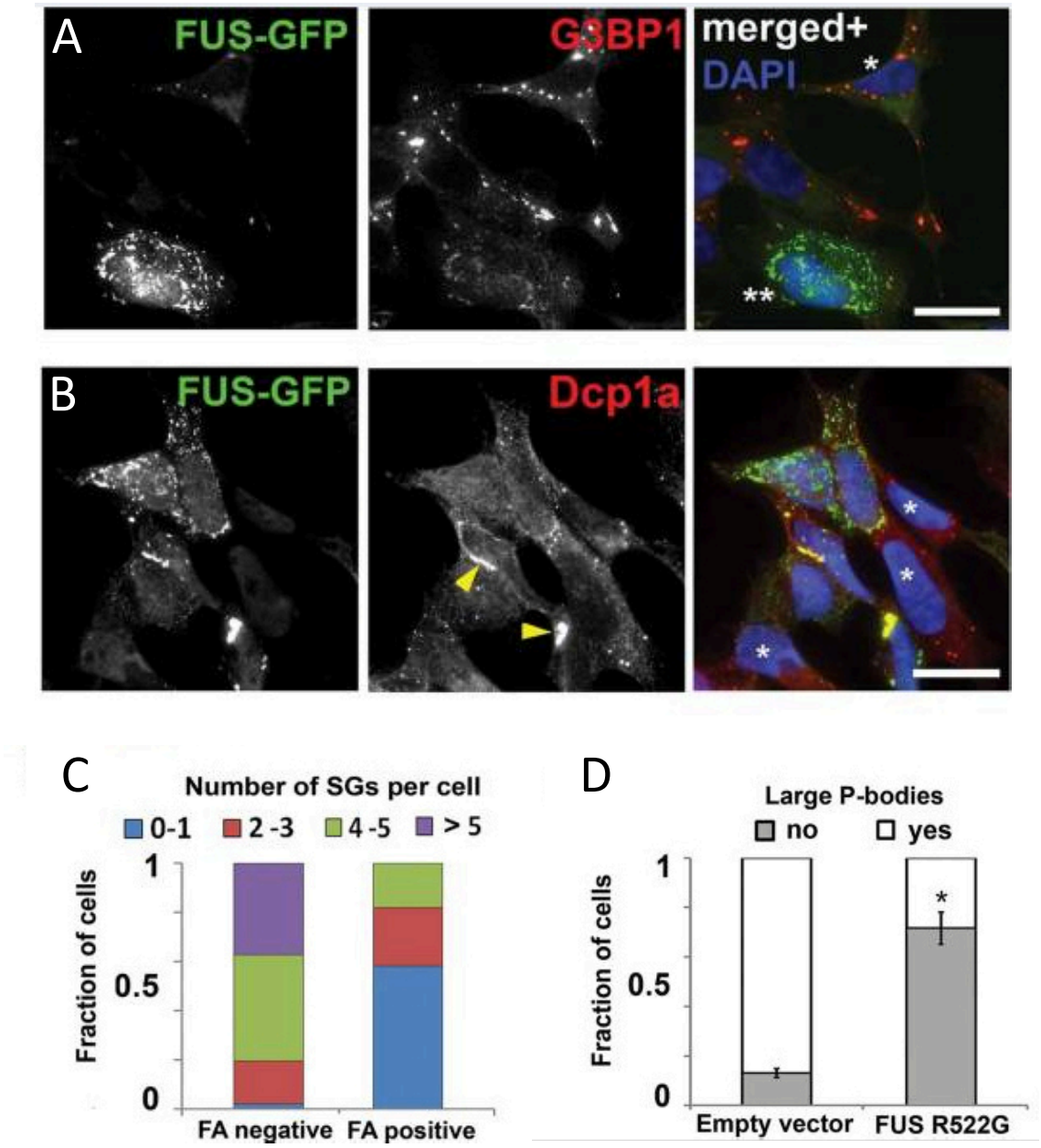

Figure 5.11. Formation of SGs and P-bodies in SH-SY5Y cells was attenuated in the presence of FAs. (A,C) FUS R522G-expressing cells with diffuse protein distribution formed regular looking SGs upon stressful exposure with sodium arsenite as revealed by staining for a SG marker, G3B1 (A, cell marked with one asterisk), while in cells with FUS accumulated in the form of FGs/FAs, formation of SGs was impaired (A, cell marked with two asterisks, and quantified in C). (B,D) Cytoplasmically accumulated FUS prevented formation of P-bodies, and Dcp1a was sequestered by a subset of FAs. Cells were considered as having P-bodies if at least two large P-bodies were evident. Asterisks in (B) indicate non-transfected cells possessing multiple P-bodies and arrows point to FAs positive for Dcp1a. Bar chart shows means ± S.E.M, * $p<0.05$. Scale bars; 10 µm.

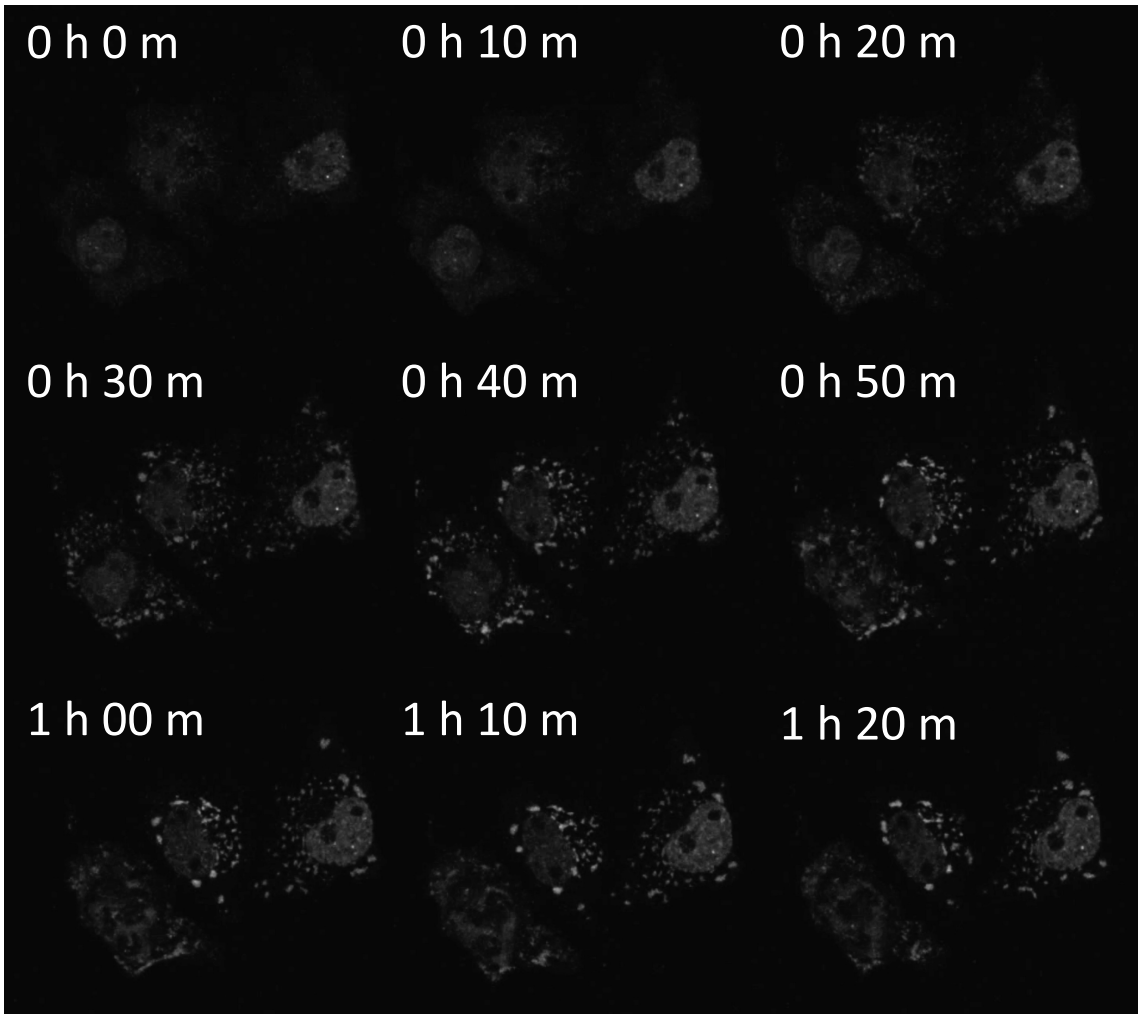

Figure 5.12. Live cell imaging of typical SGs formed in cells with diffuse distribution of FUS R522G in the cytoplasm. COS7 cells were transfected with GFP tagged-FUS R522G. 24 h post-transfection, sodium arsenite was added to the culture medium to induce oxidative stress and live cell imaging was started (time 0 h 0 m) on 3 cells with diffuse distribution of the tagged protein and no observable FGs for 1.5 h.

5.3.6 Disruption of RNA-binding motifs of cytoplasmic FUS augments its aggregation

Above it was demonstrated that the integrity of FAs formed by RNA-binding-competent forms of FUS accumulating in the cytoplasm was dependent upon the availability of non-polysomal RNA, highlighting a reversible nature of these structures. However, in previous chapters we showed that FUS, in which RNA-binding capacity is compromised due to lack of major RNA binding domains (FUS 1-359), was able to irreversibly accumulate forming aggresome-like structures in cultured cells. Furthermore, FUS 1-359 produced several ALS-like features, including the presence of large FUS cytoplasmic inclusions, when expressed neuronally in mice. As expected given its compromised RNA-binding capacity, we observed that neither aggregate structures formed by FUS 1-359 (NT-RRM, Figure 5.13A) nor their smaller precursors contained poly(A)$^+$ RNA (Figure 5.13B). Moreover, these structures were resistant to treatment with RNase A (Figure 5.13C), suggesting that RNA was not required for their integrity. An even shorter C-terminally truncated variant that additionally lacked the RRM domain (NT), also displayed similar aggresome-like structures (Figure 5.13D).

To further investigate how RNA-binding ability of FUS affected its propensity to aggregate, a series of GFP-tagged FUS deletion constructs were generated and their distribution within the cytoplasm of SH-SY5Y cells noted. Whilst dRGG3 (FUS 1-466), lacking the extreme C-terminus that included a portion of an RGG domain, displayed a similar aggregation profile across the population of transfected cells as seen with FUS R522G (Figure 5.13E), with increasing disruption of RNA binding domains a clear trend towards increased aggregation was seen. Deletion of the RRM domain (dRRM) led to an increased fraction of cells with FAs, which was further increased upon deletion of the RRM and RGG together (dRRM-dRGG3) (Figure 5.13E). Given these findings, it is clear that FUS with compromised RNA-binding capacity readily accumulates via a different mechanisms to that seen by FUS retaining its ability to bind target RNAs, where accumulation in RNA-based FGs progresses into formation of RNA-based FAs.

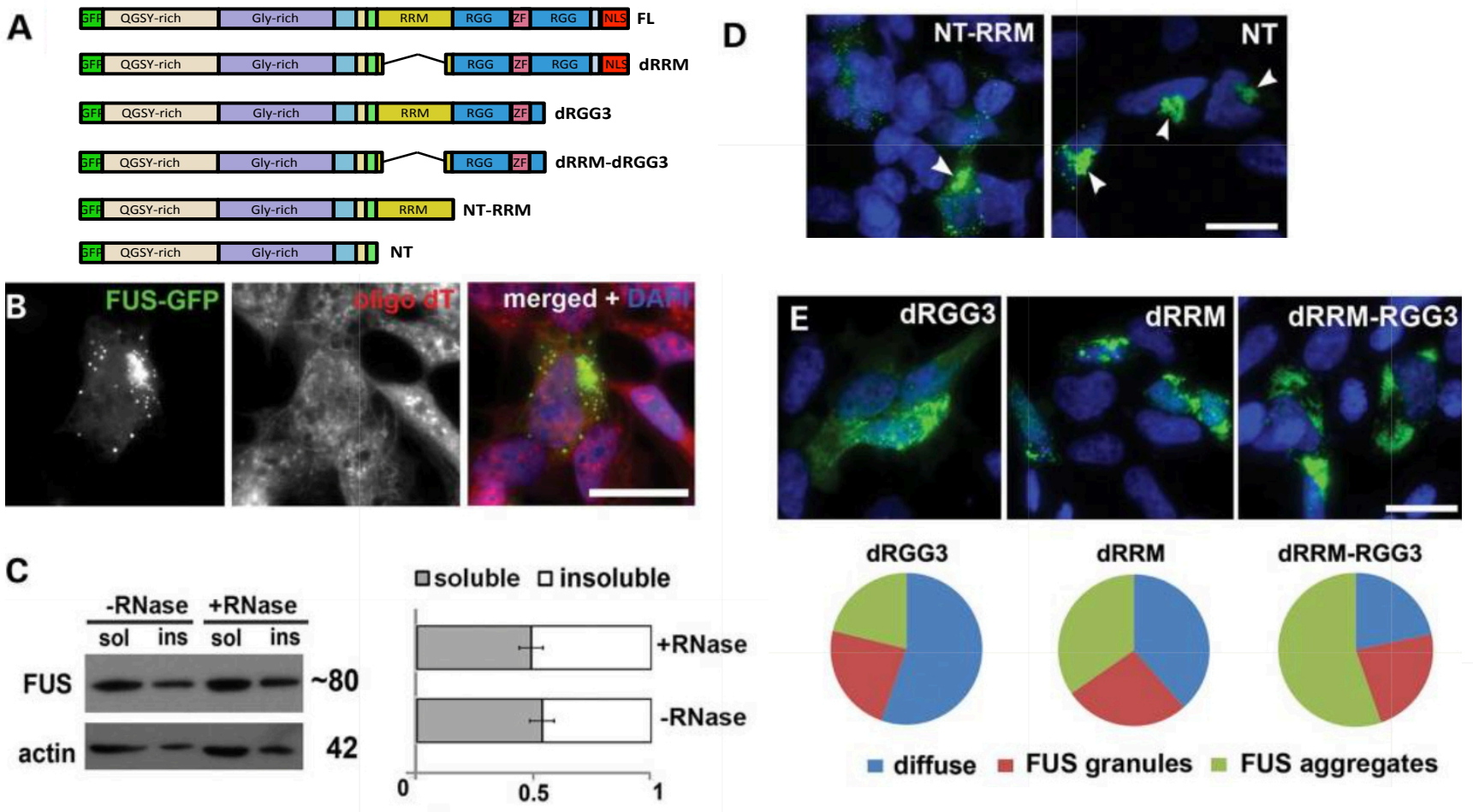

Figure 5.13. FUS with disrupted RNA binding domains readily aggregated in SH-SY5Y cells. (A) Schematic representation of GFP-tagged FUS deletion constructs with disrupted domains involved in interactions of the protein with RNA. (B) FUS 1-359 (NT-RRM) lacking major RNA-binding domains formed aggresome like structures which were negative for poly(A)$^+$ RNA as recognised by an oligo(dT) probe upon fluorescence *in situ* hybridisation. (C) Aggregates formed by FUS 1-359, present in the Triton-X-insoluble fraction were resistant to RNase A treatment. Western membrane was reprobed with anti-β-actin antibodies as a loading control. (D) Both NT-RRM and NT fragments formed frequent aggresome-like structures 24 h after transfection. (E) In SH-SY5Y cells, progressive disruption of RNA-binding domains increased the propensity of cells to form FAs, with the greatest fraction of cells containing FAs following transfection with dRRM-RGG3. See Figure 5.1 for how structures were classified. Scale bars; 10 μm.

5.3.7 Inhibition of transcription triggers RNA-independent aggregation of RNA-binding

To investigate how ALS-associated full length FUS variants that retained their RNA-binding domains would respond to reduced interaction with RNAs, the pool of newly synthesised transcripts on which FGs/FAs were formed, was reduced by transcriptional inhibition with actinomycin D. Above, this treatment reduced the proportion of cells with FAs and shifted FUS R522G from the granule-enriched insoluble fraction to the soluble fraction. Fluorescence *in situ* hybridisation experiments supported this, with FAs rapidly dissipated and almost all poly(A)$^+$ RNA removed from small FUS-positive granules that were preserved in the cytoplasm after 2 h actinomycin D treatment (Figure 5.14A). However, strikingly, following prolonged inhibition of transcription with actinomycin D, these small RNA-depleted granules again fused and formed large aggregates in cells with a high level of FUS expression (Figure 5.14B). This was also recapitulated with FUS 1-466 and FUS ΔNLS and with another transcriptional inhibitor, DRB (data not shown). These large aggregates were structurally distinct from FAs, as they were negative for RNA and were resistant to treatment with RNase (Figure 5.14C). From herein, these large RNA-free aggregates formed after transcriptional arrest by RNA-binding-competent forms of FUS will be referred to as FA(-)s. FA(-)s formed in a juxtanuclear position close to MTOC, similarly to those formed by FUS 1-359 (Figure 5.14B, D). However, similarly to their precursors, these FA(-)s were positive for DDX5 (Figure 5.14E). Contrastingly, protein markers of stress granules often found in FAs were dissociated from FA(-)s; G3B1 was lost from FA(-)s and they were only weakly positive for TIAR (Figure 5.14F). This highlighted the selectivity by which these RNA-free FA(-)s form.

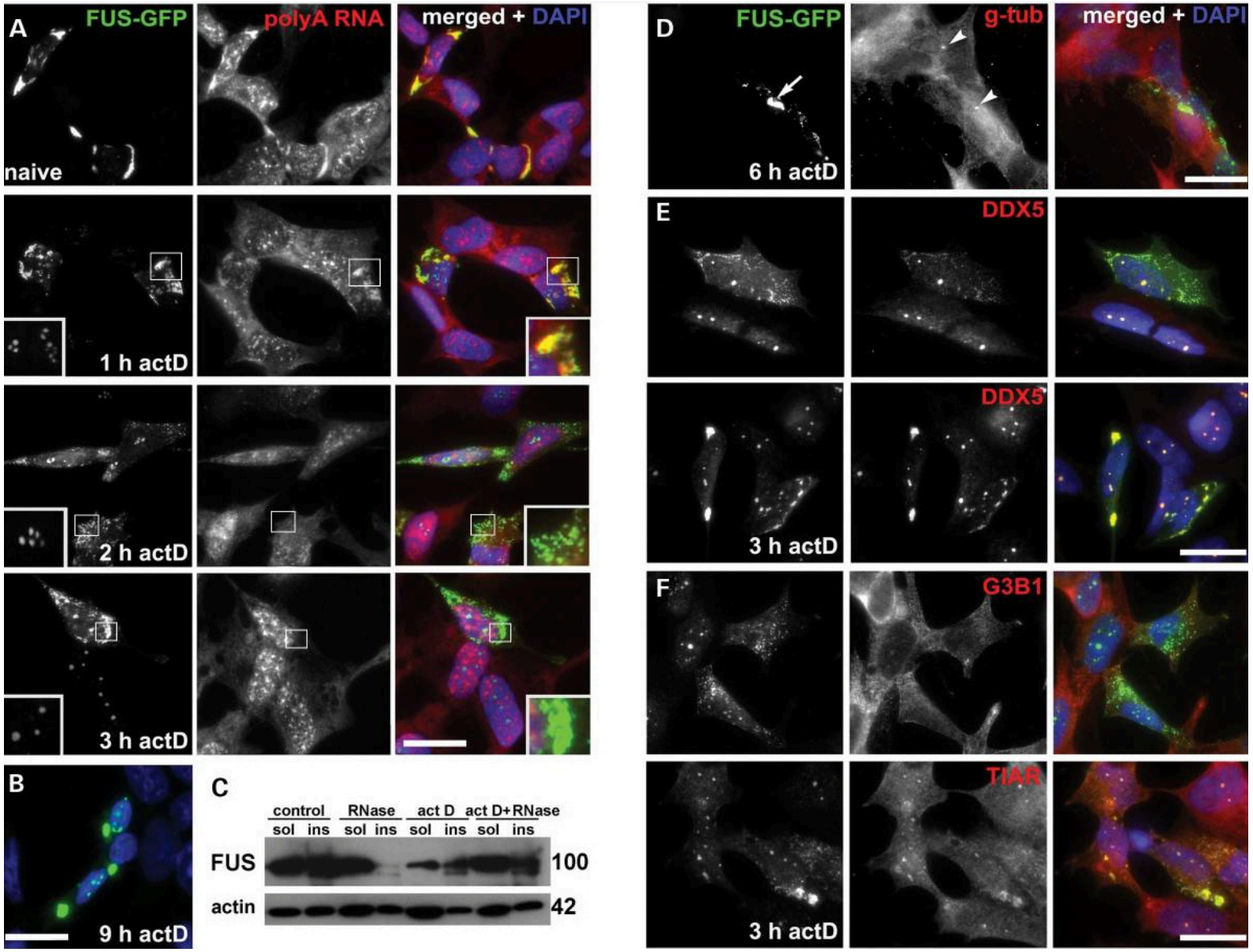
A
FUS-GFP
polyA RNA
merged + DAPI
naive
1 h actD
2 h actD
3 h actD
B
9 h actD
C
control
RNase
act D
act D+RNase
sol ins sol ins sol ins sol ins
FUS
100
actin
42
D
FUS-GFP
g-tub
merged + DAPI
6 h actD
E
DDX5
DDX5
3 h actD
F
G3B1
TIAR
3 h actD

Previous page:

Figure 5.14. Inhibition of transcription in cells expressing cytoplasmically localised FUS R522G resulted in dissipation of FAs and FGs and subsequent RNA-independent FUS aggregation. (A) *In situ* hybridisation with a fluorescent oligo(dT) probe shows dynamics of poly(A)$^+$ RNA loss from FAs and FGs and secondary aggregation leading to the formation of RNA-independent FAs (FA(-)s). Increased magnification of cytoplasmic FUS structures shown bottom right corner. Inserts in the left bottom corner represent enlarged nucleolar caps from a representative cell. Note changes in the morphology of FUS-positive nucleolar caps reflected the duration of transcriptional inhibition; several crescent-shaped caps after 1–2 h of actinomycin D treatment were replaced by dot-like FUS accumulation in their fibrillar center from 3 h onwards. (B) Products of secondary RNA-independent aggregation fused together producing large juxtanuclear aggregates after prolonged (9 h) exposure to actinomycin D. (C) Triton X-insoluble FUS species recovered from COS7 cells after 6 h actinomycin D treatment were not sensitive to RNase A. (D) Large FA(-)s (arrow) formed after prolonged (for 6 h) transcriptional repression in SH-SY5Y cells were found in the immediate vicinity of the centrosome (arrowheads) visualised by anti-γ-tubulin (g-tub) staining. DDX5 but not G3B1 co-aggregated with FUS R522G in small (E) and large (F) FA(-)s detected after 3 h of transcriptional inhibition with actinomycin D. Scale bars; A, B, D, E, 10 μm; F, 2.5 μm.

5.3.8 Transcriptional inhibition results in pathological redistribution and aggregation of predominantly nuclear FUS mutants

ALS-associated mutants tested to this point all displayed impaired nuclear import and increased presence in the cytoplasm, thought to be a key step in ALS-FUS progression. However, it was not known how a transcriptional inhibitory insult would affect other ALS-associated FUS mutants retaining nuclear localisation. GFP-tagged FUS R518K and R524T, although harboring mutations within the NLS, displayed prominent nuclear staining (Figure 5.15A, B). After 2 h treatment with actinomycin D, these variants displayed significantly increased presence in the cytoplasm (Figure 5.15B). Furthermore, prolonged treatment with actinomycin D resulted in aggregation of mutant FUS within the cytoplasm (Figure 5.15C). Consequently, transcriptional inhibition may also be a trigger for cytoplasmic mislocalisation and aggregation of otherwise nuclear FUS.

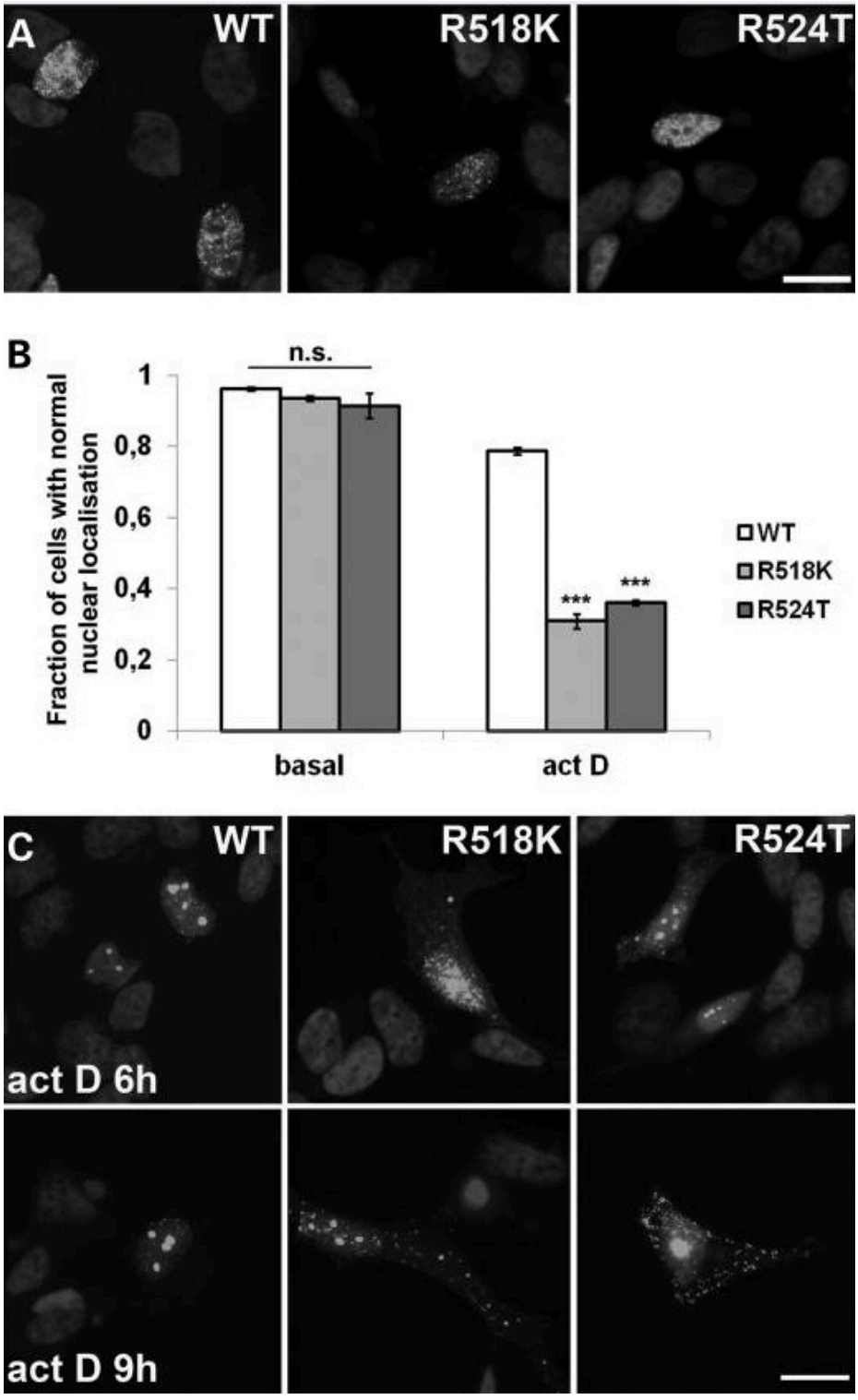

Figure 5.15. ALS-associated full length forms of FUS normally residing in the nucleus aggregated in the cytoplasm following transcriptional inhibition. (A) Nuclear distribution of WT, R518K and R524T FUS variants 24 h post-transfection in naïve SH-SY5Y cells. (B) Nuclear distribution was seen in the majority of naïve cells expressing these variants, whereas 2 h actinomycin treatment shifted mutant variants to the cytoplasm in a large fraction of cells. (C) Prolonged (6 or 9 h) treatment with actinomycin D caused formation of cytoplasmic aggregates by FUS R524T and FUS R518K variants. Bar chart in B shows means ± S.E.M, ***p<0.005. Scale bars; 10 μm.

5.4 Discussion

Here we aimed to understand the pathways leading to the final products of cytoplasmically accumulating full length ALS-associated FUS mutants, which are observed in these ALS patients' tissues post-mortem. Indeed, in ALS, missense mutations in the C-terminus of FUS are some of the most frequently occurring within the protein (Lagier-Tourenne and Cleveland, 2009) and mislocalisation to the cytoplasm and subsequent formation into large pathological inclusions is thought to be a key, but little understood, event involved in FUS pathophysiology (Dormann *et al.*, 2010; Li *et al.*, 2013). In earlier chapters we identified prominent aggregation in the cytoplasm of an experimental C-terminally truncated form of FUS with compromised RNA-binding capacity that was induced by the deletion of major RNA-binding domains. Unable to be recruited into physiological SGs, thought to provide a protective response, this protein formed higher order FUS structures and led to substantial ALS-like pathology in mice. Here we evidenced that these large FUS aggregates were RNA-free and wondered whether similar mechanisms of aggregation may occur for mutant full length forms of FUS that occur in ALS, or whether these were principally distinct.

Ourselves and others (Bosco *et al.*, 2010; Dormann *et al.*, 2010; Vance *et al.*, 2013) demonstrated that mutant FUS variants in the cytoplasm, with intact domains involved in binding target RNAs, could be taken up into physiological SGs formed upon the induction of cellular stresses, including heat shock or oxidative stress induced by sodium arsenite. However, intriguingly, we identified that these FUS variants may also aggregate in a concentration dependent manner in the absence of exogenously-applied stress, warranting further investigation. These variants, with the ability to bind RNA, accumulated on newly synthesised transcripts into small granular-like structures (FGs) following nucleation of FUS, which occurred above a certain threshold. This could potentially be coupled with a conformational change in the structure of FUS, yet this remains to be investigated. It was concluded that FGs represented a novel RNP structure, as although they resembled RNA transport granules, they also displayed several distinct features, for example they were negative or displayed only partial overlap with key components of known RNA granules (FMRP and DDX5, respectively).

Further, with live cell imaging it was shown that these FGs coalesced gradually over time to form large RNA-based FUS aggregates (FAs). This was greatly enhanced by exogenously applied cellular stress and increased presence of FAs occurred in naïve cells with elevated levels levels of phospho-eiF2α, indicating an activated stress response, probably arising from the accumulation of FUS itself. We identified that

increased availability of RNAs running off polysomes, a process that occurs under stressful cellular conditions, promoted FA formation. Moreover, interaction of FUS with a specific pool of these RNAs was required, as evolutionarily distant RNA binding domains from yeast, unlike those from the similar human protein, TDP-43, were unable to recapitulate these aggregation profiles. Additionally, the prion-like domain of FUS was also important in the formation of FAs. Previously, this domain has been shown to be physiologically important in forming higher order FUS structures following the assembly of FUS on RNA (Schwartz *et al.*, 2013) and it may be that a similar mechanism underlies FA formation in vivo.

Given the known association of FUS with induced SGs in conditions of cellular stress and the requirement of RNA for the formation of both SGs and FAs, we wondered whether SGs and FAs were distinct. Supporting this, we revealed structural and kinetic differences between FAs and induced SGs, with differing morphology and recruitment of proteins, even identifying DDX5 protein, a component of RNA transport granules (Kanai *et al.*, 2004), as a differentiating marker for FAs over SGs. We also demonstrated that these large FAs could sequester not just RNA, but also key components of SGs and P-bodies and perturb the formation of these structures. Evidence from Takanashi and Yamaguchi (2014) supports this, also finding that spontaneously forming FUS aggregates recruited RNP granule components. Therefore, FAs may disrupt the protective function that SGs are thought to have and this could be an important step in the development of cellular toxicity in these cases.

Perhaps the most surprising finding was that following prolonged transcriptional inhibition, FAs, which had initially dissipated early after transcriptional inhibition, re-accumulated to form RNA-free aggregate structures (FA(-)s) that appeared similar to those formed by RNA-binding compromised forms of FUS, although FA(-)s retained features of their predecessors, e.g. remained positive for DDX5. This suggested that an insult of transcriptional inhibition may lead to the irreversible aggregation of RNA-binding competent forms of FUS present in the cytoplasm. This provides an alternate mechanism for the irreversible aggregation of ALS-associated FUS variants into large inclusion-like aggregates, aside from the postulated coalescence of ‘pathological SGs’ (Wolozin, 2014). Furthermore, transcriptional inhibition was sufficient to also cause mislocalisation of normally nuclear ALS-associated FUS variants, e.g. FUS R518K and R524T. Notably, it has been shown previously that endogenous FUS and other FET family members also displayed a shift towards increased presence in the cytoplasm following inhibition of transcription (Zinszner *et al.*, 1997a; Marko *et al.*, 2012).

As FUS itself has been shown to be heavily involved with regulation of transcription (Schwartz *et al.*, 2012; Schwartz *et al.*, 2013; Tan *et al.*, 2012; Yang *et al.*, 2014) it is possible that its loss from the nucleus, occurring in ALS and other FUSopathies could be a physiological trigger for similar transcriptional disruption. Moreover, a state of transcriptional arrest may also be induced physiologically through ageing-induced DNA damage via oxidative stress or, more specifically, the increased DNA damage thought to occur in ALS (Hetman *et al.*, 2010; Bogdanov *et al.*, 2000). Therefore, transcriptional arrest and a subsequent reduction in the level of free RNA may induce an irreversible redistribution of RNA-based FUS aggregates into large RNA-free juxtanuclear structures. These large RNA-free structures, similar to those produced by RNA-binding-compromised FUS that led to development of neuronal toxicity in mice, may ultimately be responsible for the development of human FUSopathies.

RESULTS IV:
Interactions of FUS in the sub-nucleus:
A novel pathogenic mechanism in ALS?

6.1 Declaration

Data included within this chapter have been published within the following open access article:

Shelkovnikova TA, **Robinson HK**, Troakes C, Ninkina N, Buchman VL. Compromised paraspeckle formation as a pathogenic factor in FUSopathies. Hum Mol Genet. (2014) May 1;23(9):2298-312.

6.2 Overview

Previous chapters centred on investigating the aggregation pathways of FUS once mislocalised to the cytoplasm, thought to be an early and critical event in ALS-FUS pathogenesis through a gain of toxic FUS function mechanism. However, conversely, FUS has several known roles within the nucleus, the disruption of which may also cause pathological changes in ALS.

Recently, FUS has been identified as a component of the subnuclear body known as the paraspeckle (Naganuma *et al.*, 2012; Nishimoto *et al.*, 2013; Page *et al.*, 2011). First described in 2002 (Fox *et al.*, 2002), paraspeckles are assembled on the lncRNA, NEAT1, which is essential for formation and maintenance of these RNP structures (Clemson *et al.*, 2009; Sasaki *et al.*, 2009; Chen and Carmichael, 2009; Sunwoo *et al.*, 2009). They are observed in virtually all cultured cells (Fox and Lamond, 2010), yet they are absent in embryonic stem cells, which lack NEAT1 expression, until differentiation (Chen and Carmichael, 2009), reflecting their dynamic nature. Given their dependency on NEAT1, in mammalian tissues paraspeckles are observed with greater prevalence in tissues highly expressing NEAT1, for example surface gastric epithelial cells (Nakagawa *et al.*, 2011). In the nervous system, NEAT1 expression level is comparatively low and paraspeckles are not seen under basal conditions (Nakagawa *et al.*, 2011). However, in addition to their role in retention of A-to-I hyperedited transcripts (Zhang and Carmichael, 2001), paraspeckles are thought to have a role in the cellular response to stress. Notably, NEAT1 is greatly increased following exposure to immune stimuli such as Poly I:C. or viral infection (Imamura *et al.*, 2014; Zhang *et al.*, 2013; Saha *et al.*, 2006). Intriguingly, paraspeckle formation has been shown to be increased during early stages of ALS development in parallel with increased NEAT1 level (Nishimoto *et al.*, 2013). However, it is unclear how changes to FUS distribution observed in ALS-FUS may affect this subnuclear body. Therefore, this chapter focused on characterising the interactions of FUS with paraspeckle proteins and determining how these may be altered in ALS that is associated with FUS mutation.

6.3 Results

6.3.1 Localisation of FUS within the nucleus

In cultured neuroblastoma cells, staining for endogenous FUS protein demonstrated that the protein is predominantly localised to the nucleus with a diffuse pattern of distribution, but upon closer inspection, small puncta and variably-sized foci were observed amongst the diffuse pattern of staining. These small puncta were also recapitulated in cells where GFP-tagged full length human (WT) FUS was overexpressed and were noted in other cell lines tested, including COS7 cells (Figure 6.1A). To determine the nature of these nuclear FUS puncta, immunocytochemistry was performed with a panel of antibodies recognising core proteins of major subnuclear bodies in neuroblastoma cells. FUS was highly enriched in paraspeckles, as evidenced by colocalisation with core paraspeckle proteins, PSP1 and p54nrb, also known as NONO (Figure 6.1B). Further, FUS was excluded from nucleolar regions as recognised by ethidium bromide staining for DNA (Figure 6.2). FUS was not seen at detectable levels in coilin-positive Cajal bodies, SMN-positive gems, or PML-positive PML bodies. On the other hand, FUS was moderately enriched in Sm antigen-positive nuclear splicing speckles (Figure 6.2).

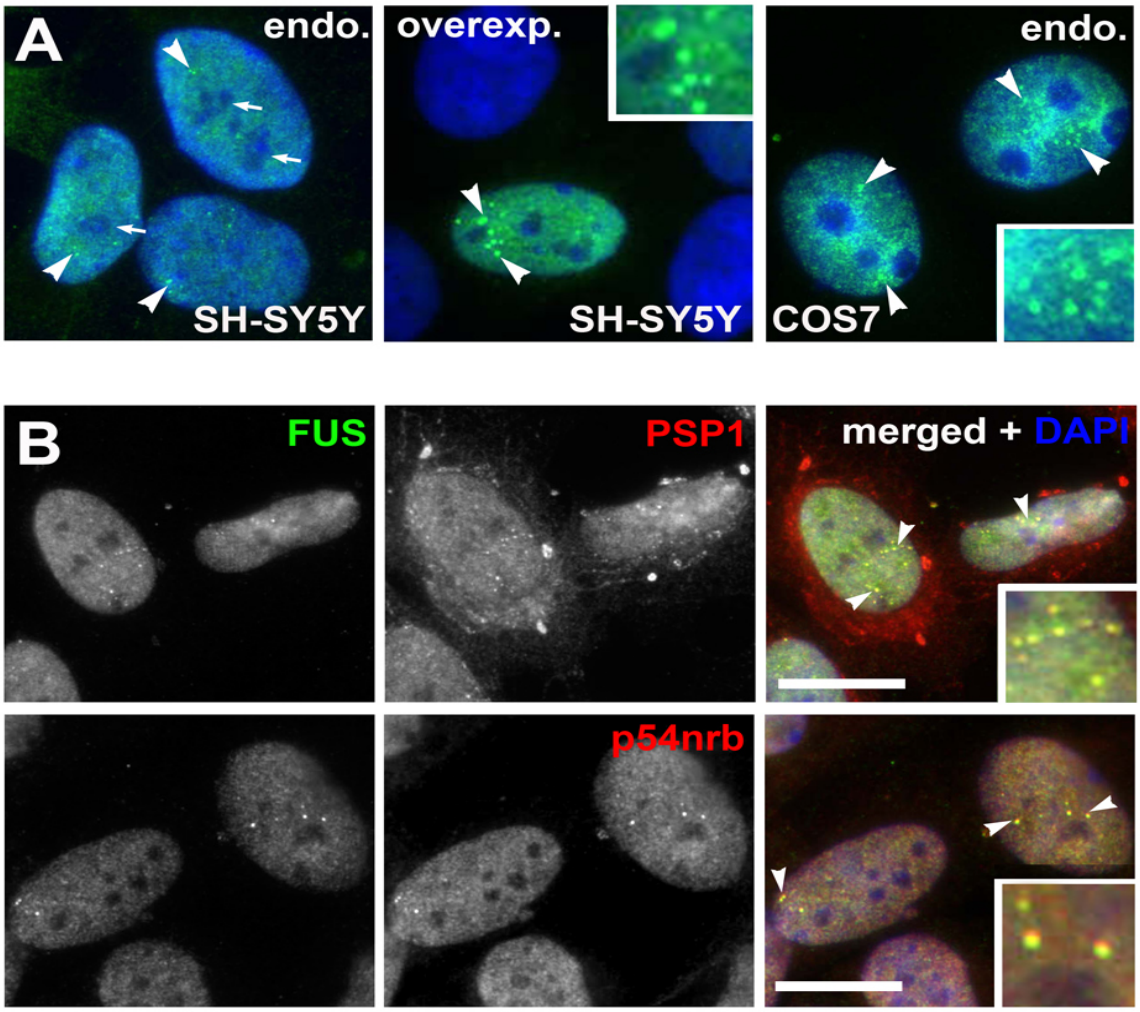

Figure 6.1. FUS protein is enriched in paraspeckles. (A) Endogenous FUS or GFP-tagged human FUS is excluded from nucleolar regions (arrows) and forms small puncta (arrowheads) in the nucleus of SH-SY5Y cells and COS7 cells. (B) FUS puncta overlap with paraspeckles, as recognised with antibodies against core paraspeckle proteins, PSP1 and p54nrb. Scale bars all panels; 10 μm. At least 3 biological repeats were performed and representative images are shown.

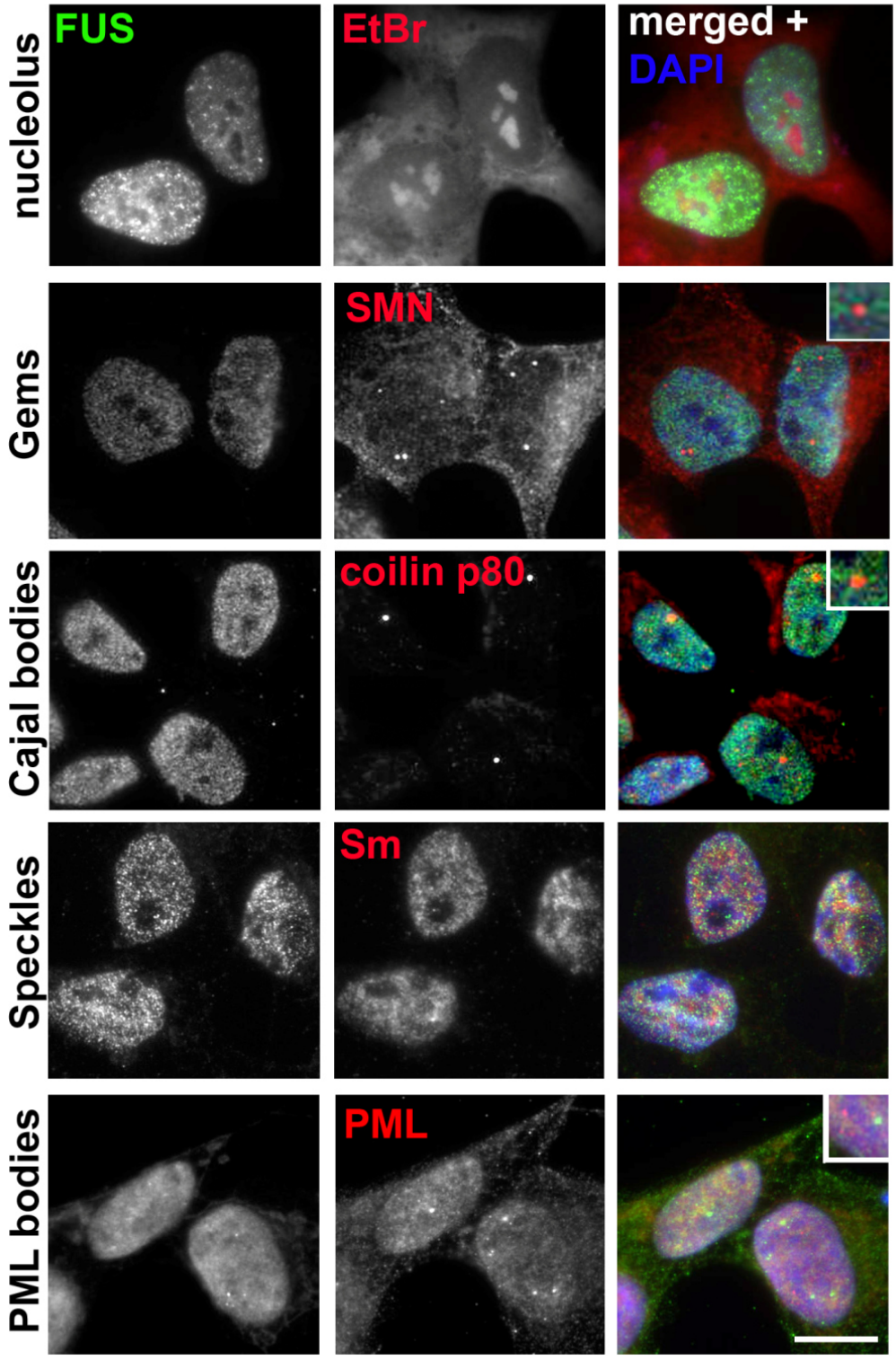

Figure 6.2. Association of FUS with additional subnuclear bodies in SH-SY5Y cells. FUS was excluded from nucleolar regions as recognised by ethidium bromide staining for DNA and was not seen at detectable levels in coilin-positive Cajal bodies, SMN-positive gems, or PML-positive PML bodies. FUS was moderately enriched in Sm antigen-positive nuclear splicing speckles. Scale bar all panels; 10 μm. At least 3 biological repeats were performed and representative images are shown.

6.3.2 FUS is recruited with other paraspeckle proteins into the same nucleolar caps

In cells where active transcription is inhibited, core paraspeckle proteins, for example PSPC1, have been shown to redistribute to form perinucleolar caps (Fox *et al.*, 2002). This has also been demonstrated for other nuclear proteins, albeit in caps distinct from those containing paraspeckle components (Shav-Tal *et al.*, 2005). Intriguingly, this behaviour has also been demonstrated for FUS (Zinszner *et al.*, 1997a), but it had not been investigated whether FUS and paraspeckle proteins are components of the same perinucleolar caps. In SH-SY5Y cells, upon global transcriptional inhibition with actinomycin D, canonical perinucleolar caps were formed by FUS (Figure 6.3A, B, FUS panels).

To determine the overlap between perinucleolar caps formed by FUS, paraspeckle proteins and other nuclear proteins known to form distinct caps (p80 coilin, and RNA helicase p68), immunocytochemistry was performed using antibodies to these proteins following treatment of cells with actinomycin D. In SH-SY5Y cells, perinucleolar caps formed by FUS were distinct from those formed by p80 coilin (Figure 6.3A), and only partially overlapped with p68-positive structures (Figure 6.3B). Partial overlap of FUS with p68, forming organised and spatially complex structures was even more pronounced in COS7 cells (Figure 6.3C). However, FUS was found to completely colocalise with paraspeckle proteins, PSPC1 and p54nrb, in the same perinucleolar caps (Figure 6.4A, B).

To establish whether FUS was essential for this recruitment of paraspeckle proteins to these perinucleolar caps, endogenous FUS was knocked down in SH-SY5Y cells using siRNA targeted to FUS. Perinucleolar caps containing paraspeckles were still formed following transcriptional inhibition in these FUS-depleted cells, suggesting FUS is not required for this process (Figure 6.4C).

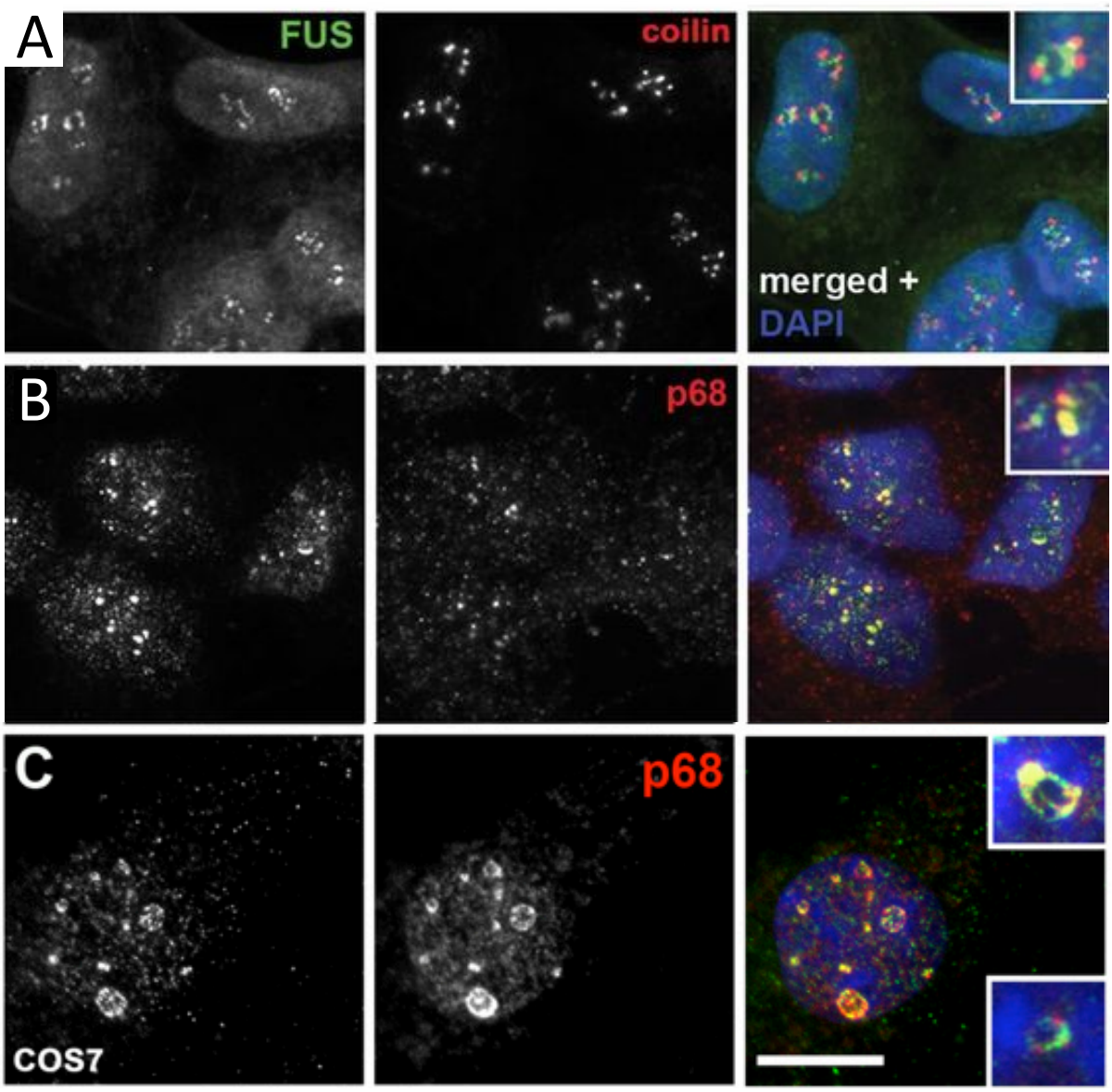

Figure 6.3. Characterisation of perinucleolar caps formed by FUS upon transcriptional inhibition. In SH-SY5Y cells, FUS is not a component of (A) p80 coilin perinucleolar caps but (B) partially colocalises with RNA helicase p68 caps. (C) FUS partial colocalisation with p68 is particularly evident in COS7 cells. Actinomycin D was added to the cells for 1.5 h prior to fixation in all experiments. Scale bars; 10 μm. At least 3 biological repeats were performed and representative images are shown.

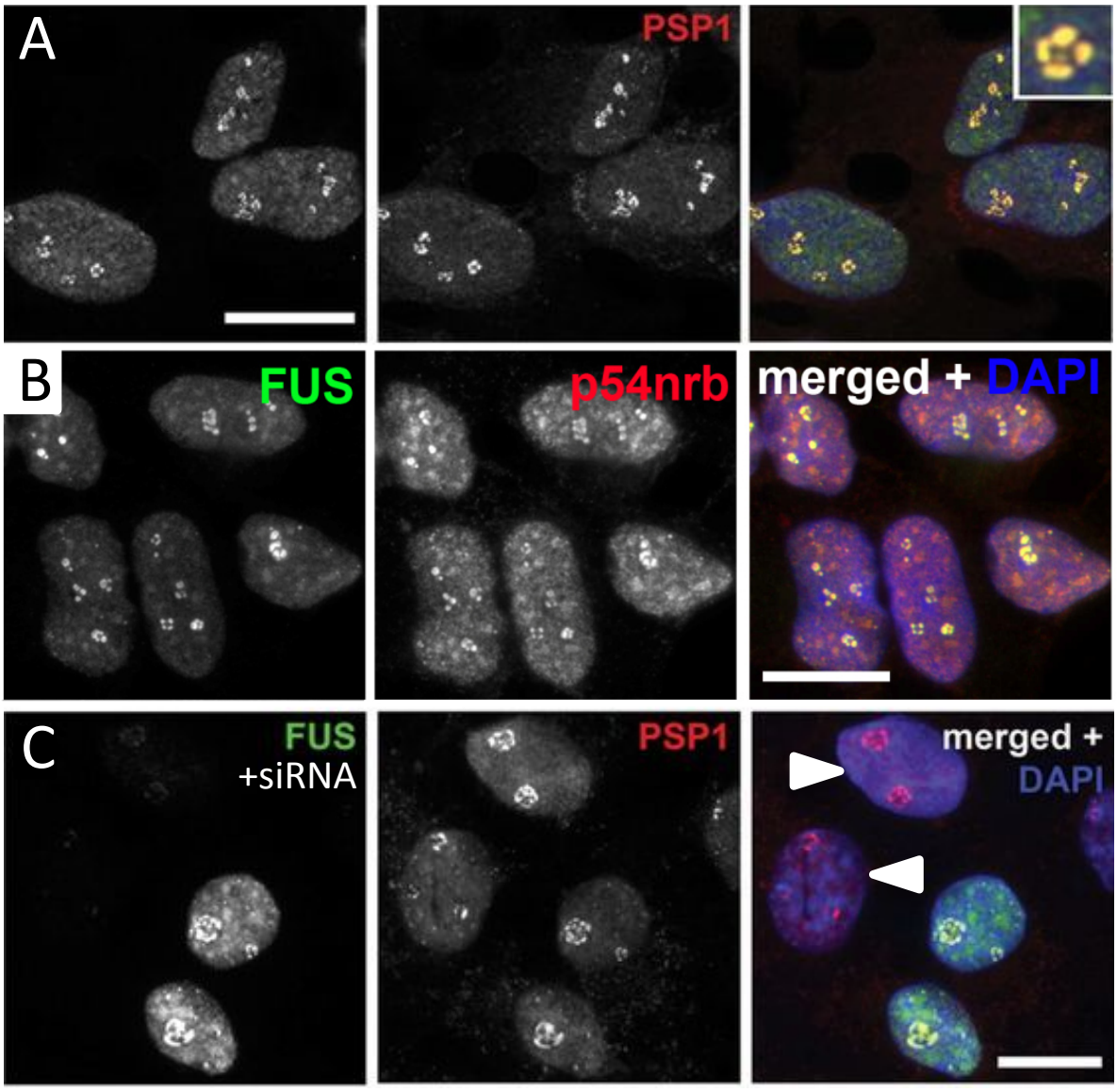

Figure 6.4. Further characterisation of perinucleolar caps formed by FUS upon transcriptional inhibition in SH-SY5Y cells. (A-B) FUS completely colocalises with caps formed by PSP1 (A) and p54nrb (B). (C) PSP1-positive perinucleolar caps still form in cells depleted of FUS (arrowheads) using siRNA. Actinomycin D was added to the cells for 1.5 h prior to fixation in all experiments. Scale bars; 10 μm. At least 3 biological repeats were performed and representative images are shown.

6.3.3 Interaction of FUS with paraspeckle protein p54nrb is RNA-dependent

To investigate whether FUS and other paraspeckle proteins could be present in the same macromolecular complexes, co-immunoprecipitation experiments were performed with GFP-tagged FUS protein expressed in SH-SY5Y cells. Following western blot analysis of proteins from these immunoprecipitates, it was shown that GFP-tagged WT FUS efficiently pulled down endogenous p54nrb (Figure 6.5A). To determine whether this interaction was RNA-dependent, lysates were treated, with RNase A. Indeed, this abolished the pull down of endogenous p54nrb by GFP-tagged WT FUS (Figure 6.5A). Further, FUS NT, lacking major RNA-binding domains, was unable to pull down p54nrb (Figure 6.5A). This interaction with p54nrb was not observed following pull down by another RNA-binding protein similar to FUS, TDP-43 (Figure 6.5B). It was also demonstrated that endogenous FUS could be pulled down from lysates of COS7 cells with antibody against p54nrb, providing further confirmation of an interaction between these two endogenous proteins (Figure 6.5C). However, the cellular location of this interaction cannot be discriminated using this approach, as FUS and p54nrb may be interacting aside from paraspeckles, elsewhere in the cell. As p54nrb, like FUS, has also been implicated in transcription (Emili *et al.*, 2002), the impact of transcriptional inhibition on the interaction observed between these two proteins was determined. DRB acts to prevent the assembly of transcriptional complexes, whereas actinomycin D stalls these complexes and prevents elongation. Pull down of p54nrb by GFP-tagged FUS was abolished following DRB treatment, but remained following global transcriptional inhibition with actinomycin D (Figure 6.5D).

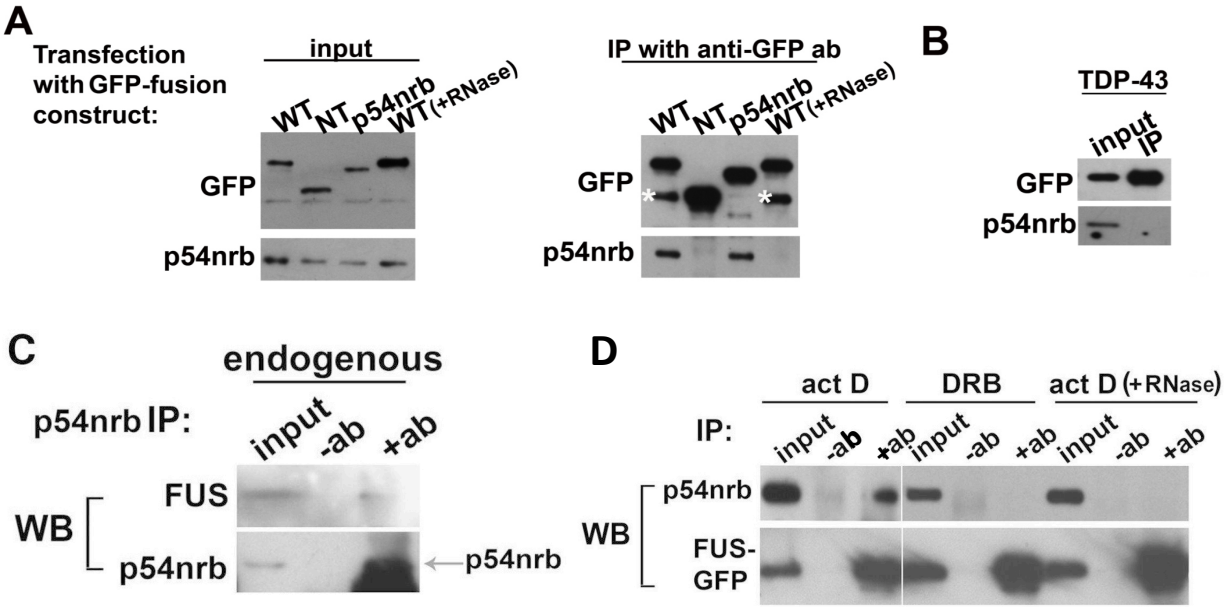

Figure 6.5. FUS interacts with p54nrb via RNA and this interaction is regulated by ongoing transcription. (A and B) Immunoprecipitation revealed an RNase-sensitive interaction of GFP-tagged full length FUS protein (WT) with p54nrb that was not seen with either GFP-tagged FUS N-terminal fragment (NT) (A) or GFP-tagged full length TDP-43 (B). SH-SY5Y cells were lysed for immunoprecipitation on anti-GFP antibody-coated beads 24 h after transfection with GFP-tagged constructs. Asterisks indicate non-specific bands. Lysates were treated with RNase A for 30 min at RT prior to incubation with beads to determine the role of RNA in the interaction. (C) Endogenous FUS was pulled down by anti-p54nrb antibody-coated beads from COS7 cells. A portion of a very intense 50 kDa immunoglobulin heavy chain band is seen just under the p54nrb band as the same antibodies were used for immunoprecipitation and western blotting. (D) FUS remains associated with p54nrb in actinomycin D but not DRB treated cells. Protein complexes of full-length GFP-tagged FUS were immunoprecipitated from lysates of SH-SY5Y cells untreated or treated with inhibitors of transcription for 1.5 h. 10% input sample was loaded alongside 100% pull-down samples for western blot. These data were produced by Dr. Tatyana Shelkovnikova.

6.3.4 Level of FUS regulates paraspeckle assembly and maintenance

FUS deficiency in the nucleus has been highlighted as a possible simplified scenario though which ALS pathology may arise. To investigate the impact of FUS depletion on paraspeckles, FUS was knocked down using siRNA. Using this approach, FUS mRNA level was reduced by ~75% and FUS protein level, 50-70% at 72 h post-transfection compared to cells transfected with scrambled siRNA (Figure 6.6C, 6.7A). Whilst overall levels of paraspeckle proteins, PSP1 and p54nrb remained unchanged following FUS knockdown (Figure 6.6C), paraspeckles disappeared from FUS-depleted cells (Figure 6.6A, B). To determine whether this may be because of an alteration in the level of NEAT1 lncRNA upon which paraspeckles are formed, qPCR was performed on these cells using primers that simultaneously detect both long (NEAT1_2) and short (NEAT1_1) isoforms of NEAT1. NEAT1 levels were significantly lower in cells treated with FUS siRNA compared with scrambled siRNA control (Figure 6.7A). Further, expression of GFP-tagged FUS led to a significant elevation of NEAT1 transcript level (Figure 6.7B). Therefore, it is likely that FUS contributes to the steady-state maintenance of NEAT1 transcript levels. In COS7 cells, expression of GFP-tagged p54nrb in cells with greatly depleted level of FUS appeared to rescue the formation of paraspeckles as several paraspeckle-like structures, positive for PSP1 formed (Figure 6.8A, B). As these structures were observed in FUS depleted cells expressing comparatively lower levels of GFP-p54nrb not known to aggregate in naïve cells, it suggests that these are true paraspeckle structures, and not simply small aggregations of overexpressed protein. This restoration cannot be attributed to restoration of NEAT1 levels as NEAT1 expression was unaltered in cells expressing GFP-tagged p54nrb (Figure 6.9A) and NEAT1 level was not rescued by p54nrb expression in cells depleted of FUS (Figure 6.9B). Therefore, p54nrb is a good candidate for substituting the architectural role of FUS in paraspeckles.

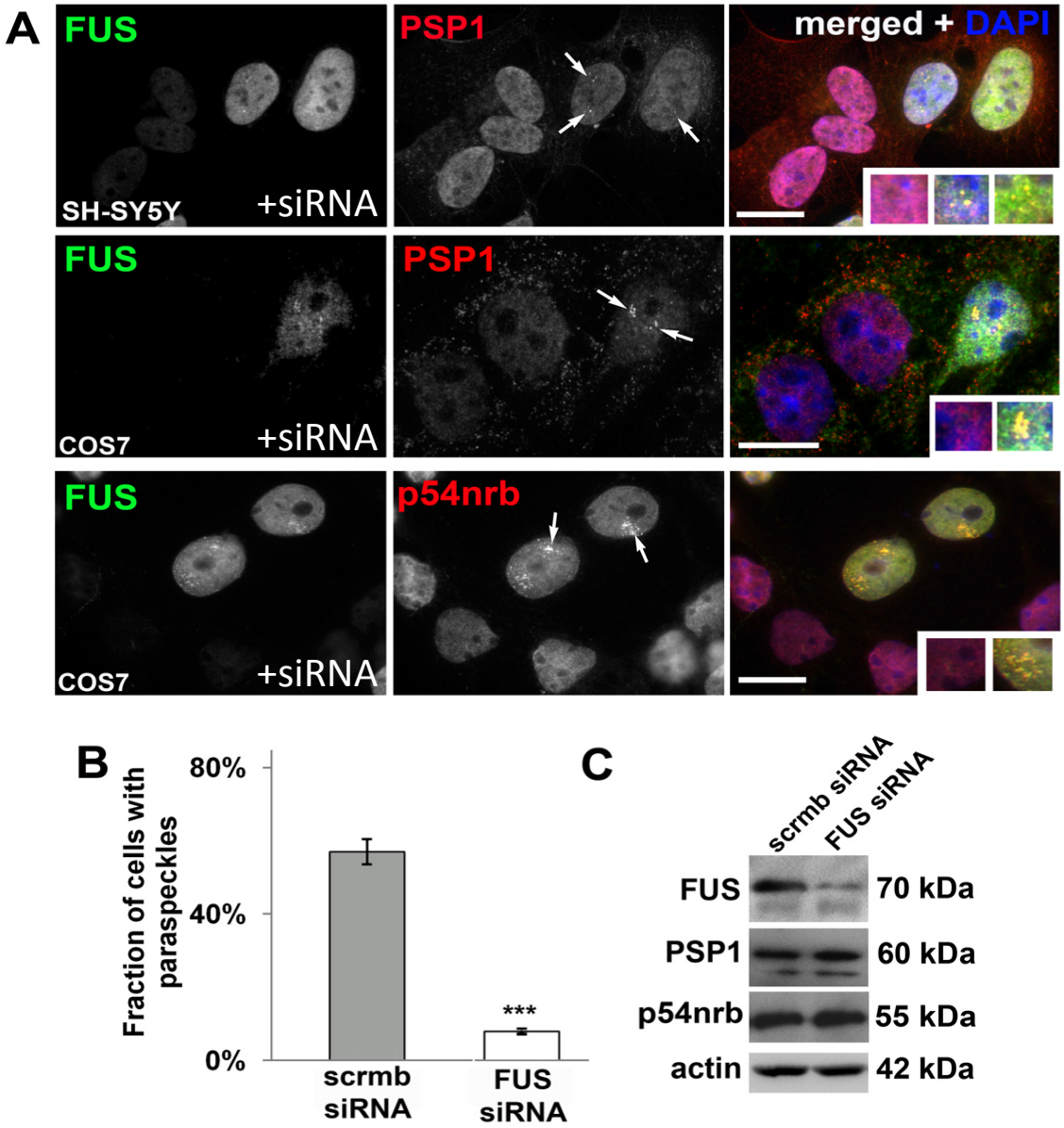

Figure 6.6. FUS knockdown with siRNA resulted in the loss of paraspeckles. (A) Representative images from SH-SY5Y and COS7 cells following knockdown of FUS with siRNA. Normal paraspeckles (arrows) remain in cells where FUS level is not depleted. (B) Quantification of the percentage of cells with paraspeckles following treatment with either scrambled or FUS-targeted siRNA. (C) Western blotting of cellular lysates following treatment with either scrambled or FUS-targeted siRNA. Whilst FUS level was depleted following knockdown with siRNA, levels of other core paraspeckle proteins, PSP1 and p54nrb remained unchanged. In all experiments, cells were transfected with either a pool of siRNA specifically targeting FUS protein (FUS siRNA) or scrambled siRNA (scrmb siRNA) and analysed 72 h post-transfection. ***$p<0.001$, n=3, (Mann–Whitney test). Bar graph represents mean±S.E.M. Scale bars, 10 μm. For (A) at least 3 biological repeats were performed and representative images are shown.

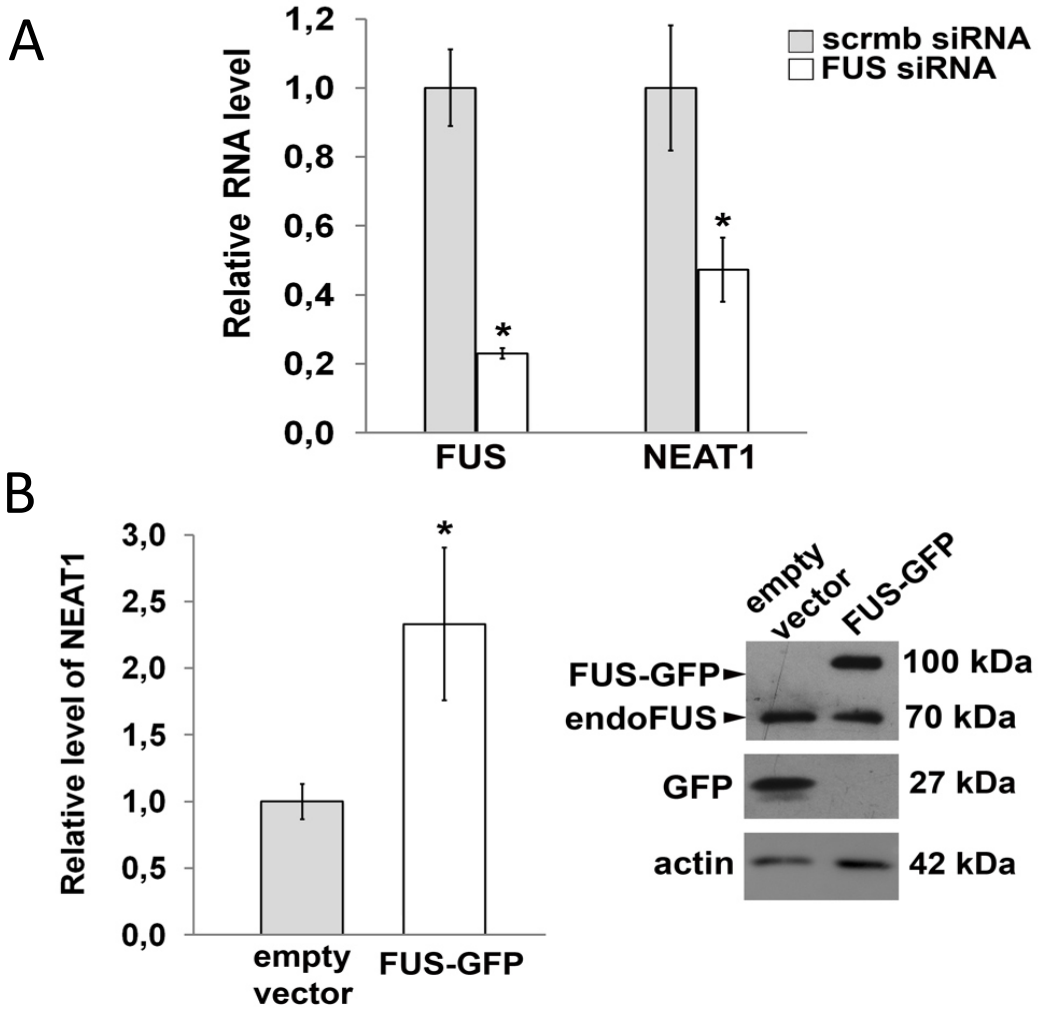

Figure 6.7. Expression of NEAT1 lncRNA was dependent upon the level of FUS expression. (A) qPCR following treatment of cells with either scrambled or FUS-targeted siRNA showed that NEAT1 transcript level was reduced following FUS knockdown. (B) qPCR following transfection of cells with either empty GFP vector or GFP-tagged FUS showed that NEAT1 level was elevated upon increased FUS expression. Western blotting with anti-FUS antibody showed approximately equal levels of FUS-GFP and endogenous FUS in total cell culture lysates, considering that efficiency of transfection was ~25%, transfected cells expressed approximately 4 times more ectopic than endogenous FUS protein. In all experiments, cells were transfected with either a pool of siRNA specifically targeting FUS protein (FUS siRNA) or scrambled siRNA (scrmb siRNA) and analysed 72 h post-transfection. *$p<0.05$, n=6, (Mann–Whitney test). Bar graph represents mean±S.E.M.

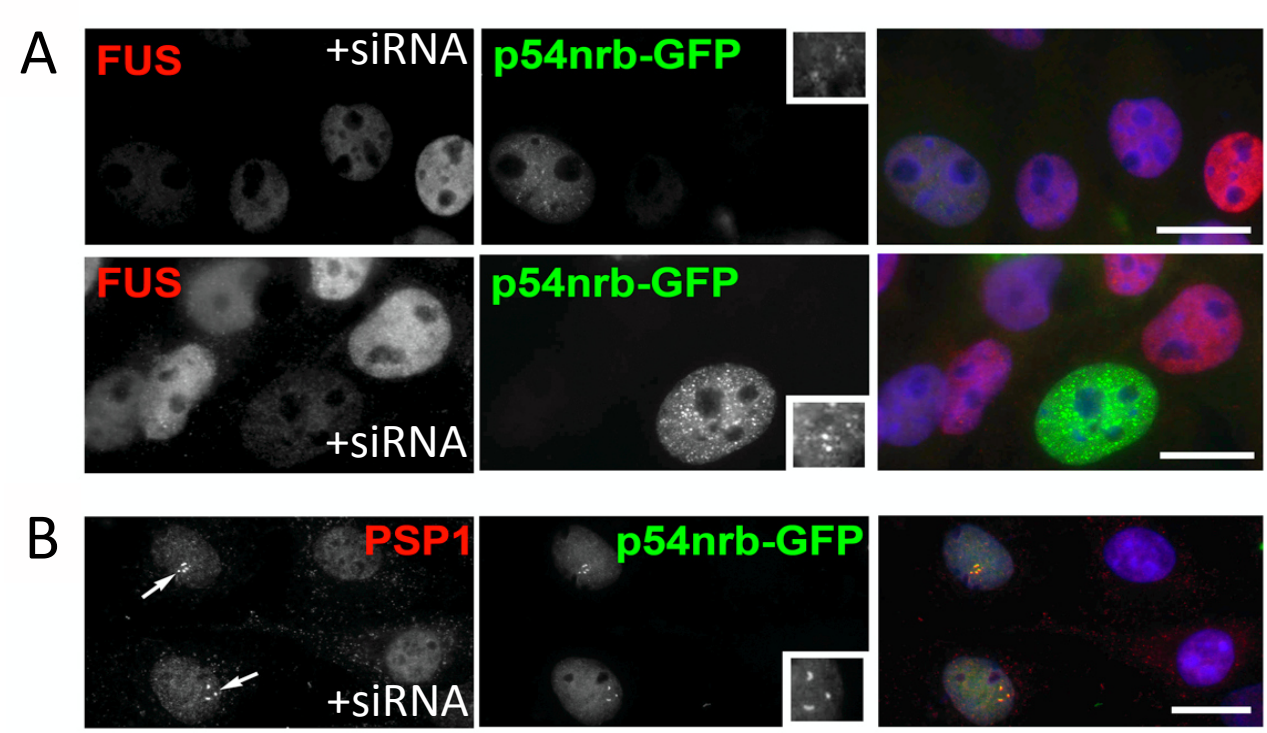

Figure 6.8. p54nrb substituted for loss of FUS function required for paraspeckle formation. (A) GFP-tagged p54nrb expressed in FUS-depleted COS7 cells formed multiple paraspeckle-like structures in a dose-dependent manner. (B) These paraspeckle-like structures were always positive for PSP1 (arrows). Scale bars, 10 μm. At least 3 biological repeats were performed and representative images are shown.

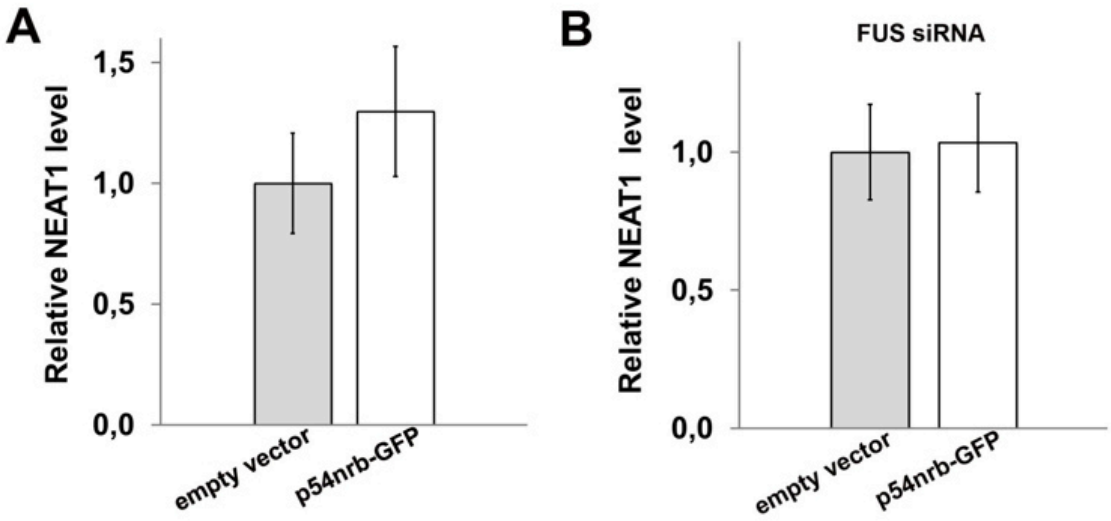

Figure 6.9. p54nrb expression level did not alter NEAT1 expression. (A) Overexpression of p54nrb did not alter NEAT1 levels in naïve cells or in (B) cells depleted of FUS protein by siRNA treatment. In A, cells were transfected with empty vector to express GFP only or with p54nrb-GFP construct; NEAT1 levels were measured 24 h post-transfection. In B, cells were transfected with FUS siRNA in combination with either empty vector or p54nrb-GFP construct followed by analysis of NEAT1 expression 72 h post-transfection. Data is compiled from 6 biological repeats.

6.3.5 Cytoplasmic aggregates of FUS trap paraspeckle proteins in cultured cells

In addition to loss of nuclear FUS function, gain of toxic function in the cytoplasm has been implicated as a possible mechanism of ALS, yet how ALS-associated mutants, which form cytoplasmic aggregates as described in previous chapters, impact the function of paraspeckles had not been investigated. In cells accumulating high levels of mutant FUS R522G protein, cytoplasmic aggregates formed and, surprisingly, these were consistently positive for p54nrb (in 80.3 ± 0.96% of all cells with aggregates) (Figure 6.10A). Likewise, this was also seen for aggregates formed by FUS ΔNLS or FUS 1-466 constructs (data not shown). Moreover, in a small fraction of cells, the presence of p54nrb in the cytoplasmic aggregates was accompanied by a strong reduction of p54nrb in the cell nucleus (Figure 6.10B). PSP1 and another core paraspeckle protein, PSF, also accumulated within the cytosolic FUS aggregates in SH-SY5Y and COS7 cells (Figure 6.10C-E, arrows).

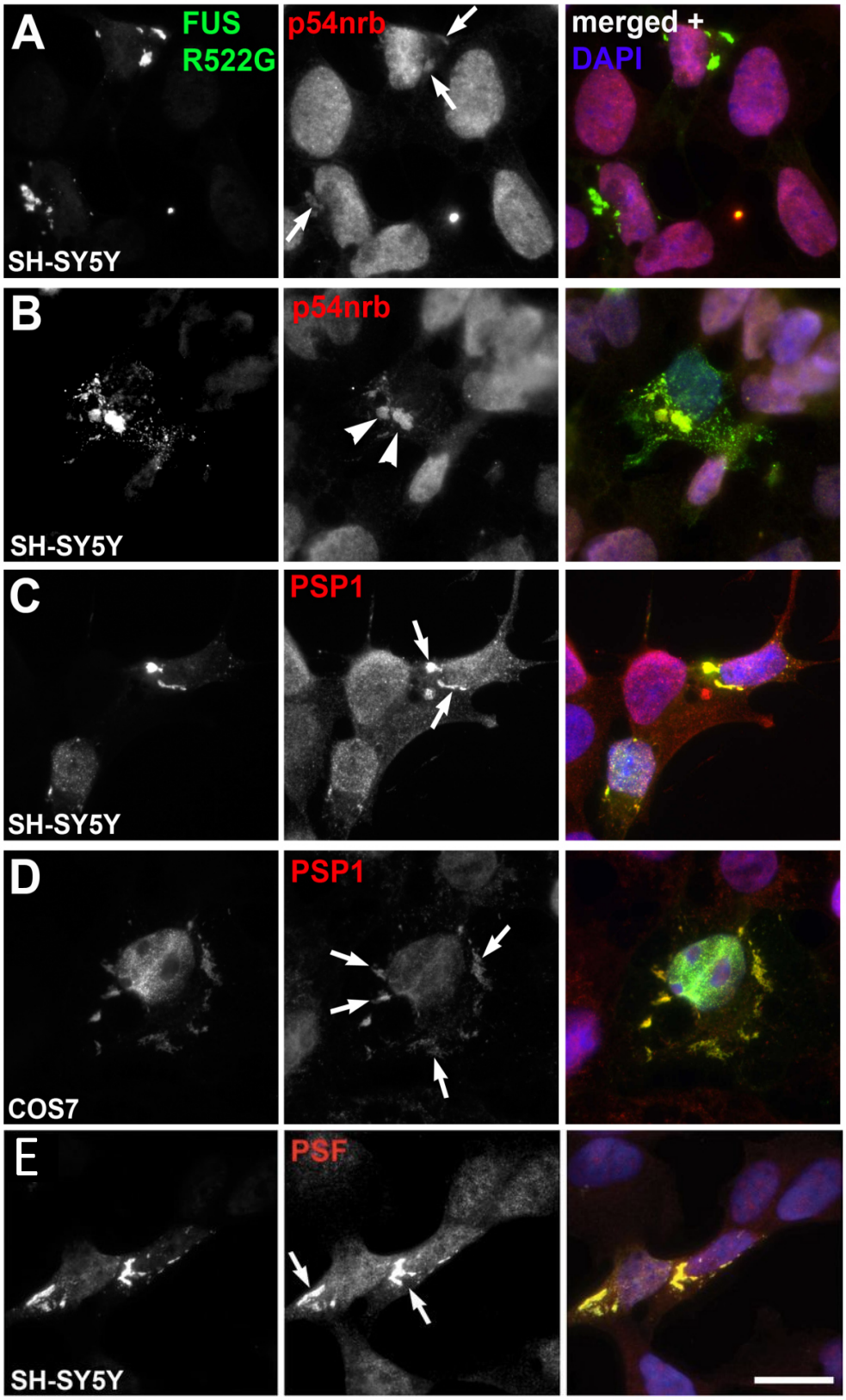

Figure 6.10. Cytoplasmic aggregates of ALS-associated FUS mutant R522G are positive for core paraspeckle proteins. (A) Cytoplasmic aggregates formed by GFP-tagged FUS harboring the ALS-associated mutation, R522G, after 24 h were positive for p54nrb (arrows). (B) In some instances these p54nrb aggregates (arrowheads), were accompanied by a strong reduction of p54nrb in the nucleus. (C-E) Cytoplasmic aggregates of FUS R522G were also positive (arrows) for (C, in COS7 cells, D, in SH-SY5Y cels) PSP1 and (E) PSF. Scale bar all panels; 10 μm. At least 3 biological repeats were performed and representative images are shown.

6.3.6 FUS inclusions in FUS 1-359 transgenic model sequester p54nrb

In addition to investigating the recruitment of p54nrb by FUS aggregates *in vitro*, given that we have a model of FUSopathy (FUS 1-359 mice) that develops pronounced FUS aggregates in the cytoplasm of neuronal cells, described in previous chapters, we sought to establish whether these *in vivo* aggregates could also sequester p54nrb. Initial characterisation of p54nrb staining in mouse nervous tissue using standard immunohistochemistry revealed that the protein was predominantly localised to the nucleus, although in some larger motor neuronal cells displayed a degree of staining in the cytoplasm (Figure 6.11A). However, in symptomatic stage FUS TG mice, p54nrb-positive aggregates were identified in the nucleus of these cells (Figure 6.11B). This method also allowed for the detection of cytoplasmic aggregates that were positive for p54nrb, although these were much rarer (Figure 6.11C, D). Using fluorescent immunohistochemistry, it was confirmed that these p54nrb-positive aggregates observed in transgenic mice directly overlapped with aggregates of FUS (Figure 6.11E-G). PSF, present predominantly in the nucleus of neurons in WT mice, was also present in a fraction of nuclear, but not cytoplasmic, FUS inclusions in FUS 1-359 mice (Figure 6.12B, C). Contrastingly, although PSP1 was detected in the cytoplasm of neurons in WT mice, we failed to detect any aggregated form of the protein in symptomatic stage FUS transgenic mice (Figure 6.12A).

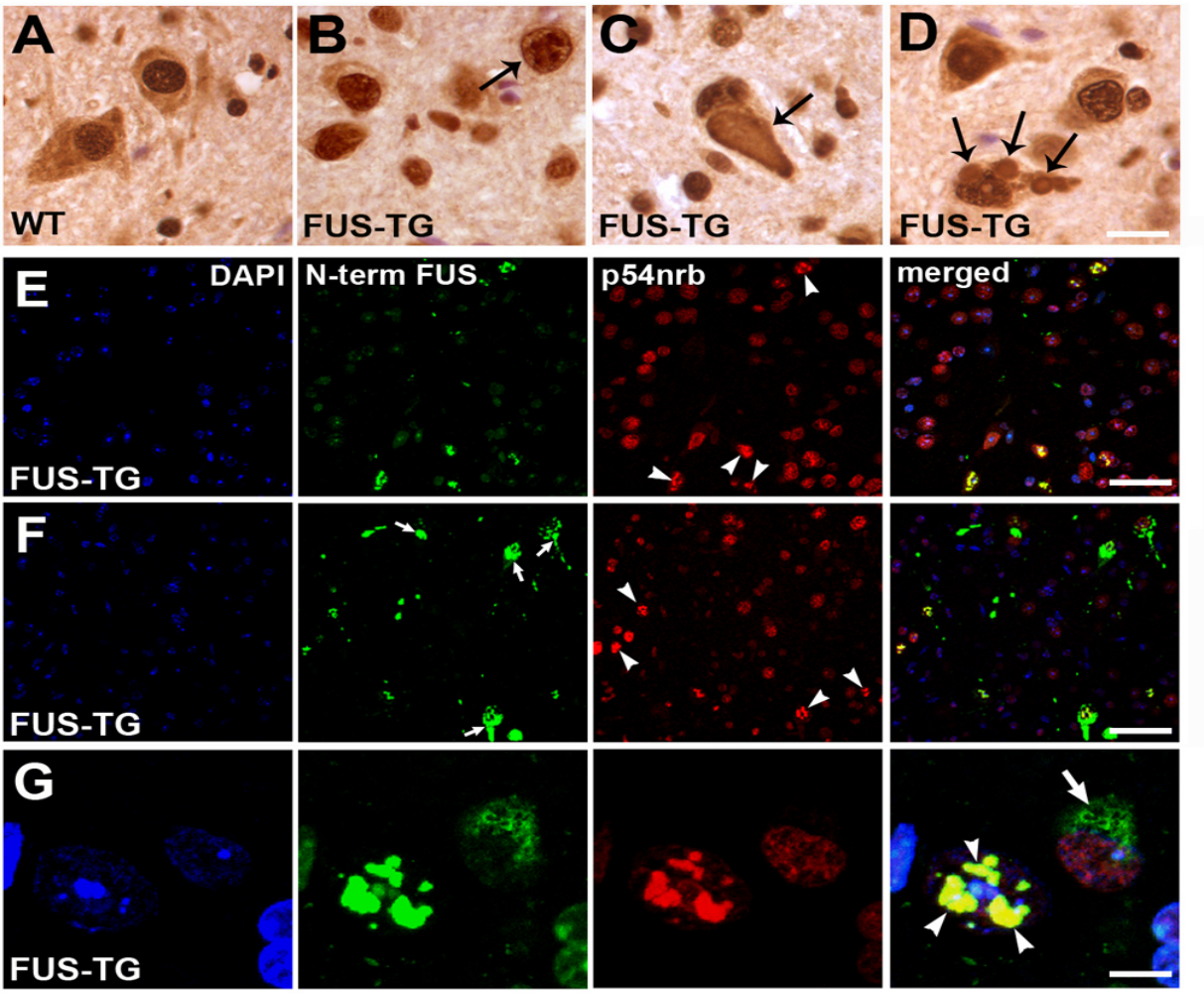

Figure 6.11. p54nrb accumulated in cytoplasmic FUS aggregates *in vivo* in spinal cord of a transgenic model of FUSopathy. (A) Standard immunohistochemistry with anti-p54nrb antibody in non-transgenic WT mouse nervous tissue revealed predominant nuclear localisation of the protein in small motor neurons and glia, although some immunoreactivity was noted in the cytoplasm of large motor neurons. (B-D) In symptomatic FUS 1-359 TG mice, p54nrb-positive aggregates (arrows) were observed in the nucleus (B), and more rarely, the cytoplasm of spinal cord motor neurons (C,D). (E-G) Fluorescent immunohistochemistry revealed colocalisation of almost all FUS-positive aggregates (arrows) in these mice with p54nrb (arrowheads). Antibodies used to recognise the N-terminus of FUS detected both truncated FUS 1-359 and endogenous FUS protein. Scale bars; A–D: 15 µm; E and F: 35 µm; G: 10 µm. Representative images are shown following analysis sections from at least 2 transgenic and 2 WT mice. Data were generated by Dr. Tatyana Shelkovnikova.

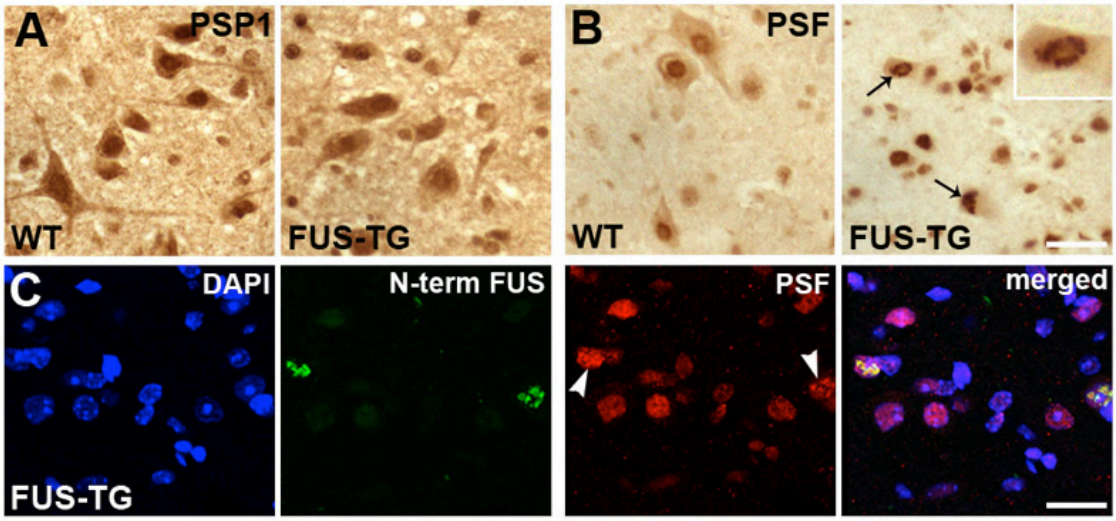

Figure 6.12. Immunoreactivity for PSP1 and PSF in spinal cord of a transgenic model of FUSopathy. (A) Although PSP1 displayed nuclear and cytoplasmic localisation in WT mice, it was not recruited into aggregates in either of these regions in FUS 1-359 mice visualised with standard immunohistochemistry using anti-PSP1 antibodies. (B) PSF was prominently localised to the nucleus in WT mice and was found in nuclear aggregates in symptomatic FUS 1-359 transgenic mice. (C) Fluorescent colocalisation revealed that nuclear FUS-positive aggregates in FUS 1-359 transgenic mice were positive for PSF. Scale bars; A and B, 30 µm; C, 20 µm. Representative images are shown following analysis sections from at least 2 transgenic and 2 WT mice. Data were generated by Dr. Tatyana Shelkovnikova.

6.3.7 p54nrb-positive inclusions are abundant in spinal motor neurons in ALS-FUS patients but not other ALS cases or healthy controls

As p54nrb was recruited to FUS aggregates both in cell culture and our transgenic model of FUSopathy, we wondered whether p54nrb could also be a component of FUS aggregates seen in human ALS patients. To investigate the distribution of p54nrb in these cases, we collaborated with Dr Claire Troakes at the MRC London Neurodegenerative Diseases Brain Bank, Institute of Psychiatry, King's College London to obtain post-mortem spinal cord sections from patients with several types of ALS alongside healthy controls and patients with other neurodegenerative diseases. Upon standard immunohistochemistry, p54nrb displayed nuclear localisation in the majority of small neurons and glial cells but strikingly, displayed prominent cytoplasmic staining in many motor neurons from non-ALS individuals (Figure 6.13A), and in some of these neurons was completely excluded from the nucleus, for instance in a case of multiple sclerosis (MS) (Figure 6.13A, MS). Multiple p54nrb immunoreactive nuclear and cytoplasmic inclusions of various sizes were noted in surviving motor neurons but not glial cells in two ALS-FUS cases studied (Figure 6.13B). These structures were not detected in any of three control non-ALS subjects (Figure 6.13A), or in three sALS cases

including one with confirmed presence of TDP-43 inclusions (Figure 6.13C, sALS-TDP), or in an ALS-SOD1 case (Figure 6.13C, ALS-SOD1).

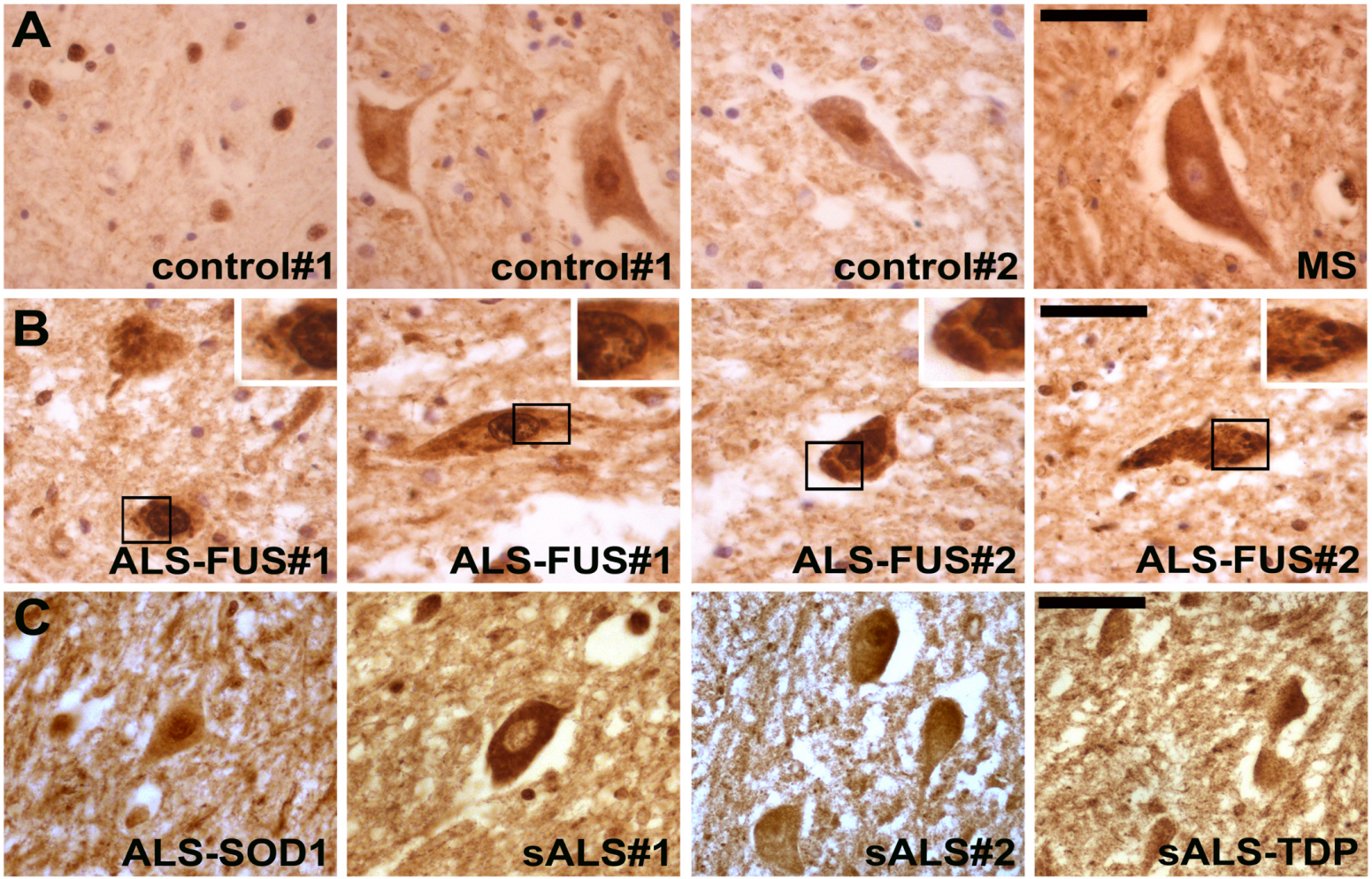

Figure 6.13. p54nrb is a constituent of cytoplasmic and nuclear inclusions in human familial ALS-FUS. (A) p54nrb is confined to the nucleus in the majority of glial cells and small neurons in the spinal cord of non-ALS individuals (control#1). However, in spinal motor neurons p54nrb is present at considerable levels in the cytoplasm. Representative images of spinal motor neurons from two healthy individuals and one MS case stained with anti-p54nrb antibody are shown. (B) Multiple nuclear and cytoplasmic p54nrb-positive inclusions are detected in two familial ALS cases with FUS mutations (ALS-FUS). (C) p54nrb is diffusely distributed in the nucleus and cytoplasm of sALS cases, including a case with confirmed TDP-43 inclusions (sALS-TDP), as well as in a case of fALS with SOD1 mutation (ALS-SOD1). Scale bars; 30 μm. These data were produced by Dr Tatyana Shelkovnikova.

6.4 Discussion

In support of findings by Naganuma *et al.* (2012), Page *et al.* (2011) and Nishimoto *et al.* (2013) we confirmed that FUS is a component of the subnuclear body known as the paraspeckle. This interaction of FUS with paraspeckles demonstrated a degree of specificity, as a number of other subnuclear bodies did not demonstrate colocalisation with FUS. Indeed, subsequent studies have confirmed our observations that FUS was excluded from nucleolar regions (Yang *et al.*, 2014) and whilst evidence suggests that there is a functional association between FUS and SMN, we did not observe FUS at detectable levels within gems, consistent with a previous report (Yamazaki *et al.*, 2012). However, we did observe a moderate enrichment of FUS in nuclear splicing speckles, subnuclear bodies known to store splicing factors (Spector and Lamond, 2011). This was not surprising given the association of FUS with spliceosomal components and the proposed function of the protein in splicing regulation (Ishigaki *et al.*, 2012; Meissner *et al.*, 2003; Zhou *et al.*, 2013).

Upon global transcriptional inhibition with actinomycin D, paraspeckle proteins redistribute to form dark perinucleolar caps, distinct from perinucleolar caps formed by other nuclear components (Shav-Tal *et al.*, 2005). We demonstrated that FUS was also recruited into canonical perinucleolar caps following treatment with actinomycin D. Using fluorescent immunocytochemistry, we confirmed that these were the same distinct caps as those formed by core paraspeckle proteins, strengthening the involvement of FUS with this dynamic subnuclear compartment.

Further, we identified an RNase sensitive association of FUS with p54nrb. This interaction was maintained following global transcriptional inhibition with actinomycin D, yet perturbed following treatment with DRB. As both FUS and p54nrb are able to interact with the C-terminal domain of RNAP2 (Emili *et al.*, 2002; Schwartz *et al.*, 2012), a plausible explanation of these data is that while the FUS–p54nrb interaction remains intact when the intercalating agent actinomycin D stalls the RNA polymerase complex and prevents elongation, this interaction becomes impaired when the assembly of a transcription unit containing FUS and p54nrb is blocked by DRB, an inhibitor of Cdk9 and other kinases that regulate integrity and activity of transcriptional complexes (Yankulov *et al.*, 1995). Taken together, this suggests that these proteins are components of the same transcriptional complex(es) and come into contact co-transcriptionally via interaction with RNAs present in these complexes.

In previous chapters, the formation of pathological FUS aggregates has been demonstrated in cell culture following expression of ALS-associated mutant forms of

FUS and also in mice expressing a C-terminally truncated form of FUS (FUS 1-359). Here we see that inclusions formed by the ALS-associated FUS R522G mutant in cell culture, were positive for the core paraspeckle protein, p54nrb, suggesting FUS inclusions can sequester the protein. This was supported by data from our mouse model and in human ALS patient tissue, where p54nrb was also found in aggregated forms in the cytoplasm and nucleus of spinal cord motor neurons. P54nrb has several roles in addition to paraspeckle formation, including transcriptional regulation (Emili *et al.*, 2002), splicing (Kameoka *et al.*, 2004). By sequestering p54nrb into aggregated forms, these normal roles of p54nrb may be augmented or disrupted, and as such, this work highlights loss of p54nrb function as a possible mechanism contributing ALS pathology, although further work characterising this will be required in the future.

Interestingly, PSF was only seen in nuclear, but not cytoplasmic aggregates in FUS 1-359 transgenic mice. Since aggregation of truncated FUS occurs extremely rapidly and after reaching a certain concentration threshold, p54nrb and PSF were more efficiently recruited into aggregates in the nucleus where they predominantly reside, while their lower levels in the cytoplasm allowed formation of cytoplasmic inclusions only in a fraction of neurons. Potentially, paraspeckles formed in motor neurons of FUS-TG mice in response to damaging effects of accumulating exogenous protein might become seeding centres for aggregation of truncated FUS, which sequester endogenous FUS-p54nrb-PSF complexes. These aggregation ‘cores’ may subsequently grow and fuse to each other to give rise to nuclear inclusions. The fact that unlike two other core paraspeckle proteins, PSP1 was not detected in final products of FUS aggregation in neurons of transgenic mice indicates selectivity of paraspeckle protein co-aggregation and not mere entrapment of entire paraspeckles.

Additionally, we observed a clear relationship between FUS and NEAT1 expression. FUS knockdown resulted in a loss of paraspeckles and the downregulation of NEAT1 expression in cultured cells. NEAT1 downregulation has previously been observed upon knockdown of p54nrb and PSF (Sasaki *et al.*, 2009), and therefore, it is likely that FUS contributes to maintenance of the steady-state level of NEAT1 transcripts in the same way as these major paraspeckle proteins. Therefore, nuclear deficiency of FUS typical of FUSopathies may impede paraspeckle formation needed for an adequate response to stress.

In this way, our data support a model whereby the protective function of paraspeckles may be overcome because of FUS mislocalisation and aggregation. Paraspeckles and NEAT1 expression are elevated in the early stages of ALS (Nishimoto *et al.*, 2013),

reflecting a protective response of the cell to an early stressful insult. Indeed, several lines of evidence support a protective role of paraspeckles. However, where nuclear FUS deficiency occurs in FUSopathies, NEAT1 level would be unable to be sustained and in turn, paraspeckle assembly and maintenance, prohibited. Sequestration of paraspeckle proteins into FUS aggregates also depletes the available pool of these proteins, further hindering paraspeckle protective response. Together these factors may contribute to neuronal pathology in FUSopathies.

GENERAL DISCUSSION

7.1 Overview

Understanding of ALS has gained substantial ground over the past 20 years, in particular, thanks to the increased knowledge provided by the identification of novel genetic contributors to the disease (Renton *et al.*, 2014). Although disruption to RNA-binding proteins, for example TDP-43 and FUS, either through mutation and/or mislocalisation of these proteins to the cytoplasm is well documented in ALS (Lagier-Tourenne *et al.*, 2010), there are several key questions remaining. How do large pathological inclusions of RNA-binding proteins form? Is pathology induced via a gain or loss of protein function? Can aggregation in the cytoplasm of these normally nuclear proteins be sufficient to produce toxicity? Answers to these questions will be useful in identifying pathways for targeting therapeutic interventions in the hope of improved outcome for patients.

This thesis has centred on understanding these processes with respect to the RNA-binding protein, FUS. We have described novel pathways through which mutant FUS can aggregate in the cytoplasm via both RNA-dependent and RNA-independent mechanisms, supporting a gain of function hypothesis elicited by the irreversible aggregation of FUS. Additionally, we sought to investigate how loss of FUS from the nucleus may affect the nuclear architecture, identifying a novel pathological mechanism of compromised paraspeckle formation that may additionally contribute to disease development and progression.

7.2 Expression of readily-aggregating FUS in the cytoplasm is an initial hit sufficient to elicit ALS-like pathology

In Chapter 3, a mouse model of FUSopathy, FUS 1-359 TG mice, was described where human FUS was experimentally C-terminally truncated to remove its NLS and major RNA-binding domains and then expressed under the control of a Thy-1 promoter. By removing these domains, the interactions of FUS with RNA normally arising from these regions were disrupted. Therefore, we were able to assess the impact of an initial hit of FUS aggregation in the cytoplasm without incurring the likely major disruption to RNA homeostasis that overexpression of full length forms would otherwise elicit.

These mice displayed several signs of ALS-like pathology, including progressive paralysis, shortened lifespan, denervation of neuromuscular junctions, muscular atrophy and degeneration of both spinal cord motor neurons and specific brainstem motor nuclei populations. Furthermore, we identified the presence of pathological FUS

inclusions within motor neurons of these mice both in the nucleus and the cytoplasm, a feature that has rarely been seen in other FUS-based models (McGoldrick *et al.*, 2013). Together this demonstrated that an initial insult of FUS aggregation in the cytoplasm in the absence of primary alterations in RNA homeostasis, was sufficient to initiate pronounced pathology.

Intriguingly, it has previously been deemed that the N-terminus prion-like domain, RRM and RGG domain are necessary to confer toxicity in yeast (Sun *et al.*, 2011). As this RGG domain was removed from our C-terminally truncated protein, it is perhaps surprising in light of this information that ALS-like pathology would be elicited. However, upon closer inspection, unlike our fragment, the protein lacking RGG domain tested within the yeast study was retained wholly in the nucleus. Therefore, our murine model also provides novel evidence that the RGG domain may not be essential to initiate pathology induced by FUS once in the cytoplasm, although the involvement of endogenous FUS sequestered by these FUS inclusions cannot be ruled out.

Our FUS 1-359 TG mouse model recapitulated several features of ALS and therefore allowed us to confirm that aggregation of FUS in the cytoplasm can elicit substantial pathology, largely supporting a gain of function hypothesis described within other FUS models (Huang *et al.*, 2011; Mitchell *et al.*, 2013). However, careful consideration will be required before these mice are used for answering future research questions. For mechanistic studies of physiological FUS interactions in the cytoplasm, it will likely be of increased relevance to use a model with improved construct validity, where the protein expressed is physiologically occurring in ALS. Whilst our mice were generated to answer our specific research question and it was not our intention to produce a 'model of ALS', there could be future research indications. As these mice have strong face validity, i.e. they produced several ALS-like features, which have not been observed following WT or mutant FUS expression in other mice (McGoldrick *et al.*, 2013), these mice might be useful predictively to test novel pharmacotherapies targeting ALS, as it would be clear whether these ALS-like features could be slowed or reversed by treatments.

7.3 A protective role of stress granules against pathological FUS aggregation

In addition to determining whether FUS aggregation in the cytoplasm could initiate an ALS-like pathology, in Chapters 4 and 5 we sought to explore the relationship between aggregating forms of FUS and their interactions with SG proteins in the pathogenesis of disease. SGs are formed in response to several types of cellular stress (Anderson

and Kedersha, 2008) and SG marker proteins have been identified in human FUS-positive inclusions post mortem (Dormann *et al.*, 2010). Furthermore, others have shown that in response to cellular stress, ALS-associated FUS variants can be sequestered into induced SGs (Bosco *et al.*, 2010). However, there are conflicting hypotheses regarding the nature of these interactions and further accumulation of FUS-positive stress-induced SGs into larger structures more typical of inclusion bodies has not been evidenced. Thus, questions remain about the origins of these FUS-positive inclusions (Li *et al.*, 2013). In Chapter 4 we showed that following oxidative stress induction with sodium arsenite that GFP-tagged mutant ALS-associated FUS variants could be sequestered into induced SGs in cultured neuroblastoma cells expressing relatively low levels of the ectopic protein, supporting previous findings by others (Bosco *et al.*, 2010; Vance *et al.*, 2013).

However, we identified that FUS lacking major RNA binding domains was unable to enter these induced SGs and instead formed large RNA-free FUS inclusions in the cytoplasm with features typical of aggresomes. Given that this form of FUS resulted in severe pathology when expressed in our transgenic mice and that existing literature suggests SGs represent a protective response by the cell to promote its survival under stressful conditions (Buchan and Parker, 2009), we concluded that recruitment of FUS into reversible SGs is likely a protective response against its pathological self-aggregation. This is contrary to ideas by some that SGs may act as precursors to large pathological inclusions, whereby these normally dynamic structures could undergo changes to become pathological entities (Wolozin, 2014; Droppelmann *et al.*, 2014). However, this notion had been based simply upon the observation of SG markers in the final products of FUS aggregation, something which we provided an alternate explanation for in Chapter 5 (discussed shortly). Having found evidence pointing towards a protective role for the recruitment of ALS-associated FUS variants to induced SGs, we wondered whether ALS-associated FUS might also aggregate pathologically and independently of SGs. Indeed, we had already demonstrated that under basal conditions these FUS variants could accumulate over time in a concentration-dependent manner and chose to further investigate this in Chapter 5.

In this chapter, whilst we observed the formation of stress-induced SGs which were able to sequester FUS mutants in cells expressing relatively low levels of the ectopic protein, we identified a novel and distinct FUS aggregation pattern in cells with a higher degree of ALS-associated FUS mislocalised to the cytoplasm. In these cells, nucleation of FUS occurred past a certain threshold independently of exogenously applied stress

where it associated with newly synthesised RNA to form small FUS granules. These clustered and formed larger RNA-based structures (FAs), a process we demonstrated to be enhanced by cellular stress. However, unlike physiological SGs, these FAs were less structurally uniform, and formed over a longer timescale compared to stress-induced SGs. Further, they contained proteins not seen within SGs, e.g. DDX5. Intriguingly, we demonstrated that these structures may recruit SG marker proteins, which could disrupt protective formation of SGs, also potentially contributing to ALS pathogenesis. This also provides an explanation as to why both ourselves (Chapter 4, Figure 4.1) and others that reported spontaneous aggregate formation in the absence of exogenously-applied stress saw immunoreactivity of these structures for SG marker proteins (Gal *et al.*, 2011; Ito *et al.*, 2011). Further, as FUS granules and FUS aggregates sequestered RNA, this would disrupt the normal transport of transcripts to distal locations, and may therefore impede local translation at the synapse. Thus, this RNA-based aggregation of FUS could also contribute towards impaired synaptic plasticity and function leading to neuronal dysfunction.

Further accumulation of stress-induced SGs that contain FUS has not been evidenced and they have been shown to rapidly disperse following the attenuation of stress (Baron *et al.*, 2013). Therefore, characterisation of this separate FUS aggregation pathway outlined in this thesis shines new light on how FUS may begin to aggregate pathologically and irreversibly in ALS.

7.4 RNA-binding activity of FUS can alter the pathways to its aggregation

Given that we had established a profound pathology in mice upon the expression of FUS that had a reduced capacity for RNA interactions, we wondered how altering the available pool of interacting RNAs might affect the aggregation of ALS-associated forms of FUS that had already formed FAs. In particular, might RNA-based aggregates of human ALS-associated mutants be transformed in response to reduced interactions with RNA?

Large RNA-based FUS aggregates formed in cells with higher levels of RNA-binding competent FUS in the cytoplasm, were readily dissipated by the immediate reduction of freely available transcripts which arose through experimentally inhibiting transcription in these cells. Yet, unexpectedly, and one of the key findings within this thesis, these aggregates reassembled into large RNA-free structures following prolonged transcriptional inhibition (Figure 7.1). Maybe as the supply of RNA is reduced, the higher-order structure of the FUS aggregate is disrupted and so the structure

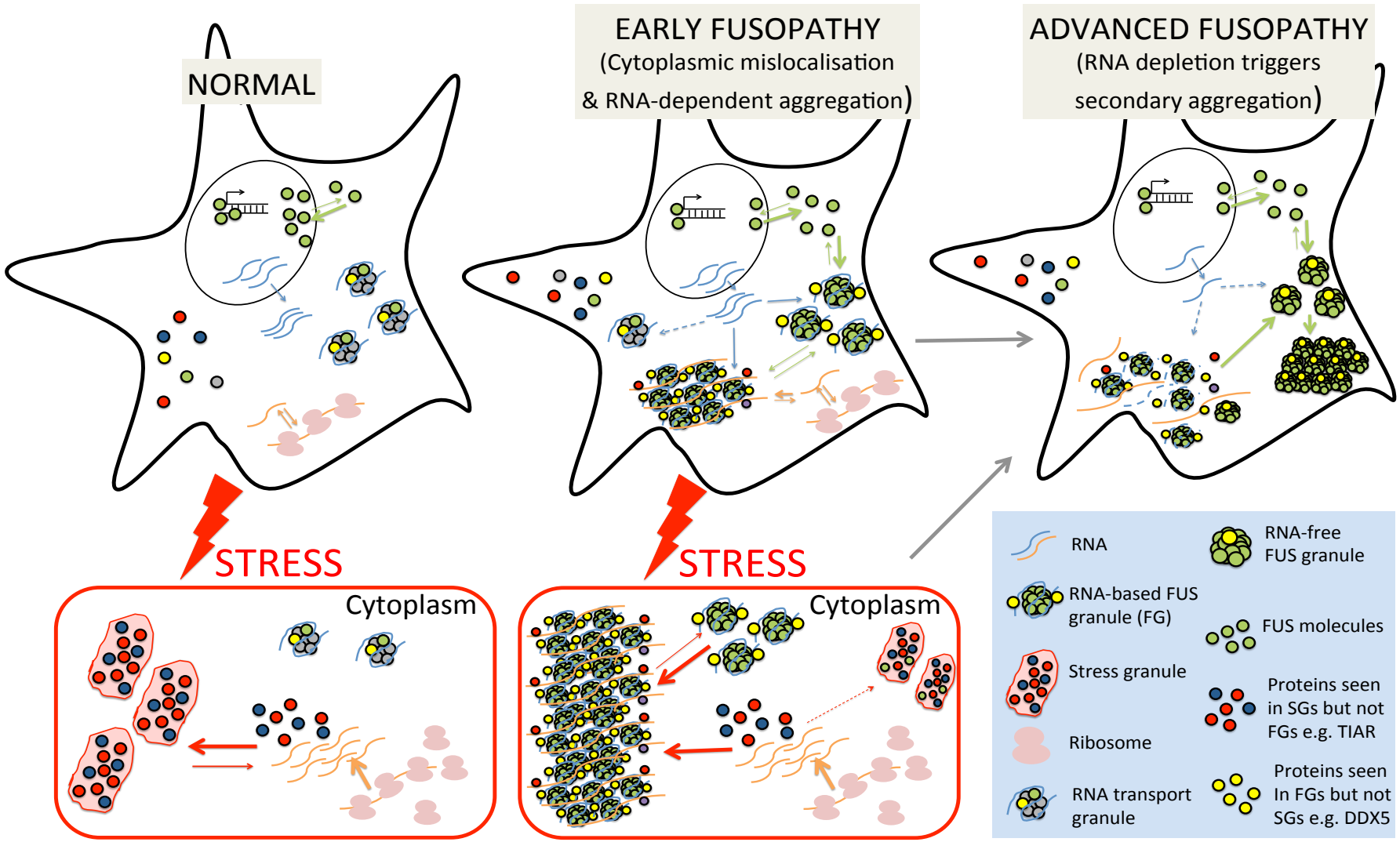

Figure 7.1. Model of FUS aggregate formation via RNA-dependent and RNA-independent mechanisms. Under normal conditions, FUS is present predominantly within the nucleus, where it is involved in several processes including transcription. In the cytoplasm, FUS is a component of RNA transport granules. Under stress, RNA runs off polysomes and is sequestered by SGs along with other specific proteins, providing a protective response. However, in early FUSopathy, FUS becomes mislocalised to the cytoplasm where above a certain threshold it aggregates in a concentration-dependent manner to form RNA-based FGs that cluster together to form large RNA-based FAs, even in the absence of stress. Stress conditions exaggerate this agglomeration and FAs can sequester RNA running off polysomes as well as newly synthesised RNA, disrupting formation of protective SGs. Reduction in available transcripts, which could occur later in the disease possibly with increasing age and disruption to normal nuclear roles of FUS, promotes the dissolution of large RNA-based FAs. These components reassemble to form RNA-free granules that accumulate to form higher order structures. This stage corresponds to the advanced stage of FUSopathy development characterised by severe cellular dysfunction and formation of pathological FUS inclusion.

collapses. Yet, the close proximity and abundance of FUS following this disruption is then sufficient to initiate self-templating, perhaps in a structurally different conformation, driven by protein-protein interactions arising from the N-terminus prion-like domain. Indeed, this domain, and to some extent the C-terminus region (amino acids 423–526) have been shown to promote aggregation of pure recombinant FUS protein *in vitro* in the absence of RNA (Sun *et al.*, 2011). One of the important implications of this work will be to guide the development of pharmacotherapies aimed at targeting ALS. For example, others have previously imagined that blocking the uptake of FUS to stress-induced SGs by disrupting its interactions with RNA may mitigate disease (Li *et al.*, 2013), yet here we demonstrate that SG formation is likely protective and provide evidence that reduced interactions with RNA promote the irreversible aggregation of FUS. Thus, it is with great caution that pharmacotherapies aimed at disrupting interaction of FUS with RNA should proceed.

Having demonstrated that the balance of FUS interacting with RNA plays a large role in determining the mechanisms by which it may aggregate *in vitro*, it would be interesting in the future to pursue how the availability of transcripts might be altered in human ALS-FUS neurons. There is evidence to suggest that transcription may be perturbed with ageing (Lu *et al.*, 2004), and as FUS is known to be directly involved with transcriptional control (Schwartz *et al.*, 2012; Schwartz *et al.*, 2013; Yang *et al.*, 2014), its loss from the nucleus could further augment these processes. Moreover, there is a strong evidence of increased DNA damage in ALS (Bogdanov *et al.*, 2000; Qiu *et al.*, 2014) and, more specifically, mislocalisation of FUS to the cytoplasm may disrupt its role in DNA repair (Mastrocola *et al.*, 2013; Wang *et al.*, 2013), both of which could reduce transcription. Furthermore, other potential regulators of transcription and translation have been implicated in ALS. For example, one theory of ALS pathogenesis suggests that cellular energy is disrupted and that motor neurons, with high energy demands, are highly susceptible to this. AMP-activated protein kinase (AMPK) is a major energy sensor regulating cellular energy homeostasis and abnormal activation of AMPK has been shown in the spinal cord and primary spinal cord neuronal cultures of a well-characterized ALS mouse model (Perera *et al.*, 2014). This is interesting as AMPK has been well implicated in transcriptional regulation and provides another mechanism through which RNA availability might be altered in ALS (McGee and Hargreaves, 2008).

Together, these features highlight that a state of reduced transcript availability is highly feasible in ALS. However, one of the limitations of this thesis is that this was not

directly evidenced. Determining the abundance of RNA transcripts in the cytoplasm of ALS patient neurons which contain FUS inclusions compared to cells displaying diffuse cytoplasmic localisation of FUS could confirm whether work outlined in this thesis directly relates to the formation of FUS-positive inclusions seen in human ALS tissues. One such option for this, although technically challenging, would be *in situ* hybridisation of a labelled oligo(dT) probe to recognise poly(A)+ mRNA abundance in human spinal cord motor neurons (Wilson *et al.*, 1997).

At the same time, we identified that not only the abundance of RNA but also the specificity of RNA interactions contributes to the aggregation propensity of FUS in the cytoplasm. Whilst replacing the C-terminus major RNA binding domains of FUS with RNA-binding domains from human TDP-43 protein with similar functionality (Honda *et al.*, 2013) was sufficient to permit the formation of RNA-based FUS granules in the absence of stress, RNA-binding domains from an evolutionary distant protein from yeast were not sufficient to compensate for this loss.

The interaction of FUS with RNA is complex and several groups have sought to identify a consensus binding sequence, albeit with differing outcomes (Iko *et al.*, 2004; Ishigaki *et al.*, 2012; Lagier-Tourenne *et al.*, 2012). Moreover, in addition to sequence, it has been suggested that secondary structure of RNAs may be an important factor when determining their interaction with FUS (Ishigaki *et al.*, 2012) and recent evidence has also shown that FUS binds RNA in a length-dependent manner, with longer RNA sequences preferentially bound (Wang *et al.*, 2015). To investigate how expressing FUS in the cytoplasm with altered specificity for RNA interactions might affect a model system, in Chapter 3 we characterised a murine model of FUS that neuronally expressed cytoplasm-mislocalised FUS lacking its RRM domain. Although the RRM domain of FUS is not one of the major RNA-binding domains of FUS, it has been proposed to impart specificity of interaction by its cooperation with RGG domains (Lerga *et al.*, 2001; Zinszner *et al.*, 1997b).

Expression of this experimental construct resulted in a dramatic phenotype in the F1 generation of transgenic mice, with severely reduced survival and an obvious tremor in a proportion of these mice. Although evidence of neurodegeneration was not observed within the brain of these mice, it is possible that dysfunction of neurons prior to cellular death may have produced the insurmountable phenotype seen in these mice. Indeed, we observed the dramatic presence of FUS RRMcyt in the cytoplasm and abundant FUS-positive inclusions in these FUS RRMcyt TG mice. This supports the notion that

disruption of FUS homeostasis can produce a significant pathology and that its interactions with RNA could also be critically important.

There are several mechanisms that can be imagined to contribute to the formation of these FUS inclusions in mice. It was shown in Chapter 4 that FUS RRMcyt could be recruited to stress-induced SGs, which may suggest that at least some protection against its aggregation may arise. However, the dynamics of this interaction with induced SGs is not clear from our work and given that FUS RRMcyt likely has altered interactions with RNA, this could augment this sequestration. Furthermore, as with FUS 1-359, we demonstrated in Chapter 3 that FUS RRMcyt was able to form large juxtanuclear structures, suggesting that aggregation outside of SGs may also contribute to the end products of FUS aggregation seen in these mice.

Whilst costly to achieve, it would be interesting to unveil the large-scale interactions of FUS mutants in the cytoplasm with RNA in the future. Using a similar method to a previous study (Colombrita *et al.*, 2012), this could be done by RNA immunoprecipitation followed by chip analysis, whereby tagged FUS mutants expressed in cultured cells are precipitated out together with bound RNA. The protein is then digested and RNAs extracted, followed by determination of all RNA sequences through Illumina or similar chip-based technology. In such a manner, it would be possible to identify RNA targets which are bound differentially by FUS mutants. This could uncover important pathways which may be disrupted not only in our murine models, but potentially in human ALS patients with various FUS mutations.

7.5 Loss of FUS function may also contribute to FUSopathy

Investigating the aggregation pathways of cytoplasmically mislocalised FUS and observing the ALS-like pathology that a primary insult of FUS aggregation in the cytoplasm produced in mice pointed towards a gain of function mechanism in the pathogenesis of ALS-FUS. This conclusion was drawn as FUS gained new functionality in the cytoplasm, forming inclusions that could sequester RNA and other proteins, including FUS, although this may later lead to a possible loss of nuclear function. We also aimed to uncover how this loss of FUS from the nucleus might contribute to the toxicity seen in several models (Hicks *et al.*, 2000; Kuroda *et al.*, 2000; Sasayama *et al.*, 2012). In particular, as FUS is predominantly a nuclear protein, how would loss of FUS disrupt the normal architecture of the nucleus and its functionality? The nucleus of a cell is thought to be highly-organised and whilst it does not contain lipid membrane-bound organelles, distinct and dynamic sub-compartments known as

subnuclear bodies provide discreet and specialised regions for a variety of processes including transcription, splicing and retention of transcripts (Dundr and Misteli, 2001; Wang *et al.*, 2002; Schmitz and Herrmann, 2008). Intriguingly, alterations to subnuclear bodies in ALS have previously been observed by other groups. For example, several groups report ALS-related deficiencies in the formation and maintenance of gems, subnuclear bodies involved in the production of certain spliceosomal components (Gertz *et al.*, 2012; Kariya *et al.*, 2012; Shan *et al.*, 2010; Yamazaki *et al.*, 2012; Ishihara *et al.*, 2013). Additionally, in SOD1-G93A mice, a model of ALS-SOD1, a fragment of excitatory amino acid transporter 2 (EAAT2) that is abnormally cleaved through oxidative stress, was shown to be conjugated with SUMO-1 and accumulated in PML bodies (Gibb *et al.*, 2007). As PML bodies are focused sites of transcription (Zhong *et al.*, 2000), abnormal accumulation of this fragment could disrupt their normal functions, providing a novel mechanism that may contribute to ALS. However, investigation into subnuclear bodies and their potential dysfunction in ALS remains in its infancy, highlighting the need for further research in this area.

In Chapter 6, confirming previous findings by others (Naganuma *et al.*, 2012; Nishimoto *et al.*, 2013; Page *et al.*, 2011), we demonstrated that under basal conditions full length WT FUS was enriched in the subnuclear body known as the paraspeckle and identified an interaction of FUS with the core paraspeckle protein, p54nrb. From previous work, it was not clear how loss of FUS from the nucleus, typical of FUSopathies, would impact paraspeckles. As such, we demonstrated that loss of FUS *in vitro*, elicited by its cellular knockdown with siRNA, caused a reduction in the level of NEAT1 lncRNA. FUS and NEAT1 are known to interact (Nishimoto *et al.*, 2013) and so it is likely that FUS is directly important in the regulation of NEAT1 expression. Simultaneously, increased expression of GFP-tagged FUS resulted in increased NEAT1 expression, supporting this idea. In cells with knocked down FUS expression, paraspeckle formation and maintenance was disrupted suggesting FUS is essential for paraspeckle formation. Further, this work agrees with evidence that high levels of NEAT1 expression are required for their presence (Clemson *et al.*, 2009).

We also identified a second novel mechanism by which FUS, mislocalised in ALS to the cytoplasm, may disrupt paraspeckle formation. We showed that FUS aggregates in the cytoplasm can sequester p54nrb. This observation *in vitro* was then confirmed in our murine model of FUSopathy (FUS 1-359 TG mice) and in human ALS-FUS patients. This recapitulation in humans is one of the key strengths of this study, providing compelling evidence for the potential role of paraspeckle disruption in human

ALS-FUS. However, non-specificity of the antibodies used cannot be completely excluded. In particular, when working with challenging human tissues, is it possible that the antibody binds aggregates non-specifically given their aggregate-prone nature rather than the antibody binding the specific protein of interest present in the aggregate?

Paraspeckles are not thought to be essential under normal conditions; they are not normally observed in neurons and NEAT1 knockout mice are healthy in the relative safety of the normal laboratory environment (Nakagawa *et al.*, 2011). However, paraspeckles are thought to provide relief against cellular stress. This notion has arisen through the increased presence of paraspeckles following a number of cellular insults (Imamura *et al.*, 2014; Zhang *et al.*, 2013; Saha *et al.*, 2006). Additionally, NEAT1 levels are increased in the brain of heroin abusers, indicating a possible protective response to this stress insult (Michelhaugh *et al.*, 2011). Thus, as FUS accumulates in the cytoplasm in conjunction with increased cellular stress, it is possible that the observed sequestration of core paraspeckle proteins and mislocalisation of FUS prevents the formation of paraspeckles, which may have otherwise provided a protective response to the stress insult (Figure 7.2). In such a way, therapies targeted to increase NEAT1 expression, may be therapeutically relevant and might prevent the exacerbation of cellular stress in ALS-FUS and other FUSopathies. Additionally, phosphorothioate-modified (PS) ASOs have been shown to be sufficient to nucleate paraspeckle-like structures in the absence of NEAT1 and so may be a viable alternative (Shen *et al.*, 2014).

In the future, it will be interesting to determine other proteins that are sequestered by FUS inclusions in the cytoplasm. Previous mass spectrometry experiments have been conducted to identify proteins interacting with detergent-insoluble TDP-43 overexpressed in HEK293 cells (Dammer *et al.*, 2012) or to determine the proteomic composition of human FTLD inclusions (Seyfried *et al.*, 2012). Similar global approaches for FUS may identify additional proteins sequestered by human FUS inclusions and lead to the identification of further disrupted pathways that could be important in the development of FUSopathies.

Furthermore, much of the work within this thesis has been based on *in vitro* cell culture systems utilising transient transfection protocols. These cell culture systems are a popular choice for early investigatory research because of their ease to work with, cost efficiency and carefully controlled environment. However, the next logical step will be to

determine whether the mechanisms outlined in this thesis are applicable to cells that stably express mutant forms of FUS. This work is ongoing in our laboratory, with a new PhD student, working to produce several CRISPR/Cas9 genome-engineered human cell lines, where the gene encoding the endogenous FUS protein has been hemizygously mutated. Future work could also incorporate the use of patient-derived induced pluripotent cells to more closely model the cellular environment in cases of human ALS.

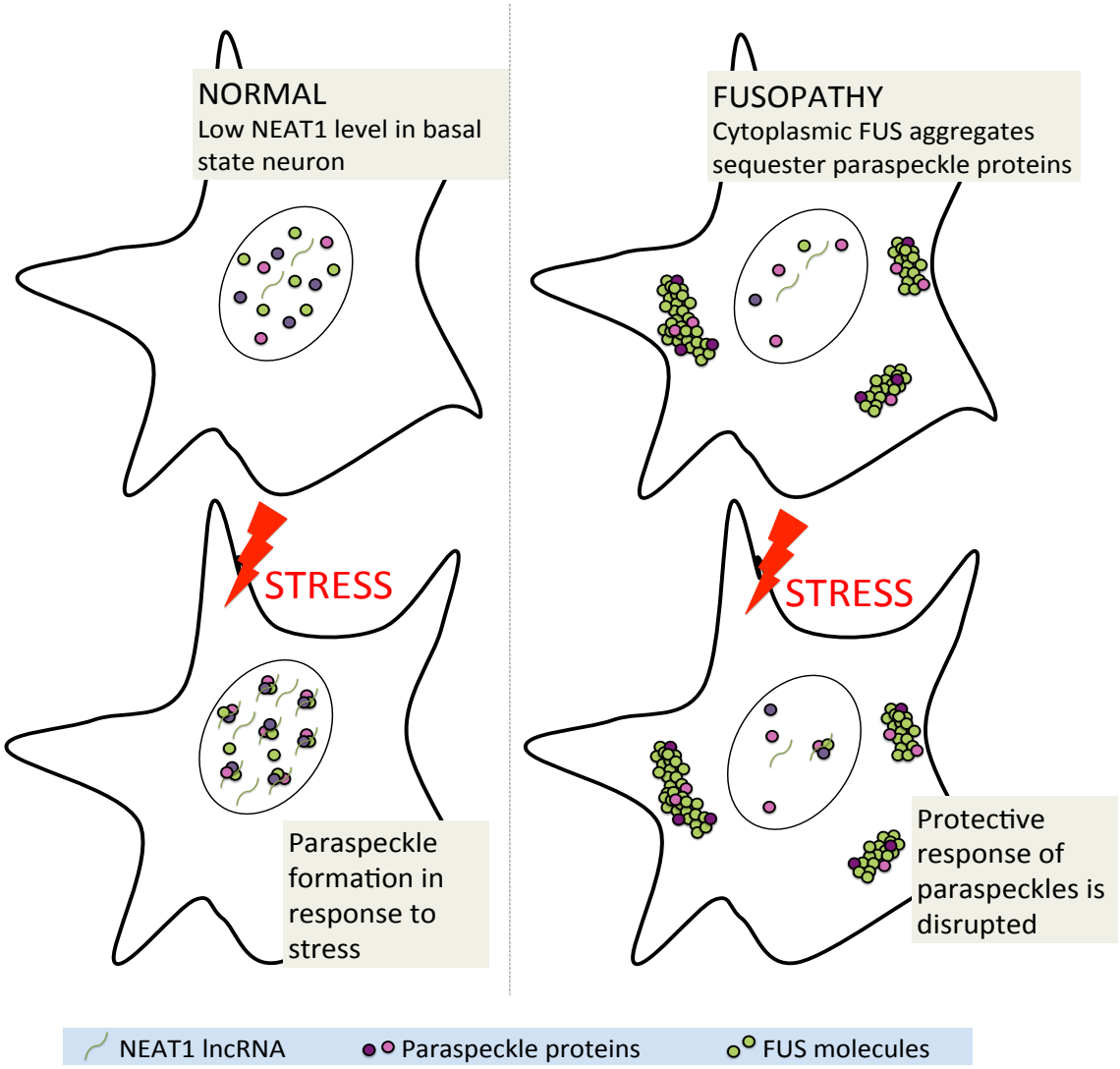

Figure 7.2. Hypothetical model of how FUS aggregation may impair a protective paraspeckle response in FUSopathies. Normally, FUS resides predominantly within the nucleus of a neuron, which expresses low levels of NEAT1 under normal conditions. Upon stress, NEAT1 expression is increase and FUS interacts with other paraspeckle proteins to form paraspeckles which could be a protective response of the cell. However, in FUSopathy, FUS is dramatically mislocalised to the cytoplasm where it can aggregate and form large inclusions. These inclusions can sequester paraspeckle proteins and loss of nuclear FUS reduces NEAT1 expression. Therefore, upon stress insult, paraspeckle formation is perturbed. This highlights how compromised paraspeckle formation may contribute to FUSopathy.

7.6 N-terminus prion-like domain of FUS and its role in aggregation

In addition to the role of FUS interactions with RNA, the contributions of the prion-like domain of FUS are key in the process of its aggregation. We have shown that this prion-like domain, thought to occur between amino acids 1-239 (Cushman *et al.*, 2010), together with RNA interaction was essential for FA formation. However, whilst preventing the pathological aggregation of FUS could be therapeutically valuable, disrupting the interactions of this prion-like domain to prevent its pathological aggregation will likely not be a viable strategy. In addition to its roles in pathological FUS aggregation, indeed others have also shown that this prion-like domain is essential for aggregation of FUS (reviewed in Gitler and Shorter (2011)), this domain is essential for mediating essential physiological roles of FUS protein. It is necessary for seeding a higher-order RNA-based assembly of FUS which enables its binding to, and regulation of, RNAP2 in transcription (Schwartz *et al.*, 2013). Further, supporting work carried out by our laboratory (Shelkovnikova *et al.*, 2014), the prion-like domain has been shown to be essential in the recruitment of FUS to paraspeckles (Hennig *et al.*, 2015). Disruption of the prion-like domain of FUS to augment its pathological interaction would therefore disturb both transcriptional regulation and paraspeckle formation, and potentially other important normal cellular functions of the protein, both of which may further contribute to progression of ALS.

7.7 Implications for ALS and concluding remarks

This thesis supports both gain of toxic FUS function and loss of normal FUS function hypotheses in the development of ALS-FUS and other neurodegenerative diseases where FUS may become mislocalised to the cytoplasm. This is in line with the wealth of literature supporting each of these possibilities. Specifically, this thesis makes several significant and novel contributions to the understanding of these processes. We have provided the first detailed characterisation of a novel pathway of FUS aggregation in instances where ALS-associated mutant FUS is mislocalised and accumulated in the cytoplasm. This pathway is distinct from recruitment into stress-induced SGs and can lead to the formation of large RNA-based FUS aggregates. Intriguingly, we demonstrated that reduced protein-RNA interaction through transcriptional inhibition resulted in the dissolution and reassembly of these FUS aggregates into higher order RNA-free structures. Alongside this, we developed a murine model of FUS aggregation by neuronal expression of an experimental form of FUS lacking major RNA-binding domains. These mice displayed pathological FUS inclusions and several additional ALS-like signs. Therefore, alterations in the interaction of FUS with RNA may augment its aggregation once mislocalised to the

cytoplasm and RNA-free FUS inclusions formed may represent similarly forming structures seen in human FUSopathy cases. This pathway, based on both RNA-dependent and RNA-independent mechanisms, demonstrates for the first time how FUS may accumulate pathologically to form large inclusions. Disruption of this pathway may be relevant for mitigating progression of FUSopathies. Furthermore, we showed how recruitment of FUS into SGs may be protective against its irreversible aggregation, providing evidence which is contrary to the view that SGs may undergo some form of change to become pathogenic. As such, future therapies aimed at disrupting SG response may not be viable for slowing ALS caused by FUS mutation. Finally, we discovered a novel loss of function mechanism that may contribute to ALS pathology via perturbed subnuclear interaction of FUS in paraspeckles. This disruption of paraspeckles may reduce the ability of neurons to overcome cellular stress. Further research into the modulation of these pathogenic mechanisms could lead to the development of additional ALS therapeutics in the future, for example, promoting paraspeckle formation may act to enhance cellular survival, although this is yet to be tested. Whilst it remains to be seen whether similar mechanisms could be relevant for ALS as a whole, work described in this thesis is valuable for understanding what happens when FUS is mislocalised to the cytoplasm, and identifies several pathological mechanisms that may be relevant for future therapeutic strategies.

APPENDIX

7.1 Plasmid profiles

7.1.1 pEGFP-C1

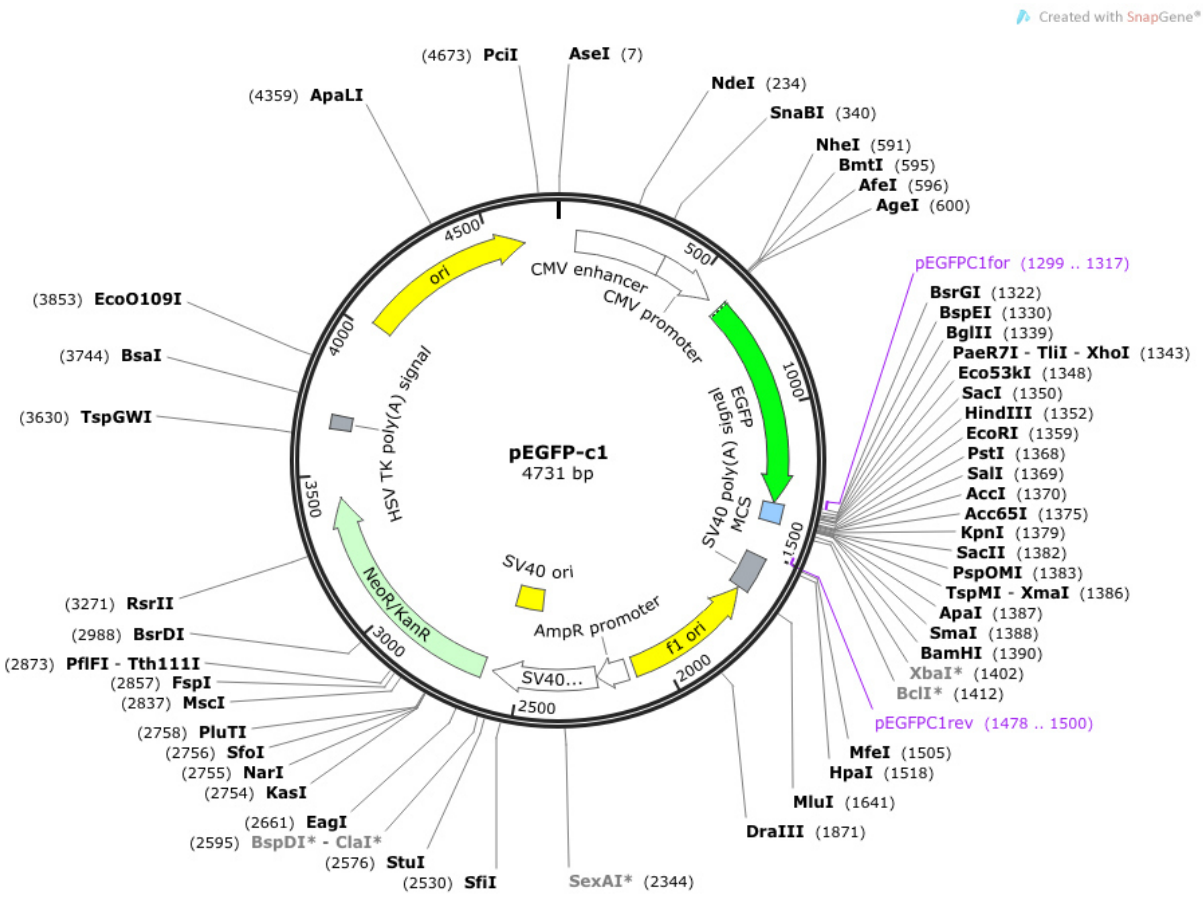

Sequencing primers (blue):

Name	Sequence (5'-3')	Length (bp)	Tm (ºC)	GC%
pEGFPC1for	GATCACTCTCGGCATGGAC	19	58.8	58
pEGFPc1rev	CATTTTATGTTTCAGGTTCAGGG	23	57.1	39

Element(s) of interest: EGFP (lime green)

Antibiotic resistance: kanamycin

Supplier: Clontech

7.1.2 pCR-BLUNT II-TOPO

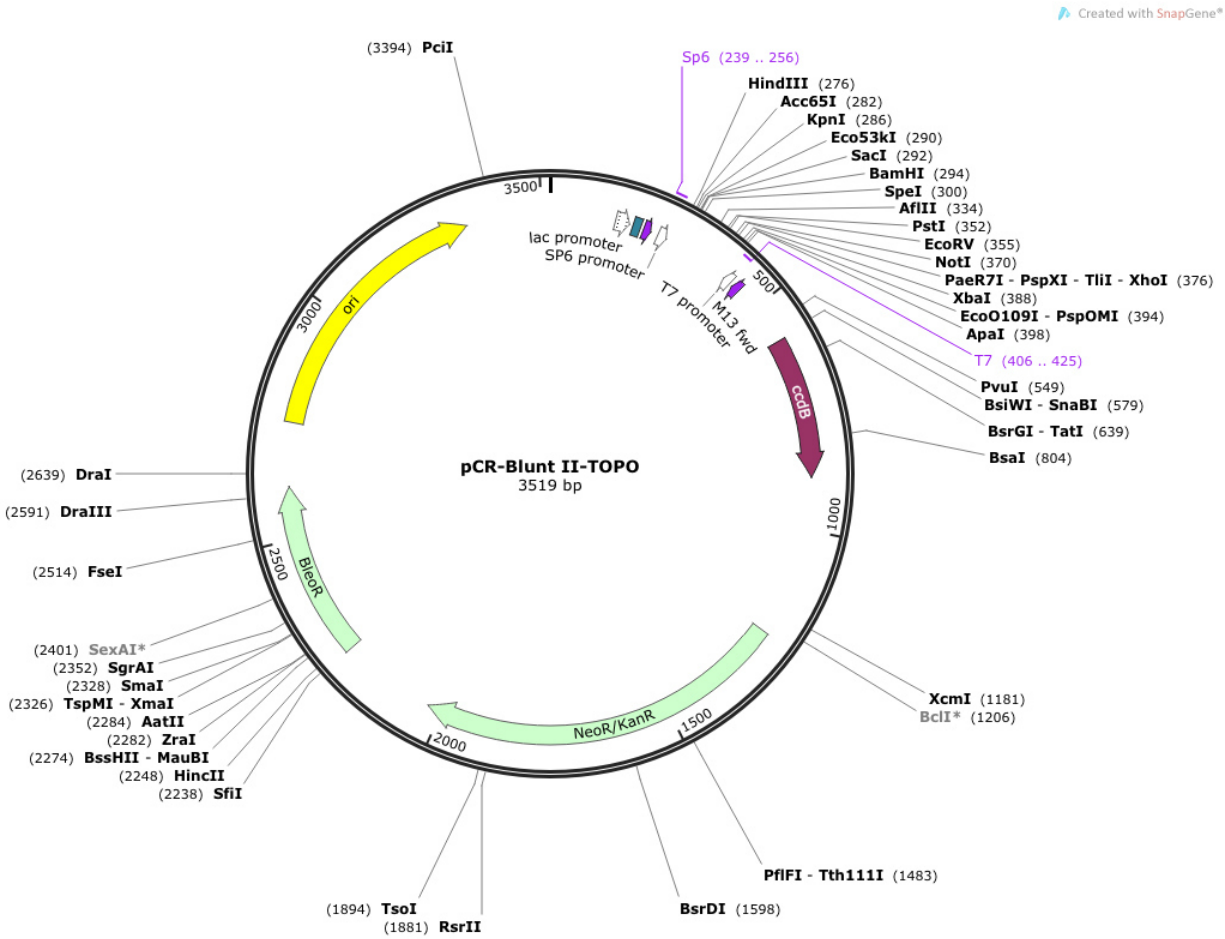

Sequencing primers (blue):

Name	Sequence (5'-3')	Length (bp)	Tm (ºC)	GC%
T7	TAATACGACTCACTATAGGG	20	53.2	40
Sp6	CATTTAGGTGACACTATAG	19	50.2	37

Antibiotic resistance: kanamycin

Supplier: Invitrogen

7.1.3 pFLAG-CMV4

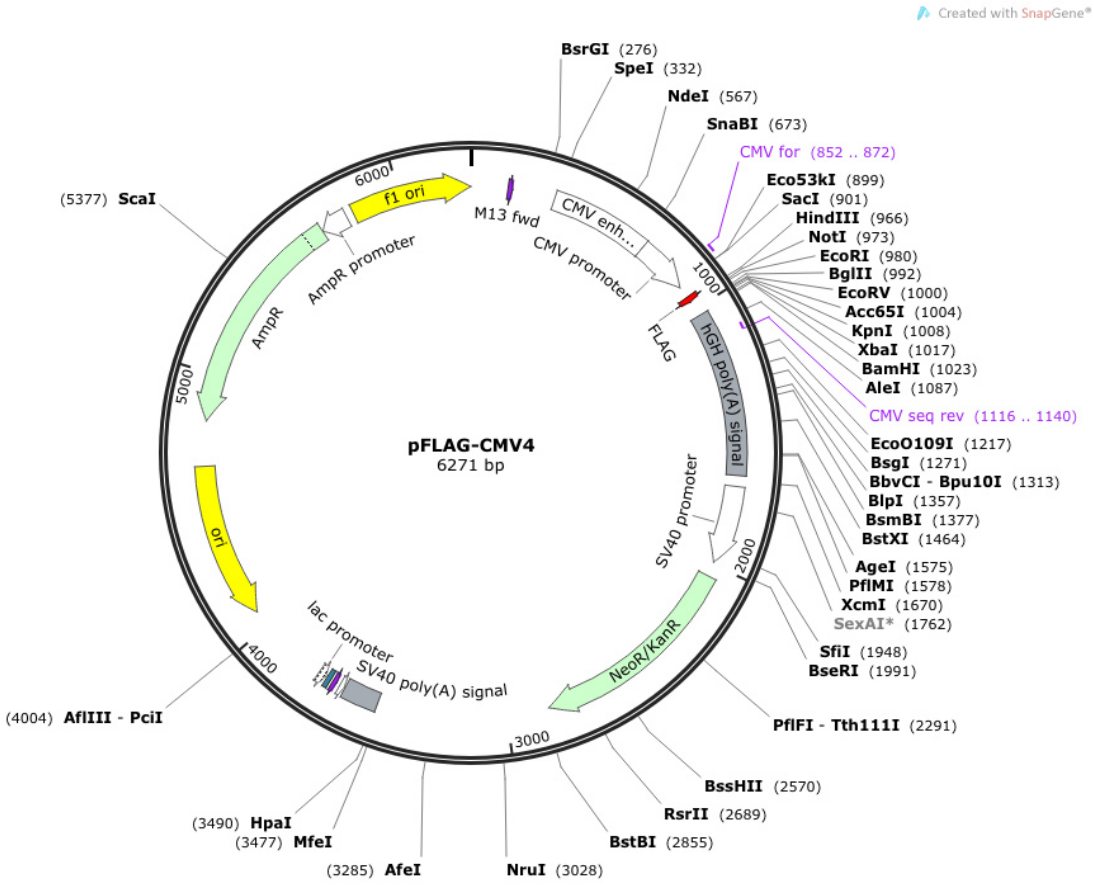

Sequencing primers (blue)

Name	Sequence (5'-3')	Length (bp)	Tm (ºC)	GC%
CMV for	CGCAAATGGGCGGTAGGCGTG	21	65.7	67
CMV seq rev	GTCAGACAAAATGATGCAACTTAAT	25	54	32

Element(s) of interest: FLAG (red)

Antibiotic resistance: kanamycin

Supplier: A kind gift from Prof. Francisco Baralle

7.2 Primers

Protein	Tag	Fragment/ mutation	Forward primer (5'-3')	Reverse primer (5'-3')	PCR template	PCR fragment size (bp)	Digest PCR product from TOPO vector	Vector
FUS	N-terminal EGFP	1-359	tctcgagctatggcctcaaacgattatac	aggatccttagaattctttaccatcaaacc	Human cDNA	1096	XhoI/BamHI	pEGFP-C1 (XhoI/BamHI)
	N-terminal EGFP	359-526 (to create WT)	gctaaagcagctattgactg	tggatccttaatacggcctctcct	Human cDNA	549	EcoRI/BamHI	FUS-1-359 in pEGFP-C1 (EcoRI/BamHI)
	N-terminal EGFP	R522G	gctaaagcagctattgactg	tggatccttaatacggcctctccccgcg	FUS WT in pEGFP-C1	550	EcoRI/BamHI	FUS-1-359 in pEGFP-C1 (EcoRI/BamHI)
	N-terminal EGFP	1-513 (ΔNLS)	gctaaagcagctattgactg	tggatccttaggaatccatcttgccagg	FUS WT in pEGFP-C1	512	EcoRI/BamHI	FUS-1-359 in pEGFP-C1 (EcoRI/BamHI)
	N-terminal EGFP	1-466 (dRGG3)	gctaaagcagctattgactg	tggatccttaacccccatgtgaga	FUS WT in pEGFP-C1	370	EcoRI/BamHI	FUS-1-359 in pEGFP-C1 (EcoRI/BamHI)
	N-terminal EGFP	ΔRRMcyt	cagtcaattgagtccggaaatcctatcaaggtc	gagtttggacaaaccacaac	FUS R522G in pEGFP-C1	753	MfeI	FUS R522G in pEGFP-C1 (MfeI)
	N-terminal EGFP	ΔRRM	cagtcaattgagtccggaaatcctatcaaggtc	gagtttggacaaaccacaac	FUS WT in pEGFP-C1	753	MfeI	FUS WT in pEGFP-C1 (MefI)
	N-terminal EGFP	CT	tctcgagaagaattctccggaaatcctaatcaa	tggatccttaatacggcctctcct	FUS WT in pEGFP-C1	523	XhoI/BamHI	pEGFP-C1 (XhoI/BamHI)
	N-terminal EGFP	RRM-CT	tctcgagctcaaggatcacgtcatgactcc	tggatccttaatacggcctctcct	FUS WT in pEGFP-C1	786	XhoI/BamHI	pEGFP-C1 (XhoI/BamHI)

	N-terminal EGFP	NT	tctcgagctatggcctcaaacgattatac					
	N-terminal EGFP	dRRM-RGG3	tctcgagctatggcctcaaacgattatac	tggatccttaacccccatgtgaga	FUS ΔRRM in pEGFP-C1	1227	XhoI/BamHI	pEGFP-C1 (XhoI/BamHI)
	N-terminal EGFP	R518K	gctaaagcagctattgactg	tggatccttaatacggcctctccctgcgatcctgtttgtg	FUS WT in pEGFP-C1	550	EcoRI/BamHI	FUS-1-359 in pEGFP-C1 (EcoRI/BamHI)
	N-terminal EGFP	R524T	gctaaagcagctattgactg	tggatccttaatacggcgtctccctgcg	FUS WT in pEGFP-C1	550	EcoRI/BamHI	FUS-1-359 in pEGFP-C1 (EcoRI/BamHI)
P54nrb	N-terminal EGFP	WT	tctcgagctatgcagagtaataaaacttttaac	tggatccttagtatcggcgacgtttgttt	Human cDNA	1416	XhoI/BamHI	pEGFP-C1 (XhoI/BamHI)
MTAP	N-terminal FLAG	WT	gacaagcttatggcctctggca	cgggatccttaatgtcttggtaataa	Human cDNA	852	HindIII/BamHI	pFLAG-CMV4 (HindIII/BamHI)
Chimeric Proteins								
	N-terminal EGFP	Sup35-FUS	tgtactcgagctatgtcggattcaaa	tcagtgaattcagacataccttgagactg	Yeast cDNA	398	XhoI/EcoRI	FUS WT in pEGFP-C1 (XhoI/EcoRI)
	N-terminal EGFP	FUS-TDP43-RRMs	gtgccgaatccacatccgatttaatagtgtt	gctaggattcctaattgtgcttaggtt	Human cDNA	513	EcoRI/BamHI	FUS FUS WT in pEGFP-C1 (EcoRI/BamHI)
	N-terminal EGFP	FUS-TDP43-RRMs-3D	agaattcgatgacatagacttgggtgacccatggaaaaca	gctaggattcctaattgtgcttaggtt	Human cDNA	505	EcoRI/BamHI	FUS FUS WT in pEGFP-C1 (EcoRI/BamHI)
	N-terminal EGFP	FUS-Npl3	tgtcacaattgaccagattgtttgttagacctt	tgtaggatccttatctgattggtggaggattgtc	Yeast cDNA	492	MfeI/BamHI	FUS WT in pEGFP-C1 (MfeI/BamHI)

7.3 Primary antibodies

Name	Type	Company
Anti G3BP1	Mouse monoclonal	BD Laboratories
Anti-β-actin	Mouse monoclonal	Clone AC-15, Sigma-Aldrich
Anti-Dcp1a	Rabbit polyclonal	Sigma-Aldrich
Anti-DDX5	Rabbit monoclonal	Clone D15E10, Cell Signalling
Anti-FLAG tag	Rabbit polyclonal	Clone M2, Sigma
Anti-FMRP	Rabbit polyclonal	Clone F4055, Sigma-Aldrich
Anti-FUS (human and mouse)	Mouse monoclonal	BD laboratories
Anti-FUS (human) (1480)	Rabbit polyclonal	A kind gift from Prof. Don Cleveland
Anti-FUS (mouse) (1482)	Rabbit polyclonal	A kind gift from Prof. Don Cleveland
Anti-FUS C-term	Mouse monoclonal	Clone 4H11, Santa Cruz
Anti-FUS N-term	Rabbit polyclonal	Abcam
Anti-FUS N-term	Mouse monoclonal	Santa Cruz
Anti-Gamma tubulin	Mouse monoclonal	Clone GTU-88, Sigma-Aldrich
Anti-GAPDH	Mouse monoclonal	Clone 6C5, Santa Cruz
Anti-GFAP	Rabbit polyclonal	Sigma-Aldrich
Anti-GFP	Mouse monoclonal	Clone 3A9, Protein Synthesis
Anti-GFP	Rabbit polyclonal	Living Colours, Clontech
Anti-HSP27	Rabbit polyclonal	Cell Signalling
Anti-LAMP1	Mouse monoclonal	Clone H4A3, BD Laboratories
Anti-LAMP2	Mouse monoclonal	Clone H4B4, BD Laboratories
Anti-NeuN	Mouse monoclonal	Clone MAB377, Chemicon
Anti-p54nrb	Rabbit polyclonal	Sigma-Aldrich
Anti-p68	Rabbit monoclonal	Clone D15E10, Cell Signalling
Anti-p80 coilin	Mouse monoclonal	BD Laboratories
Anti-phospho-eIF2alpha	Rabbit polyclonal	Abcam
Anti-PML	Chicken polyclonal	A kind gift from Prof. Ronald Hay
Anti-PSF	Rabbit polyclonal	Clone AB2, Sigma
Anti-PSP1	Rabbit polyclonal	Sigma-Aldrich

Anti-S6 ribosomal protein	Rabbit polyclonal	Cell Signalling
Anti-Sm antigen	Rabbit polyclonal	Clone Y12, Abcam
Anti-SMN	Mouse monoclonal	BD Laboratories
Anti-TIAR	Mouse monoclonal	Clone 6, BD Laboratories
Anti-Ubiquitin	Mouse monoclonal	Clone N-19, Santa Cruz
Anti-Vimentin	Mouse monoclonal	Clone RV202, BD Laboratories

REFERENCES

AL-CHALABI, A., ANDERSEN, P. M., NILSSON, P., CHIOZA, B., ANDERSSON, J. L., RUSS, C., SHAW, C. E., POWELL, J. F. & LEIGH, P. N. 1999. Deletions of the heavy neurofilament subunit tail in amyotrophic lateral sclerosis. *Hum Mol Genet,* 8**,** 157-64.

AL-CHALABI, A., FANG, F., HANBY, M. F., LEIGH, P. N., SHAW, C. E., YE, W. & RIJSDIJK, F. 2010. An estimate of amyotrophic lateral sclerosis heritability using twin data. *J Neurol Neurosurg Psychiatry,* 81**,** 1324-6.

AL-CHALABI, A. & HARDIMAN, O. 2013. The epidemiology of ALS: a conspiracy of genes, environment and time. *Nat Rev Neurol,* 9**,** 617-28.

AL-SAIF, A., AL-MOHANNA, F. & BOHLEGA, S. 2011. A mutation in sigma-1 receptor causes juvenile amyotrophic lateral sclerosis. *Ann Neurol,* 70**,** 913-9.

ALAMI, N. H., SMITH, R. B., CARRASCO, M. A., WILLIAMS, L. A., WINBORN, C. S., HAN, S. S., KISKINIS, E., WINBORN, B., FREIBAUM, B. D., KANAGARAJ, A., CLARE, A. J., BADDERS, N. M., BILICAN, B., CHAUM, E., CHANDRAN, S., SHAW, C. E., EGGAN, K. C., MANIATIS, T. & TAYLOR, J. P. 2014. Axonal transport of TDP-43 mRNA granules is impaired by ALS-causing mutations. *Neuron,* 81**,** 536-43.

ALVES-RODRIGUES, A., GREGORI, L. & FIGUEIREDO-PEREIRA, M. E. 1998. Ubiquitin, cellular inclusions and their role in neurodegeneration. *Trends Neurosci,* 21**,** 516-20.

AMADOR-ORTIZ, C., LIN, W. L., AHMED, Z., PERSONETT, D., DAVIES, P., DUARA, R., GRAFF-RADFORD, N. R., HUTTON, M. L. & DICKSON, D. W. 2007. TDP-43 immunoreactivity in hippocampal sclerosis and Alzheimer's disease. *Ann Neurol,* 61**,** 435-45.

ANDERSEN, P. M., NILSSON, P., ALA-HURULA, V., KERANEN, M. L., TARVAINEN, I., HALTIA, T., NILSSON, L., BINZER, M., FORSGREN, L. & MARKLUND, S. L. 1995. Amyotrophic lateral sclerosis associated with homozygosity for an Asp90Ala mutation in CuZn-superoxide dismutase. *Nat Genet,* 10**,** 61-6.

ANDERSON, P. & KEDERSHA, N. 2006. RNA granules. *J Cell Biol,* 172**,** 803-8.

ANDERSON, P. & KEDERSHA, N. 2008. Stress granules: the Tao of RNA triage. *Trends Biochem Sci,* 33**,** 141-50.

AOKI, N., HIGASHI, S., KAWAKAMI, I., KOBAYASHI, Z., HOSOKAWA, M., KATSUSE, O., TOGO, T., HIRAYASU, Y. & AKIYAMA, H. 2012. Localization of fused in sarcoma (FUS) protein to the post-synaptic density in the brain. *Acta Neuropathol,* 124**,** 383-94.

ARAI, T., HASEGAWA, M., AKIYAMA, H., IKEDA, K., NONAKA, T., MORI, H., MANN, D., TSUCHIYA, K., YOSHIDA, M., HASHIZUME, Y. & ODA, T. 2006. TDP-43 is a component of ubiquitin-positive tau-negative inclusions in frontotemporal lobar degeneration and amyotrophic lateral sclerosis. *Biochem Biophys Res Commun,* 351**,** 602-11.

ARMSTRONG, G. A. & DRAPEAU, P. 2013. Loss and gain of FUS function impair neuromuscular synaptic transmission in a genetic model of ALS. *Hum Mol Genet,* 22**,** 4282-92.

ARNOLD, E. S., LING, S. C., HUELGA, S. C., LAGIER-TOURENNE, C., POLYMENIDOU, M., DITSWORTH, D., KORDASIEWICZ, H. B., MCALONIS-DOWNES, M., PLATOSHYN, O., PARONE, P. A., DA CRUZ, S., CLUTARIO, K. M., SWING, D., TESSAROLLO, L., MARSALA, M., SHAW, C. E., YEO, G. W. & CLEVELAND, D. W. 2013. ALS-linked TDP-43 mutations produce aberrant RNA splicing and adult-onset motor neuron disease without aggregation or loss of nuclear TDP-43. *Proc Natl Acad Sci U S A,* 110**,** E736-45.

AYALA, Y. M., DE CONTI, L., AVENDANO-VAZQUEZ, S. E., DHIR, A., ROMANO, M., D'AMBROGIO, A., TOLLERVEY, J., ULE, J., BARALLE, M., BURATTI, E. &

BARALLE, F. E. 2011. TDP-43 regulates its mRNA levels through a negative feedback loop. *EMBO J,* 30**,** 277-88.

AYALA, Y. M., ZAGO, P., D'AMBROGIO, A., XU, Y. F., PETRUCELLI, L., BURATTI, E. & BARALLE, F. E. 2008. Structural determinants of the cellular localization and shuttling of TDP-43. *J Cell Sci,* 121**,** 3778-85.

BAECHTOLD, H., KURODA, M., SOK, J., RON, D., LOPEZ, B. S. & AKHMEDOV, A. T. 1999. Human 75-kDa DNA-pairing protein is identical to the pro-oncoprotein TLS/FUS and is able to promote D-loop formation. *J Biol Chem,* 274**,** 34337-42.

BANNWARTH, S., AIT-EL-MKADEM, S., CHAUSSENOT, A., GENIN, E. C., LACAS-GERVAIS, S., FRAGAKI, K., BERG-ALONSO, L., KAGEYAMA, Y., SERRE, V., MOORE, D. G., VERSCHUEREN, A., ROUZIER, C., LE BER, I., AUGE, G., COCHAUD, C., LESPINASSE, F., N'GUYEN, K., DE SEPTENVILLE, A., BRICE, A., YU-WAI-MAN, P., SESAKI, H., POUGET, J. & PAQUIS-FLUCKLINGER, V. 2014. A mitochondrial origin for frontotemporal dementia and amyotrophic lateral sclerosis through CHCHD10 involvement. *Brain,* 137**,** 2329-45.

BARBER, S. C. & SHAW, P. J. 2010. Oxidative stress in ALS: key role in motor neuron injury and therapeutic target. *Free Radic Biol Med,* 48**,** 629-41.

BARMADA, S. J., SKIBINSKI, G., KORB, E., RAO, E. J., WU, J. Y. & FINKBEINER, S. 2010. Cytoplasmic mislocalization of TDP-43 is toxic to neurons and enhanced by a mutation associated with familial amyotrophic lateral sclerosis. *J Neurosci,* 30**,** 639-49.

BARON, D. M., KAUSHANSKY, L. J., WARD, C. L., SAMA, R. R., CHIAN, R. J., BOGGIO, K. J., QUARESMA, A. J., NICKERSON, J. A. & BOSCO, D. A. 2013. Amyotrophic lateral sclerosis-linked FUS/TLS alters stress granule assembly and dynamics. *Mol Neurodegener,* 8**,** 30.

BAUMER, D., HILTON, D., PAINE, S. M., TURNER, M. R., LOWE, J., TALBOT, K. & ANSORGE, O. 2010. Juvenile ALS with basophilic inclusions is a FUS proteinopathy with FUS mutations. *Neurology,* 75**,** 611-8.

BECK, J., POULTER, M., HENSMAN, D., ROHRER, J. D., MAHONEY, C. J., ADAMSON, G., CAMPBELL, T., UPHILL, J., BORG, A., FRATTA, P., ORRELL, R. W., MALASPINA, A., ROWE, J., BROWN, J., HODGES, J., SIDLE, K., POLKE, J. M., HOULDEN, H., SCHOTT, J. M., FOX, N. C., ROSSOR, M. N., TABRIZI, S. J., ISAACS, A. M., HARDY, J., WARREN, J. D., COLLINGE, J. & MEAD, S. 2013. Large C9orf72 hexanucleotide repeat expansions are seen in multiple neurodegenerative syndromes and are more frequent than expected in the UK population. *Am J Hum Genet,* 92**,** 345-53.

BELLY, A., MOREAU-GACHELIN, F., SADOUL, R. & GOLDBERG, Y. 2005. Delocalization of the multifunctional RNA splicing factor TLS/FUS in hippocampal neurones: exclusion from the nucleus and accumulation in dendritic granules and spine heads. *Neurosci Lett,* 379**,** 152-7.

BELZIL, V. V., BAUER, P. O., PRUDENCIO, M., GENDRON, T. F., STETLER, C. T., YAN, I. K., PREGENT, L., DAUGHRITY, L., BAKER, M. C., RADEMAKERS, R., BOYLAN, K., PATEL, T. C., DICKSON, D. W. & PETRUCELLI, L. 2013. Reduced C9orf72 gene expression in c9FTD/ALS is caused by histone trimethylation, an epigenetic event detectable in blood. *Acta Neuropathol,* 126**,** 895-905.

BENSIMON, G., LACOMBLEZ, L. & MEININGER, V. 1994. A controlled trial of riluzole in amyotrophic lateral sclerosis. ALS/Riluzole Study Group. *N Engl J Med,* 330**,** 585-91.

BENTMANN, E., NEUMANN, M., TAHIROVIC, S., RODDE, R., DORMANN, D. & HAASS, C. 2012. Requirements for stress granule recruitment of fused in

sarcoma (FUS) and TAR DNA-binding protein of 43 kDa (TDP-43). *J Biol Chem,* 287**,** 23079-94.

BERTOLOTTI, A., LUTZ, Y., HEARD, D. J., CHAMBON, P. & TORA, L. 1996. hTAF(II)68, a novel RNA/ssDNA-binding protein with homology to the pro-oncoproteins TLS/FUS and EWS is associated with both TFIID and RNA polymerase II. *EMBO J,* 15**,** 5022-31.

BIENIOSSEK, C., PAPAI, G., SCHAFFITZEL, C., GARZONI, F., CHAILLET, M., SCHEER, E., PAPADOPOULOS, P., TORA, L., SCHULTZ, P. & BERGER, I. 2013. The architecture of human general transcription factor TFIID core complex. *Nature,* 493**,** 699-702.

BLACKHALL, L. J. 2012. Amyotrophic lateral sclerosis and palliative care: where we are, and the road ahead. *Muscle Nerve,* 45**,** 311-8.

BLAIR, I. P., WILLIAMS, K. L., WARRAICH, S. T., DURNALL, J. C., THOENG, A. D., MANAVIS, J., BLUMBERGS, P. C., VUCIC, S., KIERNAN, M. C. & NICHOLSON, G. A. 2010. FUS mutations in amyotrophic lateral sclerosis: clinical, pathological, neurophysiological and genetic analysis. *J Neurol Neurosurg Psychiatry,* 81**,** 639-45.

BOGDANOV, M., BROWN, R. H., MATSON, W., SMART, R., HAYDEN, D., O'DONNELL, H., FLINT BEAL, M. & CUDKOWICZ, M. 2000. Increased oxidative damage to DNA in ALS patients. *Free Radic Biol Med,* 29**,** 652-8.

BOLHUIS, S. & RICHTER-LANDSBERG, C. 2010. Effect of proteasome inhibition by MG-132 on HSP27 oligomerization, phosphorylation, and aggresome formation in the OLN-93 oligodendroglia cell line. *J Neurochem,* 114**,** 960-71.

BORRONI, B., BONVICINI, C., ALBERICI, A., BURATTI, E., AGOSTI, C., ARCHETTI, S., PAPETTI, A., STUANI, C., DI LUCA, M., GENNARELLI, M. & PADOVANI, A. 2009. Mutation within TARDBP leads to frontotemporal dementia without motor neuron disease. *Hum Mutat,* 30**,** E974-83.

BOSCO, D. A., LEMAY, N., KO, H. K., ZHOU, H., BURKE, C., KWIATKOWSKI, T. J., JR., SAPP, P., MCKENNA-YASEK, D., BROWN, R. H., JR. & HAYWARD, L. J. 2010. Mutant FUS proteins that cause amyotrophic lateral sclerosis incorporate into stress granules. *Hum Mol Genet,* 19**,** 4160-75.

BOUNEDJAH, O., DESFORGES, B., WU, T. D., PIOCHE-DURIEU, C., MARCO, S., HAMON, L., CURMI, P. A., GUERQUIN-KERN, J. L., PIETREMENT, O. & PASTRE, D. 2014. Free mRNA in excess upon polysome dissociation is a scaffold for protein multimerization to form stress granules. *Nucleic Acids Res,* 42**,** 8678-91.

BRADY, O. A., MENG, P., ZHENG, Y., MAO, Y. & HU, F. 2011. Regulation of TDP-43 aggregation by phosphorylation and p62/SQSTM1. *J Neurochem,* 116**,** 248-59.

BRAINCONNECTION.COM. 2014. Available: http://www.brainconnection.com.

BROOKS, B. R. 1994. El Escorial World Federation of Neurology criteria for the diagnosis of amyotrophic lateral sclerosis. Subcommittee on Motor Neuron Diseases/Amyotrophic Lateral Sclerosis of the World Federation of Neurology Research Group on Neuromuscular Diseases and the El Escorial "Clinical limits of amyotrophic lateral sclerosis" workshop contributors. *J Neurol Sci,* 124 Suppl**,** 96-107.

BRUIJN, L. I., BECHER, M. W., LEE, M. K., ANDERSON, K. L., JENKINS, N. A., COPELAND, N. G., SISODIA, S. S., ROTHSTEIN, J. D., BORCHELT, D. R., PRICE, D. L. & CLEVELAND, D. W. 1997. ALS-linked SOD1 mutant G85R mediates damage to astrocytes and promotes rapidly progressive disease with SOD1-containing inclusions. *Neuron,* 18**,** 327-38.

BRUIJN, L. I., HOUSEWEART, M. K., KATO, S., ANDERSON, K. L., ANDERSON, S. D., OHAMA, E., REAUME, A. G., SCOTT, R. W. & CLEVELAND, D. W. 1998.

Aggregation and motor neuron toxicity of an ALS-linked SOD1 mutant independent from wild-type SOD1. *Science,* 281**,** 1851-4.

BUCHAN, J. R. & PARKER, R. 2009. Eukaryotic stress granules: the ins and outs of translation. *Mol Cell,* 36**,** 932-41.

BUNINA, T. L. 1962. [On intracellular inclusions in familial amyotrophic lateral sclerosis]. *Zh Nevropatol Psikhiatr Im S S Korsakova,* 62**,** 1293-9.

BURATTI, E. & BARALLE, F. E. 2001. Characterization and functional implications of the RNA binding properties of nuclear factor TDP-43, a novel splicing regulator of CFTR exon 9. *J Biol Chem,* 276**,** 36337-43.

CELLURA, E., SPATARO, R., TAIELLO, A. C. & LA BELLA, V. 2012. Factors affecting the diagnostic delay in amyotrophic lateral sclerosis. *Clin Neurol Neurosurg,* 114**,** 550-4.

CHEN, H., QIAN, K., DU, Z., CAO, J., PETERSEN, A., LIU, H., BLACKBOURN, L. W. T., HUANG, C. L., ERRIGO, A., YIN, Y., LU, J., AYALA, M. & ZHANG, S. C. 2014. Modeling ALS with iPSCs reveals that mutant SOD1 misregulates neurofilament balance in motor neurons. *Cell Stem Cell,* 14**,** 796-809.

CHEN, L. L. & CARMICHAEL, G. G. 2009. Altered nuclear retention of mRNAs containing inverted repeats in human embryonic stem cells: functional role of a nuclear noncoding RNA. *Mol Cell,* 35**,** 467-78.

CHEN, S., SAYANA, P., ZHANG, X. & LE, W. 2013. Genetics of amyotrophic lateral sclerosis: an update. *Mol Neurodegener,* 8**,** 28.

CHEN, Y., YANG, M., DENG, J., CHEN, X., YE, Y., ZHU, L., LIU, J., YE, H., SHEN, Y., LI, Y., RAO, E. J., FUSHIMI, K., ZHOU, X., BIGIO, E. H., MESULAM, M., XU, Q. & WU, J. Y. 2011. Expression of human FUS protein in Drosophila leads to progressive neurodegeneration. *Protein Cell,* 2**,** 477-86.

CHEN, Y. Z., BENNETT, C. L., HUYNH, H. M., BLAIR, I. P., PULS, I., IROBI, J., DIERICK, I., ABEL, A., KENNERSON, M. L., RABIN, B. A., NICHOLSON, G. A., AUER-GRUMBACH, M., WAGNER, K., DE JONGHE, P., GRIFFIN, J. W., FISCHBECK, K. H., TIMMERMAN, V., CORNBLATH, D. R. & CHANCE, P. F. 2004. DNA/RNA helicase gene mutations in a form of juvenile amyotrophic lateral sclerosis (ALS4). *Am J Hum Genet,* 74**,** 1128-35.

CHESI, A., STAAHL, B. T., JOVICIC, A., COUTHOUIS, J., FASOLINO, M., RAPHAEL, A. R., YAMAZAKI, T., ELIAS, L., POLAK, M., KELLY, C., WILLIAMS, K. L., FIFITA, J. A., MARAGAKIS, N. J., NICHOLSON, G. A., KING, O. D., REED, R., CRABTREE, G. R., BLAIR, I. P., GLASS, J. D. & GITLER, A. D. 2013. Exome sequencing to identify de novo mutations in sporadic ALS trios. *Nat Neurosci,* 16**,** 851-5.

CHIANG, P. M., LING, J., JEONG, Y. H., PRICE, D. L., AJA, S. M. & WONG, P. C. 2010. Deletion of TDP-43 down-regulates Tbc1d1, a gene linked to obesity, and alters body fat metabolism. *Proc Natl Acad Sci U S A,* 107**,** 16320-4.

CHOW, C. Y., LANDERS, J. E., BERGREN, S. K., SAPP, P. C., GRANT, A. E., JONES, J. M., EVERETT, L., LENK, G. M., MCKENNA-YASEK, D. M., WEISMAN, L. S., FIGLEWICZ, D., BROWN, R. H. & MEISLER, M. H. 2009. Deleterious variants of FIG4, a phosphoinositide phosphatase, in patients with ALS. *Am J Hum Genet,* 84**,** 85-8.

CIRULLI, E. T., LASSEIGNE, B. N., PETROVSKI, S., SAPP, P. C., DION, P. A., LEBLOND, C. S., COUTHOUIS, J., LU, Y. F., WANG, Q., KRUEGER, B. J., REN, Z., KEEBLER, J., HAN, Y., LEVY, S. E., BOONE, B. E., WIMBISH, J. R., WAITE, L. L., JONES, A. L., CARULLI, J. P., DAY-WILLIAMS, A. G., STAROPOLI, J. F., XIN, W. W., CHESI, A., RAPHAEL, A. R., MCKENNA-YASEK, D., CADY, J., VIANNEY DE JONG, J. M., KENNA, K. P., SMITH, B. N., TOPP, S., MILLER, J., GKAZI, A., CONSORTIUM, F. S., AL-CHALABI, A., VAN

DEN BERG, L. H., VELDINK, J., SILANI, V., TICOZZI, N., SHAW, C. E., BALOH, R. H., APPEL, S., SIMPSON, E., LAGIER-TOURENNE, C., PULST, S. M., GIBSON, S., TROJANOWSKI, J. Q., ELMAN, L., MCCLUSKEY, L., GROSSMAN, M., SHNEIDER, N. A., CHUNG, W. K., RAVITS, J. M., GLASS, J. D., SIMS, K. B., VAN DEERLIN, V. M., MANIATIS, T., HAYES, S. D., ORDUREAU, A., SWARUP, S., LANDERS, J., BAAS, F., ALLEN, A. S., BEDLACK, R. S., HARPER, J. W., GITLER, A. D., ROULEAU, G. A., BROWN, R., HARMS, M. B., COOPER, G. M., HARRIS, T., MYERS, R. M. & GOLDSTEIN, D. B. 2015. Exome sequencing in amyotrophic lateral sclerosis identifies risk genes and pathways. *Science,* 347**,** 1436-1441.

CIURA, S., LATTANTE, S., LE BER, I., LATOUCHE, M., TOSTIVINT, H., BRICE, A. & KABASHI, E. 2013. Loss of function of C9orf72 causes motor deficits in a zebrafish model of amyotrophic lateral sclerosis. *Ann Neurol,* 74**,** 180-7.

CLAVAGUERA, F., AKATSU, H., FRASER, G., CROWTHER, R. A., FRANK, S., HENCH, J., PROBST, A., WINKLER, D. T., REICHWALD, J., STAUFENBIEL, M., GHETTI, B., GOEDERT, M. & TOLNAY, M. 2013. Brain homogenates from human tauopathies induce tau inclusions in mouse brain. *Proc Natl Acad Sci U S A,* 110**,** 9535-40.

CLEMSON, C. M., HUTCHINSON, J. N., SARA, S. A., ENSMINGER, A. W., FOX, A. H., CHESS, A. & LAWRENCE, J. B. 2009. An architectural role for a nuclear noncoding RNA: NEAT1 RNA is essential for the structure of paraspeckles. *Mol Cell,* 33**,** 717-26.

CLERY, A., BLATTER, M. & ALLAIN, F. H. 2008. RNA recognition motifs: boring? Not quite. *Curr Opin Struct Biol,* 18**,** 290-8.

CLEVELAND, D. W. 1999. From Charcot to SOD1: mechanisms of selective motor neuron death in ALS. *Neuron,* 24**,** 515-20.

CLEVELAND, D. W. & ROTHSTEIN, J. D. 2001. From Charcot to Lou Gehrig: deciphering selective motor neuron death in ALS. *Nat Rev Neurosci,* 2**,** 806-19.

COLEMAN, M. 2005. Axon degeneration mechanisms: commonality amid diversity. *Nat Rev Neurosci,* 6**,** 889-98.

COLLINGE, J. 2001. Prion diseases of humans and animals: their causes and molecular basis. *Annu Rev Neurosci,* 24**,** 519-50.

COLOMBRITA, C., ONESTO, E., MEGIORNI, F., PIZZUTI, A., BARALLE, F. E., BURATTI, E., SILANI, V. & RATTI, A. 2012. TDP-43 and FUS RNA-binding proteins bind distinct sets of cytoplasmic messenger RNAs and differently regulate their post-transcriptional fate in motoneuron-like cells. *J Biol Chem,* 287**,** 15635-47.

COLOMBRITA, C., ZENNARO, E., FALLINI, C., WEBER, M., SOMMACAL, A., BURATTI, E., SILANI, V. & RATTI, A. 2009. TDP-43 is recruited to stress granules in conditions of oxidative insult. *J Neurochem,* 111**,** 1051-61.

COLTON, C. A., ABEL, C., PATCHETT, J., KERI, J. & YAO, J. 1992. Lectin staining of cultured CNS microglia. *J Histochem Cytochem,* 40**,** 505-12.

COOPER-KNOCK, J., HEWITT, C., HIGHLEY, J. R., BROCKINGTON, A., MILANO, A., MAN, S., MARTINDALE, J., HARTLEY, J., WALSH, T., GELSTHORPE, C., BAXTER, L., FORSTER, G., FOX, M., BURY, J., MOK, K., MCDERMOTT, C. J., TRAYNOR, B. J., KIRBY, J., WHARTON, S. B., INCE, P. G., HARDY, J. & SHAW, P. J. 2012. Clinico-pathological features in amyotrophic lateral sclerosis with expansions in C9ORF72. *Brain,* 135**,** 751-64.

COOPER-KNOCK, J., HIGGINBOTTOM, A., CONNOR-ROBSON, N., BAYATTI, N., BURY, J. J., KIRBY, J., NINKINA, N., BUCHMAN, V. L. & SHAW, P. J. 2013. C9ORF72 transcription in a frontotemporal dementia case with two expanded alleles. *Neurology,* 81**,** 1719-21.

COOPER-KNOCK, J., WALSH, M. J., HIGGINBOTTOM, A., ROBIN HIGHLEY, J., DICKMAN, M. J., EDBAUER, D., INCE, P. G., WHARTON, S. B., WILSON, S. A., KIRBY, J., HAUTBERGUE, G. M. & SHAW, P. J. 2014. Sequestration of multiple RNA recognition motif-containing proteins by C9orf72 repeat expansions. *Brain,* 137**,** 2040-51.

CORBO, M. & HAYS, A. P. 1992. Peripherin and neurofilament protein coexist in spinal spheroids of motor neuron disease. *J Neuropathol Exp Neurol,* 51**,** 531-7.

CORCIA, P., VALDMANIS, P., MILLECAMPS, S., LIONNET, C., BLASCO, H., MOUZAT, K., DAOUD, H., BELZIL, V., MORALES, R., PAGEOT, N., DANEL-BRUNAUD, V., VANDENBERGHE, N., PRADAT, P. F., COURATIER, P., SALACHAS, F., LUMBROSO, S., ROULEAU, G. A., MEININGER, V. & CAMU, W. 2012. Phenotype and genotype analysis in amyotrophic lateral sclerosis with TARDBP gene mutations. *Neurology,* 78**,** 1519-26.

COUTHOUIS, J., HART, M. P., SHORTER, J., DEJESUS-HERNANDEZ, M., ERION, R., ORISTANO, R., LIU, A. X., RAMOS, D., JETHAVA, N., HOSANGADI, D., EPSTEIN, J., CHIANG, A., DIAZ, Z., NAKAYA, T., IBRAHIM, F., KIM, H. J., SOLSKI, J. A., WILLIAMS, K. L., MOJSILOVIC-PETROVIC, J., INGRE, C., BOYLAN, K., GRAFF-RADFORD, N. R., DICKSON, D. W., CLAY-FALCONE, D., ELMAN, L., MCCLUSKEY, L., GREENE, R., KALB, R. G., LEE, V. M., TROJANOWSKI, J. Q., LUDOLPH, A., ROBBERECHT, W., ANDERSEN, P. M., NICHOLSON, G. A., BLAIR, I. P., KING, O. D., BONINI, N. M., VAN DEERLIN, V., RADEMAKERS, R., MOURELATOS, Z. & GITLER, A. D. 2011. A yeast functional screen predicts new candidate ALS disease genes. *Proc Natl Acad Sci U S A,* 108**,** 20881-90.

CROZAT, A., AMAN, P., MANDAHL, N. & RON, D. 1993. Fusion of CHOP to a novel RNA-binding protein in human myxoid liposarcoma. *Nature,* 363**,** 640-4.

CUDKOWICZ, M. E., MCKENNA-YASEK, D., SAPP, P. E., CHIN, W., GELLER, B., HAYDEN, D. L., SCHOENFELD, D. A., HOSLER, B. A., HORVITZ, H. R. & BROWN, R. H. 1997. Epidemiology of mutations in superoxide dismutase in amyotrophic lateral sclerosis. *Ann Neurol,* 41**,** 210-21.

CUSHMAN, M., JOHNSON, B. S., KING, O. D., GITLER, A. D. & SHORTER, J. 2010. Prion-like disorders: blurring the divide between transmissibility and infectivity. *J Cell Sci,* 123**,** 1191-201.

DAIGLE, J. G., LANSON, N. A., JR., SMITH, R. B., CASCI, I., MALTARE, A., MONAGHAN, J., NICHOLS, C. D., KRYNDUSHKIN, D., SHEWMAKER, F. & PANDEY, U. B. 2013. RNA-binding ability of FUS regulates neurodegeneration, cytoplasmic mislocalization and incorporation into stress granules associated with FUS carrying ALS-linked mutations. *Hum Mol Genet,* 22**,** 1193-205.

DAMMER, E. B., FALLINI, C., GOZAL, Y. M., DUONG, D. M., ROSSOLL, W., XU, P., LAH, J. J., LEVEY, A. I., PENG, J., BASSELL, G. J. & SEYFRIED, N. T. 2012. Coaggregation of RNA-binding proteins in a model of TDP-43 proteinopathy with selective RGG motif methylation and a role for RRM1 ubiquitination. *PLoS One,* 7**,** e38658.

DAS, R., YU, J., ZHANG, Z., GYGI, M. P., KRAINER, A. R., GYGI, S. P. & REED, R. 2007. SR proteins function in coupling RNAP II transcription to pre-mRNA splicing. *Mol Cell,* 26**,** 867-81.

DE CARVALHO, M., DENGLER, R., EISEN, A., ENGLAND, J. D., KAJI, R., KIMURA, J., MILLS, K., MITSUMOTO, H., NODERA, H., SHEFNER, J. & SWASH, M. 2008. Electrodiagnostic criteria for diagnosis of ALS. *Clin Neurophysiol,* 119**,** 497-503.

DE VOS, K. J., CHAPMAN, A. L., TENNANT, M. E., MANSER, C., TUDOR, E. L., LAU, K. F., BROWNLEES, J., ACKERLEY, S., SHAW, P. J., MCLOUGHLIN, D. M., SHAW, C. E., LEIGH, P. N., MILLER, C. C. & GRIERSON, A. J. 2007. Familial amyotrophic lateral sclerosis-linked SOD1 mutants perturb fast axonal transport to reduce axonal mitochondria content. *Hum Mol Genet,* 16**,** 2720-8.

DEJESUS-HERNANDEZ, M., KOCERHA, J., FINCH, N., CROOK, R., BAKER, M., DESARO, P., JOHNSTON, A., RUTHERFORD, N., WOJTAS, A., KENNELLY, K., WSZOLEK, Z. K., GRAFF-RADFORD, N., BOYLAN, K. & RADEMAKERS, R. 2010. De novo truncating FUS gene mutation as a cause of sporadic amyotrophic lateral sclerosis. *Hum Mutat,* 31**,** E1377-89.

DEJESUS-HERNANDEZ, M., MACKENZIE, I. R., BOEVE, B. F., BOXER, A. L., BAKER, M., RUTHERFORD, N. J., NICHOLSON, A. M., FINCH, N. A., FLYNN, H., ADAMSON, J., KOURI, N., WOJTAS, A., SENGDY, P., HSIUNG, G. Y., KARYDAS, A., SEELEY, W. W., JOSEPHS, K. A., COPPOLA, G., GESCHWIND, D. H., WSZOLEK, Z. K., FELDMAN, H., KNOPMAN, D. S., PETERSEN, R. C., MILLER, B. L., DICKSON, D. W., BOYLAN, K. B., GRAFF-RADFORD, N. R. & RADEMAKERS, R. 2011. Expanded GGGGCC hexanucleotide repeat in noncoding region of C9ORF72 causes chromosome 9p-linked FTD and ALS. *Neuron,* 72**,** 245-56.

DENG, H. X., CHEN, W., HONG, S. T., BOYCOTT, K. M., GORRIE, G. H., SIDDIQUE, N., YANG, Y., FECTO, F., SHI, Y., ZHAI, H., JIANG, H., HIRANO, M., RAMPERSAUD, E., JANSEN, G. H., DONKERVOORT, S., BIGIO, E. H., BROOKS, B. R., AJROUD, K., SUFIT, R. L., HAINES, J. L., MUGNAINI, E., PERICAK-VANCE, M. A. & SIDDIQUE, T. 2011. Mutations in UBQLN2 cause dominant X-linked juvenile and adult-onset ALS and ALS/dementia. *Nature,* 477**,** 211-5.

DENG, H. X., ZHAI, H., BIGIO, E. H., YAN, J., FECTO, F., AJROUD, K., MISHRA, M., AJROUD-DRISS, S., HELLER, S., SUFIT, R., SIDDIQUE, N., MUGNAINI, E. & SIDDIQUE, T. 2010. FUS-immunoreactive inclusions are a common feature in sporadic and non-SOD1 familial amyotrophic lateral sclerosis. *Ann Neurol,* 67**,** 739-48.

DENG, Q., HOLLER, C. J., TAYLOR, G., HUDSON, K. F., WATKINS, W., GEARING, M., ITO, D., MURRAY, M. E., DICKSON, D. W., SEYFRIED, N. T. & KUKAR, T. 2014. FUS is phosphorylated by DNA-PK and accumulates in the cytoplasm after DNA damage. *J Neurosci,* 34**,** 7802-13.

DEPAUL, R., ABBS, J. H., CALIGIURI, M., GRACCO, V. L. & BROOKS, B. R. 1988. Hypoglossal, trigeminal, and facial motoneuron involvement in amyotrophic lateral sclerosis. *Neurology,* 38**,** 281-3.

DEWEY, C. M., CENIK, B., SEPHTON, C. F., DRIES, D. R., MAYER, P., 3RD, GOOD, S. K., JOHNSON, B. A., HERZ, J. & YU, G. 2011. TDP-43 is directed to stress granules by sorbitol, a novel physiological osmotic and oxidative stressor. *Mol Cell Biol,* 31**,** 1098-108.

DEWEY, C. M., CENIK, B., SEPHTON, C. F., JOHNSON, B. A., HERZ, J. & YU, G. 2012. TDP-43 aggregation in neurodegeneration: are stress granules the key? *Brain Res,* 1462**,** 16-25.

DOI, H., KOYANO, S., SUZUKI, Y., NUKINA, N. & KUROIWA, Y. 2010. The RNA-binding protein FUS/TLS is a common aggregate-interacting protein in polyglutamine diseases. *Neurosci Res,* 66**,** 131-3.

DOI, H., OKAMURA, K., BAUER, P. O., FURUKAWA, Y., SHIMIZU, H., KUROSAWA, M., MACHIDA, Y., MIYAZAKI, H., MITSUI, K., KUROIWA, Y. & NUKINA, N. 2008. RNA-binding protein TLS is a major nuclear aggregate-interacting

protein in huntingtin exon 1 with expanded polyglutamine-expressing cells. *J Biol Chem,* 283**,** 6489-500.

DORMANN, D. & HAASS, C. 2011. TDP-43 and FUS: a nuclear affair. *Trends Neurosci,* 34**,** 339-48.

DORMANN, D., MADL, T., VALORI, C. F., BENTMANN, E., TAHIROVIC, S., ABOU-AJRAM, C., KREMMER, E., ANSORGE, O., MACKENZIE, I. R., NEUMANN, M. & HAASS, C. 2012. Arginine methylation next to the PY-NLS modulates Transportin binding and nuclear import of FUS. *EMBO J,* 31**,** 4258-75.

DORMANN, D., RODDE, R., EDBAUER, D., BENTMANN, E., FISCHER, I., HRUSCHA, A., THAN, M. E., MACKENZIE, I. R., CAPELL, A., SCHMID, B., NEUMANN, M. & HAASS, C. 2010. ALS-associated fused in sarcoma (FUS) mutations disrupt Transportin-mediated nuclear import. *EMBO J,* 29**,** 2841-57.

DOUGLASS, C. P., KANDLER, R. H., SHAW, P. J. & MCDERMOTT, C. J. 2010. An evaluation of neurophysiological criteria used in the diagnosis of motor neuron disease. *J Neurol Neurosurg Psychiatry,* 81**,** 646-9.

DROPPELMANN, C. A., CAMPOS-MELO, D., ISHTIAQ, M., VOLKENING, K. & STRONG, M. J. 2014. RNA metabolism in ALS: when normal processes become pathological. *Amyotroph Lateral Scler Frontotemporal Degener,* 15**,** 321-36.

DUNDR, M. & MISTELI, T. 2001. Functional architecture in the cell nucleus. *Biochem J,* 356**,** 297-310.

ELBASHIR, S. M., HARBORTH, J., LENDECKEL, W., YALCIN, A., WEBER, K. & TUSCHL, T. 2001. Duplexes of 21-nucleotide RNAs mediate RNA interference in cultured mammalian cells. *Nature,* 411**,** 494-8.

EMILI, A., SHALES, M., MCCRACKEN, S., XIE, W., TUCKER, P. W., KOBAYASHI, R., BLENCOWE, B. J. & INGLES, C. J. 2002. Splicing and transcription-associated proteins PSF and p54nrb/nonO bind to the RNA polymerase II CTD. *RNA,* 8**,** 1102-11.

FARG, M. A., SUNDARAMOORTHY, V., SULTANA, J. M., YANG, S., ATKINSON, R. A., LEVINA, V., HALLORAN, M. A., GLEESON, P. A., BLAIR, I. P., SOO, K. Y., KING, A. E. & ATKIN, J. D. 2014. C9ORF72, implicated in amytrophic lateral sclerosis and frontotemporal dementia, regulates endosomal trafficking. *Hum Mol Genet,* 23**,** 3579-95.

FECTO, F., YAN, J., VEMULA, S. P., LIU, E., YANG, Y., CHEN, W., ZHENG, J. G., SHI, Y., SIDDIQUE, N., ARRAT, H., DONKERVOORT, S., AJROUD-DRISS, S., SUFIT, R. L., HELLER, S. L., DENG, H. X. & SIDDIQUE, T. 2011. SQSTM1 mutations in familial and sporadic amyotrophic lateral sclerosis. *Arch Neurol,* 68**,** 1440-6.

FERRAIUOLO, L., KIRBY, J., GRIERSON, A. J., SENDTNER, M. & SHAW, P. J. 2011. Molecular pathways of motor neuron injury in amyotrophic lateral sclerosis. *Nat Rev Neurol,* 7**,** 616-30.

FISCHER, L. R., CULVER, D. G., TENNANT, P., DAVIS, A. A., WANG, M., CASTELLANO-SANCHEZ, A., KHAN, J., POLAK, M. A. & GLASS, J. D. 2004. Amyotrophic lateral sclerosis is a distal axonopathy: evidence in mice and man. *Exp Neurol,* 185**,** 232-40.

FISCHER, U., LIU, Q. & DREYFUSS, G. 1997. The SMN-SIP1 complex has an essential role in spliceosomal snRNP biogenesis. *Cell,* 90**,** 1023-9.

FORSBERG, K., JONSSON, P. A., ANDERSEN, P. M., BERGEMALM, D., GRAFFMO, K. S., HULTDIN, M., JACOBSSON, J., ROSQUIST, R., MARKLUND, S. L. & BRANNSTROM, T. 2010. Novel antibodies reveal inclusions containing non-native SOD1 in sporadic ALS patients. *PLoS One,* 5**,** e11552.

FOX, A. H., LAM, Y. W., LEUNG, A. K., LYON, C. E., ANDERSEN, J., MANN, M. & LAMOND, A. I. 2002. Paraspeckles: a novel nuclear domain. *Curr Biol,* 12**,** 13-25.

FOX, A. H. & LAMOND, A. I. 2010. Paraspeckles. *Cold Spring Harb Perspect Biol,* 2**,** a000687.

FREISCHMIDT, A., WIELAND, T., RICHTER, B., RUF, W., SCHAEFFER, V., MULLER, K., MARROQUIN, N., NORDIN, F., HUBERS, A., WEYDT, P., PINTO, S., PRESS, R., MILLECAMPS, S., MOLKO, N., BERNARD, E., DESNUELLE, C., SORIANI, M. H., DORST, J., GRAF, E., NORDSTROM, U., FEILER, M. S., PUTZ, S., BOECKERS, T. M., MEYER, T., WINKLER, A. S., WINKELMAN, J., DE CARVALHO, M., THAL, D. R., OTTO, M., BRANNSTROM, T., VOLK, A. E., KURSULA, P., DANZER, K. M., LICHTNER, P., DIKIC, I., MEITINGER, T., LUDOLPH, A. C., STROM, T. M., ANDERSEN, P. M. & WEISHAUPT, J. H. 2015. Haploinsufficiency of TBK1 causes familial ALS and fronto-temporal dementia. *Nat Neurosci*.

FRITH, M. C., PHEASANT, M. & MATTICK, J. S. 2005. The amazing complexity of the human transcriptome. *Eur J Hum Genet,* 13**,** 894-7.

FUJII, R., OKABE, S., URUSHIDO, T., INOUE, K., YOSHIMURA, A., TACHIBANA, T., NISHIKAWA, T., HICKS, G. G. & TAKUMI, T. 2005. The RNA binding protein TLS is translocated to dendritic spines by mGluR5 activation and regulates spine morphology. *Curr Biol,* 15**,** 587-93.

FUJII, R. & TAKUMI, T. 2005. TLS facilitates transport of mRNA encoding an actin-stabilizing protein to dendritic spines. *J Cell Sci,* 118**,** 5755-65.

FUJIOKA, Y., ISHIGAKI, S., MASUDA, A., IGUCHI, Y., UDAGAWA, T., WATANABE, H., KATSUNO, M., OHNO, K. & SOBUE, G. 2013. FUS-regulated region- and cell-type-specific transcriptome is associated with cell selectivity in ALS/FTLD. *Sci Rep,* 3**,** 2388.

FUSHIMI, K., LONG, C., JAYARAM, N., CHEN, X., LI, L. & WU, J. Y. 2011. Expression of human FUS/TLS in yeast leads to protein aggregation and cytotoxicity, recapitulating key features of FUS proteinopathy. *Protein Cell,* 2**,** 141-9.

GAL, J., ZHANG, J., KWINTER, D. M., ZHAI, J., JIA, H., JIA, J. & ZHU, H. 2011. Nuclear localization sequence of FUS and induction of stress granules by ALS mutants. *Neurobiol Aging,* 32**,** 2323 e27-40.

GARCIA-MATA, R., BEBOK, Z., SORSCHER, E. J. & SZTUL, E. S. 1999. Characterization and dynamics of aggresome formation by a cytosolic GFP-chimera. *J Cell Biol,* 146**,** 1239-54.

GERTZ, B., WONG, M. & MARTIN, L. J. 2012. Nuclear localization of human SOD1 and mutant SOD1-specific disruption of survival motor neuron protein complex in transgenic amyotrophic lateral sclerosis mice. *J Neuropathol Exp Neurol,* 71**,** 162-77.

GIBB, S. L., BOSTON-HOWES, W., LAVINA, Z. S., GUSTINCICH, S., BROWN, R. H., JR., PASINELLI, P. & TROTTI, D. 2007. A caspase-3-cleaved fragment of the glial glutamate transporter EAAT2 is sumoylated and targeted to promyelocytic leukemia nuclear bodies in mutant SOD1-linked amyotrophic lateral sclerosis. *J Biol Chem,* 282**,** 32480-90.

GIJSELINCK, I., VAN LANGENHOVE, T., VAN DER ZEE, J., SLEEGERS, K., PHILTJENS, S., KLEINBERGER, G., JANSSENS, J., BETTENS, K., VAN CAUWENBERGHE, C., PERESON, S., ENGELBORGHS, S., SIEBEN, A., DE JONGHE, P., VANDENBERGHE, R., SANTENS, P., DE BLEECKER, J., MAES, G., BAUMER, V., DILLEN, L., JORIS, G., CUIJT, I., CORSMIT, E., ELINCK, E., VAN DONGEN, J., VERMEULEN, S., VAN DEN BROECK, M., VAERENBERG, C., MATTHEIJSSENS, M., PEETERS, K., ROBBERECHT, W., CRAS, P.,

MARTIN, J. J., DE DEYN, P. P., CRUTS, M. & VAN BROECKHOVEN, C. 2012. A C9orf72 promoter repeat expansion in a Flanders-Belgian cohort with disorders of the frontotemporal lobar degeneration-amyotrophic lateral sclerosis spectrum: a gene identification study. *Lancet Neurol,* 11**,** 54-65.

GIORDANA, M. T., PICCININI, M., GRIFONI, S., DE MARCO, G., VERCELLINO, M., MAGISTRELLO, M., PELLERINO, A., BUCCINNA, B., LUPINO, E. & RINAUDO, M. T. 2010. TDP-43 redistribution is an early event in sporadic amyotrophic lateral sclerosis. *Brain Pathol,* 20**,** 351-60.

GITCHO, M. A., STRIDER, J., CARTER, D., TAYLOR-REINWALD, L., FORMAN, M. S., GOATE, A. M. & CAIRNS, N. J. 2009. VCP mutations causing frontotemporal lobar degeneration disrupt localization of TDP-43 and induce cell death. *J Biol Chem,* 284**,** 12384-98.

GITLER, A. D. & SHORTER, J. 2011. RNA-binding proteins with prion-like domains in ALS and FTLD-U. *Prion,* 5**,** 179-87.

GOETZ, C. G. 2000. Amyotrophic lateral sclerosis: early contributions of Jean-Martin Charcot. *Muscle Nerve,* 23**,** 336-43.

GOLDSTEIN, L. H. & ABRAHAMS, S. 2013. Changes in cognition and behaviour in amyotrophic lateral sclerosis: nature of impairment and implications for assessment. *Lancet Neurol,* 12**,** 368-80.

GOMEZ-TORTOSA, E., GALLEGO, J., GUERRERO-LOPEZ, R., MARCOS, A., GIL-NECIGA, E., SAINZ, M. J., DIAZ, A., FRANCO-MACIAS, E., TRUJILLO-TIEBAS, M. J., AYUSO, C. & PEREZ-PEREZ, J. 2013. C9ORF72 hexanucleotide expansions of 20-22 repeats are associated with frontotemporal deterioration. *Neurology,* 80**,** 366-70.

GREDAL, O., PAKKENBERG, H., KARLSBORG, M. & PAKKENBERG, B. 2000. Unchanged total number of neurons in motor cortex and neocortex in amyotrophic lateral sclerosis: a stereological study. *J Neurosci Methods,* 95**,** 171-6.

GREENWAY, M. J., ANDERSEN, P. M., RUSS, C., ENNIS, S., CASHMAN, S., DONAGHY, C., PATTERSON, V., SWINGLER, R., KIERAN, D., PREHN, J., MORRISON, K. E., GREEN, A., ACHARYA, K. R., BROWN, R. H., JR. & HARDIMAN, O. 2006. ANG mutations segregate with familial and 'sporadic' amyotrophic lateral sclerosis. *Nat Genet,* 38**,** 411-3.

GREGORY, R. I., YAN, K. P., AMUTHAN, G., CHENDRIMADA, T., DORATOTAJ, B., COOCH, N. & SHIEKHATTAR, R. 2004. The Microprocessor complex mediates the genesis of microRNAs. *Nature,* 432**,** 235-40.

GROEN, E. J., FUMOTO, K., BLOKHUIS, A. M., ENGELEN-LEE, J., ZHOU, Y., VAN DEN HEUVEL, D. M., KOPPERS, M., VAN DIGGELEN, F., VAN HEEST, J., DEMMERS, J. A., KIRBY, J., SHAW, P. J., ARONICA, E., SPLIET, W. G., VELDINK, J. H., VAN DEN BERG, L. H. & PASTERKAMP, R. J. 2013. ALS-associated mutations in FUS disrupt the axonal distribution and function of SMN. *Hum Mol Genet,* 22**,** 3690-704.

GURNEY, M. E., PU, H., CHIU, A. Y., DAL CANTO, M. C., POLCHOW, C. Y., ALEXANDER, D. D., CALIENDO, J., HENTATI, A., KWON, Y. W., DENG, H. X. & ET AL. 1994. Motor neuron degeneration in mice that express a human Cu,Zn superoxide dismutase mutation. *Science,* 264**,** 1772-5.

GUSTAVSSON, A., SVENSSON, M., JACOBI, F., ALLGULANDER, C., ALONSO, J., BEGHI, E., DODEL, R., EKMAN, M., FARAVELLI, C., FRATIGLIONI, L., GANNON, B., JONES, D. H., JENNUM, P., JORDANOVA, A., JONSSON, L., KARAMPAMPA, K., KNAPP, M., KOBELT, G., KURTH, T., LIEB, R., LINDE, M., LJUNGCRANTZ, C., MAERCKER, A., MELIN, B., MOSCARELLI, M., MUSAYEV, A., NORWOOD, F., PREISIG, M., PUGLIATTI, M., REHM, J.,

SALVADOR-CARULLA, L., SCHLEHOFER, B., SIMON, R., STEINHAUSEN, H. C., STOVNER, L. J., VALLAT, J. M., VAN DEN BERGH, P., VAN OS, J., VOS, P., XU, W., WITTCHEN, H. U., JONSSON, B. & OLESEN, J. 2011. Cost of disorders of the brain in Europe 2010. *Eur Neuropsychopharmacol,* 21**,** 718-79.

HADANO, S., HAND, C. K., OSUGA, H., YANAGISAWA, Y., OTOMO, A., DEVON, R. S., MIYAMOTO, N., SHOWGUCHI-MIYATA, J., OKADA, Y., SINGARAJA, R., FIGLEWICZ, D. A., KWIATKOWSKI, T., HOSLER, B. A., SAGIE, T., SKAUG, J., NASIR, J., BROWN, R. H., JR., SCHERER, S. W., ROULEAU, G. A., HAYDEN, M. R. & IKEDA, J. E. 2001. A gene encoding a putative GTPase regulator is mutated in familial amyotrophic lateral sclerosis 2. *Nat Genet,* 29**,** 166-73.

HARDIMAN, O., VAN DEN BERG, L. H. & KIERNAN, M. C. 2011. Clinical diagnosis and management of amyotrophic lateral sclerosis. *Nat Rev Neurol,* 7**,** 639-49.

HAYS, A. P., NAINI, A., HE, C. Z., MITSUMOTO, H. & ROWLAND, L. P. 2006. Sporadic amyotrophic lateral sclerosis and breast cancer: Hyaline conglomerate inclusions lead to identification of SOD1 mutation. *J Neurol Sci,* 242**,** 67-9.

HENNIG, S., KONG, G., MANNEN, T., SADOWSKA, A., KOBELKE, S., BLYTHE, A., KNOTT, G. J., IYER, K. S., HO, D., NEWCOMBE, E. A., HOSOKI, K., GOSHIMA, N., KAWAGUCHI, T., HATTERS, D., TRINKLE-MULCAHY, L., HIROSE, T., BOND, C. S. & FOX, A. H. 2015. Prion-like domains in RNA binding proteins are essential for building subnuclear paraspeckles. *J Cell Biol,* 210**,** 529-39.

HETMAN, M., VASHISHTA, A. & REMPALA, G. 2010. Neurotoxic mechanisms of DNA damage: focus on transcriptional inhibition. *J Neurochem,* 114**,** 1537-49.

HEWITT, C., KIRBY, J., HIGHLEY, J. R., HARTLEY, J. A., HIBBERD, R., HOLLINGER, H. C., WILLIAMS, T. L., INCE, P. G., MCDERMOTT, C. J. & SHAW, P. J. 2010. Novel FUS/TLS mutations and pathology in familial and sporadic amyotrophic lateral sclerosis. *Arch Neurol,* 67**,** 455-61.

HICKS, G. G., SINGH, N., NASHABI, A., MAI, S., BOZEK, G., KLEWES, L., ARAPOVIC, D., WHITE, E. K., KOURY, M. J., OLTZ, E. M., VAN KAER, L. & RULEY, H. E. 2000. Fus deficiency in mice results in defective B-lymphocyte development and activation, high levels of chromosomal instability and perinatal death. *Nat Genet,* 24**,** 175-9.

HIGGINS, C. M., JUNG, C. & XU, Z. 2003. ALS-associated mutant SOD1G93A causes mitochondrial vacuolation by expansion of the intermembrane space and by involvement of SOD1 aggregation and peroxisomes. *BMC Neurosci,* 4**,** 16.

HOELL, J. I., LARSSON, E., RUNGE, S., NUSBAUM, J. D., DUGGIMPUDI, S., FARAZI, T. A., HAFNER, M., BORKHARDT, A., SANDER, C. & TUSCHL, T. 2011. RNA targets of wild-type and mutant FET family proteins. *Nat Struct Mol Biol,* 18**,** 1428-31.

HONDA, D., ISHIGAKI, S., IGUCHI, Y., FUJIOKA, Y., UDAGAWA, T., MASUDA, A., OHNO, K., KATSUNO, M. & SOBUE, G. 2013. The ALS/FTLD-related RNA-binding proteins TDP-43 and FUS have common downstream RNA targets in cortical neurons. *FEBS Open Bio,* 4**,** 1-10.

HUANG, C., TONG, J., BI, F., WU, Q., HUANG, B., ZHOU, H. & XIA, X. G. 2012. Entorhinal cortical neurons are the primary targets of FUS mislocalization and ubiquitin aggregation in FUS transgenic rats. *Hum Mol Genet,* 21**,** 4602-14.

HUANG, C., ZHOU, H., TONG, J., CHEN, H., LIU, Y. J., WANG, D., WEI, X. & XIA, X. G. 2011. FUS transgenic rats develop the phenotypes of amyotrophic lateral sclerosis and frontotemporal lobar degeneration. *PLoS Genet,* 7**,** e1002011.

HUANG, E. J., ZHANG, J., GESER, F., TROJANOWSKI, J. Q., STROBER, J. B., DICKSON, D. W., BROWN, R. H., JR., SHAPIRO, B. E. & LOMEN-HOERTH, C.

2010. Extensive FUS-immunoreactive pathology in juvenile amyotrophic lateral sclerosis with basophilic inclusions. *Brain Pathol,* 20**,** 1069-76.

HUEY, E. D., FERRARI, R., MORENO, J. H., JENSEN, C., MORRIS, C. M., POTOCNIK, F., KALARIA, R. N., TIERNEY, M., WASSERMANN, E. M., HARDY, J., GRAFMAN, J. & MOMENI, P. 2012. FUS and TDP43 genetic variability in FTD and CBS. *Neurobiol Aging,* 33**,** 1016 e9-17.

HUGHES, J. T. 1982. Pathology of amyotrophic lateral sclerosis. *Adv Neurol,* 36**,** 61-74.

HUKEMA, R. K., RIEMSLAGH, F. W., MELHEM, S., VAN DER LINDE, H. C., SEVERIJNEN, L., EDBAUER, D., MAAS, A., CHARLET-BERGUERAND, N., WILLEMSEN, R. & VAN SWIETEN, J. C. 2014. A new inducible transgenic mouse model for C9orf72-associated GGGGCC repeat expansion supports a gain-of-function mechanism in C9orf72 associated ALS and FTD. *Acta Neuropathol Commun,* 2**,** 166.

HUSI, H., WARD, M. A., CHOUDHARY, J. S., BLACKSTOCK, W. P. & GRANT, S. G. 2000. Proteomic analysis of NMDA receptor-adhesion protein signaling complexes. *Nat Neurosci,* 3**,** 661-9.

IGAZ, L. M., KWONG, L. K., XU, Y., TRUAX, A. C., URYU, K., NEUMANN, M., CLARK, C. M., ELMAN, L. B., MILLER, B. L., GROSSMAN, M., MCCLUSKEY, L. F., TROJANOWSKI, J. Q. & LEE, V. M. 2008. Enrichment of C-terminal fragments in TAR DNA-binding protein-43 cytoplasmic inclusions in brain but not in spinal cord of frontotemporal lobar degeneration and amyotrophic lateral sclerosis. *Am J Pathol,* 173**,** 182-94.

IKO, Y., KODAMA, T. S., KASAI, N., OYAMA, T., MORITA, E. H., MUTO, T., OKUMURA, M., FUJII, R., TAKUMI, T., TATE, S. & MORIKAWA, K. 2004. Domain architectures and characterization of an RNA-binding protein, TLS. *J Biol Chem,* 279**,** 44834-40.

IMAMURA, K., IMAMACHI, N., AKIZUKI, G., KUMAKURA, M., KAWAGUCHI, A., NAGATA, K., KATO, A., KAWAGUCHI, Y., SATO, H., YONEDA, M., KAI, C., YADA, T., SUZUKI, Y., YAMADA, T., OZAWA, T., KANEKI, K., INOUE, T., KOBAYASHI, M., KODAMA, T., WADA, Y., SEKIMIZU, K. & AKIMITSU, N. 2014. Long noncoding RNA NEAT1-dependent SFPQ relocation from promoter region to paraspeckle mediates IL8 expression upon immune stimuli. *Mol Cell,* 53**,** 393-406.

ISHIGAKI, S., MASUDA, A., FUJIOKA, Y., IGUCHI, Y., KATSUNO, M., SHIBATA, A., URANO, F., SOBUE, G. & OHNO, K. 2012. Position-dependent FUS-RNA interactions regulate alternative splicing events and transcriptions. *Sci Rep,* 2**,** 529.

ISHIHARA, T., ARIIZUMI, Y., SHIGA, A., KATO, T., TAN, C. F., SATO, T., MIKI, Y., YOKOO, M., FUJINO, T., KOYAMA, A., YOKOSEKI, A., NISHIZAWA, M., KAKITA, A., TAKAHASHI, H. & ONODERA, O. 2013. Decreased number of Gemini of coiled bodies and U12 snRNA level in amyotrophic lateral sclerosis. *Hum Mol Genet,* 22**,** 4136-47.

ITO, D., SEKI, M., TSUNODA, Y., UCHIYAMA, H. & SUZUKI, N. 2011. Nuclear transport impairment of amyotrophic lateral sclerosis-linked mutations in FUS/TLS. *Ann Neurol,* 69**,** 152-62.

JAARSMA, D., ROGNONI, F., VAN DUIJN, W., VERSPAGET, H. W., HAASDIJK, E. D. & HOLSTEGE, J. C. 2001. CuZn superoxide dismutase (SOD1) accumulates in vacuolated mitochondria in transgenic mice expressing amyotrophic lateral sclerosis-linked SOD1 mutations. *Acta Neuropathol,* 102**,** 293-305.

JOHNSON, B. S., SNEAD, D., LEE, J. J., MCCAFFERY, J. M., SHORTER, J. & GITLER, A. D. 2009. TDP-43 is intrinsically aggregation-prone, and

amyotrophic lateral sclerosis-linked mutations accelerate aggregation and increase toxicity. *J Biol Chem,* 284**,** 20329-39.

JOHNSON, J. O., MANDRIOLI, J., BENATAR, M., ABRAMZON, Y., VAN DEERLIN, V. M., TROJANOWSKI, J. Q., GIBBS, J. R., BRUNETTI, M., GRONKA, S., WUU, J., DING, J., MCCLUSKEY, L., MARTINEZ-LAGE, M., FALCONE, D., HERNANDEZ, D. G., AREPALLI, S., CHONG, S., SCHYMICK, J. C., ROTHSTEIN, J., LANDI, F., WANG, Y. D., CALVO, A., MORA, G., SABATELLI, M., MONSURRO, M. R., BATTISTINI, S., SALVI, F., SPATARO, R., SOLA, P., BORGHERO, G., CONSORTIUM, I., GALASSI, G., SCHOLZ, S. W., TAYLOR, J. P., RESTAGNO, G., CHIO, A. & TRAYNOR, B. J. 2010. Exome sequencing reveals VCP mutations as a cause of familial ALS. *Neuron,* 68**,** 857-64.

JOHNSON, J. O., PIORO, E. P., BOEHRINGER, A., CHIA, R., FEIT, H., RENTON, A. E., PLINER, H. A., ABRAMZON, Y., MARANGI, G., WINBORN, B. J., GIBBS, J. R., NALLS, M. A., MORGAN, S., SHOAI, M., HARDY, J., PITTMAN, A., ORRELL, R. W., MALASPINA, A., SIDLE, K. C., FRATTA, P., HARMS, M. B., BALOH, R. H., PESTRONK, A., WEIHL, C. C., ROGAEVA, E., ZINMAN, L., DRORY, V. E., BORGHERO, G., MORA, G., CALVO, A., ROTHSTEIN, J. D., CONSORTIUM, I., DREPPER, C., SENDTNER, M., SINGLETON, A. B., TAYLOR, J. P., COOKSON, M. R., RESTAGNO, G., SABATELLI, M., BOWSER, R., CHIO, A. & TRAYNOR, B. J. 2014. Mutations in the Matrin 3 gene cause familial amyotrophic lateral sclerosis. *Nat Neurosci,* 17**,** 664-6.

JOHNSTON, J. A., WARD, C. L. & KOPITO, R. R. 1998. Aggresomes: a cellular response to misfolded proteins. *J Cell Biol,* 143**,** 1883-98.

JONSSON, P. A., ERNHILL, K., ANDERSEN, P. M., BERGEMALM, D., BRANNSTROM, T., GREDAL, O., NILSSON, P. & MARKLUND, S. L. 2004. Minute quantities of misfolded mutant superoxide dismutase-1 cause amyotrophic lateral sclerosis. *Brain,* 127**,** 73-88.

JU, S., TARDIFF, D. F., HAN, H., DIVYA, K., ZHONG, Q., MAQUAT, L. E., BOSCO, D. A., HAYWARD, L. J., BROWN, R. H., JR., LINDQUIST, S., RINGE, D. & PETSKO, G. A. 2011. A yeast model of FUS/TLS-dependent cytotoxicity. *PLoS Biol,* 9**,** e1001052.

KABASHI, E., BERCIER, V., LISSOUBA, A., LIAO, M., BRUSTEIN, E., ROULEAU, G. A. & DRAPEAU, P. 2011. FUS and TARDBP but not SOD1 interact in genetic models of amyotrophic lateral sclerosis. *PLoS Genet,* 7**,** e1002214.

KAMEOKA, S., DUQUE, P. & KONARSKA, M. M. 2004. p54(nrb) associates with the 5' splice site within large transcription/splicing complexes. *EMBO J,* 23**,** 1782-91.

KANAI, Y., DOHMAE, N. & HIROKAWA, N. 2004. Kinesin transports RNA: isolation and characterization of an RNA-transporting granule. *Neuron,* 43**,** 513-25.

KANDEL, E. R. 2013. *Principles of neural science.* New York: McGraw-Hill.

KANEB, H. M., FOLKMANN, A. W., BELZIL, V. V., JAO, L. E., LEBLOND, C. S., GIRARD, S. L., DAOUD, H., NOREAU, A., ROCHEFORT, D., HINCE, P., SZUTO, A., LEVERT, A., VIDAL, S., ANDRE-GUIMONT, C., CAMU, W., BOUCHARD, J. P., DUPRE, N., ROULEAU, G. A., WENTE, S. R. & DION, P. A. 2015. Deleterious mutations in the essential mRNA metabolism factor, hGle1, in amyotrophic lateral sclerosis. *Hum Mol Genet,* 24**,** 1363-73.

KARIYA, S., RE, D. B., JACQUIER, A., NELSON, K., PRZEDBORSKI, S. & MONANI, U. R. 2012. Mutant superoxide dismutase 1 (SOD1), a cause of amyotrophic lateral sclerosis, disrupts the recruitment of SMN, the spinal muscular atrophy protein to nuclear Cajal bodies. *Hum Mol Genet,* 21**,** 3421-34.

KARIYA, S., SAMPSON, J. B., NORTHROP, L. E., LUCCARELLI, C. M., NAINI, A. B., RE, D. B., HIRANO, M. & MITSUMOTO, H. 2014. Nuclear localization of SMN

and FUS is not altered in fibroblasts from patients with sporadic ALS. *Amyotroph Lateral Scler Frontotemporal Degener*.

KATO, M., HAN, T. W., XIE, S., SHI, K., DU, X., WU, L. C., MIRZAEI, H., GOLDSMITH, E. J., LONGGOOD, J., PEI, J., GRISHIN, N. V., FRANTZ, D. E., SCHNEIDER, J. W., CHEN, S., LI, L., SAWAYA, M. R., EISENBERG, D., TYCKO, R. & MCKNIGHT, S. L. 2012. Cell-free formation of RNA granules: low complexity sequence domains form dynamic fibers within hydrogels. *Cell,* 149**,** 753-67.

KATO, S., SHIMODA, M., WATANABE, Y., NAKASHIMA, K., TAKAHASHI, K. & OHAMA, E. 1996. Familial amyotrophic lateral sclerosis with a two base pair deletion in superoxide dismutase 1: gene multisystem degeneration with intracytoplasmic hyaline inclusions in astrocytes. *J Neuropathol Exp Neurol,* 55**,** 1089-101.

KATZ, J. S., KATZBERG, H. D., WOOLLEY, S. C., MARKLUND, S. L. & ANDERSEN, P. M. 2012. Combined fulminant frontotemporal dementia and amyotrophic lateral sclerosis associated with an I113T SOD1 mutation. *Amyotroph Lateral Scler,* 13**,** 567-9.

KEDERSHA, N. & ANDERSON, P. 2007. Mammalian stress granules and processing bodies. *Methods Enzymol,* 431**,** 61-81.

KEDERSHA, N., CHO, M. R., LI, W., YACONO, P. W., CHEN, S., GILKS, N., GOLAN, D. E. & ANDERSON, P. 2000. Dynamic shuttling of TIA-1 accompanies the recruitment of mRNA to mammalian stress granules. *J Cell Biol,* 151**,** 1257-68.

KENT, L., VIZARD, T. N., SMITH, B. N., TOPP, S. D., VANCE, C., GKAZI, A., MILLER, J., SHAW, C. E. & TALBOT, K. 2014. Autosomal dominant inheritance of rapidly progressive amyotrophic lateral sclerosis due to a truncation mutation in the fused in sarcoma (FUS) gene. *Amyotroph Lateral Scler Frontotemporal Degener***,** 1-6.

KIERNAN, M. C., VUCIC, S., CHEAH, B. C., TURNER, M. R., EISEN, A., HARDIMAN, O., BURRELL, J. R. & ZOING, M. C. 2011. Amyotrophic lateral sclerosis. *Lancet,* 377**,** 942-55.

KIM, H. J., KIM, N. C., WANG, Y. D., SCARBOROUGH, E. A., MOORE, J., DIAZ, Z., MACLEA, K. S., FREIBAUM, B., LI, S., MOLLIEX, A., KANAGARAJ, A. P., CARTER, R., BOYLAN, K. B., WOJTAS, A. M., RADEMAKERS, R., PINKUS, J. L., GREENBERG, S. A., TROJANOWSKI, J. Q., TRAYNOR, B. J., SMITH, B. N., TOPP, S., GKAZI, A. S., MILLER, J., SHAW, C. E., KOTTLORS, M., KIRSCHNER, J., PESTRONK, A., LI, Y. R., FORD, A. F., GITLER, A. D., BENATAR, M., KING, O. D., KIMONIS, V. E., ROSS, E. D., WEIHL, C. C., SHORTER, J. & TAYLOR, J. P. 2013. Mutations in prion-like domains in hnRNPA2B1 and hnRNPA1 cause multisystem proteinopathy and ALS. *Nature,* 495**,** 467-73.

KIMBALL, S. R., HORETSKY, R. L., RON, D., JEFFERSON, L. S. & HARDING, H. P. 2003. Mammalian stress granules represent sites of accumulation of stalled translation initiation complexes. *Am J Physiol Cell Physiol,* 284**,** C273-84.

KINO, Y., WASHIZU, C., AQUILANTI, E., OKUNO, M., KUROSAWA, M., YAMADA, M., DOI, H. & NUKINA, N. 2011. Intracellular localization and splicing regulation of FUS/TLS are variably affected by amyotrophic lateral sclerosis-linked mutations. *Nucleic Acids Res,* 39**,** 2781-98.

KOKUBO, Y., KUZUHARA, S., NARITA, Y., KIKUGAWA, K., NAKANO, R., INUZUKA, T., TSUJI, S., WATANABE, M., MIYAZAKI, T., MURAYAMA, S. & IHARA, Y. 1999. Accumulation of neurofilaments and SOD1-immunoreactive products in a patient with familial amyotrophic lateral sclerosis with I113T SOD1 mutation. *Arch Neurol,* 56**,** 1506-8.

KOPITO, R. R. 2000. Aggresomes, inclusion bodies and protein aggregation. *Trends Cell Biol,* 10**,** 524-30.

KRAEMER, B. C., SCHUCK, T., WHEELER, J. M., ROBINSON, L. C., TROJANOWSKI, J. Q., LEE, V. M. & SCHELLENBERG, G. D. 2010. Loss of murine TDP-43 disrupts motor function and plays an essential role in embryogenesis. *Acta Neuropathol,* 119**,** 409-19.

KRYNDUSHKIN, D., WICKNER, R. B. & SHEWMAKER, F. 2011. FUS/TLS forms cytoplasmic aggregates, inhibits cell growth and interacts with TDP-43 in a yeast model of amyotrophic lateral sclerosis. *Protein Cell,* 2**,** 223-36.

KURODA, M., SOK, J., WEBB, L., BAECHTOLD, H., URANO, F., YIN, Y., CHUNG, P., DE ROOIJ, D. G., AKHMEDOV, A., ASHLEY, T. & RON, D. 2000. Male sterility and enhanced radiation sensitivity in TLS(-/-) mice. *EMBO J,* 19**,** 453-62.

KWIATKOWSKI, T. J., JR., BOSCO, D. A., LECLERC, A. L., TAMRAZIAN, E., VANDERBURG, C. R., RUSS, C., DAVIS, A., GILCHRIST, J., KASARSKIS, E. J., MUNSAT, T., VALDMANIS, P., ROULEAU, G. A., HOSLER, B. A., CORTELLI, P., DE JONG, P. J., YOSHINAGA, Y., HAINES, J. L., PERICAK-VANCE, M. A., YAN, J., TICOZZI, N., SIDDIQUE, T., MCKENNA-YASEK, D., SAPP, P. C., HORVITZ, H. R., LANDERS, J. E. & BROWN, R. H., JR. 2009. Mutations in the FUS/TLS gene on chromosome 16 cause familial amyotrophic lateral sclerosis. *Science,* 323**,** 1205-8.

KWON, I., XIANG, S., KATO, M., WU, L., THEODOROPOULOS, P., WANG, T., KIM, J., YUN, J., XIE, Y. & MCKNIGHT, S. L. 2014. Poly-dipeptides encoded by the C9ORF72 repeats bind nucleoli, impede RNA biogenesis, and kill cells. *Science*.

LAAKSOVIRTA, H., PEURALINNA, T., SCHYMICK, J. C., SCHOLZ, S. W., LAI, S. L., MYLLYKANGAS, L., SULKAVA, R., JANSSON, L., HERNANDEZ, D. G., GIBBS, J. R., NALLS, M. A., HECKERMAN, D., TIENARI, P. J. & TRAYNOR, B. J. 2010. Chromosome 9p21 in amyotrophic lateral sclerosis in Finland: a genome-wide association study. *Lancet Neurol,* 9**,** 978-85.

LAGIER-TOURENNE, C., BAUGHN, M., RIGO, F., SUN, S., LIU, P., LI, H. R., JIANG, J., WATT, A. T., CHUN, S., KATZ, M., QIU, J., SUN, Y., LING, S. C., ZHU, Q., POLYMENIDOU, M., DRENNER, K., ARTATES, J. W., MCALONIS-DOWNES, M., MARKMILLER, S., HUTT, K. R., PIZZO, D. P., CADY, J., HARMS, M. B., BALOH, R. H., VANDENBERG, S. R., YEO, G. W., FU, X. D., BENNETT, C. F., CLEVELAND, D. W. & RAVITS, J. 2013. Targeted degradation of sense and antisense C9orf72 RNA foci as therapy for ALS and frontotemporal degeneration. *Proc Natl Acad Sci U S A,* 110**,** E4530-9.

LAGIER-TOURENNE, C. & CLEVELAND, D. W. 2009. Rethinking ALS: the FUS about TDP-43. *Cell,* 136**,** 1001-4.

LAGIER-TOURENNE, C., POLYMENIDOU, M. & CLEVELAND, D. W. 2010. TDP-43 and FUS/TLS: emerging roles in RNA processing and neurodegeneration. *Hum Mol Genet,* 19**,** R46-64.

LAGIER-TOURENNE, C., POLYMENIDOU, M., HUTT, K. R., VU, A. Q., BAUGHN, M., HUELGA, S. C., CLUTARIO, K. M., LING, S. C., LIANG, T. Y., MAZUR, C., WANCEWICZ, E., KIM, A. S., WATT, A., FREIER, S., HICKS, G. G., DONOHUE, J. P., SHIUE, L., BENNETT, C. F., RAVITS, J., CLEVELAND, D. W. & YEO, G. W. 2012. Divergent roles of ALS-linked proteins FUS/TLS and TDP-43 intersect in processing long pre-mRNAs. *Nat Neurosci,* 15**,** 1488-97.

LANSON, N. A., JR., MALTARE, A., KING, H., SMITH, R., KIM, J. H., TAYLOR, J. P., LLOYD, T. E. & PANDEY, U. B. 2011. A Drosophila model of FUS-related neurodegeneration reveals genetic interaction between FUS and TDP-43. *Hum Mol Genet,* 20**,** 2510-23.

LEE, B. J., CANSIZOGLU, A. E., SUEL, K. E., LOUIS, T. H., ZHANG, Z. & CHOOK, Y. M. 2006. Rules for nuclear localization sequence recognition by karyopherin beta 2. *Cell,* 126**,** 543-58.

LEE, Y. B., CHEN, H. J., PERES, J. N., GOMEZ-DEZA, J., ATTIG, J., STALEKAR, M., TROAKES, C., NISHIMURA, A. L., SCOTTER, E. L., VANCE, C., ADACHI, Y., SARDONE, V., MILLER, J. W., SMITH, B. N., GALLO, J. M., ULE, J., HIRTH, F., ROGELJ, B., HOUART, C. & SHAW, C. E. 2013. Hexanucleotide repeats in ALS/FTD form length-dependent RNA foci, sequester RNA binding proteins, and are neurotoxic. *Cell Rep,* 5**,** 1178-86.

LEFEBVRE, S., BURGLEN, L., REBOULLET, S., CLERMONT, O., BURLET, P., VIOLLET, L., BENICHOU, B., CRUAUD, C., MILLASSEAU, P., ZEVIANI, M. & ET AL. 1995. Identification and characterization of a spinal muscular atrophy-determining gene. *Cell,* 80**,** 155-65.

LEIGH, P. N., WHITWELL, H., GAROFALO, O., BULLER, J., SWASH, M., MARTIN, J. E., GALLO, J. M., WELLER, R. O. & ANDERTON, B. H. 1991. Ubiquitin-immunoreactive intraneuronal inclusions in amyotrophic lateral sclerosis. Morphology, distribution, and specificity. *Brain,* 114 (Pt 2)**,** 775-88.

LERGA, A., HALLIER, M., DELVA, L., ORVAIN, C., GALLAIS, I., MARIE, J. & MOREAU-GACHELIN, F. 2001. Identification of an RNA binding specificity for the potential splicing factor TLS. *J Biol Chem,* 276**,** 6807-16.

LEVINE, T. P., DANIELS, R. D., GATTA, A. T., WONG, L. H. & HAYES, M. J. 2013. The product of C9orf72, a gene strongly implicated in neurodegeneration, is structurally related to DENN Rab-GEFs. *Bioinformatics,* 29**,** 499-503.

LI, Y. R., KING, O. D., SHORTER, J. & GITLER, A. D. 2013. Stress granules as crucibles of ALS pathogenesis. *J Cell Biol,* 201**,** 361-72.

LILLO, P. & HODGES, J. R. 2009. Frontotemporal dementia and motor neurone disease: overlapping clinic-pathological disorders. *J Clin Neurosci,* 16**,** 1131-5.

LINDHOLM, D., WOOTZ, H. & KORHONEN, L. 2006. ER stress and neurodegenerative diseases. *Cell Death Differ,* 13**,** 385-92.

LING, S. C., POLYMENIDOU, M. & CLEVELAND, D. W. 2013. Converging mechanisms in ALS and FTD: disrupted RNA and protein homeostasis. *Neuron,* 79**,** 416-38.

LIU, Q. & DREYFUSS, G. 1996. A novel nuclear structure containing the survival of motor neurons protein. *EMBO J,* 15**,** 3555-65.

LIU, Q., FISCHER, U., WANG, F. & DREYFUSS, G. 1997. The spinal muscular atrophy disease gene product, SMN, and its associated protein SIP1 are in a complex with spliceosomal snRNP proteins. *Cell,* 90**,** 1013-21.

LIU, X., NIU, C., REN, J., ZHANG, J., XIE, X., ZHU, H., FENG, W. & GONG, W. 2012. The RRM domain of human fused in sarcoma protein reveals a non-canonical nucleic acid binding site. *Biochim Biophys Acta*.

LIU, Y. J., JU, T. C., CHEN, H. M., JANG, Y. S., LEE, L. M., LAI, H. L., TAI, H. C., FANG, J. M., LIN, Y. L., TU, P. H. & CHERN, Y. 2015. Activation of AMP-activated protein kinase alpha1 mediates mislocalization of TDP-43 in amyotrophic lateral sclerosis. *Hum Mol Genet,* 24**,** 787-801.

LIU-YESUCEVITZ, L., BILGUTAY, A., ZHANG, Y. J., VANDERWEYDE, T., CITRO, A., MEHTA, T., ZAARUR, N., MCKEE, A., BOWSER, R., SHERMAN, M., PETRUCELLI, L. & WOLOZIN, B. 2010. Tar DNA binding protein-43 (TDP-43) associates with stress granules: analysis of cultured cells and pathological brain tissue. *PLoS One,* 5**,** e13250.

LIU-YESUCEVITZ, L., LIN, A. Y., EBATA, A., BOON, J. Y., REID, W., XU, Y. F., KOBRIN, K., MURPHY, G. J., PETRUCELLI, L. & WOLOZIN, B. 2014. ALS-

linked mutations enlarge TDP-43-enriched neuronal RNA granules in the dendritic arbor. *J Neurosci,* 34**,** 4167-74.

LOGROSCINO, G., TRAYNOR, B. J., HARDIMAN, O., CHIO, A., COURATIER, P., MITCHELL, J. D., SWINGLER, R. J. & BEGHI, E. 2008. Descriptive epidemiology of amyotrophic lateral sclerosis: new evidence and unsolved issues. *J Neurol Neurosurg Psychiatry,* 79**,** 6-11.

LOGROSCINO, G., TRAYNOR, B. J., HARDIMAN, O., CHIO, A., MITCHELL, D., SWINGLER, R. J., MILLUL, A., BENN, E. & BEGHI, E. 2010. Incidence of amyotrophic lateral sclerosis in Europe. *J Neurol Neurosurg Psychiatry,* 81**,** 385-90.

LOMEN-HOERTH, C., ANDERSON, T. & MILLER, B. 2002. The overlap of amyotrophic lateral sclerosis and frontotemporal dementia. *Neurology,* 59**,** 1077-9.

LU, T., PAN, Y., KAO, S. Y., LI, C., KOHANE, I., CHAN, J. & YANKNER, B. A. 2004. Gene regulation and DNA damage in the ageing human brain. *Nature,* 429**,** 883-91.

LUK, K. C., SONG, C., O'BRIEN, P., STIEBER, A., BRANCH, J. R., BRUNDEN, K. R., TROJANOWSKI, J. Q. & LEE, V. M. 2009. Exogenous alpha-synuclein fibrils seed the formation of Lewy body-like intracellular inclusions in cultured cells. *Proc Natl Acad Sci U S A,* 106**,** 20051-6.

LUTHI, A., VAN DER PUTTEN, H., BOTTERI, F. M., MANSUY, I. M., MEINS, M., FREY, U., SANSIG, G., PORTET, C., SCHMUTZ, M., SCHRODER, M., NITSCH, C., LAURENT, J. P. & MONARD, D. 1997. Endogenous serine protease inhibitor modulates epileptic activity and hippocampal long-term potentiation. *J Neurosci,* 17**,** 4688-99.

LUZIO, J. P., PRYOR, P. R. & BRIGHT, N. A. 2007. Lysosomes: fusion and function. *Nat Rev Mol Cell Biol,* 8**,** 622-32.

MACHAMER, J. B., COLLINS, S. E. & LLOYD, T. E. 2014. The ALS gene FUS regulates synaptic transmission at the Drosophila neuromuscular junction. *Hum Mol Genet*.

MACKENZIE, I. R., BIGIO, E. H., INCE, P. G., GESER, F., NEUMANN, M., CAIRNS, N. J., KWONG, L. K., FORMAN, M. S., RAVITS, J., STEWART, H., EISEN, A., MCCLUSKY, L., KRETZSCHMAR, H. A., MONORANU, C. M., HIGHLEY, J. R., KIRBY, J., SIDDIQUE, T., SHAW, P. J., LEE, V. M. & TROJANOWSKI, J. Q. 2007. Pathological TDP-43 distinguishes sporadic amyotrophic lateral sclerosis from amyotrophic lateral sclerosis with SOD1 mutations. *Ann Neurol,* 61**,** 427-34.

MAEKAWA, S., AL-SARRAJ, S., KIBBLE, M., LANDAU, S., PARNAVELAS, J., COTTER, D., EVERALL, I. & LEIGH, P. N. 2004. Cortical selective vulnerability in motor neuron disease: a morphometric study. *Brain,* 127**,** 1237-51.

MAJOUNIE, E., RENTON, A. E., MOK, K., DOPPER, E. G., WAITE, A., ROLLINSON, S., CHIO, A., RESTAGNO, G., NICOLAOU, N., SIMON-SANCHEZ, J., VAN SWIETEN, J. C., ABRAMZON, Y., JOHNSON, J. O., SENDTNER, M., PAMPHLETT, R., ORRELL, R. W., MEAD, S., SIDLE, K. C., HOULDEN, H., ROHRER, J. D., MORRISON, K. E., PALL, H., TALBOT, K., ANSORGE, O., CHROMOSOME, A. L. S. F. T. D. C., FRENCH RESEARCH NETWORK ON, F. F. A., CONSORTIUM, I., HERNANDEZ, D. G., AREPALLI, S., SABATELLI, M., MORA, G., CORBO, M., GIANNINI, F., CALVO, A., ENGLUND, E., BORGHERO, G., FLORIS, G. L., REMES, A. M., LAAKSOVIRTA, H., MCCLUSKEY, L., TROJANOWSKI, J. Q., VAN DEERLIN, V. M., SCHELLENBERG, G. D., NALLS, M. A., DRORY, V. E., LU, C. S., YEH, T. H., ISHIURA, H., TAKAHASHI, Y., TSUJI, S., LE BER, I., BRICE, A., DREPPER, C., WILLIAMS, N., KIRBY, J., SHAW, P., HARDY, J., TIENARI, P. J., HEUTINK, P.,

MORRIS, H. R., PICKERING-BROWN, S. & TRAYNOR, B. J. 2012. Frequency of the C9orf72 hexanucleotide repeat expansion in patients with amyotrophic lateral sclerosis and frontotemporal dementia: a cross-sectional study. *Lancet Neurol,* 11**,** 323-30.

MANNEN, T., IWATA, M., TOYOKURA, Y. & NAGASHIMA, K. 1977. Preservation of a certain motoneurone group of the sacral cord in amyotrophic lateral sclerosis: its clinical significance. *J Neurol Neurosurg Psychiatry,* 40**,** 464-9.

MANNOJI, H., YEGER, H. & BECKER, L. E. 1986. A specific histochemical marker (lectin Ricinus communis agglutinin-1) for normal human microglia, and application to routine histopathology. *Acta Neuropathol,* 71**,** 341-3.

MARKO, M., VLASSIS, A., GUIALIS, A. & LEICHTER, M. 2012. Domains involved in TAF15 subcellular localisation: dependence on cell type and ongoing transcription. *Gene,* 506**,** 331-8.

MARUYAMA, H., MORINO, H., ITO, H., IZUMI, Y., KATO, H., WATANABE, Y., KINOSHITA, Y., KAMADA, M., NODERA, H., SUZUKI, H., KOMURE, O., MATSUURA, S., KOBATAKE, K., MORIMOTO, N., ABE, K., SUZUKI, N., AOKI, M., KAWATA, A., HIRAI, T., KATO, T., OGASAWARA, K., HIRANO, A., TAKUMI, T., KUSAKA, H., HAGIWARA, K., KAJI, R. & KAWAKAMI, H. 2010. Mutations of optineurin in amyotrophic lateral sclerosis. *Nature,* 465**,** 223-6.

MASTROCOLA, A. S., KIM, S. H., TRINH, A. T., RODENKIRCH, L. A. & TIBBETTS, R. S. 2013. The RNA-binding protein fused in sarcoma (FUS) functions downstream of poly(ADP-ribose) polymerase (PARP) in response to DNA damage. *J Biol Chem,* 288**,** 24731-41.

MAY, S., HORNBURG, D., SCHLUDI, M. H., ARZBERGER, T., RENTZSCH, K., SCHWENK, B. M., GRASSER, F. A., MORI, K., KREMMER, E., BANZHAF-STRATHMANN, J., MANN, M., MEISSNER, F. & EDBAUER, D. 2014. C9orf72 FTLD/ALS-associated Gly-Ala dipeptide repeat proteins cause neuronal toxicity and Unc119 sequestration. *Acta Neuropathol*.

MCCORD, J. M. & FRIDOVICH, I. 1969. Superoxide dismutase. An enzymic function for erythrocuprein (hemocuprein). *J Biol Chem,* 244**,** 6049-55.

MCGEE, S. L. & HARGREAVES, M. 2008. AMPK and transcriptional regulation. *Front Biosci,* 13**,** 3022-33.

MCGOLDRICK, P., JOYCE, P. I., FISHER, E. M. & GREENSMITH, L. 2013. Rodent models of amyotrophic lateral sclerosis. *Biochim Biophys Acta,* 1832**,** 1421-36.

MEISSNER, M., LOPATO, S., GOTZMANN, J., SAUERMANN, G. & BARTA, A. 2003. Proto-oncoprotein TLS/FUS is associated to the nuclear matrix and complexed with splicing factors PTB, SRm160, and SR proteins. *Exp Cell Res,* 283**,** 184-95.

MENZIES, F. M., GRIERSON, A. J., COOKSON, M. R., HEATH, P. R., TOMKINS, J., FIGLEWICZ, D. A., INCE, P. G. & SHAW, P. J. 2002. Selective loss of neurofilament expression in Cu/Zn superoxide dismutase (SOD1) linked amyotrophic lateral sclerosis. *J Neurochem,* 82**,** 1118-28.

MERNER, N. D., GIRARD, S. L., CATOIRE, H., BOURASSA, C. V., BELZIL, V. V., RIVIERE, J. B., HINCE, P., LEVERT, A., DIONNE-LAPORTE, A., SPIEGELMAN, D., NOREAU, A., DIAB, S., SZUTO, A., FOURNIER, H., RAELSON, J., BELOUCHI, M., PANISSET, M., COSSETTE, P., DUPRE, N., BERNARD, G., CHOUINARD, S., DION, P. A. & ROULEAU, G. A. 2012. Exome sequencing identifies FUS mutations as a cause of essential tremor. *Am J Hum Genet,* 91**,** 313-9.

MICHELHAUGH, S. K., LIPOVICH, L., BLYTHE, J., JIA, H., KAPATOS, G. & BANNON, M. J. 2011. Mining Affymetrix microarray data for long non-coding RNAs:

altered expression in the nucleus accumbens of heroin abusers. *J Neurochem,* 116**,** 459-66.

MICHELITSCH, M. D. & WEISSMAN, J. S. 2000. A census of glutamine/asparagine-rich regions: implications for their conserved function and the prediction of novel prions. *Proc Natl Acad Sci U S A,* 97**,** 11910-5.

MIGUEL, L., AVEQUIN, T., DELARUE, M., FEUILLETTE, S., FREBOURG, T., CAMPION, D. & LECOURTOIS, M. 2012. Accumulation of insoluble forms of FUS protein correlates with toxicity in Drosophila. *Neurobiol Aging,* 33**,** 1008 e1-15.

MILLER, R. G., MITCHELL, J. D., LYON, M. & MOORE, D. H. 2003. Riluzole for amyotrophic lateral sclerosis (ALS)/motor neuron disease (MND). *Amyotroph Lateral Scler Other Motor Neuron Disord,* 4**,** 191-206.

MITCHELL, J. C., MCGOLDRICK, P., VANCE, C., HORTOBAGYI, T., SREEDHARAN, J., ROGELJ, B., TUDOR, E. L., SMITH, B. N., KLASEN, C., MILLER, C. C., COOPER, J. D., GREENSMITH, L. & SHAW, C. E. 2013. Overexpression of human wild-type FUS causes progressive motor neuron degeneration in an age- and dose-dependent fashion. *Acta Neuropathol,* 125**,** 273-88.

MIZIELINSKA, S., GRONKE, S., NICCOLI, T., RIDLER, C. E., CLAYTON, E. L., DEVOY, A., MOENS, T., NORONA, F. E., WOOLLACOTT, I. O., PIETRZYK, J., CLEVERLEY, K., NICOLL, A. J., PICKERING-BROWN, S., DOLS, J., CABECINHA, M., HENDRICH, O., FRATTA, P., FISHER, E. M., PARTRIDGE, L. & ISAACS, A. M. 2014. C9orf72 repeat expansions cause neurodegeneration in Drosophila through arginine-rich proteins. *Science*.

MIZUNO, Y., AMARI, M., TAKATAMA, M., AIZAWA, H., MIHARA, B. & OKAMOTO, K. 2006. Transferrin localizes in Bunina bodies in amyotrophic lateral sclerosis. *Acta Neuropathol,* 112**,** 597-603.

MORI, K., WENG, S. M., ARZBERGER, T., MAY, S., RENTZSCH, K., KREMMER, E., SCHMID, B., KRETZSCHMAR, H. A., CRUTS, M., VAN BROECKHOVEN, C., HAASS, C. & EDBAUER, D. 2013. The C9orf72 GGGGCC Repeat Is Translated into Aggregating Dipeptide-Repeat Proteins in FTLD/ALS. *Science*.

MORLANDO, M., DINI MODIGLIANI, S., TORRELLI, G., ROSA, A., DI CARLO, V., CAFFARELLI, E. & BOZZONI, I. 2012. FUS stimulates microRNA biogenesis by facilitating co-transcriptional Drosha recruitment. *EMBO J,* 31**,** 4502-10.

MUNCH, C., SEDLMEIER, R., MEYER, T., HOMBERG, V., SPERFELD, A. D., KURT, A., PRUDLO, J., PERAUS, G., HANEMANN, C. O., STUMM, G. & LUDOLPH, A. C. 2004. Point mutations of the p150 subunit of dynactin (DCTN1) gene in ALS. *Neurology,* 63**,** 724-6.

MUNOZ, D. G., NEUMANN, M., KUSAKA, H., YOKOTA, O., ISHIHARA, K., TERADA, S., KURODA, S. & MACKENZIE, I. R. 2009. FUS pathology in basophilic inclusion body disease. *Acta Neuropathol,* 118**,** 617-27.

MURAKAMI, T., YANG, S. P., XIE, L., KAWANO, T., FU, D., MUKAI, A., BOHM, C., CHEN, F., ROBERTSON, J., SUZUKI, H., TARTAGLIA, G. G., VENDRUSCOLO, M., KAMINSKI SCHIERLE, G. S., CHAN, F. T., MOLONEY, A., CROWTHER, D., KAMINSKI, C. F., ZHEN, M. & ST GEORGE-HYSLOP, P. 2012. ALS mutations in FUS cause neuronal dysfunction and death in Caenorhabditis elegans by a dominant gain-of-function mechanism. *Hum Mol Genet,* 21**,** 1-9.

MUSCULAR DYSTROPHY ASSOCIATION. 2014. *Signs and symptoms of amyotrophic lateral sclerosis* [Online]. Available: http://www.mda.org [Accessed 17th March 2014].

NAGANUMA, T., NAKAGAWA, S., TANIGAWA, A., SASAKI, Y. F., GOSHIMA, N. & HIROSE, T. 2012. Alternative 3'-end processing of long noncoding RNA initiates construction of nuclear paraspeckles. *EMBO J,* 31**,** 4020-34.

NAGY, D., KATO, T. & KUSHNER, P. D. 1994. Reactive astrocytes are widespread in the cortical gray matter of amyotrophic lateral sclerosis. *J Neurosci Res,* 38**,** 336-47.

NAKAGAWA, S., NAGANUMA, T., SHIOI, G. & HIROSE, T. 2011. Paraspeckles are subpopulation-specific nuclear bodies that are not essential in mice. *J Cell Biol,* 193**,** 31-9.

NAKAYA, T., ALEXIOU, P., MARAGKAKIS, M., CHANG, A. & MOURELATOS, Z. 2013. FUS regulates genes coding for RNA-binding proteins in neurons by binding to their highly conserved introns. *RNA,* 19**,** 498-509.

NEUMANN, M., BENTMANN, E., DORMANN, D., JAWAID, A., DEJESUS-HERNANDEZ, M., ANSORGE, O., ROEBER, S., KRETZSCHMAR, H. A., MUNOZ, D. G., KUSAKA, H., YOKOTA, O., ANG, L. C., BILBAO, J., RADEMAKERS, R., HAASS, C. & MACKENZIE, I. R. 2011. FET proteins TAF15 and EWS are selective markers that distinguish FTLD with FUS pathology from amyotrophic lateral sclerosis with FUS mutations. *Brain,* 134**,** 2595-609.

NEUMANN, M., KAHLE, P. J., GIASSON, B. I., OZMEN, L., BORRONI, E., SPOOREN, W., MULLER, V., ODOY, S., FUJIWARA, H., HASEGAWA, M., IWATSUBO, T., TROJANOWSKI, J. Q., KRETZSCHMAR, H. A. & HAASS, C. 2002. Misfolded proteinase K-resistant hyperphosphorylated alpha-synuclein in aged transgenic mice with locomotor deterioration and in human alpha-synucleinopathies. *J Clin Invest,* 110**,** 1429-39.

NEUMANN, M., ROEBER, S., KRETZSCHMAR, H. A., RADEMAKERS, R., BAKER, M. & MACKENZIE, I. R. 2009. Abundant FUS-immunoreactive pathology in neuronal intermediate filament inclusion disease. *Acta Neuropathol,* 118**,** 605-16.

NEUMANN, M., SAMPATHU, D. M., KWONG, L. K., TRUAX, A. C., MICSENYI, M. C., CHOU, T. T., BRUCE, J., SCHUCK, T., GROSSMAN, M., CLARK, C. M., MCCLUSKEY, L. F., MILLER, B. L., MASLIAH, E., MACKENZIE, I. R., FELDMAN, H., FEIDEN, W., KRETZSCHMAR, H. A., TROJANOWSKI, J. Q. & LEE, V. M. 2006. Ubiquitinated TDP-43 in frontotemporal lobar degeneration and amyotrophic lateral sclerosis. *Science,* 314**,** 130-3.

NISHIMOTO, Y., NAKAGAWA, S., HIROSE, T., OKANO, H. J., TAKAO, M., SHIBATA, S., SUYAMA, S., KUWAKO, K., IMAI, T., MURAYAMA, S., SUZUKI, N. & OKANO, H. 2013. The long non-coding RNA nuclear-enriched abundant transcript 1_2 induces paraspeckle formation in the motor neuron during the early phase of amyotrophic lateral sclerosis. *Mol Brain,* 6**,** 31.

NISHIMURA, A. L., MITNE-NETO, M., SILVA, H. C., RICHIERI-COSTA, A., MIDDLETON, S., CASCIO, D., KOK, F., OLIVEIRA, J. R., GILLINGWATER, T., WEBB, J., SKEHEL, P. & ZATZ, M. 2004. A mutation in the vesicle-trafficking protein VAPB causes late-onset spinal muscular atrophy and amyotrophic lateral sclerosis. *Am J Hum Genet,* 75**,** 822-31.

NISHITOH, H., KADOWAKI, H., NAGAI, A., MARUYAMA, T., YOKOTA, T., FUKUTOMI, H., NOGUCHI, T., MATSUZAWA, A., TAKEDA, K. & ICHIJO, H. 2008. ALS-linked mutant SOD1 induces ER stress- and ASK1-dependent motor neuron death by targeting Derlin-1. *Genes Dev,* 22**,** 1451-64.

NOMURA, T., WATANABE, S., KANEKO, K., YAMANAKA, K., NUKINA, N. & FURUKAWA, Y. 2014. Intranuclear aggregation of mutant FUS/TLS as a molecular pathomechanism of amyotrophic lateral sclerosis. *J Biol Chem,* 289**,** 1192-202.

OAKLEY, B. R. 1995. Cell biology. A nice ring to the centrosome. *Nature,* 378**,** 555-6.

OKAMOTO, K., HIRAI, S., AMARI, M., WATANABE, M. & SAKURAI, A. 1993. Bunina bodies in amyotrophic lateral sclerosis immunostained with rabbit anti-cystatin C serum. *Neurosci Lett,* 162**,** 125-8.

OKAMOTO, K., MIZUNO, Y. & FUJITA, Y. 2008. Bunina bodies in amyotrophic lateral sclerosis. *Neuropathology,* 28**,** 109-15.

OKAMOTO, K., NAGAI, T., MIYAWAKI, A. & HAYASHI, Y. 2004. Rapid and persistent modulation of actin dynamics regulates postsynaptic reorganization underlying bidirectional plasticity. *Nat Neurosci,* 7**,** 1104-12.

OKAMOTO, Y., IHARA, M., URUSHITANI, M., YAMASHITA, H., KONDO, T., TANIGAKI, A., OONO, M., KAWAMATA, J., IKEMOTO, A., KAWAMOTO, Y., TAKAHASHI, R. & ITO, H. 2011. An autopsy case of SOD1-related ALS with TDP-43 positive inclusions. *Neurology,* 77**,** 1993-5.

ORLACCHIO, A., BABALINI, C., BORRECA, A., PATRONO, C., MASSA, R., BASARAN, S., MUNHOZ, R. P., ROGAEVA, E. A., ST GEORGE-HYSLOP, P. H., BERNARDI, G. & KAWARAI, T. 2010. SPATACSIN mutations cause autosomal recessive juvenile amyotrophic lateral sclerosis. *Brain,* 133**,** 591-8.

OROZCO, D., TAHIROVIC, S., RENTZSCH, K., SCHWENK, B. M., HAASS, C. & EDBAUER, D. 2012. Loss of fused in sarcoma (FUS) promotes pathological Tau splicing. *EMBO Rep,* 13**,** 759-64.

PAGE, T., GITCHO, M. A., MOSAHEB, S., CARTER, D., CHAKRAVERTY, S., PERRY, R. H., BIGIO, E. H., GEARING, M., FERRER, I., GOATE, A. M., CAIRNS, N. J. & THORPE, J. R. 2011. FUS immunogold labeling TEM analysis of the neuronal cytoplasmic inclusions of neuronal intermediate filament inclusion disease: a frontotemporal lobar degeneration with FUS proteinopathy. *J Mol Neurosci,* 45**,** 409-21.

PASINELLI, P., BELFORD, M. E., LENNON, N., BACSKAI, B. J., HYMAN, B. T., TROTTI, D. & BROWN, R. H., JR. 2004. Amyotrophic lateral sclerosis-associated SOD1 mutant proteins bind and aggregate with Bcl-2 in spinal cord mitochondria. *Neuron,* 43**,** 19-30.

PASINELLI, P. & BROWN, R. H. 2006. Molecular biology of amyotrophic lateral sclerosis: insights from genetics. *Nat Rev Neurosci,* 7**,** 710-23.

PERERA, N. D., SHEEAN, R. K., SCOTT, J. W., KEMP, B. E., HORNE, M. K. & TURNER, B. J. 2014. Mutant TDP-43 deregulates AMPK activation by PP2A in ALS models. *PLoS One,* 9**,** e90449.

PIAO, Y. S., WAKABAYASHI, K., KAKITA, A., YAMADA, M., HAYASHI, S., MORITA, T., IKUTA, F., OYANAGI, K. & TAKAHASHI, H. 2003. Neuropathology with clinical correlations of sporadic amyotrophic lateral sclerosis: 102 autopsy cases examined between 1962 and 2000. *Brain Pathol,* 13**,** 10-22.

POKRISHEVSKY, E., GRAD, L. I., YOUSEFI, M., WANG, J., MACKENZIE, I. R. & CASHMAN, N. R. 2012. Aberrant localization of FUS and TDP43 is associated with misfolding of SOD1 in amyotrophic lateral sclerosis. *PLoS One,* 7**,** e35050.

PRASANTH, K. V., PRASANTH, S. G., XUAN, Z., HEARN, S., FREIER, S. M., BENNETT, C. F., ZHANG, M. Q. & SPECTOR, D. L. 2005. Regulating gene expression through RNA nuclear retention. *Cell,* 123**,** 249-63.

QIU, H., LEE, S., SHANG, Y., WANG, W. Y., AU, K. F., KAMIYA, S., BARMADA, S. J., FINKBEINER, S., LUI, H., CARLTON, C. E., TANG, A. A., OLDHAM, M. C., WANG, H., SHORTER, J., FILIANO, A. J., ROBERSON, E. D., TOURTELLOTTE, W. G., CHEN, B., TSAI, L. H. & HUANG, E. J. 2014. ALS-associated mutation FUS-R521C causes DNA damage and RNA splicing defects. *J Clin Invest,* 124**,** 981-99.

RAJPUT, A., RAJPUT, A. H., RAJPUT, M. L., ENCARNACION, M., BERNALES, C. Q., ROSS, J. P., FARRER, M. J. & VILARINO-GUELL, C. 2014. Identification of FUS p.R377W in essential tremor. *Eur J Neurol,* 21**,** 361-3.

RAVITS, J., APPEL, S., BALOH, R. H., BAROHN, R., BROOKS, B. R., ELMAN, L., FLOETER, M. K., HENDERSON, C., LOMEN-HOERTH, C., MACKLIS, J. D., MCCLUSKEY, L., MITSUMOTO, H., PRZEDBORSKI, S., ROTHSTEIN, J., TROJANOWSKI, J. Q., VAN DEN BERG, L. H. & RINGEL, S. 2013. Deciphering amyotrophic lateral sclerosis: what phenotype, neuropathology and genetics are telling us about pathogenesis. *Amyotroph Lateral Scler Frontotemporal Degener,* 14 Suppl 1**,** 5-18.

RAVITS, J., LAURIE, P., FAN, Y. & MOORE, D. H. 2007. Implications of ALS focality: rostral-caudal distribution of lower motor neuron loss postmortem. *Neurology,* 68**,** 1576-82.

REAUME, A. G., ELLIOTT, J. L., HOFFMAN, E. K., KOWALL, N. W., FERRANTE, R. J., SIWEK, D. F., WILCOX, H. M., FLOOD, D. G., BEAL, M. F., BROWN, R. H., JR., SCOTT, R. W. & SNIDER, W. D. 1996. Motor neurons in Cu/Zn superoxide dismutase-deficient mice develop normally but exhibit enhanced cell death after axonal injury. *Nat Genet,* 13**,** 43-7.

REDDI, A. R. & CULOTTA, V. C. 2013. SOD1 integrates signals from oxygen and glucose to repress respiration. *Cell,* 152**,** 224-35.

REINER, A., MEDINA, L., FIGUEREDO-CARDENAS, G. & ANFINSON, S. 1995. Brainstem motoneuron pools that are selectively resistant in amyotrophic lateral sclerosis are preferentially enriched in parvalbumin: evidence from monkey brainstem for a calcium-mediated mechanism in sporadic ALS. *Exp Neurol,* 131**,** 239-50.

RENTON, A. E., CHIO, A. & TRAYNOR, B. J. 2014. State of play in amyotrophic lateral sclerosis genetics. *Nat Neurosci,* 17**,** 17-23.

RENTON, A. E., MAJOUNIE, E., WAITE, A., SIMON-SANCHEZ, J., ROLLINSON, S., GIBBS, J. R., SCHYMICK, J. C., LAAKSOVIRTA, H., VAN SWIETEN, J. C., MYLLYKANGAS, L., KALIMO, H., PAETAU, A., ABRAMZON, Y., REMES, A. M., KAGANOVICH, A., SCHOLZ, S. W., DUCKWORTH, J., DING, J., HARMER, D. W., HERNANDEZ, D. G., JOHNSON, J. O., MOK, K., RYTEN, M., TRABZUNI, D., GUERREIRO, R. J., ORRELL, R. W., NEAL, J., MURRAY, A., PEARSON, J., JANSEN, I. E., SONDERVAN, D., SEELAAR, H., BLAKE, D., YOUNG, K., HALLIWELL, N., CALLISTER, J. B., TOULSON, G., RICHARDSON, A., GERHARD, A., SNOWDEN, J., MANN, D., NEARY, D., NALLS, M. A., PEURALINNA, T., JANSSON, L., ISOVIITA, V. M., KAIVORINNE, A. L., HOLTTA-VUORI, M., IKONEN, E., SULKAVA, R., BENATAR, M., WUU, J., CHIO, A., RESTAGNO, G., BORGHERO, G., SABATELLI, M., HECKERMAN, D., ROGAEVA, E., ZINMAN, L., ROTHSTEIN, J. D., SENDTNER, M., DREPPER, C., EICHLER, E. E., ALKAN, C., ABDULLAEV, Z., PACK, S. D., DUTRA, A., PAK, E., HARDY, J., SINGLETON, A., WILLIAMS, N. M., HEUTINK, P., PICKERING-BROWN, S., MORRIS, H. R., TIENARI, P. J. & TRAYNOR, B. J. 2011. A hexanucleotide repeat expansion in C9ORF72 is the cause of chromosome 9p21-linked ALS-FTD. *Neuron,* 72**,** 257-68.

RINGHOLZ, G. M., APPEL, S. H., BRADSHAW, M., COOKE, N. A., MOSNIK, D. M. & SCHULZ, P. E. 2005. Prevalence and patterns of cognitive impairment in sporadic ALS. *Neurology,* 65**,** 586-90.

RIPPS, M. E., HUNTLEY, G. W., HOF, P. R., MORRISON, J. H. & GORDON, J. W. 1995. Transgenic mice expressing an altered murine superoxide dismutase gene provide an animal model of amyotrophic lateral sclerosis. *Proc Natl Acad Sci U S A,* 92**,** 689-93.

ROBBERECHT, W. & PHILIPS, T. 2013. The changing scene of amyotrophic lateral sclerosis. *Nat Rev Neurosci,* 14**,** 248-64.

ROCHE, J. C., ROJAS-GARCIA, R., SCOTT, K. M., SCOTTON, W., ELLIS, C. E., BURMAN, R., WIJESEKERA, L., TURNER, M. R., LEIGH, P. N., SHAW, C. E. & AL-CHALABI, A. 2012. A proposed staging system for amyotrophic lateral sclerosis. *Brain,* 135**,** 847-52.

ROGELJ, B., EASTON, L. E., BOGU, G. K., STANTON, L. W., ROT, G., CURK, T., ZUPAN, B., SUGIMOTO, Y., MODIC, M., HABERMAN, N., TOLLERVEY, J., FUJII, R., TAKUMI, T., SHAW, C. E. & ULE, J. 2012. Widespread binding of FUS along nascent RNA regulates alternative splicing in the brain. *Sci Rep,* 2**,** 603.

ROSEN, D. R., BOWLING, A. C., PATTERSON, D., USDIN, T. B., SAPP, P., MEZEY, E., MCKENNA-YASEK, D., O'REGAN, J., RAHMANI, Z., FERRANTE, R. J. & ET AL. 1994. A frequent ala 4 to val superoxide dismutase-1 mutation is associated with a rapidly progressive familial amyotrophic lateral sclerosis. *Hum Mol Genet,* 3**,** 981-7.

ROSEN, D. R., SIDDIQUE, T., PATTERSON, D., FIGLEWICZ, D. A., SAPP, P., HENTATI, A., DONALDSON, D., GOTO, J., O'REGAN, J. P., DENG, H. X. & ET AL. 1993. Mutations in Cu/Zn superoxide dismutase gene are associated with familial amyotrophic lateral sclerosis. *Nature,* 362**,** 59-62.

ROSS, C. A. & POIRIER, M. A. 2004. Protein aggregation and neurodegenerative disease. *Nat Med,* 10 Suppl**,** S10-7.

ROTUNNO, M. S. & BOSCO, D. A. 2013. An emerging role for misfolded wild-type SOD1 in sporadic ALS pathogenesis. *Front Cell Neurosci,* 7**,** 253.

ROWLAND, L. P. 2001. How amyotrophic lateral sclerosis got its name: the clinical-pathologic genius of Jean-Martin Charcot. *Arch Neurol,* 58**,** 512-5.

ROWLAND, L. P. & SHNEIDER, N. A. 2001. Amyotrophic lateral sclerosis. *N Engl J Med,* 344**,** 1688-700.

RUTHERFORD, N. J., FINCH, N. A., DEJESUS-HERNANDEZ, M., CROOK, R. J., LOMEN-HOERTH, C., WSZOLEK, Z. K., UITTI, R. J., GRAFF-RADFORD, N. R. & RADEMAKERS, R. 2012. Pathogenicity of exonic indels in fused in sarcoma in amyotrophic lateral sclerosis. *Neurobiol Aging,* 33**,** 424 e23-4.

SABATELLI, M., MONCADA, A., CONTE, A., LATTANTE, S., MARANGI, G., LUIGETTI, M., LUCCHINI, M., MIRABELLA, M., ROMANO, A., DEL GRANDE, A., BISOGNI, G., DORONZIO, P. N., ROSSINI, P. M. & ZOLLINO, M. 2013. Mutations in the 3' untranslated region of FUS causing FUS overexpression are associated with amyotrophic lateral sclerosis. *Hum Mol Genet,* 22**,** 4748-55.

SACCON, R. A., BUNTON-STASYSHYN, R. K., FISHER, E. M. & FRATTA, P. 2013. Is SOD1 loss of function involved in amyotrophic lateral sclerosis? *Brain,* 136**,** 2342-58.

SAHA, S., MURTHY, S. & RANGARAJAN, P. N. 2006. Identification and characterization of a virus-inducible non-coding RNA in mouse brain. *J Gen Virol,* 87**,** 1991-5.

SAMA, R. R., WARD, C. L., KAUSHANSKY, L. J., LEMAY, N., ISHIGAKI, S., URANO, F. & BOSCO, D. A. 2013. FUS/TLS assembles into stress granules and is a prosurvival factor during hyperosmolar stress. *J Cell Physiol,* 228**,** 2222-31.

SARNA, J. R. & HAWKES, R. 2011. Patterned Purkinje cell loss in the ataxic sticky mouse. *Eur J Neurosci,* 34**,** 79-86.

SASAKI, Y. T., IDEUE, T., SANO, M., MITUYAMA, T. & HIROSE, T. 2009. MENepsilon/beta noncoding RNAs are essential for structural integrity of nuclear paraspeckles. *Proc Natl Acad Sci U S A,* 106**,** 2525-30.

SASAYAMA, H., SHIMAMURA, M., TOKUDA, T., AZUMA, Y., YOSHIDA, T., MIZUNO, T., NAKAGAWA, M., FUJIKAKE, N., NAGAI, Y. & YAMAGUCHI, M. 2012. Knockdown of the Drosophila fused in sarcoma (FUS) homologue causes deficient locomotive behavior and shortening of motoneuron terminal branches. *PLoS One,* 7**,** e39483.

SAWADA, K., KALAM AZAD, A., SAKATA-HAGA, H., LEE, N. S., JEONG, Y. G. & FUKUI, Y. 2009. Striking pattern of Purkinje cell loss in cerebellum of an ataxic mutant mouse, tottering. *Acta Neurobiol Exp (Wars),* 69**,** 138-45.

SCHIFFER, D., CORDERA, S., CAVALLA, P. & MIGHELI, A. 1996. Reactive astrogliosis of the spinal cord in amyotrophic lateral sclerosis. *J Neurol Sci,* 139 Suppl**,** 27-33.

SCHIFFER, D., CORDERA, S., GIORDANA, M. T., ATTANASIO, A. & PEZZULO, T. 1995. Synaptic vesicle proteins, synaptophysin and chromogranin A in amyotrophic lateral sclerosis. *J Neurol Sci,* 129 Suppl**,** 68-74.

SCHMITTGEN, T. D. & LIVAK, K. J. 2008. Analyzing real-time PCR data by the comparative C(T) method. *Nat Protoc,* 3**,** 1101-8.

SCHMITZ, M. L. & HERRMANN, H. 2008. Functional architecture of the cell nucleus. *Biochim Biophys Acta,* 1783**,** 2041-3.

SCHWARTZ, J. C., EBMEIER, C. C., PODELL, E. R., HEIMILLER, J., TAATJES, D. J. & CECH, T. R. 2012. FUS binds the CTD of RNA polymerase II and regulates its phosphorylation at Ser2. *Genes Dev,* 26**,** 2690-5.

SCHWARTZ, J. C., WANG, X., PODELL, E. R. & CECH, T. R. 2013. RNA seeds higher-order assembly of FUS protein. *Cell Rep,* 5**,** 918-25.

SELTMAN, R. E. & MATTHEWS, B. R. 2012. Frontotemporal lobar degeneration: epidemiology, pathology, diagnosis and management. *CNS Drugs,* 26**,** 841-70.

SEPHTON, C. F., GOOD, S. K., ATKIN, S., DEWEY, C. M., MAYER, P., 3RD, HERZ, J. & YU, G. 2010. TDP-43 is a developmentally regulated protein essential for early embryonic development. *J Biol Chem,* 285**,** 6826-34.

SEPHTON, C. F., TANG, A. A., KULKARNI, A., WEST, J., BROOKS, M., STUBBLEFIELD, J. J., LIU, Y., ZHANG, M. Q., GREEN, C. B., HUBER, K. M., HUANG, E. J., HERZ, J. & YU, G. 2014. Activity-dependent FUS dysregulation disrupts synaptic homeostasis. *Proc Natl Acad Sci U S A,* 111**,** E4769-78.

SEYFRIED, N. T., GOZAL, Y. M., DONOVAN, L. E., HERSKOWITZ, J. H., DAMMER, E. B., XIA, Q., KU, L., CHANG, J., DUONG, D. M., REES, H. D., COOPER, D. S., GLASS, J. D., GEARING, M., TANSEY, M. G., LAH, J. J., FENG, Y., LEVEY, A. I. & PENG, J. 2012. Quantitative analysis of the detergent-insoluble brain proteome in frontotemporal lobar degeneration using SILAC internal standards. *J Proteome Res,* 11**,** 2721-38.

SHAHIDULLAH, M., LE MARCHAND, S. J., FEI, H., ZHANG, J., PANDEY, U. B., DALVA, M. B., PASINELLI, P. & LEVITAN, I. B. 2013. Defects in synapse structure and function precede motor neuron degeneration in Drosophila models of FUS-related ALS. *J Neurosci,* 33**,** 19590-8.

SHAN, X., CHIANG, P. M., PRICE, D. L. & WONG, P. C. 2010. Altered distributions of Gemini of coiled bodies and mitochondria in motor neurons of TDP-43 transgenic mice. *Proc Natl Acad Sci U S A,* 107**,** 16325-30.

SHAV-TAL, Y., BLECHMAN, J., DARZACQ, X., MONTAGNA, C., DYE, B. T., PATTON, J. G., SINGER, R. H. & ZIPORI, D. 2005. Dynamic sorting of nuclear components into distinct nucleolar caps during transcriptional inhibition. *Mol Biol Cell,* 16**,** 2395-413.

SHAW, C. E., ENAYAT, Z. E., POWELL, J. F., ANDERSON, V. E., RADUNOVIC, A., AL-SARRAJ, S. & LEIGH, P. N. 1997. Familial amyotrophic lateral sclerosis. Molecular pathology of a patient with a SOD1 mutation. *Neurology,* 49**,** 1612-6.

SHELKOVNIKOVA, T. A., ROBINSON, H. K., TROAKES, C., NINKINA, N. & BUCHMAN, V. L. 2014. Compromised paraspeckle formation as a pathogenic factor in FUSopathies. *Hum Mol Genet,* 23**,** 2298-312.

SHEN, W., LIANG, X. H. & CROOKE, S. T. 2014. Phosphorothioate oligonucleotides can displace NEAT1 RNA and form nuclear paraspeckle-like structures. *Nucleic Acids Res,* 42**,** 8648-62.

SHIBATA, N., HIRANO, A., KOBAYASHI, M., SASAKI, S., KATO, T., MATSUMOTO, S., SHIOZAWA, Z., KOMORI, T., IKEMOTO, A., UMAHARA, T. & ET AL. 1994. Cu/Zn superoxide dismutase-like immunoreactivity in Lewy body-like inclusions of sporadic amyotrophic lateral sclerosis. *Neurosci Lett,* 179**,** 149-52.

SHIBATA, N., HIRANO, A., KOBAYASHI, M., SIDDIQUE, T., DENG, H. X., HUNG, W. Y., KATO, T. & ASAYAMA, K. 1996. Intense superoxide dismutase-1 immunoreactivity in intracytoplasmic hyaline inclusions of familial amyotrophic lateral sclerosis with posterior column involvement. *J Neuropathol Exp Neurol,* 55**,** 481-90.

SHUMAN, S. 1991. Recombination mediated by vaccinia virus DNA topoisomerase I in Escherichia coli is sequence specific. *Proc Natl Acad Sci U S A,* 88**,** 10104-8.

SHUMAN, S. 1994. Novel approach to molecular cloning and polynucleotide synthesis using vaccinia DNA topoisomerase. *J Biol Chem,* 269**,** 32678-84.

SIMPSON, C. L., LEMMENS, R., MISKIEWICZ, K., BROOM, W. J., HANSEN, V. K., VAN VUGHT, P. W., LANDERS, J. E., SAPP, P., VAN DEN BOSCH, L., KNIGHT, J., NEALE, B. M., TURNER, M. R., VELDINK, J. H., OPHOFF, R. A., TRIPATHI, V. B., BELEZA, A., SHAH, M. N., PROITSI, P., VAN HOECKE, A., CARMELIET, P., HORVITZ, H. R., LEIGH, P. N., SHAW, C. E., VAN DEN BERG, L. H., SHAM, P. C., POWELL, J. F., VERSTREKEN, P., BROWN, R. H., JR., ROBBERECHT, W. & AL-CHALABI, A. 2009. Variants of the elongator protein 3 (ELP3) gene are associated with motor neuron degeneration. *Hum Mol Genet,* 18**,** 472-81.

SLEEMAN, J. E. & TRINKLE-MULCAHY, L. 2014. Nuclear bodies: new insights into assembly/dynamics and disease relevance. *Curr Opin Cell Biol,* 28C**,** 76-83.

SMITH, B. N., TICOZZI, N., FALLINI, C., GKAZI, A. S., TOPP, S., KENNA, K. P., SCOTTER, E. L., KOST, J., KEAGLE, P., MILLER, J. W., CALINI, D., VANCE, C., DANIELSON, E. W., TROAKES, C., TILOCA, C., AL-SARRAJ, S., LEWIS, E. A., KING, A., COLOMBRITA, C., PENSATO, V., CASTELLOTTI, B., DE BELLEROCHE, J., BAAS, F., TEN ASBROEK, A. L., SAPP, P. C., MCKENNA-YASEK, D., MCLAUGHLIN, R. L., POLAK, M., ASRESS, S., ESTEBAN-PEREZ, J., MUNOZ-BLANCO, J. L., SIMPSON, M., CONSORTIUM, S., VAN RHEENEN, W., DIEKSTRA, F. P., LAURIA, G., DUGA, S., CORTI, S., CEREDA, C., CORRADO, L., SORARU, G., MORRISON, K. E., WILLIAMS, K. L., NICHOLSON, G. A., BLAIR, I. P., DION, P. A., LEBLOND, C. S., ROULEAU, G. A., HARDIMAN, O., VELDINK, J. H., VAN DEN BERG, L. H., AL-CHALABI, A., PALL, H., SHAW, P. J., TURNER, M. R., TALBOT, K., TARONI, F., GARCIA-REDONDO, A., WU, Z., GLASS, J. D., GELLERA, C., RATTI, A., BROWN, R. H., JR., SILANI, V., SHAW, C. E., LANDERS, J. E. & CONSORTIUM, S. 2014. Exome-wide Rare Variant Analysis Identifies TUBA4A Mutations Associated with Familial ALS. *Neuron,* 84**,** 324-31.

SPECTOR, D. L. & LAMOND, A. I. 2011. Nuclear speckles. *Cold Spring Harb Perspect Biol,* 3.

SREEDHARAN, J., BLAIR, I. P., TRIPATHI, V. B., HU, X., VANCE, C., ROGELJ, B., ACKERLEY, S., DURNALL, J. C., WILLIAMS, K. L., BURATTI, E., BARALLE, F.,

DE BELLEROCHE, J., MITCHELL, J. D., LEIGH, P. N., AL-CHALABI, A., MILLER, C. C., NICHOLSON, G. & SHAW, C. E. 2008. TDP-43 mutations in familial and sporadic amyotrophic lateral sclerosis. *Science,* 319**,** 1668-72.

STALLINGS, N. R., PUTTAPARTHI, K., LUTHER, C. M., BURNS, D. K. & ELLIOTT, J. L. 2010. Progressive motor weakness in transgenic mice expressing human TDP-43. *Neurobiol Dis,* 40**,** 404-14.

SUN, S., LING, S. C., QIU, J., ALBUQUERQUE, C. P., ZHOU, Y., TOKUNAGA, S., LI, H., QIU, H., BUI, A., YEO, G. W., HUANG, E. J., EGGAN, K., ZHOU, H., FU, X. D., LAGIER-TOURENNE, C. & CLEVELAND, D. W. 2015. ALS-causative mutations in FUS/TLS confer gain and loss of function by altered association with SMN and U1-snRNP. *Nat Commun,* 6**,** 6171.

SUN, Z., DIAZ, Z., FANG, X., HART, M. P., CHESI, A., SHORTER, J. & GITLER, A. D. 2011. Molecular determinants and genetic modifiers of aggregation and toxicity for the ALS disease protein FUS/TLS. *PLoS Biol,* 9**,** e1000614.

SUNWOO, H., DINGER, M. E., WILUSZ, J. E., AMARAL, P. P., MATTICK, J. S. & SPECTOR, D. L. 2009. MEN epsilon/beta nuclear-retained non-coding RNAs are up-regulated upon muscle differentiation and are essential components of paraspeckles. *Genome Res,* 19**,** 347-59.

TAKANASHI, K. & YAMAGUCHI, A. 2014. Aggregation of ALS-linked FUS mutant sequesters RNA binding proteins and impairs RNA granules formation. *Biochem Biophys Res Commun,* 452**,** 600-7.

TALBOT, K. 2009. Motor neuron disease: the bare essentials. *Pract Neurol,* 9**,** 303-9.

TALBOT, K. 2013. Should all patients with ALS have genetic testing? *J Neurol Neurosurg Psychiatry*.

TAN, A. Y. & MANLEY, J. L. 2009. The TET family of proteins: functions and roles in disease. *J Mol Cell Biol,* 1**,** 82-92.

TAN, A. Y. & MANLEY, J. L. 2010. TLS inhibits RNA polymerase III transcription. *Mol Cell Biol,* 30**,** 186-96.

TAN, A. Y., RILEY, T. R., COADY, T., BUSSEMAKER, H. J. & MANLEY, J. L. 2012. TLS/FUS (translocated in liposarcoma/fused in sarcoma) regulates target gene transcription via single-stranded DNA response elements. *Proc Natl Acad Sci U S A,* 109**,** 6030-5.

TAO, Z., WANG, H., XIA, Q., LI, K., LI, K., JIANG, X., XU, G., WANG, G. & YING, Z. 2015. Nucleolar stress and impaired stress granule formation contribute to C9orf72 RAN translation-induced cytotoxicity. *Hum Mol Genet*.

TEYSSOU, E., TAKEDA, T., LEBON, V., BOILLEE, S., DOUKOURE, B., BATAILLON, G., SAZDOVITCH, V., CAZENEUVE, C., MEININGER, V., LEGUERN, E., SALACHAS, F., SEILHEAN, D. & MILLECAMPS, S. 2013. Mutations in SQSTM1 encoding p62 in amyotrophic lateral sclerosis: genetics and neuropathology. *Acta Neuropathol,* 125**,** 511-22.

THERRIEN, M., ROULEAU, G. A., DION, P. A. & PARKER, J. A. 2013. Deletion of C9ORF72 results in motor neuron degeneration and stress sensitivity in C. elegans. *PLoS One,* 8**,** e83450.

THOMAS, M., ALEGRE-ABARRATEGUI, J. & WADE-MARTINS, R. 2013. RNA dysfunction and aggrephagy at the centre of an amyotrophic lateral sclerosis/frontotemporal dementia disease continuum. *Brain,* 136**,** 1345-60.

TOOMBS, J. A., MCCARTY, B. R. & ROSS, E. D. 2010. Compositional determinants of prion formation in yeast. *Mol Cell Biol,* 30**,** 319-32.

TRAYNOR, B. J., CODD, M. B., CORR, B., FORDE, C., FROST, E. & HARDIMAN, O. M. 2000. Clinical features of amyotrophic lateral sclerosis according to the El Escorial and Airlie House diagnostic criteria: A population-based study. *Arch Neurol,* 57**,** 1171-6.

TROOST, D., SILLEVIS SMITT, P. A., DE JONG, J. M. & SWAAB, D. F. 1992. Neurofilament and glial alterations in the cerebral cortex in amyotrophic lateral sclerosis. *Acta Neuropathol,* 84**,** 664-73.

TSUIJI, H., IGUCHI, Y., FURUYA, A., KATAOKA, A., HATSUTA, H., ATSUTA, N., TANAKA, F., HASHIZUME, Y., AKATSU, H., MURAYAMA, S., SOBUE, G. & YAMANAKA, K. 2013. Spliceosome integrity is defective in the motor neuron diseases ALS and SMA. *EMBO Mol Med,* 5**,** 221-34.

TURNER, B. J. & TALBOT, K. 2008. Transgenics, toxicity and therapeutics in rodent models of mutant SOD1-mediated familial ALS. *Prog Neurobiol,* 85**,** 94-134.

TURNER, M. R., BARNWELL, J., AL-CHALABI, A. & EISEN, A. 2012. Young-onset amyotrophic lateral sclerosis: historical and other observations. *Brain,* 135**,** 2883-91.

URWIN, H., JOSEPHS, K. A., ROHRER, J. D., MACKENZIE, I. R., NEUMANN, M., AUTHIER, A., SEELAAR, H., VAN SWIETEN, J. C., BROWN, J. M., JOHANNSEN, P., NIELSEN, J. E., HOLM, I. E., DICKSON, D. W., RADEMAKERS, R., GRAFF-RADFORD, N. R., PARISI, J. E., PETERSEN, R. C., HATANPAA, K. J., WHITE, C. L., 3RD, WEINER, M. F., GESER, F., VAN DEERLIN, V. M., TROJANOWSKI, J. Q., MILLER, B. L., SEELEY, W. W., VAN DER ZEE, J., KUMAR-SINGH, S., ENGELBORGHS, S., DE DEYN, P. P., VAN BROECKHOVEN, C., BIGIO, E. H., DENG, H. X., HALLIDAY, G. M., KRIL, J. J., MUNOZ, D. G., MANN, D. M., PICKERING-BROWN, S. M., DOODEMAN, V., ADAMSON, G., GHAZI-NOORI, S., FISHER, E. M., HOLTON, J. L., REVESZ, T., ROSSOR, M. N., COLLINGE, J., MEAD, S. & ISAACS, A. M. 2010. FUS pathology defines the majority of tau- and TDP-43-negative frontotemporal lobar degeneration. *Acta Neuropathol,* 120**,** 33-41.

VAN BLITTERSWIJK, M., DEJESUS-HERNANDEZ, M., NIEMANTSVERDRIET, E., MURRAY, M. E., HECKMAN, M. G., DIEHL, N. N., BROWN, P. H., BAKER, M. C., FINCH, N. A., BAUER, P. O., SERRANO, G., BEACH, T. G., JOSEPHS, K. A., KNOPMAN, D. S., PETERSEN, R. C., BOEVE, B. F., GRAFF-RADFORD, N. R., BOYLAN, K. B., PETRUCELLI, L., DICKSON, D. W. & RADEMAKERS, R. 2013a. Association between repeat sizes and clinical and pathological characteristics in carriers of C9ORF72 repeat expansions (Xpansize-72): a cross-sectional cohort study. *Lancet Neurol,* 12**,** 978-88.

VAN BLITTERSWIJK, M., WANG, E. T., FRIEDMAN, B. A., KEAGLE, P. J., LOWE, P., LECLERC, A. L., VAN DEN BERG, L. H., HOUSMAN, D. E., VELDINK, J. H. & LANDERS, J. E. 2013b. Characterization of FUS mutations in amyotrophic lateral sclerosis using RNA-Seq. *PLoS One,* 8**,** e60788.

VAN DEN BOSCH, L., VAN DAMME, P., BOGAERT, E. & ROBBERECHT, W. 2006. The role of excitotoxicity in the pathogenesis of amyotrophic lateral sclerosis. *Biochim Biophys Acta,* 1762**,** 1068-82.

VANCE, C., ROGELJ, B., HORTOBAGYI, T., DE VOS, K. J., NISHIMURA, A. L., SREEDHARAN, J., HU, X., SMITH, B., RUDDY, D., WRIGHT, P., GANESALINGAM, J., WILLIAMS, K. L., TRIPATHI, V., AL-SARAJ, S., AL-CHALABI, A., LEIGH, P. N., BLAIR, I. P., NICHOLSON, G., DE BELLEROCHE, J., GALLO, J. M., MILLER, C. C. & SHAW, C. E. 2009. Mutations in FUS, an RNA processing protein, cause familial amyotrophic lateral sclerosis type 6. *Science,* 323**,** 1208-11.

VANCE, C., SCOTTER, E. L., NISHIMURA, A. L., TROAKES, C., MITCHELL, J. C., KATHE, C., URWIN, H., MANSER, C., MILLER, C. C., HORTOBAGYI, T., DRAGUNOW, M., ROGELJ, B. & SHAW, C. E. 2013. ALS mutant FUS disrupts nuclear localisation and sequesters wild-type FUS within cytoplasmic stress granules. *Hum Mol Genet*.

VANDEN BROECK, L., CALLAERTS, P. & DERMAUT, B. 2014. TDP-43-mediated neurodegeneration: towards a loss-of-function hypothesis? *Trends Mol Med,* 20**,** 66-71.

VASQUEZ, R. J., HOWELL, B., YVON, A. M., WADSWORTH, P. & CASSIMERIS, L. 1997. Nanomolar concentrations of nocodazole alter microtubule dynamic instability in vivo and in vitro. *Mol Biol Cell,* 8**,** 973-85.

VERBEECK, C., DENG, Q., DEJESUS-HERNANDEZ, M., TAYLOR, G., CEBALLOS-DIAZ, C., KOCERHA, J., GOLDE, T. E., DAS, P., RADEMAKERS, R., DICKSON, D. W. & KUKAR, T. 2012. Expression of Fused in sarcoma mutations in mice recapitulates the neuropathology of FUS proteinopathies and provides insight into disease pathogenesis. *Mol Neurodegener,* 7**,** 53.

WAIBEL, S., NEUMANN, M., RABE, M., MEYER, T. & LUDOLPH, A. C. 2010. Novel missense and truncating mutations in FUS/TLS in familial ALS. *Neurology,* 75**,** 815-7.

WAITE, A. J., BAUMER, D., EAST, S., NEAL, J., MORRIS, H. R., ANSORGE, O. & BLAKE, D. J. 2014. Reduced C9orf72 protein levels in frontal cortex of amyotrophic lateral sclerosis and frontotemporal degeneration brain with the C9ORF72 hexanucleotide repeat expansion. *Neurobiol Aging,* 35**,** 1779 e5-1779 e13.

WALKER, A. K., SOO, K. Y., SUNDARAMOORTHY, V., PARAKH, S., MA, Y., FARG, M. A., WALLACE, R. H., CROUCH, P. J., TURNER, B. J., HORNE, M. K. & ATKIN, J. D. 2013. ALS-associated TDP-43 induces endoplasmic reticulum stress, which drives cytoplasmic TDP-43 accumulation and stress granule formation. *PLoS One,* 8**,** e81170.

WANG, I. F., REDDY, N. M. & SHEN, C. K. 2002. Higher order arrangement of the eukaryotic nuclear bodies. *Proc Natl Acad Sci U S A,* 99**,** 13583-8.

WANG, J. W., BRENT, J. R., TOMLINSON, A., SHNEIDER, N. A. & MCCABE, B. D. 2011. The ALS-associated proteins FUS and TDP-43 function together to affect Drosophila locomotion and life span. *J Clin Invest,* 121**,** 4118-26.

WANG, W. Y., PAN, L., SU, S. C., QUINN, E. J., SASAKI, M., JIMENEZ, J. C., MACKENZIE, I. R., HUANG, E. J. & TSAI, L. H. 2013. Interaction of FUS and HDAC1 regulates DNA damage response and repair in neurons. *Nat Neurosci,* 16**,** 1383-91.

WANG, X., ARAI, S., SONG, X., REICHART, D., DU, K., PASCUAL, G., TEMPST, P., ROSENFELD, M. G., GLASS, C. K. & KUROKAWA, R. 2008. Induced ncRNAs allosterically modify RNA-binding proteins in cis to inhibit transcription. *Nature,* 454**,** 126-30.

WANG, X., SCHWARTZ, J. C. & CECH, T. R. 2015. Nucleic acid-binding specificity of human FUS protein. *Nucleic Acids Res*.

WATANABE, M., DYKES-HOBERG, M., CULOTTA, V. C., PRICE, D. L., WONG, P. C. & ROTHSTEIN, J. D. 2001. Histological evidence of protein aggregation in mutant SOD1 transgenic mice and in amyotrophic lateral sclerosis neural tissues. *Neurobiol Dis,* 8**,** 933-41.

WEGORZEWSKA, I. & BALOH, R. H. 2011. TDP-43-based animal models of neurodegeneration: new insights into ALS pathology and pathophysiology. *Neurodegener Dis,* 8**,** 262-74.

WEGORZEWSKA, I., BELL, S., CAIRNS, N. J., MILLER, T. M. & BALOH, R. H. 2009. TDP-43 mutant transgenic mice develop features of ALS and frontotemporal lobar degeneration. *Proc Natl Acad Sci U S A,* 106**,** 18809-14.

WIJESEKERA, L. C. & LEIGH, P. N. 2009. Amyotrophic lateral sclerosis. *Orphanet J Rare Dis,* 4**,** 3.

WILL, C. L. & LUHRMANN, R. 2011. Spliceosome structure and function. *Cold Spring Harb Perspect Biol,* 3.

WILS, H., KLEINBERGER, G., JANSSENS, J., PERESON, S., JORIS, G., CUIJT, I., SMITS, V., CEUTERICK-DE GROOTE, C., VAN BROECKHOVEN, C. & KUMAR-SINGH, S. 2010. TDP-43 transgenic mice develop spastic paralysis and neuronal inclusions characteristic of ALS and frontotemporal lobar degeneration. *Proc Natl Acad Sci U S A,* 107**,** 3858-63.

WILSON, K. H., SCHAMBRA, U. B., SMITH, M. S., PAGE, S. O., RICHARDSON, C. D., FREMEAU, R. T. & SCHWINN, D. A. 1997. In situ hybridization: identification of rare mRNAs in human tissues. *Brain Res Brain Res Protoc,* 1**,** 175-85.

WOLOZIN, B. 2014. Physiological protein aggregation run amuck: stress granules and the genesis of neurodegenerative disease. *Discov Med,* 17**,** 47-52.

WU, C. H., FALLINI, C., TICOZZI, N., KEAGLE, P. J., SAPP, P. C., PIOTROWSKA, K., LOWE, P., KOPPERS, M., MCKENNA-YASEK, D., BARON, D. M., KOST, J. E., GONZALEZ-PEREZ, P., FOX, A. D., ADAMS, J., TARONI, F., TILOCA, C., LECLERC, A. L., CHAFE, S. C., MANGROO, D., MOORE, M. J., ZITZEWITZ, J. A., XU, Z. S., VAN DEN BERG, L. H., GLASS, J. D., SICILIANO, G., CIRULLI, E. T., GOLDSTEIN, D. B., SALACHAS, F., MEININGER, V., ROSSOLL, W., RATTI, A., GELLERA, C., BOSCO, D. A., BASSELL, G. J., SILANI, V., DRORY, V. E., BROWN, R. H., JR. & LANDERS, J. E. 2012. Mutations in the profilin 1 gene cause familial amyotrophic lateral sclerosis. *Nature,* 488**,** 499-503.

WU, L. S., CHENG, W. C., HOU, S. C., YAN, Y. T., JIANG, S. T. & SHEN, C. K. 2010. TDP-43, a neuro-pathosignature factor, is essential for early mouse embryogenesis. *Genesis,* 48**,** 56-62.

WU, Y. R., FOO, J. N., TAN, L. C., CHEN, C. M., PRAKASH, K. M., CHEN, Y. C., BEI, J. X., AU, W. L., CHANG, C. W., WONG, T. Y., LIU, J. J., ZHAO, Y. & TAN, E. K. 2013. Identification of a novel risk variant in the FUS gene in essential tremor. *Neurology,* 81**,** 541-4.

XIA, G., MCFARLAND, K. N., WANG, K., SARKAR, P. S., YACHNIS, A. T. & ASHIZAWA, T. 2013. Purkinje cell loss is the major brain pathology of spinocerebellar ataxia type 10. *J Neurol Neurosurg Psychiatry,* 84**,** 1409-11.

XIA, R., LIU, Y., YANG, L., GAL, J., ZHU, H. & JIA, J. 2012. Motor neuron apoptosis and neuromuscular junction perturbation are prominent features in a Drosophila model of Fus-mediated ALS. *Mol Neurodegener,* 7**,** 10.

XIAO, S., MCLEAN, J. & ROBERTSON, J. 2006. Neuronal intermediate filaments and ALS: a new look at an old question. *Biochim Biophys Acta,* 1762**,** 1001-12.

XU, Y. F., GENDRON, T. F., ZHANG, Y. J., LIN, W. L., D'ALTON, S., SHENG, H., CASEY, M. C., TONG, J., KNIGHT, J., YU, X., RADEMAKERS, R., BOYLAN, K., HUTTON, M., MCGOWAN, E., DICKSON, D. W., LEWIS, J. & PETRUCELLI, L. 2010. Wild-type human TDP-43 expression causes TDP-43 phosphorylation, mitochondrial aggregation, motor deficits, and early mortality in transgenic mice. *J Neurosci,* 30**,** 10851-9.

YAMAZAKI, T., CHEN, S., YU, Y., YAN, B., HAERTLEIN, T. C., CARRASCO, M. A., TAPIA, J. C., ZHAI, B., DAS, R., LALANCETTE-HEBERT, M., SHARMA, A., CHANDRAN, S., SULLIVAN, G., NISHIMURA, A. L., SHAW, C. E., GYGI, S. P., SHNEIDER, N. A., MANIATIS, T. & REED, R. 2012. FUS-SMN protein interactions link the motor neuron diseases ALS and SMA. *Cell Rep,* 2**,** 799-806.

YANG, L., GAL, J., CHEN, J. & ZHU, H. 2014. Self-assembled FUS binds active chromatin and regulates gene transcription. *Proc Natl Acad Sci U S A,* 111**,** 17809-14.

YANKULOV, K., YAMASHITA, K., ROY, R., EGLY, J. M. & BENTLEY, D. L. 1995. The transcriptional elongation inhibitor 5,6-dichloro-1-beta-D-ribofuranosylbenzimidazole inhibits transcription factor IIH-associated protein kinase. *J Biol Chem,* 270**,** 23922-5.

ZHANG, D., IYER, L. M., HE, F. & ARAVIND, L. 2012. Discovery of Novel DENN Proteins: Implications for the Evolution of Eukaryotic Intracellular Membrane Structures and Human Disease. *Front Genet,* 3**,** 283.

ZHANG, J., OKABE, K., TANI, T. & FUNATSU, T. 2011. Dynamic association-dissociation and harboring of endogenous mRNAs in stress granules. *J Cell Sci,* 124**,** 4087-95.

ZHANG, Q., CHEN, C. Y., YEDAVALLI, V. S. & JEANG, K. T. 2013. NEAT1 long noncoding RNA and paraspeckle bodies modulate HIV-1 posttranscriptional expression. *MBio,* 4**,** e00596-12.

ZHANG, Y. J., JANSEN-WEST, K., XU, Y. F., GENDRON, T. F., BIENIEK, K. F., LIN, W. L., SASAGURI, H., CAULFIELD, T., HUBBARD, J., DAUGHRITY, L., CHEW, J., BELZIL, V. V., PRUDENCIO, M., STANKOWSKI, J. N., CASTANEDES-CASEY, M., WHITELAW, E., ASH, P. E., DETURE, M., RADEMAKERS, R., BOYLAN, K. B., DICKSON, D. W. & PETRUCELLI, L. 2014. Aggregation-prone c9FTD/ALS poly(GA) RAN-translated proteins cause neurotoxicity by inducing ER stress. *Acta Neuropathol,* 128**,** 505-24.

ZHANG, Y. J., XU, Y. F., COOK, C., GENDRON, T. F., ROETTGES, P., LINK, C. D., LIN, W. L., TONG, J., CASTANEDES-CASEY, M., ASH, P., GASS, J., RANGACHARI, V., BURATTI, E., BARALLE, F., GOLDE, T. E., DICKSON, D. W. & PETRUCELLI, L. 2009. Aberrant cleavage of TDP-43 enhances aggregation and cellular toxicity. *Proc Natl Acad Sci U S A,* 106**,** 7607-12.

ZHANG, Y. J., XU, Y. F., DICKEY, C. A., BURATTI, E., BARALLE, F., BAILEY, R., PICKERING-BROWN, S., DICKSON, D. & PETRUCELLI, L. 2007. Progranulin mediates caspase-dependent cleavage of TAR DNA binding protein-43. *J Neurosci,* 27**,** 10530-4.

ZHANG, Z. & CARMICHAEL, G. G. 2001. The fate of dsRNA in the nucleus: a p54(nrb)-containing complex mediates the nuclear retention of promiscuously A-to-I edited RNAs. *Cell,* 106**,** 465-75.

ZHANG, Z. C. & CHOOK, Y. M. 2012. Structural and energetic basis of ALS-causing mutations in the atypical proline-tyrosine nuclear localization signal of the Fused in Sarcoma protein (FUS). *Proc Natl Acad Sci U S A,* 109**,** 12017-21.

ZHENG, W., DENG, X., LIANG, H., SONG, Z., GAO, K., YANG, Y. & DENG, H. 2013. Genetic analysis of the fused in sarcoma gene in Chinese Han patients with essential tremor. *Neurobiol Aging,* 34**,** 2078 e3-4.

ZHONG, S., SALOMONI, P. & PANDOLFI, P. P. 2000. The transcriptional role of PML and the nuclear body. *Nat Cell Biol,* 2**,** E85-90.

ZHOU, Y., LIU, S., LIU, G., OZTURK, A. & HICKS, G. G. 2013. ALS-associated FUS mutations result in compromised FUS alternative splicing and autoregulation. *PLoS Genet,* 9**,** e1003895.

ZHOU, Y., LIU, S., OZTURK, A. & HICKS, G. G. 2014. FUS-regulated RNA metabolism and DNA damage repair: Implications for amyotrophic lateral sclerosis and frontotemporal dementia pathogenesis. *Rare Dis,* 2**,** e29515.

ZHOU, Z., LICKLIDER, L. J., GYGI, S. P. & REED, R. 2002. Comprehensive proteomic analysis of the human spliceosome. *Nature,* 419**,** 182-5.

ZINSZNER, H., IMMANUEL, D., YIN, Y., LIANG, F. X. & RON, D. 1997a. A topogenic role for the oncogenic N-terminus of TLS: nucleolar localization when transcription is inhibited. *Oncogene,* 14**,** 451-61.

ZINSZNER, H., SOK, J., IMMANUEL, D., YIN, Y. & RON, D. 1997b. TLS (FUS) binds RNA in vivo and engages in nucleo-cytoplasmic shuttling. *J Cell Sci,* 110 (Pt 15)**,** 1741-50.

ZU, T., LIU, Y., BANEZ-CORONEL, M., REID, T., PLETNIKOVA, O., LEWIS, J., MILLER, T. M., HARMS, M. B., FALCHOOK, A. E., SUBRAMONY, S. H., OSTROW, L. W., ROTHSTEIN, J. D., TRONCOSO, J. C. & RANUM, L. P. 2013. RAN proteins and RNA foci from antisense transcripts in C9ORF72 ALS and frontotemporal dementia. *Proc Natl Acad Sci U S A,* 110**,** E4968-77.